ULTRASTRUCTURAL PATHOLOGY OF HUMAN GASTROINTESTINAL TUMOURS

Volume One

Thesis Submitted for the Degree of Ph. D.
of the University of Glasgow

By

Tariq Mohamed Al-Yassin, M.B. Ch.B.

From

The Department of Pathology,

Royal Infirmary, Glasgow

April 1976

CONTENTS

ACKNOWLEDGEMENTS

I am deeply indebted to Dr. P.G. Toner for his supervision, interest, constructive advice and constant encouragement throughout this work.

I am also most grateful to Professor R.B. Goudie for giving me the opportunity to work in his laboratory.

I would like to thank the staff of the Department of Surgery, Glasgow Royal Infirmary for the provision of the surgical biopsies used in this study. I am grateful to the staff of the E.M. suite for their invaluable technical advice, to Dr. A. McLay for his help with the x-ray microanalysis technique, and to Mr. T. Parker for assistance with the light micrographs.

I wish also to express my thanks to the University of Basrah, Basrah, Iraq for financial support received during the three years of this study.

Finally, I am most appreciative to my wife for her patience, encouragement and support throughout this period.

SUMMARY

This thesis consists of an ultrastructural study of 129 neoplasms of the human alimentary tract. Included are observations on 39 samples of control human tissues, including hitherto poorly described features of the normal human oesophagus. All tissues examined were from freshly fixed biopsy or resection specimens. The techniques used were those of conventional transmission electron microscopy. Some limited studies employed ultracytochemical methods to demonstrate carbohydrate and acid phosphatase activity. In these studies, X-ray microanalysis was also employed to confirm the identity of the reaction product.

The normal squamous epithelium and submucosal glands of the human oesophagus were investigated in detail. The fine structure of squamous epithelium was found to be similar to that of non keratinized epithelium in other situations. Certain features not previously noted included the occurrence of occasional cilia, intracytoplasmic desmosomes and nuclear bodies. Langerhans cells, which have been described in the epidermis and in other squamous locations, were also observed in oesophageal squamous mucosa. The submucosal glands were comparable to the labial salivary glands.

Ultrastructural investigation of well differentiated squamous cell carcinoma of the human oesophagus revealed various similarities to, and aberrations from, the normal patterns of oesophageal squamous cell differentiation. Particular features of note included frequent intracytoplasmic desmosomes and curious thick-walled vesicles. Langerhans cells were observed in these tumours, as in the normal mucosa.

The normal gastric mucosa was studied as a control material. There were no particular features of note, the finding corresponding to the published literature. The cases of primary gastric carcinoma fall into two main groups, those with mucous secretion granules identical to the granules of gastric mucous cells and those without mucous secretion granules. There were other fine structural details which

served to distinguish these two groups. In cases of secondary gastric carcinoma, some bore a close structural resemblance to equivalent primary gastric tumours and contained mucous secretion granules identical to those of gastric mucous cells, while others contained no mucous granules. Metastatic signet ring cell carcinoma was similar in many respects to previous reports of primary signet ring cell carcinoma. However, among the observed structural differences were the occurrence of tubulovesicular structures similar to those of normal gastric parietal cells and of frequent intracytoplasmic desmosomes. Gastric carcinoma was particularly distinguished by the presence of a variety of structurally aberrant organelles. The most poorly differentiated tumours retained the adhesion specialisations typical of epithelial cells, in contrast to the findings in gastric lymphoma, in which desmosomes were absent.

The normal colonic morphology as studied in this work showed no particular features at variance with previous reports. The villous papillomas and colonic carcinomas examined displayed the fine structural features in common with the immature cells of the lower one third of the colonic crypt. The aggregates of dark cells in villous papilloma had features reminiscent of various cell types associated with fluid and electrolyte transport in other sites. Two distinctive features of primary well differentiated colonic carcinoma were the occurrence of an aberrant tubular form of granular endoplasmic reticulum and the presence of doughnut-shaped carbohydrate-rich inclusions, possibly representing a secretory product.

Various distinctive intranuclear and intracytoplasmic inclusions were observed in the course of this work, mainly in neoplastic cells in different sites. These had not previously been described in either normal or neoplastic cells of the human alimentary tract. The possible diagnostic relevance of such features is discussed.

Using a periodic acid thiocarbohydrazide silver proteinate technique a carbohydrate component was demonstrated in various sites

in the normal and neoplastic tissues studied. In most normal and neoplastic cells of the human alimentary tract, acid phosphatase was confined to the lysosomes. However, in both normal squamous epithelium and well differentiated squamous cell carcinoma, acid phosphatase activity was also found in the intercellular spaces, although the membrane-coating granules were negative. The reaction products of both of these cytochemical procedures were examined by x-ray microanalytical techniques.

CHAPTER ONE

GENERAL INTRODUCTION

The electron microscope has now become an essential tool in biological research. After the impressive improvements of the 1950's in the techniques of fixation, embedding and sectioning, there was a rapid expansion of basic ultrastructural knowledge. The detailed fine structural features of cellular anatomy were explored and correlated with the functional aspects of cell biology. Much of the fundamental structural basis of cellular organisation was found to be common to all normal cells. Moreover, particular variations of cell structure were found to correlate with specific functions. Various fine structural features peculiar to certain types of cells and tissues can form the basis for their confident identification. The contribution which the electron microscope has made to our knowledge of the structure and function of normal cells has provided us with the essential basis for the detailed study of the ultrastructure of disease.

The early descriptions of tumour ultrastructure dealt with the general fine structure of neoplastic cells (Bernhard 1958; Dalton and Felix, 1956; Mercer, 1961). Various quantitative deviations of tumour cells from normal have been documented, but there is no single ultrastructural feature which distinguishes a neoplastic cell from a normal cell with any certainty. The same problem is not unfamiliar in histology, where it is often the pattern or organisation of the cells rather than their cytology that leads us to the diagnosis of malignancy.

Subsequent ultrastructural studies have shown both striking similarities and obvious differences between the normal and

neoplastic tissues of many organs. It is clear that the neoplastic cell often mimics to a substantial extent the patterns of differentiation of its cell or tissue of origin; the standard rules for tumour classification by light microscopy can thus be seen to apply equally at the ultrastructural level. For example, the typical malignant melanoma shares certain distinctive fine structural features with the normal melanoblast (Klug and Gunther, 1972) the islet cell tumour, whether of beta cell or other origin, with its parent cell (Goldenberg, Goldenberg and Benditt, 1969; Suzuki and Matsuyama 1971) the carcinoid tumour with the argentaffin cell (Bensch, Gordon and Miller, 1965). In ultrastructure as in histology, the difficulties of classification and diagnosis tend to increase with advancing anaplasia. Nevertheless, some ultrastructural clues to histogenesis may persist in neoplastic cells which have regressed beyond the threshold of accurate histological classification. In such cases, ultrastructural examination has been shown to give a more accurate diagnosis than is possible with light microscopy (Ashworth and Stembridge, 1964; Lynn, Martin and Kingsley, 1967; Rosi and Rodriguez, 1968). It has been estimated that a more accurate diagnosis can be reached in between 4% to 8% of biopsies with the assistance of electron microscopy (Gyorkey, Min, Krisko and Gyorkey 1975).

It is clear from this that electron microscopy is not simply an academic exercise, but has a considerable, and to some extent still unrealised potential for routine tumour diagnosis particularly in relation to "problem" cases. However, the

atypical or problem case can only be understood against the widest possible background of knowledge of the typical case, and of the normal ultrastructure of the tissue or organ concerned. Although the gathering of such background knowledge is an unspectacular activity it provides the indispensable frame of reference for the pathologist who seeks to exploit ultrastructure for the purposes of diagnosis. It was with this in mind that the work of this thesis was undertaken.

There are many considerations which underline the suitability of the human alimentary tract as a target for detailed ultrastructural investigation. These include the multiplicity of cell types each elaborately specialised in ultrastructural terms; the frequency and clinical importance of gastro-intestinal neoplasms; the common occurrence of histopathological uncertainty as to the site of origin of intra-abdominal metastatic tumours; and the relatively limited scope of many of the previous ultrastructural investigations in this field.

This study set out first to define the range of normal fine structure in those tissues which had not received detailed attention by previous workers. Its second, and major aim, was to investigate the fine structure of some of the common neoplasms of the alimentary tract with a view to establishing a valid baseline for the study of future atypical cases. Its final aim was to explore the application of two basic cytochemical methods to the study of normal and neoplastic cells, with a view to confirming the identity of certain ultrastructural features. An opportunity was also taken to make a preliminary study of the

x-ray microanalytical approach to cytochemistry. These aims were all, to a greater or lesser extent, successfully realised. The accumulated data are presented region by region, with separate chapters concerning topics of special interest.

CHAPTER TWO

MATERIALS AND METHODS

MATERIALS AND METHODS

1 - Conventional Electron Microscopy

Tissues were obtained from biopsy and resection specimens as shown in Table 1. Four to eight blocks each measuring 0.5 - 1 mm in diameter were taken from the tissue, using a fresh razor blade for dissection. The blocks were immediately fixed in pre-chilled 2% glutaraldehyde in phosphate buffer (pH 7.2) at 4°C for 4 - 6 hours, washed in phosphate buffer, post fixed in 1 - 2% osmium tetroxide in distilled water at room temperature for 35 - 90 minutes and washed in distilled water for 10 minutes. The embedding schedule used is shown in Table 2. The tissue blocks were kept in small glass bottles until the final stage, and the different fluids changed with a pasteur pipette.

Tissue from the same specimens was also prepared for light microscopy by conventional methods and submitted to routine histopathological examination. Thick sections (2µm) from 2 - 4 Epon blocks from each case were cut on the LKB Ultratome III, stained with 1% methylene blue in boric acid and examined by light microscopy to confirm tissue identity and to allow selection of the area to be sectioned for electron microscopy. Ultrathin sections (30 - 50 nm) were mounted on copper grids, stained with 2% uranyl acetate in distilled water and with lead citrate, and examined in the Philips EM 200 and Philips EM 301 electron microscopes.

The electron micrographs were made on Ilford plates, type EM - 5, Kodak electron microscope cut film, and Kodak 35 mm roll film. The negatives were printed on Ilford photographic papers of different grades and developed using the Ilford automatic processor. The prints were subsequently fixed, washed and glazed.

2 - Ultracytochemistry

The following techniques were used.

i - Periodic acid thiocarbohydrazide silver proteinate technique.

Small pieces (0.5 - 1 mm) of the normal and neoplastic tissues described above, were freshly fixed in 2% glutaraldehyde in phosphate buffer (pH 7.2) for 4 - 6 hours, and processed and embedded in Epon as for conventional electron microscopy, omitting post fixation in osmium tetroxide.

Ultrathin sections were mounted on stainless steel grids and processed by the periodic acid thiocarbohydrazide silver proteinate (PATCH) method described by Pearse (1972) which is based on that of Thiery (1967). The method is shown in Table 3.

ii - Acid phosphatase technique.

Small pieces of normal and neoplastic tissues were freshly fixed in 5% glutaraldehyde in Cacodylate buffer (pH 7.4) at $4^{\circ}C$ for 4 hours. The tissue was then minced into even smaller pieces using a fresh razor blade; 50µm cryostat sections were also used. The tissue was washed with acetate buffer containing 7.5% sucrose. For localisation of acid phosphatase, a modified Gomori method was used (Etherton and Botham. 1970; Holt and Hicks, 1961) as detailed in Table 4.

The substrate mixture used has the following composition: 10 ml of 1.25% sodium β-glycerophosphate (pH 5); 20 ml of 0.2% lead nitrate; 10 ml of distilled water; 10 ml of tris maleate buffer. Control experiments were carried out on substrate - free media or media containing inhibitors such as NaF. Ultrathin sections were cut as usual mounted on copper grids and examined unstained.

iii - X -ray microanalytical technique.

Specimens processed for periodic acid thiocarbohydrazide silver proteinate, and acid phosphatase, were subjected to x - ray microanalysis for verification of the reaction products. Analysis was performed on a Philips EM 301 transmission electron microscope which had facilities for scanning microscopy and which was equipped with an EDAX retractable energy-dispersive x-ray spectrometer coupled to an EDAX 707A analyser with an 8K Data General Nova Computer for spectral manipulation.

TABLE I

Origin and Nature of the Specimens Examined.

Location	Benign Tumour	Primary Carcinoma	Secondary Carcinoma	Normal Tissue
Oesophagus	-	20	-	15
Stomach	-	35	18	10
Small Intestine	-	-	-	6
Large Intestine	10	33	11	8
Ampulla of Vater	-	2	-	-

TABLE 2

The Embedding Schedule

Process	Details
1. Dehydration	10 per cent ethanol 3 changes of 10 minutes each
2. Clearing	Propylene oxide 2 changes of 10 minutes each
3. Infiltration	Propylene oxide : Epon mixture 1:1 for 30 minutes
4. Infiltration	Propylene oxide : Epon mixture 1:3 for 90 minutes
5. Embedding	Epon mixture in gelatin capsules and rubber mould
6. Polymerization	35°C, 45°C and 60°C ovens each 24 hours

TABLE 3

Periodic acid thiocarbohydrazide silver proteinate technique

1. Float or immerse the sections mounted on the grids in 1% periodic acid in distilled water at room temperature for 60 minutes.
2. Rinse the grids in distilled water.
3. Immerse in 1% thiocarbohydrazide in 5% acetic acid for 1 - 2 hours at 60°c.
4. Wash in 5% acetic acid at 45°C for 5 - 10 minutes.
5. Rinse in distilled water.
6. Float or immerse the grids in 1% silver proteinate solution in distilled water in dark at room temperature for 30 - 45 minutes.
7. Rinse in distilled water and dry by filter paper.
8. Examine sections unstained by uranyl acetate or lead citrate.
9. Process control sections without periodic acid or without thiocarbohydrazide treatment.

TABLE 4

Acid Phosphatase Technique

1. Incubate tissue with substrate mixture at 37°C for 60 to 90 minutes.
2. Wash with Cacodylate buffer (pH 7.4) for 5 minutes.
3. Post-fix in 2% osmium tetroxide in Cacodylate buffer at 4°C for 2 hours.
4. Wash in distilled water for 5 minutes.
5. Process and embed as for conventional electron microscopy.
6. Examine sections unstained by Uranyl acetate or lead citrate.

CHAPTER THREE

NORMAL MORPHOLOGY

INTRODUCTION

The fine structure of normal human gastric (Lillibridge, 1964; Rubin, Ross, Sleisenger and Jeffries, 1968) and colonic mucosa (Pittman and Pittman, 1966; Lorenzsonn and Trier, 1968; Jimenez, Ambrosius, Boom and Leuze, 1971) has been previously described. It is not proposed to describe or illustrate these structures in detail, since the observations undertaken in the course of this work were in agreement with previous reports. A brief summary of the principal features of control tissue from stomach and colon is accompanied by a few representative micrographs.

The human oesophagus, however, has not been fully explored at the ultrastructural level, either in relation to the squamous mucosa or the submucosal glands. The main part of this chapter deals with the fine structure of the non-keratinised human oesophageal mucosa, drawing comparisons with similar surfaces, such as buccal mucosa and cervix uteri. The submucosal glands are examined in detail and compared in ultrastructural terms with mucus secreting labial salivary glands, to which they bear a histological resemblance.

The Langerhans cell, first identified by histological techniques in the upper layers of the epidermis, is now best characterised electron-microscopically, by the presence of its distinctive cytoplasmic inclusions and by absence of epithelial adhesion specialisations and tonofilaments. Cells of this type have now been identified in various squamous epithelia, including skin (Birbeck, Breathnach and Everall, 1961; Zelickson, 1965), buccal mucosa (Waterhouse and Squire, 1967), the female genital tract (Younes, Robertson and Bencosme, 1968), the sheep rumen (Gemmell, 1973) and the upper alimentary tract of the mouse (Bock, 1974). Speculations as to their nature and function

remain unresolved, although the earlier view that they were effete melanocytes (Masson, 1926, 1951) has now largely been discounted. The present study reports the occurrence of morphologically typical Langerhans cells in the normal human oesophagus and draws comparisons with the intra-epithelial lymphocytes.

OBSERVATIONS

1. Squamous epithelium of oesophagus.

The epithelial cells can be assigned to three layers, basal, intermediate and superficial, each with its characteristic fine structural features. The basal cells are cuboidal or oblong, with centrally placed nuclei which have occasional indentations (Fig. 1). The cytoplasm is relatively unspecialised, with moderate numbers of mitochondria, a small Golgi apparatus, free ribosomes but little organised endoplasmic reticulum. There are also moderate numbers of membrane - limited dense bodies. Fine bundles of tonofilaments are scattered throughout the cytoplasm and are inserted into the cytoplasmic plates of the desmosomes. Distinct intercellular spaces are crossed by interdigitating folds and projections of cytoplasm. The base, resting on the basal lamina, shows numerous hemidesmosomes, each consisting of a single dark plate with inserted tonofilaments, along with the extracellular lamina which is typical of this structure. The basal lamina itself, 40 to 50 nm in thickness, is separated from the base of the epithelium by a pale interspace of around 50 to 65 nm (Fig. 2).

In the intermediate zone of the epithelium, the cells are larger and flatter than basal cells (Fig. 3). They may have coarser bundles of tonofilaments but they are similar to basal cells in terms of their mitochondria, endoplasmic reticulum, ribosome distribution and Golgi apparatus.

The desmosomes appear more prominent in the superficial part of the intermediate layer. However, at some sites, often where the intercellular space is widened and conventional desmosomes are absent, occasional intracytoplasmic desmosomes are encountered (Fig. 4). These paradoxical structures have all of the morphology of typical desmosomes, with laminated structure and inserted tonofilaments, but they lie embedded within the cytoplasm instead of forming an attachment with another cell. These intracytoplasmic desmosomes have no demonstrable link with the cell surface or with any intracytoplasmic membrane system. A further feature of the intermediate zone is the occurrence of "membrane-coating granules" in the more distal cells. These are described more fully below. Occasional single cilia project into the intercellular space (Figs. 5,6).

The cells of the superficial zone of the mucosa are flattened, lying parallel to the surface. They retain their nuclei and have diffuse tonofilaments in a rather pale cytoplasmic matrix (Fig. 7). Cytoplasmic vacuolation is common in the deeper cells of this zone. This is associated with the presence of glycogen. There are fewer desmosomes at this level in the epithelium and the cytoplasmic projections at the cell surface only rarely appear to interdigitate. At the luminal free surface there are many finger-like projections, probably representing sectioned folds or flaps of cytoplasm (Fig. 8). The cell membrane is particularly prominent here, due to a significant increase in the thickness and staining reaction of its inner cytoplasmic leaflet (Fig. 9), while the outer leaflet and the pale interspace remain unaltered. "Membrane-coating" granules are seen in the cells of the superficial layer.

The membrane-coating granules of the human oesophageal mucosa are similar to those seen in other non-keratinised epithelia. They are small heterogeneous oval or round granules, from 60 to 350 nm in diameter, limited by a trilaminar membrane (Fig. 10). The location and size of the dense content within its pale halo is variable, at least partly as a result of plane-of-section effects. Some granules show a faint internal lamination (Fig. 11), but this is never as pronounced as in keratinised epithelium, where the distinctive periodicity of these granules is their most striking property. Membrane-coating granules occur in the distal cells of the intermediate zone of the human oesophagus, and in the superficial zone. The granules gather at the margin of the cell and dense material resembling their contents is often seen in the intercellular space (Fig. 12).

There are two other features of note in the oesophageal mucosa. The presence of Langerhans cells is described in detail below. The difficulties in distinguishing in some instances between Langerhans cells and lymphocytes raised the question of a relationship between these two cell types. In general, however, the balance of evidence favours a histiocytic origin for the Langerhans cell. Nuclear bodies are occasionally encountered at all levels in the oesophageal epithelium (Fig. 1). They consist of aggregates of microfibrillar material, up to 600 nm in diameter, not demarcated positively from the nuclear substance. The nature of these structures remains obscure. The nuclear bodies seen in this and other sites are described in detail in a subsequent chapter of this thesis.

2. Submucosal glands of oesophagus.

The oesophageal glands are situated in the submucous connective tissue, connected to the surface by a straight duct. They are

composed of lobules, each consisting of acinar and ductal structures. The acini are lined by predominantly mucus secreting columnar epithelium, the ducts by cuboidal or stratified epithelium.

Four acinar cell types can be identified in human oesophageal submucosal glands. The predominant mucous cells are recognised by their numerous large pale secretion granules. Occasional subsidiary secretory cells are seen, with similar cytoplasmic characteristics but different granule patterns. Myoepithelial cells are readily identified by their characteristic location and cytoplasmic filaments. Finally, typical oncocytes are sometimes encountered close to the origin of the duct system.

The mucous cells are closely packed, pyramidal in shape and connected by conventional junctional complexes. The bulging luminal surface (Fig. 19) bears short sparse microvilli. The nucleus is pushed to the periphery or to the base of the cell by the accumulated mass of secretion (Fig. 20). These mucus granules are pale and sometimes foamy in texture. With the fixation procedures used in this study, individual limiting membranes are not observed, and granules frequently coalesce. There is a rim of well organised granular endoplasmic reticulum at the basal andperinuclear areas, and an elaborate Golgi system is seen in favourable sections. The mitochondria are scattered towards the cell base. They have no particularly distinctive features. There are occasional microtubular inclusions within mitochondria (Fig. 21). These tubules, 15 - 25 nm in diameter, are orderly in their arrangement, usually straight or slightly curved and in longitudinal section they display a fine transverse periodicity. Finally, there are intracytoplasmic membrane-limited microfibrillar bundles, associated with pale vacuoles (Figs. 20 , 22, 25). These are distributed throughout the cytoplasm,

often lying between secretion granules.

The less common subsidiary secretory cells of the acinus (Fig. 23) are interposed between mucous cells, or lie at the junction of the acinus and duct. The secretory granules are distinct from those of the mucous cells, being membrane-limited, smaller, rather more dense, and homogeneous or stippled in texture. In other respects, these subsidiary cells are not dissimilar to the mucous cells. A further group of cells distinguished by the presence of numerous cytoplasmic filaments has smaller granules, often with a denser core and pale halo (Fig. 24). Occasional similar cells (Fig. 26) have few of these distinctive granules, or even none at all. Such cells have a less elaborate endoplasmic reticulum then their granulated counterparts.

The myoepithelial cells (Fig. 27) are flattened spindle shaped cells, connected by desmosomes to the overlying epithelial cells. They rest upon the continuous acinar basement membrane. The cytoplasm contains sparse mitochondria and few membrane systems, but is rich in myofilaments similar to those of smooth muscle, with typical attachment zones at the cell base.

Oncocytes are found in small numbers in the submucosal glands, occasionally in small clusters between duct and acinus (Fig. 28). Their characteristic numerous, closely packed mitochondria may appear round, oval or elongated (Figs. 29, 31). They have numerous cristae and occasional dense intramitochondrial granules. There is, in addition, a small Golgi system, a moderate complement of free ribosomes and a scattering of membrane-limited dense bodies. The centrally placed nucleus has a slightly irregular outline. The oncocytes have no unusual surface features. They are connected to adjacent cells by junctional complexes and desmosomes. they rest on

the basement membrane without basal specialisations and their free surface borders the gland lumen with few if any microvilli.

Various other features which have been described in previous studies of salivary tissue were not encountered in these glands. These include secretory canaliculi, intraepithelial nerve terminals and intranuclear inclusions. Unmyelinated nerves are, however, frequently found in the periacinar connective tissue, often close to the basal lamina (Fig. 30). As well as mitochondria, these axons contain small agranular and large dense-cored vesicles.

3. Ducts of submucosal glands.

Their lining ranges from flattened cuboidal epithelium (Fig. 32) at the junction of acinus and duct through two layers (Fig. 33), to a stratified pattern. The luminal surface is covered by short irregular microvilli; the contact surfaces have junctional complexes, desmosomes, and some interdigitations. Evenly distributed microfilaments are more numerous in the cuboidal than the columnar cells. Granular endoplasmic reticulum is very sparse, but free ribosomes are present in moderate numbers. In the apical cytoplasm there are some empty smooth-walled vesicles from 70 to 140 nm in diameter, along with membrane-limited multilocular bodies and pleomorphic dense granules. Myoepithelial cells similar to those of the acinus are present in ducts with a simple epithelial lining, but are absent from ducts lined by stratified epithelium.

4. Langerhans cells.

The oesophageal clear cells, which I have identified as Langerhans cells (Fig. 34), are found in the middle and superficial layers of the normal squamous mucosa and do not occur in basal layer or beneath the basal lamina. They are often irregular in outline (Fig. 35) with cytoplasmic protrusions which extent out from the perikaryon

between the surrounding squamous cells. As a result of this dendritic pattern not all sections pass through the perikaryon. In some fields, the Langerhans cell is represented only by a small cytoplasmic island interpolated between the epithelial cells.

The relative pallor of the Langerhans cell cytoplasm is in contrast with the denser matrix of adjacent squamous cells. Langerhans cells are further distinguished (Fig. 34) by the complete absence of the desmosomes and tonofilaments which are such a prominent feature of the normal squamous mucosa. Their cytoplasm (Figs. 38, 39) contains moderate numbers of free ribosomes, profiles of granular endoplasmic reticulum, a well developed Golgi apparatus with lamellae and vacuoles, often with a related centriole, and a few round or oval mitochondria, without particular structural distinction.

The nucleus is irregular in contour, often with deep invaginations, and may contain one, or rarely two nucleoli. However, not all Langerhans cells correspond to this pattern. Cells such as those shown in Fig. 40 and 41, with typical Langerhans granules, have a much less elaborate degree of cytoplasmic organisation. It is of course, difficult to exclude the possibility that such variations are simply the consequence of selection of different planes of section through different cells.

The single most distinctive feature of these cells is the presence of typical Langerhans granules (Figs. 36, 38, 39), rod-shaped inclusions up to 460 nm in length. A median section of a Langerhans cell in oesophagus may display many of these granules. They have a characteristic linear laminated internal structure and in slightly tangential sections show an apparent periodic substructure. On occasions the rod-shaped Langerhans granule is seen to connect directly with the cell membrane (Fig. 37). Some granules have a

rounded expansion at one end measuring up to 150 nm in diameter (Fig. 39). These are the distinctive 'tennis racket' structures which are described in the epidermal Langerhans cells. In addition to these organelles, there are moderate numbers of membrane limited electron dense bodies, possibly of lysosomal nature.

A second clear cell found in the human oesophagus is the typical intra-epithelial lymphocyte (Fig. 42) which is similar in appearance to those found in the intestine (Toner and Ferguson, 1971). These are also distinguished by their lack of tonofilaments and desmosomes, but they differ from typical Langerhans cells in several respects. They do not have the characteristic Langerhans granules. their cytoplasmic organelles are in general less well organised, and their nuclear morphology tends to differ from that of the Langerhans cell, in having a more prominent heterochromatin component. Nevertheless, it remains difficult in some cases to make a firm distinction on the basis of morphology between lymphocytes and Langerhans cells. Some cells containing unequivocal Langerhans granules (Fig. 41) are in most other respects indistinguishable from lymphocytes (Fig. 43). Perhaps some of the cells presumed to be lymphocytes (Fig. 43) are in fact Langerhans cells, their granules lying by chance outwith the plane of section. There is no doubt that the well differentiated Langerhans cell (Fig. 34) and the typical lymphocyte (Fig. 42) are readily separated, but the borderline between the less classical examples of the two cell types is at best indistinct. I did not identify any cells of melanocytic type in this study despite a careful search for premelanosomes.

5. Stomach

The fine structure of human gastric mucosa which was studied as control material is in accordance with previous descriptions

(Lillibridge, 1964; Rubin, Ross, Sleisenger and Jeffries, 1968; Toner, Carr and Wyburn, 1971).

The surface mucous cells have an apical aggregate of round or oval granules which have a closely applied limiting membrane and mottled or stippled appearance (Fig. 45). Their cytoplasm also contains a supranuclear Golgi apparatus and a moderately organised endoplasmic reticulum. The luminal surface bears few short microvilli with an inconspicuous fuzzy coat. The cells are connected by junctional complexes and desmosomes and rest on a basement membrane. The mucous neck cells (Fig. 44) have denser granules than the surface mucous cells, and sometimes the granules have eccentrically placed dense areas (Fig 50). The chief cells (Fig. 46) are pyramidal in shape and have basally placed nuclei. Their cytoplasm contains pale granules, elaborate endoplasmic reticulum, well developed Golgi apparatus, scattered mitochondria and moderate numbers of irregular and pleomorphic dense bodies (Fig. 54). The parietal cells (Figs. 47, 48) are pyramidal in shape and have basally situated nuclei. Their cytoplasm contains numerous oval or round mitochondria, profiles of sections through the canaliculi, numerous tubulovesicles and moderate numbers of dense bodies which are composed of myelin figures and granular and amorphous material (Fig. 53). The endocrine cells (Fig. 49) are pyramidal in shape and occasionally reach the lumen. The cytoplasm contains few mitochondria, small Golgi apparatus and few scattered cisternae of endoplasmic reticulum. The secretory granules are scattered below and around the centrally placed nucleus.

6. Colon.

The fine structure of the normal colonic mucosa studied as control material is similar to that of previous reports (Pittman

and Pittman, 1966; Lorenzsonn and Trier, 1968; Jimenez, Ambrosius, Boom and Leuze, 1971). The columnar absorptive cells are connected by junctional complexes and desmosomes. Their luminal surface (Fig. 60) is covered by numerous microvilli, with a prominent fuzzy coat of rather fine filaments. Small spherical vesicles are present between the microvilli. These cells have numerous mitochondria, a supranuclear Golgi apparatus of moderate size and scattered cisternae of endoplasmic reticulum. There are membrane-limited vesicles in the apical cytoplasm. Their basal nuclei are oval in shape. The goblet cells (Figs. 60, 61) have dark nuclei which are pushed basally or laterally together with the cytoplasmic organelles by the accumulated mucus granules. Small membrane-limited dense bodies are present in moderate numbers in the cytoplasm of both absorptive and goblet cells (Fig. 62). The cells of the lower one third of the colonic crypt (Fig. 63, 64) have numerous mitochondria, scattered endoplasmic reticulum, numerous free ribosomes, a small Golgi apparatus, numerous membrane-limited apical vesicles and numerous lateral interdigitations. Their centrally placed nuclei are irregular and frequently segmented (Fig. 65).

CHAPTER FOUR

SQUAMOUS CELL CARCINOMA

OF OESOPHAGUS

INTRODUCTION

The histological classification of tumours relies substantially upon the tendency of the neoplastic cell to mimic the patterns of differentiation of its cell or tissue of origin. This principle applies equally in the ultrastructural field. Thus, for example. a typical malignant melanoma shares certain distinctive fine structural features with the normal melanoblast (Gyorkey, Min, Krisko and Gyorkey 1975). In ultrastructure as in histology, the difficulties of classification tend to increase with advancing anaplasia.

The published descriptions of squamous cell carcinoma in various sites (Greene, Brown and Kivertie, 1969; Lin, Lin, Yeh and Tu, 1969) bear out this principle. As might be expected, the more anaplastic the tumour, the less close is its correspondence to the conventional ultrastuructural pattern of squamous differentiation. Nevertheless, some subcellular clues to histogenesis may present in neoplastic cells which have regressed beyond the threshold of accurate histological classification. In such cases, fine structural examination may lead to a more accurate diagnosis than is possible with light microscopy. For this reason, the detailed analysis of the full range of ultrastructural variation of common tumours such as squamous carcinoma is of more than simply academic significance.

The present study is confined to the ultrastructural aspects of well differentiated squamous carcinoma in a site not hitherto studied in detail. the human oesophagus. It is attempted first to highlight the persisting similarities between the cancer cell and its normal counterpart as described in detail in Chapter 3. and then to point out its principal cytological aberrations.

OBSERVATIONS

The histological pattern of a typical case in this series is shown in Figure 69. All of the tumours examined in this study were of well-differentiated squamous type, with "cell nest" or "epithelial pearl" formation.

Throughout these tumours, there are many striking ultrastructural similarities between the neoplastic cells and their normal counterparts, as described above in Chapter 3. The majority of cells have a cytoplasmic matrix of moderate density corresponding to that of the basal cell of normal oesophageal epithelium (Fig. 70). The same basic cytoplasmic components are seen: these include ribosomes, granular endoplasmic reticulum, mitochondria and Golgi system. Some variations from normal patterns are seen, such as a general increase in the free ribosome population and a lesser degree of elaboration of the cytoplasmic membrane systems. Virtually all tumour cells contain the cytoplasmic tonofilaments which are typical of squamous cells both in oesophagus and elsewhere. As a general rule they are coarser and denser than those of normal cells. In some cells these tonofilaments are randomly distributed in course bundles, while others have fine bundles scattered mainly around the nucleus.

Perhaps the single most distinctive feature of squamous epithelium is the prominence of desmosomes, which link cell to cell. This feature is also typical of squamous carcinoma. The desmosomes are indistinguishable, in their essentials, from normal. They measure from 20 to 45 nm in thickness and from 200 to 350 nm in length. They are, however, rather less numerous and orderly in their arrangement than those of the normal epithelium.

Another typical feature of the normal oesophageal squamous epithelium is the presence of the so-called "membrane-coating" granules, which are released from the maturing squamous cell and are believed to contribute in some fundamental way to the physical properties of the epithelium. Similar granules are found in neoplastic squamous cells (Fig. 71). They are limited by a conventional trilaminar membrane and consist of a dense core surrounded by a pale halo. Their distribution in the tumour is irregular.

At low magnifications, the most striking aberrations of the neoplastic squamous cells are those of size and contour (Fig. 73). Small cells and large cells are readily identified, as in histology. Ultrastructural examination displays clearly the irregularity of cell outline which contrastswith the regularity of normal oesophageal epithelium. The extent of the intercellular space varies widely, from a minimal contact gap of 20 nm,to wide separations of 200 nm. Small and large cytoplasmic protrusions, not seen in normal epithelium, may intervene between cells widening the gap, while numerous tiny projections cover the tumour cell surface. Bulbous protrusions (Fig. 74) from tumour cells are rarely attached to their neighbours by desmosomes and in general are devoid of tonofilaments, despite their presence elsewhere in the cytoplasm.

The nuclear morphology of the tumour cells also varies from that of normal epithelium. Binucleate cells are common (Fig. 70), as are mitotic figures. The nuclei of tumour cells are generally larger than normal and may be lobulated and segmented, with multiple deep invaginations of the nuclear envelope, forming cytoplasmic channels whose apex may contact one of several prominent nucleoli (Fig. 75). When cut transversely, such channels may appear as islands of cytoplasm stranded within the centre of the nucleus (Fig. 76). Pale

euchromatin is more prominent, and dense heterochromatin less so than in normal cells. Occasional ring-shaped nucleoli are only seen in neoplastic cells (Fig. 93).

Curious inclusions, or "nuclear bodies" are consistently present in tumour cells but are only rarely seen in normal epithelium. These bodies measure 60 to 80 nm in diameter and consist of a variable central core surrounded by a microfibrillar cortex. These nuclear bodies are described in detail in Chapter 7.

A few cells in these tumours have either a strikingly pale or an unusually dense cytoplasmic matrix (Fig. 77). These "light" and "dark" cells (Lin, Lin, Yeh and Tu, 1969), are scattered singly between the main population. The high density of the dark cell is attributable in part to increased numbers of cytoplasmic tonofilaments. The light cells are relatively deficient in tonofilaments as well as showing a distinctive pallor of the cytoplasmic matrix. Their nuclei are also pale.

The maturing squamous cell of the superficial layers of the normal oesophageal mucosa displays a distinctive thickening of its cell membrane, due to increased density of the inner leaflet of its trilaminar structure. There is no corresponding specialisation of the neoplastic cell membrane.

A curious feature of the tumour cells in this study was the frequent occurrence of intracytoplasmic desmosomes (Figs. 78 79). This paradoxical structure has been recognised in various other situations and is occasionally seen in normal oesophagus. It consists of the characteristic laminated desmosome structure complete with attached cytoplasmic tonofilaments. Its membrane components however, are not in continuity with the surface membrane

of the cell or with any extensive intracytoplasmic membrane system, in as much as this can be determined by tilting the section to exclude continuity with an obliquely sectioned membrane surface (Figs. 82, 83, 84). Intracytoplasmic desmosomes are particularly common in mitotic figures, where conventional desmosomes are infrequent, and in the cells of the epithelial pearl, where the cytoplasm is packed with coarse bundles of tonofilaments.

The boundary between normal epithelium and underlying connective tissue in the oesophageal mucosa is marked by a continuous filamentous dense layer, the basal lamina. This closely follows the contours of the base of the epithelium. Hemidesmosomes are present at the cell surface which lies in contact with this basal lamina. In squamous carcinoma the groups of tumour cells are sometimes similarly demarcated from the surrounding stroma (Fig. 70): the basal lamina is continuous, although the hemidesmosomes are less conspicuous than in normal epithelium. Elsewhere, however, the basal lamina is virtually absent from tumour cells, or widely breached by pseudopodial cytoplasmic projections which extend from the malignant cells into the surrounding stroma (Fig. 80). Where the basal lamina is deficient, hemidesmosomes are also absent from the surface of the tumour cell.

The cells of the epithelial pearl have no counterpart in normal human oesophagus; they more closely resemble keratinising epithelial cells from the epidermis. Their nuclei are condensed and pyknotic (Fig. 81), finally disintegrating. Their cytoplasmic organelles are largely replaced by numerous randomly oriented tonofilaments, which may also appear within the nucleus (Figs. 81, 85). Dense cytoplasmic keratohyalin granules are seen sometimes in these

cells (Fig. 86) but in no others in the tumours examined. A distinctive variety of intracytoplasmic inclusion occurs in these cells. These structures (Figs. 87 88), conveniently termed "thick-walled vesicles" are round or oval in contour, at times with a focal invagination, their diameter being from 300 to 600 nm. They are apparently partitioned from the cytoplasm by an intact limiting envelope, consisting of two dense laminae, each about 8 nm in thickness, separated by a 5 nm interspace in which a 7 nm periodicity occurs. The material enclosed within these vesicles closely resembles the cytoplasmic matrix, but continuity with it is not observed.

There are occasional pleomorphic membrane-limited dense bodies in the cytoplasm of neoplastic cells (Fig. 93).

Finally, an occasional finding in cases of squamous carcinoma is the occurrence of Langerhans cells. These normal inhabitants of the human oesophageal mucosa are recognised by their distinctive cytoplasmic inclusions (Fig. 89).

CHAPTER FIVE

GASTRIC TUMOURS

INTRODUCTION

In recent years gastric carcinoma has been investigated by various workers, using the techniques of electron microscopy (Aiboshi, 1960; Izumi, 1962; Onoe, 1962; Goldman and Ming, 1968). Some quantitative differences have been described between cancer cells and their normal counterparts, such as the irregularities of the contours of neoplastic cells and their nuclei and the increased numbers of their microvilli. The ultrastructure of metastatic gastric carcinoma has, however, not yet been fully explored.

Two ultrastructural types of gastric cancer have been described by Sasano, Nakamura, Arai and Akazaki (1969). These are called the gastric and intestinal type, the distinction being made on the basis of the presence or absence of mucous secretion granules, goblet cells and brush border.

In the present investigation, an attempt was made to look at several aspects of the ultrastructure of gastric cancer: firstly to compare gastric cancer cells with the normal cell populations of the human stomach; secondly to explore the concept of the two ultrastructural types of gastric carcinoma; and thirdly to examine some examples of metastatic gastric tumours.

OBSERVATIONS

1. Well Differentiated Gastric Adenocarcinoma

The criteria of Sasano et al (1969) were used in the assessment of these cases. The two types of gastric carcinoma recognized by these workers were distinguished on the basis of the presence or absence of mucous secretion granules, similar to those of gastric mucous cells, of goblet cells and of a well-developed brush border. In the present study, the occurrence was confirmed of two ultrastructural types of

gastric adenocarcinoma, each with its characteristic features; those of gastric cell type which contained mucous secretion granules identical to those of gastric mucous cells, and those of intestinal cell type which did not contain mucous granules but had long microvilli and were interspersed with goblet cells. These two types of gastric carcinoma correspond to those of Sasano et al (1969). The present study revealed additional fine structural details, not previously described, which were found to assist in distinguishing these two patterns.

a) Gastric type The histology of a typical case of this type of gastric carcinoma is shown in Figure 95.

The columnar neoplastic cells (Fig. 96) are arranged in an acinar pattern. They are closely packed and connected by conventional junctional complexes and desmosomes, with few lateral interdigitations. Their luminal surface bears few short and irregular microvilli with the fuzzy coat of short filaments similar to those of gastric mucous cells. The neoplastic cells rest on a continuous fibrillar lamina densa. The cytoplasmic matrix is of moderate density comparable to that of gastric mucous cells.

The most distinctive feature of the neoplastic cells of this type of gastric carcinoma is the presence of an aggregate of granules in the apical cytoplasm. The fine structure of these granules (Figs. 97, 98) is identical to that of the mucous secretion granules of gastric mucous cells (Figs. 44, 45). They are oval or round in shape and have a closely applied limiting membrane and a homogenous or mottled appearance. The amount of these granules is variable from case to case and even from cell to cell within one case. The neoplastic cells have a supranuclear Golgi apparatus of moderate size, a few scattered cisternae of granular endoplasmic reticulum, numerous ribosomes and moderate numbers of mitochondria.

In this type of gastric carcinoma, various structural aberrations of some cytoplasmic organelles were noted, particularly the mitochondria, endoplasmic reticulum and membranous structures. Some mitochondria were seen to display tubular or vesicular cristae with an electron lucent intramitochondrial matrix (Fig. 99). Others had concentric cristae (Fig. 101) or contained rod-shaped inclusions (Fig. 100), 10 to 15 nm. in diameter. These intramitochondrial inclusions displayed internal periodicity. Crystalline inclusions in dilated cisternae of the granular endoplasmic reticulum are seen in this type of gastric carcinoma (Fig. 102). These intracisternal inclusions, which occur in some cells of every case examined, are composed of long parallel and curved rod-shaped structures of about 10 to 17 nm. in diameter. Concentric membranous structures (Fig. 103) were also seen. These inclusions, which sometimes contained moderately dense material, showed no consistent structural relationship to any other cytoplasmic organelle. The membranes surrounding these inclusions are trilaminar structures, thicker than those of the mitochondria and endoplasmic reticulum.

b) Intestinal type The histological pattern of a typical case of this type of gastric carcinoma is shown in Figure 104.

The striking feature of the neoplastic cells of this type of gastric carcinoma is their dissimilarity to the gastric mucous cells. Not only was there an absence of mucous granules, but in addition these cells possessed numerous long microvilli which resembled those of intestinal cells.

The neoplastic cells are tall and columnar in type, arranged in an acinar pattern around spaces of variable size (Fig. 105). Their apex bears more numerous and taller microvilli (Fig. 106) than those of normal gastric epithelium and gastric type adenocarcinoma. Each microvillus has a long microfilamentous core inserted into the apical

cytoplasm (Fig. 108). Small spherical vesicles are sometimes seen between the microvilli. Similar vesicles were not seen in normal gastric cells or in the gastric type of carcinoma. The fuzzy coat is prominent and is composed of rather fine filaments. The neoplastic cells rest on a continuous fibrillar lamina densa similar to that of normal gastric epithelium. The cells are connected by typical junctional complexes and desmosomes and have numerous lateral interdigitations, particularly at their basal parts (Fig. 107).

The cytoplasm is of moderate density and contains no mucous secretion granules. There is, however, a well developed supranuclear Golgi apparatus, with scattered cisternae of granular endoplasmic reticulum, moderate numbers of ribosomes and oval or round mitochondria (Fig. 109), features more or less similar to those of tumours of gastric cell type. There are some apparently empty membrane-limited vesicles in the supranuclear and apical cytoplasm. Similar vesicles are also sometimes seen to contain dense material, particularly when they lie in the supranuclear region (Fig. 114). Such vesicles are absent from gastric carcinoma of gastric cell type.

Goblet cells are occasionally seen in this type of gastric carcinoma, but not in normal gastric mucosa or in gastric type carcinoma. These goblet cells have dark nuclei which are pushed basally, together with the cytoplasmic organelles, by their accumulated mucous granules (Fig. 110). They are interposed between the less differentiated cancer cells and they have few short irregular microvilli.

The nuclei of both types of gastric carcinoma are larger and more irregular than those of normal gastric epithelium. They are basally or centrally situated and contain prominent nucleoli. Deep invaginations of the nuclear envelope may form channels of cytoplasm

leading to the nucleoli (Figs. 111, 112, 113). Nuclear bodies and coiled inclusions are also found in the nuclei of both types of gastric carcinoma. These features are described in greater detail in Chapter 7.

In the cytoplasm of both types of gastric carcinoma there are moderate numbers of membrane-limited homogenous and pleomorphic dense bodies (Figs. 115, 116).

2. Poorly Differentiated Gastric Carcinoma

There are two types of poorly differentiated gastric carcinoma, distinguished by the presence or absence of mucous secretion granules identical to those of gastric mucous cells, and by their tendency towards acinar formation. These two types of tumour are similar in most other cytoplasmic and nuclear features.

Those cases of poorly differentiated carcinoma which contained mucous granules also showed occasional acinus-like spaces (Fig. 117). The neoplastic cells arranged around these spaces have cytoplasmic projections extending into the lumen. These projections lack the microfilamentous core of microvilli, and have no obvious fuzzy coat. The mucous secretion granules are identical to those of gastric mucous cells. They have a closely applied limiting membrane and a mottled or stippled appearance. There are eccentrically placed dark areas in some of these granules (Fig. 119). The granules are distributed throughout the cytoplasm with frequent aggregations in the apical cytoplasm.

The other type of poorly differentiated carcinoma did not contain mucous secretion granules and showed no tendency to form acinus-like spaces.

The cells of both types rest on a continuous basal lamina (Fig. 118), and are connected by desmosomes which appear to be less

prominent and orderly than those of well differentiated gastric carcinoma. The cytoplasm of both types contains a moderately well developed Golgi apparatus, small to moderate numbers of mitochondria, scattered cisternae of granular endoplasmic reticulum and numerous ribosomes (Fig. 120). Their nuclei are large and irregular, and contain prominent nucleoli and nuclear bodies. Intranuclear coiled inclusions similar to those of well differentiated gastric carcinoma, although present in every case, are encountered only rarely and demand careful search of many sections. These features are described in detail in Chapter 7.

3. Gastric Lymphoma

A single case of gastric lymphoma was examined, to serve as comparison with the cases of carcinoma described above.

The compact cells of gastric lymphoma (Fig. 121) are more closely packed than those of poorly differentiated gastric carcinoma. There are no distinct intercellular spaces such as those which separate the cells of carcinoma, and the neoplastic lymphoid cells lack the distinctive epithelial adhesion specialisations seen in the epithelial neoplasms of the stomach (Fig. 122).

The cytoplasm of the neoplastic cells contains scantier organelles than in cases of gastric carcinoma. There are few mitochondria, no organised granular endoplasmic reticulum and only an occasional diminutive Golgi system. Variable amounts of free ribosomes, occasional membrane-limited vesicles and membrane-limited dense bodies are encountered. Occasional cells with strikingly pale cytoplasm and very scanty organelles (Fig. 122) are seen.

The nuclei are large, irregular and may be segmented or binucleated. The nucleoli are prominent. The nuclei of lymphoma are generally darker than those of carcinoma, with a chromatin pattern

reminiscent of mature lymphocytes.

4. Metastatic Gastric Tumours

All metastatic gastric tumours examined in this study were obtained from omental deposits or mesenteric lymph node deposits of gastric carcinoma, the primary site being confirmed at laparotomy.

a) Well differentiated metastatic gastric adenocarcinoma The histology of a typical case of this series is shown in Figure 130.

In all cases of metastatic gastric adenocarcinoma examined in the present study, the neoplastic cells had features reminiscent of gastric mucous cells. The low columnar cells are arranged around wide lumina and have few irregular apical microvilli (Fig. 133). Each microvillus has a microfilamentous core which does not extend into the apical cytoplasm. The fuzzy coat consists of rather fine filaments. The cells are separated from the underlying stroma by a continuous basal lamina. They are connected by junctional complexes and desmosomes and frequently interdigitate at their basal parts. The cytoplasm is of moderate density and contains an apical aggregate of granules (Figs. 131, 132) identical to those of gastric mucous cells (Figs. 44, 45, 50). The individual granules are enclosed by a closely applied limiting membrane, and have a dense homogenous, stippled or mottled appearance. There are eccentrically placed dense areas in some of these granules (Fig. 131) similar to those of gastric mucous neck cells (Fig. 50). The number of granules present in the tumour cells is variable. The cytoplasm contains a Golgi apparatus of moderate size, scattered cisternae of granular endoplasmic reticulum, numerous ribosomes and moderate numbers of mitochondria. Frequently seen in the cytoplasm are apparently empty spaces which are not limited by a membrane.

Various atypical cytoplasmic organelles were seen. Aberrations occurred particularly in the mitochondria, endoplasmic reticulum and membranous structures. Some mitochondria were found to display tubular or vesicular cristae with an electron lucent intramitochondrial matrix (Figs. 136, 137). Others were ring-shaped (Figs. 138, 139), displayed concentric cristae (Figs. 140, 141), or contained a central inclusion of material which resembled the surrounding cytoplasmic matrix (Figs. 142, 143). This appearance could perhaps be explained on the basis of an invaginated "cup-shaped" mitochondrion, such as that shown in Figure 144.

Some dilated cisternae of granular endoplasmic reticulum are sometimes seen to contain arrays of tubular inclusions (Figs. 145, 146). These tubular structures are convoluted and smooth surfaced. Curious arrays of granular endoplasmic reticulum are sometimes seen to be continuous with aggregates of smooth endoplasmic reticulum (Fig. 148). Distinctive membranous structures are sometimes present in the cytoplasm of metastatic gastric adenocarcinoma (Fig. 147). These consist of a network of convoluted smooth-surfaced membranes, with intervening dense material. There is no apparent structural relationship between these inclusions and any other cytoplasmic organelle.

The large basally situated nuclei are irregular in outline and round in shape. Their prominent nucleoli may show structural aberrations. Ring-shaped nucleoli, some with a nucleolar cap, are seen (Figs. 134, 135). Nuclear bodies with a dense central core and microfibrillar cortex (Fig. 133) are also seen, as detailed in Chapter 7.

b) Poorly differentiated metastatic gastric carcinoma The histology of a typical case of poorly differentiated metastatic gastric carcinoma is shown in Figure 152.

Ultrastructurally, there are small and large cells with pale cytoplasmic matrix and irregular contours (Fig. 153). These cells are closely packed with no distinct intercellular spaces or lateral interdigitations.

The solid masses of neoplastic cells are separated by a fibrillar lamina densa from the surrounding stroma (Fig. 155). True acinar spaces are not seen but typical microvilli are sometimes encountered at the surface of groups of cells (Fig. 154). These microvilli are simple cytoplasmic extensions with rounded tips, covered by the cell membrane and containing a fine filamentous core, but with no obvious fuzzy coat. Perhaps the most distinctive remaining feature of these epithelial tumours is the occurrence of typical desmosomes which connect the adjacent neoplastic cells (Fig. 157). However, these desmosomes are less prominent and less frequent and orderly in their arrangement than those of well differentiated tumours.

The pale cytoplasm of the neoplastic cells contains moderate numbers of vacuolated mitochondria, scattered cisternae of granular endoplasmic reticulum, numerous ribosomes, membrane-limited dense bodies and an occasional very small Golgi zone. There are no secretory granules of mucous neck cell pattern. The nuclei are pale, large and irregular. Their prominent nucleoli are frequently peripherally located.

Occasional dark cells, with numerous vacuolated mitochondria, are seen between the pale cells. Their cytoplasm also contains numerous ribosomes and scattered cisternae of endoplasmic reticulum.

They rest on a continuous basal lamina and may have vestigial short microvilli (Fig. 156). Their nuclei are dark and irregular.

c) Signet ring cell metastatic gastric carcinoma The histology of a typical case of signet ring cell metastatic gastric carcinoma is shown in Figure 159.

In low magnification electron micrographs the cells are dark, irregular, and surrounded by electron-lucent material identical to that of their secretion granules (Fig. 161). The signet ring cells are frequently found in lymphatic vessels (Fig. 160).

The irregular surface of the cell is covered by numerous finger-like cytoplasmic projections, extending into wide intercellular spaces. There are desmosomes connecting adjacent neoplastic cells. The distribution of these desmosomes is quite irregular. They are rarely seen between those neoplastic cells which are seen to lie within a lymphatic vessel.

The signet ring cells frequently rest on dense fibrillar lamina densa (Fig. 162), but are not arranged in an acinar pattern.

The dense cytoplasm contains numerous mitochondria and ribosomes, a well developed Golgi apparatus and moderate numbers of cisternae of granular endoplasmic reticulum. There are also numerous secretion granules. They measure up to 2.5 μm. in diameter, and in many instances appear not to be limited by a membrane, perhaps partly as a result of plane of section effect. They are electron-lucent or pale in appearance, and may be scattered throughout the cytoplasm. More typically, they are aggregated in one area, pushing the nucleus to the side.

There are certain cytoplasmic inclusions seen only in signet ring cells and not in other gastric neoplasms. These include intracytoplasmic "acinus-like" structures and tubulovesicular inclusions.

Intracytoplasmic desmosomes are frequently seen (Fig. 163). They consist of two dark plates with a central lamination. These intracytoplasmic desmosomes may display "tennis racket" profiles due to their connection with a rounded expansion of 60 to 80 nm. in diameter. These expansions consist of cytoplasmic vesicles limited by a trilaminar membrane (Fig. 164).

The intracytoplasmic "acinus-like" structure, which may be single or multiple, is a saccular inclusion entirely surrounded by cytoplasm and lined by short irregular microvilli (Figs. 165, 166). The microvilli (Fig. 167) have a microfibrillar core which extends into the cytoplasm of the tumour cell. These inclusions, in other words, are intracellular microcysts. They are lined by a trilaminar membrane and are not connected to the cell surface.

The tubulovesicular inclusions (Fig. 168) are apparently empty spaces of about 60 to 350 nm. in diameter, often with a concentric central inclusion of material resembling the surrounding cytoplasmic matrix. In some instances this appearance of a concentric inclusion can be seen to have arisen through a process of invagination of a cytoplasmic process into the otherwise empty vesicle. The membrane limiting these structures is similar to that of the cell surface. These tubulovesicular structures are to some degree reminiscent of similar features seen in normal gastric parietal cells (Fig. 48).

Signet ring cell nuclei are large, dark and irregular. They are frequently seen to be compressed by surrounding mucous secretion granules, which may also appear within the nuclear material. Intranuclear inclusions of various types are sometimes seen. These may contain tubular structures of about 20 to 45 nm. in diameter (Fig. 169), resembling the lamellae of Golgi system. Also frequently seen in the nuclei of signet ring cells, are small dark inclusions

(Fig. 170) of about 40 to 60 nm. in diameter surrounded by a pale halo. They are dispersed individually in the nucleus or may form aggregates.

d) Metastatic gastric lymphoma In the one case examined, the pale irregular cells are closely packed without distinct intercellular spaces (Fig. 158). The neoplastic cells do not rest on a basal lamina and are not connected by the epithelial adhesion specialisations of poorly differentiated metastatic gastric carcinoma as described above. The microvilli seen in the typical carcinoma are also absent. The pale cytoplasm of lymphoma cells contains few mitochondria, numerous free ribosomes, a small Golgi zone and very few scattered cisternae of endoplasmic reticulum. The appearances are identical in all important respects with the primary tumour described above. Occasional dark cells, having vacuolated cytoplasm and shrunken dark nuclei, are seen. These are thought to be degenerate tumour cells.

CHAPTER SIX

COLONIC TUMOURS

INTRODUCTION

Villous papillomas of colon have already been the subject of substantial numbers of histochemical (Szernoblisky and Tsou, 1968; Lipkin, 1971; Makal, Korhonen and Lilius, 1971) and fine structural studies (Fisher and Sharkey, 1962; Imai, Saito and Stein, 1965; Spjut and Smith, 1967; Ioachim, Delaney and Madrazo, 1974). This is no doubt due to their frequency of occurrence, their malignant potential (Enterline, Evans, Mercado-Lugo, Miller and Fitts, 1962; Morson, 1968) and their interesting association with severe electrolyte and fluid loss (Davies, Seavey and Sessions, 1961; Wells, Moron and Cooper, 1962).

Colonic carcinoma has also been intensively investigated (Birbeck and Dukes, 1963; Imai and Stein, 1963; Spjut and Smith, 1967; Cardoso, Diener, Alvorez, Elizabeth and Maldonado, 1971; Jenkinson and Dawson, 1971). These previous fine structural studies have been confined to the well differentiated types of colonic carcinoma leaving the more poorly differentiated varieties to be examined in detail. The present investigation set out to complete this work: to make direct ultrastructural comparisons between villous papilloma and colonic carcinoma; to compare the features of colonic carcinoma in its primary and its metastatic sites; and finally to explore certain ultracytochemical properties of colonic tumours.

OBSERVATIONS

1. Villous Papilloma

The ten villous papillomas examined here were located in rectum and sigmoid colon. They had the typical histological features of finger-like projections consisting of a fibro-vascular core covered by crowded tall columnar cells (Figs. 171, 172).

The tall slender columnar cells of villous papilloma (Figs. 173, 174) rest on a fibrillar dense lamina densa 30 to 50 nm. in thickness which separates the base of the cells from the underlying stroma. The microvilli which cover the luminal surface are in general shorter, fewer and less regular then those of normal colonic cells. Occasionally, the microvilli may be either more plentiful or almost entirely absent. At the free surface, between the microvilli of the cells of villous papilloma, there are numerous small round vesicles, similar to those seen in the same situation in normal colonic cells. In conventional electron micrographs, the cells of villous papilloma appear to lack the well marked glycocalyx or fuzzy coat of the normal colonic mucosal cells. In thin sections stained with the periodic acid thiocarbohydrazide silver proteinate procedure to demonstrate cell coat mucopoly-saccharides, an electron dense reaction product is seen at the surface of the apical cell membrane (Figs. 177, 178) but not at the lateral or basal surfaces.

The cells have moderate numbers of ribosomes, lying free in the cytoplasm or attached to the scattered cisternae of the endoplasmic reticulum (Fig. 175). There is a well developed supranuclear Golgi apparatus. The mitochondria are numerous, measuring up to 1.5 μm. in diameter. They have shelf-like cristae with a prominent intramitochondrial matrix (Fig. 176). They are dispersed throughout the cytoplasm, but basal aggregates of mitochondria are also seen. In the apical and supranuclear cytoplasm, apparently empty membrane-limited vesicles of about 20 to 30 nm. in diameter are present. In thin sections stained with the silver proteinate procedure, a thin layer of electron dense reaction product is seen just inside the limiting membrane, while the rest of the content of the vesicle remains

unstained (Figs. 177, 178). Apical concentrations of mucous granules are frequently seen, and may project above the luminal surface of the adjacent cells.

The nuclei are slightly irregular, centrally located and larger than those of normal cells. They are round or oval in shape and may display shallow or deep indentations, with prominent compact nucleoli (Fig. 179). Nuclear bodies, about 60 to 80 nm. in diameter are encountered (Chapter 7).

The intercellular spaces are of normal dimensions, and the lateral surfaces of the cells are irregular and frequently interdigitate. In this respect they resemble the cells of the lower one third of the colonic crypt. The cells are connected by conventional junctional complexes with occasional exaggeration of the desmosomal component.

At the basal parts of the cells of villous papilloma there are sometimes round or oval intracellular inclusions which measure up to 6.5 µm. in length (Fig. 180). They have a peripheral rim of electron dense material and are limited by single membrane. The material of the inclusions consists of fine fibrillar and granular components.

A distinctive feature of villous papilloma is the occurrence of aggregates of cells with dark basal cytoplasm, almost entirely packed with round or oval mitochondria (Figs. 181, 182, 183). There are also numerous apparently empty intracellular vacuoles, measuring up to 900 nm. in diameter. These vacuoles are scattered between the mitochondria. The dark cells form extensive lateral interdigitations with adjacent cells. These complex interdigitations are produced by the interlocking of matching projections and invaginations of cytoplasm. The density of the dark cells is attributable partly to the increased numbers of mitochondria which seem to compress the cytoplasmic matrix. Their dark irregular nuclei are centrally located. In other respects,

such as the appearance of the cell apex, the dark cells are not dissimilar to the principal cells of villous papilloma as described above.

Mature goblet and absorptive cells are only very rarely encountered. Paneth or endocrine cells were not seen.

2. Well Differentiated Colonic Carcinoma

All cases of primary well differentiated carcinoma of large intestine examined in this series showed a well formed glandular pattern (Fig. 184).

The neoplastic cells, arranged in acinar patterns, are columnar and sometimes heap on each other with pseudostratification (Fig. 189). As in villous papilloma, the microvilli of cancer cells are irregular and fewer (Fig. 186) than those of normal colonic cells, but they are similar in fine structure. The long filamentous core extends from the tip to the apical cytoplasm. As in normal colonic mucosa and villous papilloma, there are small round vesicles, up to 90 nm. in diameter, lying between the microvilli of cancer cells (Fig. 187). They form rows, parallel and close beside the microvilli. The fine fibrillar fuzzy coat is less prominent than that of normal colonic cells but is similar to that of villous papilloma. In the lumen of acini, distal to the microvilli, electron dense material with various irregular vacuoles and inclusions may be seen (Fig. 186). This material most probably represents a mixture of secretory product and cell debris.

The lateral surfaces of cancer cells appear to have fewer interdigitations (Fig. 188) than are seen in villous papilloma and normal colonic mucosa. The adjacent lateral surfaces of the cells are connected by junctional complexes and desmosomes, more or less similar to those of normal colonic mucosa.

The basement membrane is a continuous fibrillar dense interface which separates cancer cells from the underlying stroma (Fig. 189). Occasionally, the continuity of the basement membrane is breached by cytoplasmic projections from cancer cells (Fig. 191).

Cancer cells in general have less organised cytoplasmic organelles than those of villous papilloma and normal colonic mucosa (Fig. 190). The variable numbers of small oval or round mitochondria are dispersed throughout the cytoplasm and have no particularly distinctive features. The moderate numbers of ribosomes lie free in the cytoplasm or are attached to the sparse cisternae of granular endoplasmic reticulum. The small Golgi apparatus consists of the usual lamellae and vesicles (Fig. 188). There are moderate numbers of small homogenous or pleomorphic membrane-limited dense inclusions (Figs. 188, 199). Apparently empty membrane-limited vesicles are present in the apical cytoplasm (Fig. 194).

There are two distinctive cytoplasmic inclusions in cancer cells which have no counterparts in villous papilloma. These are rounded doughnut-like inclusions and a curious hexagonal network of tubular structures. The rounded inclusions (Figs. 193, 194) are present in the apical cytoplasm of cancer cells and are composed of dense central material surrounded by less dense zone and limited by a membrane. The network of tubules showing hexagonal stacking appears to be in continuity with the cisternae of granular endoplasmic reticulum, with similar contents but a smooth surface. Each tubule of the network has a diameter of about 40 to 55nm. This seems to represent a specialisation of the endoplasmic reticulum (Figs. 195, 196).

The nuclei of cancer cells are larger and more irregular than those of villous papilloma and normal colonic mucosa, and are sometimes segmented (Fig. 190), with deep invaginations of the nuclear envelope

which may form channels of cytoplasm leading to prominent nucleoli (Figs. 197, 198). The nucleoli themselves are compact and peripherally located. They sometimes adopt bizarre shapes, such as a cribriform configuration with fibrillar material within the holes (Fig. 192).

Nuclear bodies, which are rarely found in normal colonic cells, are frequently encountered in colonic carcinoma and in villous papilloma. They are described in detail in Chapter 7 along with other cytoplasmic and nuclear inclusions found in tumour cells, including microfibrillar and lattice structures and paired profiles. Apart from the nuclear body, such inclusions are not found in normal colonic mucosa or in villous papilloma, and their occurrence in human tissue is a rare phenomenon.

3. Poorly Differentiated Colonic Carcinoma

The histology of a typical case of poorly differentiated colonic carcinoma is shown in Figure 201A.

The cells of poorly differentiated colonic carcinoma are of widely varying size, and are closely packed (Fig. 200). Two populations are encountered, those with dark and those with pale cytoplasm. The predominant pale cells have scanty organelles, consisting of a few small mitochondria, a small Golgi apparatus, moderate numbers of ribosomes and occasional cisternae of endoplasmic reticulum. Their nuclei are also pale and contain more euchromatin than heterochromatin. The nuclei sometimes appear to be segmented, with connecting nuclear bands.

The few dark cells are interposed between light cells. The density of their cytoplasmic matrix is attributable to their more plentiful organelles, including numerous mitochondria and ribosomes. They have dark nuclei.

Groups of cells are seen to rest on a continuous basement membrane

(Fig. 202), forming a central luminal space (Fig. 201). In such a case, the luminal surface bears only occasional short microvilli with no obvious fuzzy coat. In the apical cytoplasm there are some apparently empty membrane-limited vesicles.

In all cases of poorly differentiated carcinoma of colon, desmosomes are seen to connect cancer cells. These adhesion specialisations are fewer than in cases of well differentiated carcinoma.

4. Metastatic Colonic Carcinoma

All speciments examined consisted of well differentiated adenocarcinomatous deposits in mesenteric lymph nodes taken from cases of known primary colonic carcinoma (Fig. 185).

The cells are of low columnar pattern, arranged around wide lumina (Fig. 203). Their luminal surface bears shorter, broader and more irregular microvilli (Fig. 204) than those of primary colonic carcinoma, although they are similar in frequency. The microfilamentous core of the microvillus is less prominent than in primary colonic carcinoma and does not extend to the apical cytoplasm. Numerous small round vesicles similar to those of normal colonic mucosa are present between the microvilli and in lumina of the glands. These vesicles measure up to 90 nm. in diameter and frequently aggregate (Fig. 204). The inconspicuous fine fibrillar fuzzy coat is similar to that of primary colonic carcinoma. Electron dense material is frequently seen in the lumina of the glands (Fig. 207). This material most probably represents a mixture of secretory product and cell debris.

The cells are connected by junctional complexes and desmosomes, and have lateral interdigitations similar to those of primary colonic carcinoma. The neoplastic cells rest on a continuous basement membrane (Fig. 205) which separates them from the underlying stroma.

The cytoplasmic matrix is of moderate density. In the apical cytoplasm, there are apparently empty membrane-limited vesicles up to 250 nm. in diameter which occasionally contain small dense inclusions. The oval or elongated mitochondria are dispersed throughout the cytoplasm or at times aggregated at the apical (Fig. 204) or basal regions (Fig. 205). A small supranuclear Golgi apparatus, numerous ribosomes, scattered cisternae of granular endoplasmic reticulum and moderate numbers of dense and pleomorphic membrane-limited structures are the other principal organelles.

The nuclei are large irregular and basally placed. They contain prominent nucleoli which are sometimes located close to deeply invaginating channels of cytoplasm (Fig. 206) similar to those seen in primary colonic carcinoma.

CHAPTER SEVEN

NUCLEAR AND CYTOPLASMIC INCLUSIONS

INTRODUCTION

Previous electron microscopic studies of the human alimentary canal in health and disease have dwelt mainly on the conventional organelles. In particular, no mention has been made of nuclear and cytoplasmic inclusions such as have been described in various other situations, both normal and pathological (Patrizi and Middlekamp, 1969; Robertson 1964; Aristila and Hopsu-Haru, 1967; Bouteille, Kalifat and Delarue, 1967; Buttner and Horstmann, 1967; Masurousky, Benitz and Murray, 1970; Straile, Tipnis, Mann and Clark, 1975). During the present study of normal and neoplastic cells of the alimentary canal, a wide range of inclusions was encountered, some confined to the nucleus, others found also in the cytoplasm. The distribution and diversity of these structures has been catalogued and their possible significance is discussed.

OBSERVATIONS

1. Nuclear Bodies

These are round or oval intranuclear inclusions which are not separated from the surrounding chromatin by any limiting membrane. They measure up to 600 nm in diameter, when found in normal tissues (Figs. 218, 219, 220). They usually occur singly, and apparently bear no consistent relationship to the nucleolus. In occasional sections two nuclear bodies may occur in a single nucleus. The involved nuclei are of normal appearance in other respects, with no unusual irregularity or invagination. Inclusions such as these are seen in both epithelial cells and others, including fibroblasts, smooth muscle cells, lymphocytes and plasma cells.

Nuclear bodies are particularly abundant in the nuclei of cancer cells, where they may bear a relationship to the nucleolus (Figs. 221,222).

As in normal cells, they are round or oval, with a variable central core and a microfibrillar cortex. They measure from 400 to 1800 nm in diameter. In most instances they are separated from the surrounding chromatin by a clear halo. A single nucleus may contain more than one such inclusion: when multiple, they may lie in close proximity to one another (Figs. 221 223, 224). In purely descriptive terms, it is possible to subdivide these inclusions into three groups which may correspond to some extent with classifications proposed by other authors (Bouteille et al 1967; Popoff and Stewart, 1968). The first group consists of simple aggregates of microfibrillar material (Figs. 227,228). The second group displays a vacuolated central core with a surrounding microfibrillar cortex (Figs. 229,230). The third group shows a dense homogeneous or granular core, contained again within a microfibrillar cortex (Figs. 225 226).

A more elaborate classification of these structures has not been attempted for the following reason. On examination of different planes of section, as shown by semi-serial sectioning, it appears that the central core of a single nuclear body may show quite different morphological features at different levels (Figs. 231, 232, 233). Sequences of micrographs may be taken from a single nuclear body to demonstrate all of the appearances described above (Figs. 234, 235, 236). Tangential sectioning of the outer microfibrillar cortex would give the impression of the simplest form of inclusion, described above as the first group, while different planes of section through the core could account for the other variants. While this observation cannot be taken to exclude the possible existence of a variety of types of nuclear body, it must to some extent call into question the validity of the more elaborate forms of classification.

2. Paired profiles, Fibrillar and Lattice inclusions

The inclusions described under this heading have been encountered

in primary and secondary rectal carcinoma, but not in normal rectal mucosa nor in the other tumours of the alimentary tract included in this study. Their distribution was found to be irregular and they were only identifiable at relatively high microscopic magnifications. In any given tumour, these inclusions tended to occur more frequently in some areas than in others. The paired profiles, found in both nucleus and cytoplasm, consist of straight or slightly curved parallel aggregates of rather ill-defined linear pairs, often suggesting the parallel walls of longitudinally sectioned microtubules (Figs. 237, 238, 239). The separation of each pair is around 10 - 15 nm, the overall dimensions of the aggregate being up to 750 nm in length and 150 nm in breadth. Against a tubular identity is the apparent absence of any circular profiles, which might correspond to transversely sectioned elements. Instead, however, intermittent linear grouping of dense spots 4 to 7 nm in diameter, might represent transversely sectioned fibrils alternating with those components seen in longitudinal section. The oblong or oval fibrillar inclusions are also found in both nucleus and cytoplasm, although again without evidence of continuity. In the nucleus (Figs. 240, 241) they occupy an area apparently free of chromatin granules, without any consistent association with the nucleolus. Intracytoplasmic aggregates (Fig. 242) are often more orderly in their arrangement. Such aggregates are quite common in mitotic figures (Fig. 243). They consist of roughly parallell, straight or slightly undulating microfibrils, each unit measure 3 to 6 nm in diameter. The oblong or oval lattice structures are only seen in nuclei (Figs. 244, 245). They consist of paracrystalline material showing parallel periodicity in two directions.

3. Intranuclear Coiled Inclusions

These round or oval structures (Figs. 246, 247) were encountered in all cases of gastric carcinoma studied, but in no other alimentary tract tumour in this series. They bear no consistent relationship to any particular part of the nucleus. They consist of numerous dense coiled threads, each measuring 20 to 30 nm in diameter. An appearance of beading is suggested when the threads lie vertical to the plane of section

CHAPTER EIGHT

ULTRACYTOCHEMISTRY

INTRODUCTION

The present study set out with the limited objective of exploring the application of two ultracytochemical procedures, in both normal and neoplastic tissues. The periodic acid thiocarbohydrazide silver proteinate procedure was used to demonstrate carbohydrates, while a modified Gomori's method was used to demonstrate acid phosphatase activity. The reaction product of both procedures was subjected to X-ray microanalysis to confirm its identity.

OBSERVATIONS

1. Periodic acid thiocarbohydrazide silver proteinate.

The reaction product took the form of a granular electron dense deposit. All control sections examined showed a complete absence of reaction product.

a. Normal Squamous Epithelium of Oesophagus. The finely granular reaction product is located in the intercellular spaces and on the outer leaflet of the cell membrane in the superficial part of the mucosa (Figs. 13, 14). No deposit is seen on the desmosomes. Inside the cells, the reaction product is seen only in the membrane-coating granules (Fig. 13) and the cytoplasmic vacuoles of the superficial layers (Figs. 15, 16).

b. Normal Gastric Mucosa. A fine granular silver deposit is found in the lumen, on the fuzzy coat and in the secretion granules of mucous cells (Figs. 51, 52). A deposit-free zone exists between the apical surface of gastric mucous cells and the reaction product in the lumen. Unstained areas are also seen in some mucous granules.

c. Normal Colonic Mucosa. A fine granular dense reaction product is seen on the fuzzy coat, apical cell membrane and membrane-limited vesicles of colonic cells (Fig. 209).

d. Squamous Cell Carcinoma of Oesophagus. The reaction product is confined to the membrane-coating granules (Fig. 72). No reaction product is seen in the intercellular spaces or on the cell membrane, in contrast with the normal oesophageal squamous epithelium.

e. Gastric Carcinoma. A fine granular deposit is seen on the fuzzy coat, in the gland lumen and in the mucous secretion granules of the gastric cell type of adenocarcinoma (Figs. 123, 124). Unstained areas similar to those seen in gastric mucous cells were found in the mucous granules of the tumours. A striking fine granular deposit is seen on the fuzzy coat, the apical cell membrane and the membrane-limited vesicles in the apical and supranuclear parts of the cells of the intestinal type of gastric carcinoma (Figs. 125, 126). The distribution of the reaction product is similar in both primary and secondary carcinoma (Figs. 149, 150). The apparently empty intracytoplasmic vacuoles seen in metastatic gastric carcinoma (Fig. 133) also showed a granular stain deposit (Fig. 151).

f. Colonic Neoplasms. The reaction product is found on the apical surface of the cells of villous papilloma (Figs. 177, 178). Positive staining is also found just inside the limiting membrane of the vesicles which are present in the apical cytoplasm. In primary colonic carcinoma, a fine granular deposit is seen on the fuzzy coat and the apical cell membrane (Fig. 210). The apparently empty membrane-limited vesicles and the rounded doughnut-like structures (Figs. 193, 194) also showed a positive reaction (Figs. 211, 212, 213). A heavy deposit is found in the gland lumen, fuzzy coat and membrane-limited vesicles of metastatic colonic carcinoma (Fig. 208).

2. Acid phosphatase.

The lead phosphate deposit appears as a coarse granular or homogeneous electron dense material in all specimens of normal and neoplastic tissues studied. No reaction product is found in control sections.

a. Normal Squamous Epithelium of Oesophagus. Lead phosphate deposits appear as coarse granular dense material in the intercellular spaces and on the cell membrane (Figs. 17, 18). The deposit on the cell surface is found on short and discrete lengths of the cell membrane. No reaction product occurs in the membrane-coating granules or any other cytoplasmic structure.

b. Normal Gastric Mucosa. Dense deposits are seen in all of the small round homogeneous or pleomorphic membrane-limited dense bodies of gastric mucous, chief and parietal cells (Figs. 56, 57, 58, 59). The myelin figures which are frequently seen in parietal cells (Fig. 53) show only a peripheral deposit of reaction product (Figs. 55, 59). Similarly, some areas in the pleomorphic bodies give a negative reaction (Fig. 58).

c. Normal Colonic Mucosa. In both absorptive and goblet cells, acid phosphatase activity is confined to small membrane-limited dense bodies (Figs. 66, 67, 68). The reaction product appears as a homogeneous or granular deposit.

d. Squamous Cell Carcinoma of Oesophagus. As in normal squamous epithelium of oesophagus, the reaction product is seen in the intercellular spaces and on the cell membrane of squamous cell carcinoma (Figs. 90, 91). It is also found in the pleomorphic membrane-limited dense bodies (Figs. 92, 94) which are infrequently seen in the cytoplasm of tumour cells (Fig. 93). No acid phosphatase activity is found in membrane-coating granules or any other intracytoplasmic organelles.

e. Gastric Carcinoma. Lead phosphate deposit is found in the small homogeneous and large pleomoephic membrane-limited dense bodies of gastric carcinoma (Figs. 127, 128, 129).

f. Colonic Carcinoma. The acid phosphatase activity in colonic carcinoma is found in the small round homogeneous or multivesicular bodies (Figs. 214, 215, 216) and in the large pleomorphic membrane-limited dense bodies (Fig. 217).

3. X-Ray Microanalysis.

Selected sections from the specimens processed for periodic acid thiocarbohydrazide silver proteinate and acid phosphatase were subjected to X-ray microanalysis. Analysis of the sections stained with the periodic acid thiocarbohydrazide silver proteinate has confirmed the presence of a heavy silver deposit in the dense reaction product at various sites (Fig. 248). With the large peak of silver, a small sulphur peak is also found. Analysis of deposit-free areas of the same sections stained with periodic acid thiocarbohydrazide silver proteinate showed no significant spectral line of silver (Fig. 249). The presence of heavy deposits of lead in the dense acid phosphatase reaction product has also been confirmed by X-ray analysis (Figs. 250, 252). With the large lead peak, a small osmium peak was also found. Analysis of clear areas from the same sections showed no significant lead deposit (Figs. 251, 253).

CHAPTER NINE

DISCUSSION

1. Normal Morphology

The squamous mucosa of the human oesophagus closely corresponds to the non-keratinised epithelium of the buccal mucosa (Zelickson and Hartmann, 1962 ; Hashimoto, Dibella and Shklar, 1966) and cervical mucosa (Hackemann, Grubb and Hill, 1968). This applies in particular to the membrane-coating granules (Grubb, Hackemann and Hill, 1968 ; Hayward and Hackemann, 1973). These granules lack the distinctive lamination seen in keratinising epithelium (Matoltsy and Parakkal, 1965 ; Rowden, 1966), although traces of this differentiation were occasionally recognised. Absent also was any evidence of keratohyalin granules in the oesophagus, despite their identification in non-keratinised cervical squamous epithelium (Hackemann et al, 1968).

There are two features of the oesophageal mucosa which have not been reported in other equivalent sites. These are the intracytoplasmic desmosomes and the nuclear bodies. Intracytoplasmic desmosomes are of rare occurrence, tending to be seen particularly at points where adjacent cells seem to have pulled apart and lack conventional desmosomal adhesion. This might be taken to support the view that their occurrence is related to defective intercellular adhesion (Mishima and Pinkus, 1968 ; Seiji and Mizuno, 1969 ; Takaki, Masutani and Kawada, 1971). Perhaps the residual hemidesmosome is retracted into the cell and pinched off, forming a twin for itself from the resultant small intracellular vacuole. The nuclear bodies encountered in the present study are equivalent to similar structures described as a normal cellular component in other sites (Buttner and Horstmann, 1967 ; Dupuy-Coin, Lazar, Kalifat and Bouteille, 1969). While their normal occurrence in human oesophagus can be affirmed, their functional significance remains obscure. These structures are dealt with in greater detail in Chapter 7.

The submucosal glands of the human oesophagus can best be compared with the human labial salivary glands (Tandler, Denning,

Mandel and Kutscher, 1969). Their principal mucous cells are virtually identical in many respects, such as general granule morphology and the occurrence of 'duplex' inclusions, the vacuolar and fibrillar aggregates described in Chapter 3. Tandler et al. (1969) believe that these inclusions are discharged along with the mucus, but there is no direct evidence from the present study to support this view. Somewhat similar filamentous bundles have been described in adipose cells in relation to lipid droplets, but again their function is unknown (Wood, 1967). The occasional arrays of microtubules observed in the present study within mitochondria have no counterpart in previous studies of salivary tissue.

The subsidiary acinar secretory cells have granules of greater density than those of the more numerous mucous cells. They resemble to some extent the mucus granules of gastric mucous cells (Lillibridge, 1964 ; Rubin, Ross, Sleisenger and Jeffries, 1968). In the labial salivary glands Tandler et al. (1969) reported a similar degree of variation in granule morphology. The cells containing smaller granules of heterogeneous pattern, or on occasion few if any granules, may correspond to the "inactive mucous cells" of Goetsch (1910). Perhaps they are immature forms. More likely they are transitional between acinar and duct cells, in a situation analogous to that of the centroacinar cells of pancreas.

The myoepithelial cells of oesophageal glands are confined to the acini and the adjacent ducts. They display no unusual features and can be compared directly with those of salivary tissue (Tandler, Denning, Mandel and Kutscher, 1970). It is curious that the otherwise meticulous histological study of Goetsch (1910) should have made no mention of these cells.

The oncocytes of the present study correspond to those previously reported in normal salivary glands (Tandler, 1966b ; Bogart, 1970) and elsewhere (Roth, Olen and Hansen, 1962 ; Tandler and Shipkey, 1964 ; Balough and Roth, 1965 ; McGavran, 1965 ; Tandler, 1966a). The

ultrastructure of these cells and their occurrence at the junction of duct and acinus gives no clue to their origin, thought variously to be from duct cells (Chauncey, Shklar and Brooks, 1962 ; Shklar and Chauncey, 1965), from myoepithelial cells (Hubner, Paulussen and Kleinsasser, 1967) and from acinar secretory cells (Voth, 1962). The distinctive oncocytoma (Tandler, 1966a), which shares the same ultrastructural features, is described in various situations, but, surprisingly, apparently not in oesophagus.

The main duct cells described above do not appear to contribute mucus secretion to the product of the gland, nor do they appear to have the large-scale fluid and electrolyte transfer functions which are inferred from the ultrastructural features of striated duct cells in salivary tissue. It is uncertain whether the small apical vesicles reflect a secretory or an absorptive function.

Finally, the innervation of the oesophageal submucosal glands is by indirect contact, since neural elements are found only in periacinar connective tissues and do not enter the epithelium as reported in salivary tissue (Tandler and Ross, 1969 ; Hand, 1970). This difference may well be related to their different function, the more sophisticated direct control of the salivary tissue perhaps reflecting the immediate responsiveness of salivary secretion to stimulation from higher centres.

The Langerhans cells of the human oesophagus are morphologically identical to those previously reported in the epidermis (Birbeck, Breathnach and Everall, 1961 ; Zelickson, 1965) and in the squamous mucosa of cervix (Younes, Robertson and Bencosme, 1968). These intra-epithelial Langerhans cells are not found in other than a stratified squamous location. The original view of Masson (1926, 1951) that the Langerhans cell represents an effete melanocyte, has already been discredited by the observation that the Langerhans cells develop normally in animals experimentally deprived of the neural crest, from which the melanocyte is known to be derived (Breathnach, Silvers, Smith and Heyner, 1968). The absence of any identifiable melanocytes in the

specimens of oesophagus which have been studied here may serve as circumstantial evidence in support of this experimental study. There is, in any case, little ultrastructural relationship between the Langerhans granule and the premelanosome or melanin granules.

The relatively common topographical relationship between the Langerhans granule and the Golgi apparatus has encouraged the view that this might be the site of its origin or synthesis (Breathnach, 1964 ; Niebauer, Krawczyk, Kidd and Wilgram, 1969) the subsequent discharge of the granule being indicated by its commonly observed continuity with the cell membrane. Equally persuasive, however, is the view that the granules form at the cell surface by a process of endocytosis (Hashimoto, 1971) akin to the specialised variety of micropinocytosis which is seen in macrophages, although tracer studies have so far failed to support an active phagocytic role for the Langerhans cell (Wolff and Schreiner, 1970 ; Sagbiel, 1972).

Perhaps the most interesting of recent findings are reports of the identification of typical Langerhans granules in cells far removed from an epithelial location. Cells of Langerhans type have been described, for example, in lymphatic vessel (Silberberg, Baer and Rosenthall, 1974), in lymph nodes, both human (Shamoto, Kaplan and Katch, 1971 ; Vernon, Fountain, Krebs, Horta-Barbosa, Fuccillo and Sever, 1973) and rabbit (Konodo, 1969), and in the dermis (Kiistala and Mustakallio, 1968). Moreover, many reports have been published of typical Langerhans granules in the cells of histiocytic lesions (Tarnowski and Hashimoto, 1967 ; Hashimoto and Tarnowski, 1968; Watson and Swedo, 1968 ; Gianotti and Kaputo, 1969 ; Morales, Fine, Horn and Watson, 1969 ; Imamura and Muroya, 1971 ; Hashimoto and Protzker, 1973).

These reports provide us with cause to consider a "mesenchymal" origin and function for the intra-epithelial Langerhans cell. For example, a possible function as "epidermoclast" has been proposed by Prunieras (1969) along with the suggestion that the Langerhans cell might have a role in the capture of antigenic material in the skin. The

observation by Silberberg (1973) of the juxaposition of Langerhans cells and mononuclear cells at sites of contact allergic reactions was taken by him as support for such a role. The ability of Langerhans cells to incorporate labelled thymidine (Giacometti and Montagna, 1967) and to divide within the epithelium suggests that they may well be more than mere transient migrants in this site. This behaviour recalls the similar proliferative capacity of the intra-epithelial lymphocyte of the intestinal tract. Indeed, Billingham and Silvers (1965) have proposed the lymphocyte as a potential relative of the Langerhans cell. It is difficult to distinguish consistently between the simple intra-epithelial lymphocyte of the oesophagus and the less well developed members of the Langerhans cell population. Some cells would certainly have qualified as lymphocytes, had there not been seen a single typical Langerhans granule within the otherwise featureless cytoplasm. On this purely structural basis it seems possible that the Langerhans cell might be related to the intra-epithelial lymphocyte. Even so, it remains unexplained that lymphocytes should be virtually universal inhabitants of epithelial surfaces of all kinds, whereas the distinctive intra-epithelial Langerhans cell seems so far to be confined to stratified squamous surfaces.

The work of Reams (1973) goes against the growing body of opinion in favour of a mesenchymal origin. His experiments suggest that the epidermal Langerhans cell in the mouse is of purely ectodermal origin.

Perhaps the Langerhans cells which have been described in various sites in health and disease do not represent a single homogeneous population with a common histogenetic origin. The occurrence of a particular ultrastructural specialisation in different cells is in itself an inadequate basis for proof of a common origin or identity. It may be that the Langerhans granule is a nonspecific cellular inclusion derived from an activity shared by different cells, both normal and neoplastic, of epithelial and mesenchymal origin, just as the simple micropinocytotic vesicle or caveola is seen in sites as diverse as smooth muscle, endothelium, serosal mesothelium and some epithelial cells.

Nevertheless, until this negative hypothesis can be more fully substantiated, the Langerhans granule will remain as circumstantial evidence to link those cells in which it is known to occur, particularly in association with squamous cells. It is interesting to speculate upon the possible factors in the biology of stratified squamous epithelium which might encourage, or perhaps demand, the presence of this curious population of presumptive mesenchymal visitors. Perhaps the relatively long turnover time of these surfaces is accompanied by an accumulation of intercellular 'garbage' the removal of which calls for a highly specialised variety of scavenger cell.

2. Squamous Cell Carcinoma of Oesophagus

No single ultrastructural feature is diagnostic of malignancy (Bernhard, 1958 ; Mercer, 1961), although many cytological variations serve to distinguish the cancer cell from its normal counterpart. The striking irregularities of nuclear and cytoplasmic contours observed in this study are perhaps the most obvious of these variations. The loss of cellular polarity, the tendency to become detached from neighbouring cells and the frequent occurrence of cytoplasmic pseudopodia all reflect the disorderly behaviour patterns of the malignant cell. The irregularity of nuclear contour, with frequently occurring channels and indentations may have some functional significance, since they imply an increased nucleocytoplasmic interface. Alternatively, these irregular contours may simply be the static representation of a greatly increased dynamic fluctuation of nuclear morphology without necessarily implying a particular functional significance in relation to nucleocytoplasmic interchange.

The wide range of variation of tonofilament morphology from cell to cell, and even within a single cell, may be related to the reduction in the number and organisation of the desmosomes. This feature was also noted in carcinoma of cervix (Luibel, Sanders and Ashworth, 1960), lung (Greene, Brown and Divertie, 1969) and skin (Martinez-Palomo, 1971),

and in squamous cell carcinoma transplants (Edward and Makk, 1960). It may be that deficient intercellular connections are related to the variability of cell shape and even to the invasiveness of neoplastic cell populations. The amoeboid pseudopodia of tumour cells in the present study were certainly only rarely attached to adjacent cells by desmosomes and were usually free from tonofilaments.

The significance of the presence or absence of the epithelial basal lamina around cancer cells is not easily determined. While it is tempting to interpret the projection of tumour cell pseudopodia through gaps in the basal lamina as evidence of invasive behaviour, it is not certain that this behaviour is a prerequisite for invasion. It is worth recalling that some non-neoplastic cells can show similar instability in relation to their basal laminae (Toner and Ferguson, 1971), although such behaviour is much more common in neoplasms (Ashworth, Stembridge and Luibel, 1961 ; Frei, 1962 ; Frithiof, 1969 ; Kobayasi, 1969 ; Woods and Smith, 1969 ; Friedmann, 1971 ; Ozzelo, 1971).

The wide variation of ultrastructural differentiation seen within a histologically typical series of squamous carcinoma emphasizes the instability of the neoplastic cell. The light cells, for example, relatively infrequent in the present series, formed the major cell population in the least differentiated cases of anaplastic nasopharyngeal carcinoma described by Lin et al. (1969). The epithelial pearls, on the other hand, represent a degree of squamous differentiation which goes beyond the normal limits of the healthy human oesophageal mucosa, and has features in common with the keratinisation process of epidermis (Brody, 1960).

The significance of the regular occurrence of intracytoplasmic desmosomes in oesophageal squamous carcinoma is obscure, although their authentic, if rare, appearance in normal squamous epithelium described in Chapter 3 shows that this is an abnormality of degree rather than of quality. In recent years, intracytoplasmic desmosomes have been described by various workers in different lesions, including Bowen's disease (Seiji and Mizuno, 1969 ; Yeh, Chen, How and Deng,

1974), Keratoacanthoma (Takaki, Masutani and Kawada, 1971 ; Fisher, McCoy and Wechsler, 1972), Gottron's Carcinoid papillomatosis (Caputo and Prandi, 1972) and nasopharyngeal carcinoma (Lin et al, 1969). Nor is this finding exclusive to tumours derived from squamous epithelia, since intracytoplasmic desmosomes are particularly common in metastatic signet-ring cell carcinoma of stomach described in Chapter 5.

The mode of formation of these intracytoplasmic desmosomes is still uncertain. In Gottron's Carcinoid papillomatosis (Caputo and Prandi, 1972) vesicles were found to form at the cell surface by a process akin to micropinocytosis. The subsequent adhesion of opposite faces of such vesicles was believed to give rise to the desmosome specialisation. Another factor possibly related to the formation of intracytoplasmic desmosomes is defective intercellular adhesion (Mishima and Pinkus, 1968 ; Seiji and Mizuno, 1969 ; Takaki, Masutani and Kawada 1971). In the present study, vesicle formation as described by Caputo and Prandi (1972) was not observed and therefore, although such a process would be entirely compatible with the mechanism of desmosome formation proposed by Krawczyk and Wilgram (1973), the present observations provide no specific support for their theory. When cell contact is lost, during mitosis or in abnormal keratinisation, it may be that residual hemidesmosomes are retracted and incorporated into the cytoplasm within a vesicle where they then induce the formation of matching specialisations. However, the absence of asymmetric complexes in the present material makes this seem an unlikely mechanism, although it must be conceded that, in certain circumstances, asymmetrical desmosomes have been observed (Hay and Revel, 1969 ; Overton, 1973), their precise significance being uncertain.

It has been suggested by Allen and Potten (1975) amongst others that modification of cell to cell contact in a maturing squamous epithelium is effected through whole desmosomal isolation and

engulfment by one of its parent cells. A high turnover of cells is to be expected in oesophageal carcinoma and, therefore, such a theory of desmosome resorption in remodelling cell boundaries would explain the unusual frequency of intracytoplasmic desmosomes in mitotic figures and epithelial pearls.

Equally enigmatic are the "thick-walled vesicles" of squamous cell carcinoma of oesophagus. These structures remain a curious but distinctive feature of this material. Such specialisation has not been previously described in squamous carcinoma in other sites, nor in any other alimentary tract neoplasm examined in this work.

Despite these many cytological aberrations, the most striking overall feature of the ultrastructure of well differentiated oesophageal squamous carcinoma is the persisting fundamental correspondence between the neoplastic cell and its normal parent. The ultrastructural parameters of a well differentiated squamous carcinoma are as distinctive, in their own way, as its histological parameters. It remains to be seen whether detailed analysis of the ultrastructure of such tumours, perhaps allied to quantitative morphological studies, may lead to future correlations with biological behaviour. In the meantime, the distinctive ultrastructural features of squamous carcinoma can at times assist in confirming the diagnosis in a tumour which by histological criteria is too anaplastic to categorise with confidence.

3. Gastric tumours

The present observations substantiate the previous report (Sasano et al. 1969) that there are two ultrastructural types of gastric carcinoma, their distinction being made on the basis of the presence or absence of mucous secretion granules, goblet cells and long microvilli. Both types showed the quantitative deviations from normal which have already been described previously in gastric carcinoma (Aiboshi, 1960 ; Onoe, 1963 ; Goldman and Ming, 1968), such as nuclear irregularity,

prominence of nucleoli, and variability of cytoplasmic organelles.

In ultrastructural terms, the classification of neoplasms according to their histogenetic origin can best be achieved by recognising cytological similarities between tumour cells and their normal counterparts. The gastric cell type of adenocarcinoma (Figs. 97, 98) appears to be most closely related to the gastric mucous cells (Figs. 44, 45), on the basis of granule morphology. The cells of the intestinal type of adenocarcinoma (Figs. 106, 107) did not resemble any of the normal gastric cell populations. On the other hand, the presence of long microvilli (Fig. 108) and of goblet cells (Fig. 110) was strongly reminiscent of intestinal differentiation, such as occurs in intestinal metaplasia in gastric mucosa (Goldman and Ming, 1968). The early reports of the fine structure of gastric carcinoma (Izumi, 1962) suggested that gastric cancers with long microvilli and goblet cells might take origin in such areas of intestinal metaplasia in the gastric mucosa.

There are other ultrastructural details encountered in the present study of gastric carcinoma which have not previously been reported. In the cytoplasm of the gastric cell type of tumour, there occur mitochondrial aberrations, intracisternal inclusions and membranous structures. In the nuclei of all types of gastric carcinoma, intranuclear coiled inclusions and nuclear bodies are found.

The mitochondria with tubular and vesicular cristae (Fig. 99) are similar to those of steroid secreting cells (Belt and Pease, 1956 ; Idelman, 1970). Those with concentric cristae (Fig. 101) are similar to the mitochondria described in renal clear cell carcinoma (Seljelid and Ericsson, 1965). Intramitochondrial rod-shaped inclusions similar to those described in gastric carcinoma (Fig. 100) have been reported to occur in human liver cells (Mugnaini, 1964). The significance of these mitochondrial alterations is obscure, although they seemed to distinguish the gastric type from the intestinal type of carcinoma. As yet, no functional relevance can be ascribed to them.

Equally enigmatic is the nature of the intracisternal rod-shaped inclusions and the membranous structures. These rod-shaped inclusions (Fig. 102) differ from those of the mitochondria (Fig. 100) in being less orderly in their arrangement and in showing no periodicity. The membranous structures (Fig. 103) can be distinguished from mitochondria with concentric cristae (Fig. 101) only in that their membranes are thicker than those of mitochondrial cristae. The association of these membranous structures with different shaped mitochondria, suggesting some possible relationship, could perhaps be clarified by future work using cytochemical procedures to demonstrate mitochondrial enzymes.

The most distinctive feature of both types of primary gastric carcinoma was the occurrence of the intranuclear coiled inclusions. These inclusions have not previously been described in normal gastric cells or in other human neoplasms. Although their nature is obscure, their possible significance in the differential diagnosis of gastric carcinoma is discussed, together with the nuclear bodies, under a separate heading.

Poorly differentiated gastric carcinoma differs from well differentiated tumours. It has neither the brush border and goblet cells of the intestinal type, nor the cytoplasmic aberrations of the gastric type. Both poorly and well differentiated carcinomas contained the intranuclear coiled inclusions. Only one distinction of significance could be made between different cases of poorly differentiated gastric carcinoma ; some contained granules of mucous secretory type, whereas others had none. It may be that this echoes the much clearer distinction between the gastric and intestinal cell types of well-differentiated tumour.

Well differentiated metastatic gastric carcinoma appears to have a fine structure in keeping with its primary site. All of the specimens of metastatic gastric carcinoma studied here were obtained from cases of gastric cell type carcinoma, since they contained mucous secretion

granules (Figs. 131, 132) identical to those of gastric mucous cells (Figs. 44, 45) and showed the expected structural alterations in some cytoplasmic organelles. These aberrations, however, and particularly those of the mitochondria, were more pronounced than in primary carcinoma. The intracisternal inclusions(Figs. 145, 146) of metastatic carcinoma differ from the rod-shaped inclusions of primary carcinoma (Fig. 102) in being tubular in cross-section and wider in diameter. They are similar to the undulating tubules described in the endoplasmic reticulum of some human lesions (Hurd, Eigenbrodt and Ziff, 1969 ; Norton, 1969 ; Jenson, Spjut, Smith and Rapp, 1971 ; Uzman, Saito and Kasac, 1971). The nature of these intracisternal tubules is still obscure. Immunofluorescence and tissue culture studies (Pinkus, Blacklow, Grimely and Bellanti, 1970) failed to support a viral origin for similar intracisternal tubules in systemic lupus erythematosus (Gyorkey, Min, Sinkovics and Gyorkey, 1969).

The ring-shaped nucleoli of metastatic carcinoma (Figs. 134, 135) have no counterpart in primary carcinoma. Their significance is unknown, but they are similar to those encountered in squamous cell carcinoma of oesophagus described in the present study, and in some human lesions such as lymphoma and leukemia (Smetana, Gyorkey, Gyorkey and Busch, 1970).

The poorly differentiated metastatic gastric carcinomas also resembled their corresponding primary tumours to a significant degree. They formed microvilli (Fig. 154) and basement membrane (Fig. 155) and were connected by typical desmosomes (Fig. 157), in contrast to gastric lymphoma (Fig. 158), which showed none of these features. However, the acinar spaces, mucous secretion granules and intranuclear coiled inclusions which were seen in primary poorly differentiated gastric carcinoma, were not found in secondary deposits.

The cases of metastatic signet ring cell gastric carcinoma described in this study are similar in some respects to the previous descriptions of primary signet ring cell carcinoma (Goldman and Ming, 1968 ; Sasano et al, 1969). This applies particularly to the appearance

of mucous granules and other cytoplasmic structures, such as mitochondria, Golgi apparatus and endoplasmic reticulum. The mucous secretion granules of signet ring cell carcinoma are more reminiscent of those of intestinal goblet cells than of gastric mucous cells.

The present series, by chance, included no case of primary signet ring cell carcinoma, all examples of this tumour being from metastases. There are some fine structural details of metastatic signet ring cell carcinoma which have not been described in the published reports of the primary tumour. These include intracytoplasmic saccular structures, tubulovesicles, intracytoplasmic desmosomes and intranuclear dense and tubular inclusions.

The saccular structures (Figs. 165, 166) have no counterpart in the normal gastric mucosa. They differ from the canaliculi of gastric parietal cells (Fig. 47) in being entirely located within the cytoplasm, unconnected to the cell surface. Their microvilli (Fig. 167) have a microfilamentous core which is not present in those lining the canaliculi of gastric parietal cells. Equivalent saccular inclusions have been described in some cases of poorly differentiated gastric carcinoma (Konodo, Tamura and Taniguchi, 1970), in malignant cells in a serous effusion due to carcinoma of breast (Springs and Jerrome, 1975) and in both primary and metastatic carcinoma of breast (Battifora, 1975). In these situations, it has been suggested that the intracytoplasmic saccular structures result from the failure to discharge accumulated secretion.

The tubulovesiclar (Fig. 168) structures described above appear surprisingly similar to those of gastric parietal cells (Fig. 48). Since they display a unit membrane similar to that of the cell membrane, these tubulovesiclar structures may well be related to the irregular surface of the neoplastic cell. Their significance in signet ring cell carcinoma is obscure, although the tubulovesicles of gastric parietal cells are probably related to the electrolyte and fluid transport mechanism (Rubin, Ross, Sleisenger and Jeffries, 1968). There is no evidence for

acid secretion by the cells of gastric carcinoma, although there is no obvious theoretical bar to the occurrence of such a function.

The significance of the frequent occurrence of intracytoplasmic desmosomes in metastatic signet ring cell but not in any other type of gastric carcinoma is obscure. Intracytoplasmic desmosomes have already been described in different lesions, including Bowen's disease (Yeh, Chen, How and Deng, 1974), Keratoacanthoma (Fisher, McCoy and Wechsler, 1972) and Gottron's carcinoid papillomatosis (Caputo and Prandi, 1972) as well as in the cases of squamous cell carcinoma of human oesophagus described in chapter 4. The mode of formation of these intracytoplasmic desmosomes is still uncertain, the possibilities being reviewed in detail in the discussion of squamous carcinoma in this chapter. In Gottron's carcinoid papillomatosis (Caputo and Prandi, 1972) the vesicles were found to form at the cell surface by a process akin to micropinocytosis. The adhesion of opposite faces of such vesicles was believed to give rise to the "tennis racket" desmosomes and subsequently to the typical desmosome specialisations. The frequent occurrence of vesicles and "tennis racket" desmosomes (Figs. 163, 164) in the present study tends to support this view. However, defective intercellular adhesion is another possibly relevant factor related to the formation of intracytoplasmic desmosomes (Mishima and Pinkus, 1968 ; Seiji and Mizuno, 1969 ; Takaki, Masutani and Kawada, 1971). Signet ring cell carcinoma is of course particularly distinguished by the lack of cellular adhesion and the infiltrating spread of separate single cells.

Equally enigmatic is the nature of the intranuclear tubules and dense intranuclear inclusions in metastatic signet ring cell carcinoma. Intranuclear tubules similar to those described in the present study (Fig. 169) have been found in intracranial chicken sarcoma (Bucciarelli, 1966) and in pulmonary adenomas and adenocarcinomas of mice (Flaks and Flaks, 1970). In Rous sarcoma (Bucciarelli, 1966) these intranuclear tubules have been suggested to be related to altered fragments of nuclear material. Dense inclusions identical to those described above were reported in some cases of colonic carcinoma

(Fig. 170) (Spjut and Smith, 1967). They were thought to be related to fixation artifact. These inclusions were seen in the present study in all cases of metastatic signet ring cell gastric carcinoma examined but in no other similarly processed neoplasm of the alimentary canal. If this represents a fixation artifact, it is a strikingly consistent and specific form of artifact. It seems more probable that it represents a true structural feature of this type of cancer. Morphologically, these inclusions are not dissimilar to the surrounding chromatin ; they may perhaps represent abnormal aggregates of chromatin granules.

In conclusion, it is evident from the wide range of variation of gastric carcinoma in the present study, that the neoplastic cell can display many cytological aberrations. However, despite these deviations, the neoplastic cells at all levels of differentiation retained their epithelial identity. They were still connected by desmosomes, rested on a basal lamina and tended to form acinar spaces and microvilli. The presence in some gastric cancers of mucous secretion granules identical to those of gastric mucous cells is a clue for their identification. This is in contrast with the cells of gastric lymphoma, which lack epithelial adhesion specialisations, basal lamina, acinar spaces and secretion granules of any kind (Figs. 121, 122). The limited availability of cases of alimentary lymphoma makes it difficult to generalise, but the comparisons made here support the view that ultrastructural examination may have an important role to play in the accurate differential diagnosis of anaplastic tumours of the gut.

4. Colonic Tumours

The main ultrastructural features of villous papilloma already published include the occurrence of membrane-bound inclusions (Fisher and Sharkey, 1962), the presence of dark cells (Imai, Saito and Stein, 1965 ; Spjut and Smith, 1967), the immaturity of the cells (Kaye, Fenoglio, Pascal and Lane, 1973) and the widened intercellular spaces (Ioachim, Delaney and Madrazo, 1973). Apart from the widened intercellular spaces, all of these features were encountered in the

present study.

However, the dark cells described by previous authors in villous papilloma did not correspond to the aggregates of dark cells noted in the present series. The cells previously described did not have the numerous closely packed mitochondria, the intracellular vacuoles and the pronounced lateral interdigitations described in the present study. They were also dispersed singly between the principal cells of villous papilloma, giving rise to the view that they might represent degenerating goblet cells (Spjut and Smith, 1967).

In the present study, the aggregates of dark cells are the most distinctive feature of villous papilloma. The close-packed aggregates of mitochondria, the pale intracellular vacuoles and the exuberant lateral interdigitations (Figs. 181, 183) were not seen in the present series of colonic carcinoma or in samples of normal colonic mucosa. It might be relevant that cells of other types known to be involved in electrolyte and fluid transport, such as the cells of the renal tubules (Tisher, Bulger and Trump, 1966) share certain similarities of fine structure with these dark cells. The nature of these aggregates of cells is unknown. Perhaps they might represent modified goblet cells. On the other hand, it is interesting to speculate,on the basis of their fine structure, that they might be related to the fluid and electrolyte loss which is known to occur in some cases of villous papilloma (Wells, Moron and Cooper, 1962).

The intracellular inclusions of villous papilloma (Fig. 180) correspond to the membrane-bound inclusions which have been described in various lesions of the alimentary tract (Fisher and Sharley, 1962). These were considered to represent the degenerating nuclei of both intra-epithelial lymphocytes and epithelial cells. The inclusion bodies described by Fisher and Sharkey (1962) differ from those seen in the present study only in being intercellularly located. Similar inclusions were not encountered during this study either in normal colonic mucosa or in cases of carcinoma of colon.

The present study is also in agreement with the previous report

(Kaye et al, 1973) that the cells of villous papilloma closely resemble the immature epithelium of the lower one third of the colonic crypt (Figs. 63, 64). Particular similarities exist between their microvilli, junctional complexes, lateral margins and secretory product.

The neoplastic cells of the present series of well differentiated colonic carcinoma can also be compared with the undifferentiated epithelium of the lower one third of the colonic crypt (Fig. 65). This particularly applies to the appearance of their nuclei and the absence of the goblet cell type of mucous granules. Because of this absence of mucous granules, early studies (Birbeck and Dukes, 1963) drew comparisons with the mature absorptive cells of colonic mucosa ; the correspondence with immature crypt cells is, however, much closer. In both villous papilloma and well differentiated colonic carcinoma, this correspondence applied to details of the apical cell surface. The tumour cells lack the prominent fuzzy coat and long and well organised microvilli of the mature colonic mucosal cells. The spherical membrane-limited vesicles frequently seen between the microvilli of normal colonic cells (Fig. 60) are, however, also present in both colonic carcinoma (Fig. 187) and villous papilloma (Fig. 175).

The penetration of the basal lamina of colonic carcinoma by cytoplasmic projections from the neoplastic cells has been considered to be the most characteristic feature of malignancy (Imai and Stein, 1963 ; Cardoso, Diener, Alvarez, Elizabeth and Maldonado, 1971), since such a phenomenon was not seen in normal colonic mucosa. Similar appearances, however, have also been described in some villous papillomas (Imai et al, 1965). In the present study, the penetration of the basal lamina by cytoplasmic projections was confined to colonic carcinoma, and was not seen in villous papilloma or in normal mucosa.

There are other ultrastructural features confined only to colonic carcinoma. These include doughnut-like inclusions, a network of tubular structures and different nuclear and cytoplasmic inclusions.

The doughnut-like inclusions (Figs. 193, 194) of colonic carcinoma have previously been thought to be of viral origin (Mueller, Menefee and Ivler, 1960) or to consist of engulfed cytoplasmic material (Spjut and Smith,

1967). These doughnut-like inclusions contained carbohydrates, as shown by the periodic acid silver proteinate procedure and were consistently located in the apical cytoplasm in all cases of primary colonic carcinoma examined in the present study. It is believed that they might represent heterogeneous secretory granules.

The network of tubular structures (Figs. 196, 196) most probably represents an abnormal arrangement of cisternae of the endoplasmic reticulum, since continuity with the more conventional form of endoplasmic reticulum is frequently seen. This inclusion has not previously been described in colonic carcinoma.

The most distinctive feature of rectal carcinoma studied here was the occurrence of nuclear and cytoplasmic inclusions not seen in normal colonic mucosa or in villous papilloma. These inclusions are discussed later under a separate heading.

The cells of poorly differentiated colonic carcinoma (Fig. 200) showed less cytoplasmic organisation than those of well differentiated colonic carcinoma (Fig. 190). They did not closely resemble any of the normal colonic cells, but they were still connected by typical desmosomes (Fig. 201) rested on a basal lamina (Fig. 202) and formed acinar spaces (Fig. 201). The characteristic feature of this type of carcinoma was the occurrence of dark and light cells similar to those seen in poorly differentiated nasopharyngeal neoplasms (Lin et al, 1969). Similar light and dark cells were not seen in cases of well differentiated colonic carcinoma. The dark cells of poorly differentiated colonic carcinoma (Fig. 200) differ from the dark goblet cells of villous papilloma described by Spjut and Smith (1967) in having no mucous secretion granules, and from the dark cells described in the present series of villous papilloma (Fig. 181) in having no lateral interdigitations or intracytoplasmic vacuoles. These light and dark cells most probably represent different degrees of neoplastic differentiation (Lin et al, 1969).

The neoplastic cells of well differentiated metastatic colonic carcinoma (Fig. 203) are in many respects similar to those of primary well differentiated colonic carcinoma (Fig. 190). The same correspondence

is seen with the undifferentiated cells of the lower one third of the colonic crypt (Fig. 65). One apparent difference between the cases of primary and of metastatic colonic carcinoma examined here was the absence, from the secondary deposits of the doughnut-like inclusions and the network of tubular structures which occurred in the primary site.

Cases of metastatic rectal carcinoma also showed the nuclear and cytoplasmic inclusions described above in primary rectal tumours. This is in contrast with metastatic gastric carcinoma, which did not display the distinctive intranuclear coiled inclusions typical of primary tumours. The significance of these inclusions is discussed later under a separate heading.

Finally, the small spherical membrane-limited vesicles found between the microvilli of colonic tumours, are identical to those seen in normal colonic mucosal cells. Although their significance is quite unknown, such vesicles are particularly numerous in metastatic colonic carcinoma (Fig. 204). The occurrence of these vesicles also in intestinal type of gastric carcinoma, renders them nonspecific and of little diagnostic value as to the origin of tumours.

5. Nuclear and cytoplasmic inclusions in normal and malignant cells in the human alimentary canal

Nuclear bodies have already been described in various other situations in both normal (Buttner and Horstmann, 1967 ; Krishan, Uzman and Hedley-Whyte, 1967 ; Henry and Petts, 1969 ; Dupuy-Coin, Lazar, Kalifat and Bouteille, 1972) and abnormal cells (Robertson, 1964 ; Swanbeck and Thyresson, 1964 ; Bouteille, Kalifat and Delarue, 1967). Histochemically, they have been found to contain ribonucleoprotein (Dupuy-Coin, Kalifat and Bouteille, 1972) and have been proposed as sites of protein synthesis (Dupuy-Coin and Bouteille, 1975) The frequent occurrence of nuclear bodies in close proximity to the nucleolus in pathological cells has suggested some relationship between the nucleolus and the nuclear body (Kierszenmann, 1969 ; Smetana, Gyorkey, Gyorkey

and Busch, 1971 ; Sobrinho-Sumes and Goncalves, 1974).

The nuclear bodies described above are morphologically identical to those previously described in various other situations (Ghadially, 1975). It is believed, from the study of multiple sections, that some of the different morphological types of nuclear body described here and in previous reports could possibly represent different planes of section through a single basic structure. Their function is uncertain but their occurrence in normal cells suggests that they may play some part in normal nuclear metabolism. Their morphological alterations in neoplasia may be related to cellular hyperactivity.

The occurrence of microtubules, microfibrillar and lattice inclusions in human cells seems to be a rarer phenomenon. Such structures have been described in certain pathological conditions of human nervous tissue (Robertson and Maclean, 1965 ; Perier and Vanderhaeghen, 1967 ; Hadfield, David and Rosenblum, 1972), but have been more widely reported in other animal species (Chandler, 1966 ; Chandler and Willis, 1966 ; Karlsson, 1966 ; Boquist, 1969 ; Seite, 1970 ; Seite, Escaig and Couineau, 1971 ; Gourantan, 1972 ; Nagl, 1973), and in plants (Evert and Deshponde, 1970 ; Wergin, Gruber and Newcomb, 1970 ; Tanaka and Mizunaga, 1974). Microfibrillar structures in animal cells have been considered to be a normal component of nuclei (Clattenburg, Singh and Montemurro, 1972) limited to certain cells of certain species (Siegesmuno, Dutta and Fox, 1964).

Perhaps their occurrence in neoplastic human cells should be regarded as an inappropriate formation of organelles not usually found in normal circumstances in man. It is of interest that structures similar to those described in the present investigation have also been found in virus-infected cells (Dubois-Dalcq and Buyes, 1972 ; Bingen and Kirn, 1973 ; Vela and Lee, 1974 ; Bingen and Kirn, 1975). The possibility exists that such inclusions in the cells of rectal carcinoma may represent some viral product. The intranuclear coiled structures seen in gastric carcinoma are equally enigmatic. They bear no relationship to any known organelle and have no counterpart in normal

stomach. Similar structures, however, have been observed in the growing oocyte of the prepubertal mouse (Chouinard, 1973), at a particular stage in the differentiation of this cell, in relation to functional hyperactivity.

Finally, it remains to be seen how far the occurrence of inclusions such as those described above may contribute to the differential diagnosis of human neoplasma. The association of particular types of inclusion with tumours in stomach and large bowel was certainly consistent within the present series. It is important that such inclusions should be sought specifically in the course of any ultrastructural studies of human neoplasia in order to allow the assessment of their value as diagnostic pointers. It is not inconceivable that in the future there might emerge therapeutic and prognostic implications of findings such as these.

6. Ultracytochemistry

In the present investigation, carbohydrate-rich compounds and acid phosphatase activity were demonstrated in normal epithelium and in tumours of the human alimentary canal.

The fine structural distribution of carbohydrates, in relation to the normal squamous epithelium of human oesophagus, was similar to that described in human oral epithelium (Hayward and Hackemann, 1973) and skin (Hashimoto, Gross, Nelson and Lever, 1966). Carbohydrates were abundant in the membrane-coating granules and on the cell membranes of the superficial layers. In non keratinised squamous epithelium of oesophagus, carbohydrates were also abundant in the cytoplasmic vacuoles of the superficial cells. This corresponds to the presence of glycogen which is known to occur here.

Apart from the presence of carbohydrates in the membrane-coating granules, the neoplastic cells of squamous carcinoma showed similar staining properties to the basal cells of normal squamous epithelium of oesophagus. Their cell membrane did not have the carbohydrate-rich compounds of the superficial cells of normal squamous epithelium.

The surface coat of normal and neoplastic cells of stomach and colon consistently showed positive carbohydrate staining, similar to that of cat (Ito, 1965) and of rat intestinal cells (Romberg and Leblond, 1967). The source of such carbohydrates was found within the cells (Ito, 1965 ; Bennett, Leblond and Haddad, 1974) and radioactive glycoprotein precursors have been traced through Golgi system to the surface coat.

Carbohydrates were also present in the membrane-limited vesicles of the intestinal type of gastric carcinoma and of colonic tumours. The significance of the presence of carbohydrates in these vesicles is obscure as is the nature of the vesicles themselves. The exact nature of doughnut-like inclusions of colonic carcinoma is also unknown. The presence of positive carbohydrate staining in these inclusions might suggest a secretory function rather than a viral origin (Mueller, Menefee and Ivler, 1960).

Carbohydrates were also demonstrated in mucous secretion granules of gastric mucous cells and gastric carcinoma, but not in mucous granules of colonic goblet cells. This is perhaps related to the type of mucous substance present in these locations (Lev, 1965 ; Makela, Korhonen and Lilius, 1971).

The numerous small homogeneous and large heterogeneous membrane-limited dense inclusions of the normal epithelial and neoplastic cells of human alimentary canal studied in the present work were found to be lysosomes, since they showed acid phosphatase activity. No significant differences were seen between the different lysosomes of normal and neoplastic cells.

In normal squamous epithelium and in squamous cell carcinoma of human oesophagus, non-lysosomal acid phosphatase activity was present in the intercellular spaces and on the cell membrane. Acid phosphatase activity in intercellular spaces and on the cell membrane has also been reported in keratinised epithelium of mouse tongue (Weinstock and Wilgram, 1970). Since these authors also found acid phosphatase activity in membrane-coating granules and in the Golgi

apparatus of keratinised epithelium, they suggested that the enzyme is produced in the Golgi system and carried by membrane-coating granules into the intercellular spaces to be involved in the desquamation of cells of stratum corneum. Acid phosphatase activity in the present study, however, was not seen either in membrane-coating granules or in the Golgi system of normal epithelium or of squamous carcinoma of oesophagus. The present observations thus conflict with the work of Weinstock and Wilgram (1970), but leave unresolved the question of the origins of intercellular acid phosphatase activity.

Finally, x-ray microanalysis has confirmed the presence of silver deposits in the reaction product of the carbohydrate staining, and lead deposits in the reaction product of acid phosphatase preparations. The ease with which such histochemical reaction products can be detected with this apparatus raises the possibility of future applications of microanalysis in histochemistry. In theory, at least, any elemental reaction product with atomic number greater than 10 is amenable to microanalytical study, irrespective of its electron scattering potential, and thus its electron contrast. This will prove a fruitful field for further study.

CHAPTER TEN

CONCLUSIONS

In its initial concept, the scope of this investigation was very wide. In practical terms, the limits were set by time and by the availability of suitable tissues. In all, 129 neoplasms and 39 samples of normal tissue were studied in detail. Numerous blocks were sectioned and examined. The permanent record, amounting to nearly 5000 negatives, understates the detailed scrutiny to which each case was subjected, since in many instances features already recorded photographically in one case were merely noted, without photography, in subsequent examples of that tumour. Consequently, many hours of screening were often represented by only a handful of micrographs. The numerous observations made in the course of this work have already been set down in the preceding chapters. In conclusion, however, the following points have been selected as being of particular interest, and perhaps worthy of further study.

1. Langerhans Cells. These curious cells, shown here to be normal inhabitants of the human oesophageal mucosa, are still unexplained. It would be of interest to attempt to define their function and to investigate possible variations under experimental and pathological conditions, such as in inflammatory disease and following experimental trauma and exposure to carcinogenic agents. Their observed occurrence in squamous carcinoma reflects the basic affinity of these cells for tissues undergoing squamous differentiation.

2. Intracytoplasmic Desmosomes. The occurrence of these specialisations in normal human oesophagus was not hitherto recorded, and their prominence in squamous carcinoma was of interest, although already described in certain circumstances. Of greater interest was their unexpected regular appearance in metastatic signet-ring cell carcinoma of stomach. Since this specialisation may reflect defective cellular adhesion mechanisms, its further study might correlate with

behavioural differences between certain neoplasms. It would be of interest to attempt quantitation of this feature in different cases, relating the results to clinical parameters.

3. Nuclear and Cytoplasmic Inclusions. Although their significance remains obscure, the wide variety of inclusions described in these different tumours deserves more detailed investigation. The occurrence of certain inclusions in tumours arising only in particular anatomical sites raises the possibility that specific ultrastructural markers might become available to assist in the detailed differential diagnosis of certain tumours. This possibility could only be properly assessed in the light of a much larger series of neoplasms.

4. Non lysosomal acid phosphatase. The occurrence of extracellular acid phosphatase activity in oesophageal squamous mucosa and in squamous carcinoma is unexplained. Further study of this enzyme activity would be of interest, in an attempt to define its source and its significance.

5. Dark Cells of Villous Papilloma. It would be of interest to explore the possible relationship of these cells to fluid and electrolyte transport, as suggested by their ultrastructural features. Quantitative measurements of their occurrence could be correlated with biochemical findings in particular cases. Short term tissue-culture studies could also be of interest.

6. X-ray Analysis in Cytochemistry. This new technique is at present limited in its application to biological problems. It is at its most effective in the precise identification and localisation of specific elements in high concentration, such as in cytochemical reaction products. The ease with which this was accomplished in the present

study suggests that wider applications of this technique should be looked for in the field of cytochemistry. In theory, for example, X-ray analysis could discriminate between two different reaction products in the same tissue, and could identify the presence of concentrations of elements without the need for electron dense deposits.

In conclusion, it is clear that this thesis represents a possible starting point for many further studies. It is hoped to pursue some of these in subsequent work.

REFERENCES

Aiboshi, I. (1960) Electron microscopic studies of human cancers. ii. Studies on fine structure of gastric cancer cells. Sapporo Medical Journal, 17,234-248.

Allen, T.D. & Potten, C.S. (1975) Desmosomal form,, fate and function in mammalian. Journal of Ultrastructure Research, 51,94-105.

Aristila, A.V. & Hopsu-Haru, V.K. (1967) Nuclear and cytoplasmic microfilaments in the pineal chief cells of the rat. Zeitschrift fur Zellforschung, 80,22-28.

Ashworth, C.T., Stembridge, V.A. & Luibel, F.J. (1961) A study of basement membrane of normal epithelium, carcinoma in situ and invasive carcinoma of uterine cervix, utilizing electron microscopy and histochemical methods. Acta Cytologica, 5,369-384.

Ashworth, C.T. & Stembridge, V.A. (1964) Utility of fomalin-fixed surgical and autopsy specimens for electron microscopy. American Journal of Clinical Pathology, 42,466-480.

Balough, K. & Roth, S.I. (1965) Histochemical and electron microscopic studies of eosinophilic granular cells (oncocytes) in tumours of the parotid gland. Laboratory Investigation, 14,310-320.

Battifora, H. (1975) Intracytoplasmic lumina in breast carcinoma. A helpful histopathologic feature. Archives of Pathology, 99,614-617.

Belt, W.D. & Pease, D.C. (1956) Mitochondrial structure in sites of steroid secretion. Journal of Biophysical and Biochemical Cytology,2(supplement),369-374.

Bennett, G., Leblond, C.P. & Haddad, A. (1974) Migration of glycoprotein from the Golgi apparatus to the surface of various cell types as shown by radioautography after labeled fucose injection into rats. Journal of Cell Biology, 60,258-285.

Bensch, K.G., Gordon, G.B. & Miller, L.R. (1965) Electron microscopic and biochemical studies on the bronchial carcinoid tumour. Cancer, 18,592-602.

Bernhard, W. (1958) Electron microscopy of tumour cells and tumour viruses. A review. Cancer Research, 18,491-509.

Billingham, R.E. & Silver, W.K. (1965) Some unsolved problems in the biology of skin. In biology of the skin and hair growth, ed. Lyne, A.G. & Shorts, B.F. Sydney: Angus Robertson.

Bingen, A. & Kirn, A. (1973) Modifications ultrastructurales precoces des noyaux des hepatocytes de souris au cours de I' hepatite degenerative aigue provaquee par le fu (frog virus 3). Journal of Ultrastructure Research, 45,343-355.

Bingen, A. & Kirn, A. (1975) Fibrillar bodies in hepatocyte nuclei during the course of the toxic hepatitis produced by frog virus 3 in mice. Journal of Ultrastructure Research, 50,167-173.

Birbeck, M.S., Breathnach, A.S. & Everall, J.D. (1961) An electron microscopic study of basal melanocytes and high level clear cells (Langerhans cells) in vitilligo. Journal of Investigative Dermatology, 37,51-64.

Birbeck, M.S. & Dukes, C.E. (1963) Electron microscopy of rectal neoplasms. Proceedings of the Royal Society of Medicine,56,793-797.

Bock, P. (1974) Fine structure of Langerhans cells in the stratified epithelia of the oesophagus and stomach of mice. Zeitschrift fur Zellforschung und Microskopische Anatomie, 147,237-247.

Bogart, B.I. (1970) The effect of aging on the rat submandibular gland: an ultrastructural, cytochemical and biochemical study. Journal of Morphology, 130,337-351.

Boquist, L. (1969) Intranuclear rods in pancreatic islet β-cells. Journal of Cell Biology, 43,377-381.

Bouteille, M., Kalifat, S.R. & Delarue, J. (1967) Ultrastructural variations of nuclear bodies in human disease. Journal of Ultrastructure Research, 19, 474-486.

Breathnach, A.S. (1964) Observations on cytoplasmic organelles in Langerhans cells of human epidermis. Journal of Anatomy,98,265-270.

Breathnach, A.S., Silver, W.K., Smith, J. & Heyner, S. (1968) Langerhans cells in mouse skin experimentally deprived of its neural crest component. Journal of Investigative Dermatology, 50,,147- 160.

Brody, I. (1960) The ultrastructure of the tonofilaments in the keratinisation process of normal human epidermis. Journal of Ultrastructure Research, 4,264-297.

Bucciarelli, E. (1966) Intranuclear cisternae resembling structures of the Golgi complex. Journal of Cell Biology, 30,664-665.

Buttner, D.W. & Horstmann, E. (1967) Haben die sphaeridion in den zellkernen kranker gewebe eine pathognomonische bedeutung. Virchows Archiv fur Pathologische Anatomie, 343,142-163.

Buttner, D.W. & Horstmann, E. (1967) Das sphaeridion eine weit verbreitete differenzierung des karyoplasma. Zeitschrift fur Zellforschung, 77,589- 605.

Caputo, R. & Prandi, G. (1972) Intracytoplasmic desmosomes. Journal of Ultrastructure Research, 41,358-368.

Cardoso, J.M., Diener, K.A., Alvarez, E.E., Elizabeth, Q. & Maldonaldo, M. (1971) Electron micoscopy of adenocarcinoma of the colon. American Journal of Pathology, 22,301-307.

Chandler, R.L. (1966) Intranuclear structures in neurons. Nature, 209, 1260.

Chandler, R.L. &Willis, R. (1966) An intranuclear fibrillar lattice in neurons. Journal of Cell Science, 1,283-286.

Chauncey, H.H., Shklar, G. & Brooks, R.A. (1962) Histochemistry of human salivary gland tumours. Oral Surgery, 15,950-964.

Chouinard, L.A. (1973) An electron microscope study of the extranucleolar bodies during growth of the oocyte in the prepubertal mouse. Journal of Cell Science, 12,55-69.

Clattenburg, R.E., Singh, R.P. & Montemurro, D.G. (1972) Intranuclear filamentous inclusions in neurons of the rabbit hypothalamus. Journal of Ultrastructure Research, 39,549-555.

Dalton, A.J. & Felix, M.D. (1956) The electron microscopy of normal and malignant cells. Annals of Science,63,1117-1140.

Davies, J.E., Seavey, P.W. & Sessions, J.T. (1961) Villous adenomas of the rectum and sigmoid colon with severe fluid and electrolyte depletion. Annals of Surgery, 155,806-812.

Dubois-Dalcq, M. & Buyse, M. (1972) Herpes virus hominis type 2 and intranuclear tubular structures in organised nervous tissue culture. Acta Neuropathologica, 22,170-179.

Dupuy-Coin, A.M., Lazar, P., Kalifat, S.R. & Bouteille, M. (1969) A method of quantitation of nuclear bodies in electron microscopy. Journal of Ultrastructure Research, 27,244-249.

Dupuy-Coin, A.M., Kalifat, S.R. & Bouteille, M. (1972) Nuclear bodies as proteinaceous structures containing ribonucleoproteins. Journal of Ultrastructure Research, 38,174-187.

Dupuy-Coin, A.M. & Bouteille, M. (1975) Protein renewal in nuclear bodies as studied by quantitative ultrastructural autoradiography. Experimental Cell Research, 90,111-118.

Edwards, G.A. & Makk, L. (1960) A comparative micromorphologic study of normal human epidermis and a human squamous cell carcinoma transplant. American Journal of Pathology, 37,101-120.

Enterline, H.T., Evans, G.W., Mercado-Lugo, R., Miller, L. & Fitts, W.T. (1962) Malignant potential of adenomas of colon and rectum. Journal of the American Medical Association, 179,322-330.

Etherton, J.E. & Botham, C.M. (1970) Factors affecting lead capture methods for the fine localisation of rat lung acid phosphatase. Histochemical Journal, 2,507-519.

Evert, R.F. & Deshpande, B.P. (1970) Nuclear P protein in seive elements of Tilia Americana. Journal of Cell Biology, 44,462-466.

Fisher, E.R. & Sharkey, D.A. (1962) The ultrastructure of colonic polyps and cancer with special reference to the epithelial inclusion bodies of Leuchtenberger. Cancer, 15,160-170.

Fisher, E.R., McCoy,M.M. & Wechsler, H.L. (1972) Analysis of histopathological and electron microscopic determinants of keratoacanthoma and squamous cell carcinoma. Cancer, 29,1387-1397.

Flaks, B. & Flaks, A. (1970) Fine structure of nuclear inclusions in murine pulmonary tumour cells. Cancer Research, 30,1437-1443.

Frei, J.V. (1962) The fine structure of the basement membrane in epidermal tumours. Journal of Cell Biology, 15,335-344.

Friedmann, I. (1971) Electron microscopy in head and neck oncology. Acta Otolaryngologica, 71,115-122.

Frithiof, L. (1969) Ultrastructure of the basement membrane in normal and hyperplastic human oral epithelium compared with that in preinvasive and invasive carcinoma. Acta Pathologica Microbiologica Scandinavica (supplement),200.

Gemmel, R.T. (1973) Langerhans cells in the ruminal epithelium of the sheep. Journal of Ultrastructure Research, 43,256-259.

Ghadially, F.N. (1975)Ultrastructural pathology of the cell. Atext and atlas of physiological and pathological alterations in cell fine structure. London and Boston: Butterworth.

Giacometti, L. & Montagna, W. (1967) Langerhans cells: uptake of tritiated thymidine. Science, 157,439-440.

Gianotti, F. & Caputo, R. (1969) Skin ultrastructure in Hand-Schuller-Christian disease: report on abnormal Langerhans cells. Archives of Dermatology, 100,342-349.

Goetsch, E. (1910) The structure of the mammalian oesophagus. American Journal of Anatomy, 10,1-40.

Goldenberg, V.E., Goldenberg, N.S. & Benditt, E.P. (1969) Ultrastructural features of functioning α-and β- celltumours. Cancer, 24,236-247.

Goldman, H. & Ming, S. (1968) Fine struucture of intestinal metaplasia and adenocarcinoma of the human stomach. Laboratory Investigation, 18,203-210.

Gouranton, J. (1972) Development of an intranuclear non occluded rod shaped virus in some midgut cells of an adult insect, Gyrinus natator L. Journal of Ultrastructure Research, 39,281-294.

Greene, J.G., Brown, A.L. & Divertie, M.B. (1969) Fine structure of squamous cell carcinoma of the lung. Mayo Clinic Proceedings, 44,85-95.

Grubb, C., Hackemann, M. & Hill, K.R. (1968) Small granules and plasma membrane thickening in human cervical squamous epithelium. Journal of Ultrastructure Research, 22,458-468.

Gyorkey, F., Min, K.W., Sinkovics, J.G. & Gyorkey, P. (1969) Systemic lupus erythematosus and myxovirus. New England Journal of Medicine, 280, 333.

Gyorkey, F., Min, K.W., Krisko, I. & Gyorkey, P. (1975) The usefulness of electron microscopy in the diagnosis of human tumours. Human Pathology, 6,421-441.

Hackemann, M., Grubb, C. & Hill, K.R. (1968) The ultrastructure of normal squamous epithelium of human cervix uteri. Journal of Ultrastructure Research, 22,443-457.

Hadfield, H.G., David, R.B. & Rosenblum, W.I. (1972) Coiled nucleocapsid configuration in subacute sclerosing panencephalitis. Acta Neuropathologica, 21,263-268.

Hand, A.R. (1970) Nerve acinar cell relationships in the rat parotid gland. Journal of Cell Biology, 47,540-543.

Hashimoto, K. (1971) Langerhans cell granule. An endocytotic organelle. Archives of Dermatology, 104,148-165.

Hashimoto, K., Dibella, R.J. & Shklar, G. (1966) Electron microscopic studies of the normal human buccal mucosa. Journal of Investigative Dermatology, 47,512-525.

Hashimoto, K., Gross, B.G., Nelson, R. & Lever, W.F. (1966) The ultrastructure of the skin of human embryo. Journal of Investigative Dermatology, 47,205-217.

Hashimoto, K. & Pritzker, M.S. (1973) Electron microscopic study of reticulo-histiocytoma: an unusual case of congenital self-healing reticulo-histiocytosis. Archives of Dermatology, 107,263-270.

Hashimoto, K. & Tarnowski, W.M. (1968) Some new aspects of Langerhans cells. Archives of Dermatology, 97,450-464.

Haye, E. & Revel, J.P. (1969) Fine structure of the developing avian cornea, ed. Karger, S. & Basel, A.G.

Hayward, A.F. & Hackemann, M. (1973) Electron microscopy of membrane-coating granules and a cell surface coat in keratinized and nonkeratinized human oral epithelium. Journal of Ultrastructure Research, 43,205-219.

Henry, K. & Petts, V. (1969) Nuclear bodies in human thymus. Journal of Ultrastructure Research, 27,330-343.

Holt, S.J. & Hicks, R.M. (1961) The localization of acid phosphatase in rat liver cells as revealed by combined cytochemical staining and electron microscopy. Journal of Biophysical and Biochemical Cytology, 11,47-66.

Hubner, G., Paulussen, F. & Kleinsasser, D. (1967) Zur feinstruktur und genese der onkocyten. Virchows Archiv fur Pathologische Anatomie, 343, 34-50.

Hurd, E.R., Eigenbrodt, E. & Ziff, M. (1969) Cytoplasmic tubular structures in kidney biopsies in systemic lupus erythematosus. Arthritis Rheum 12,541-542.

Idelman, S. (1970) Ultrastructure of the mammalian adrenal certex. International Review of Cytology, 27,181-281.

Imai, H. & Stein, A.A. (1963) Ultrastructure of adenocarcinoma of the colon. Gastroenterology, 45,410-418.

Imai, H., Saito, S. & Stein, A.A. (1965) Ultrastructure of adenomatous polyps and villous adenomas of the large intestine. Gastroenterology, 48, 188-197.

Imamura, M. & Muroya, K. (1971) Lymph node ultrastructure in Hand-Schuller-Christian disease. Cancer, 27,956-964.

Ioa chim, N., Delaney, W.E. & Madrazo, A. (1974) Villous adenoma of the colon and rectum: an ultrastructural study. Cancer, 34,586-596.

Ito, S. (1965) The enteric surface coat on cat intestinal microvilli. Journal of Cell Biology, 27,475-491.

Ito, S. (1965) Radioactive labeling of the surface coat on enteric microvilli. Anatomical Record, 151,489.

Izumi, G. (1962) Electron microscopic studies of human cancer. iii. On the difference in fine structure of gastric cancer cells from the viewpoint of histological differentiation. Sapporo Medical Journal, 21,250-272.

Jenkinson, J.A. & Dawson, I.M. (1971) The value of electron microscope studies in diagnosing malignant change in ulcerative colitis. Gut,12,110-118.

Jenson, A.B., Spjut, H.J., Smith, M.N. & Rapp, F. (1971) Intracellular branched tubular structures in osteosarcoma. Cancer, 27,1440-1448.

Jimenez, J.M., Ambrosius, K., Boom, R. & Leuze, E. (1971) Ultramicroscopic structure of the human sigmoid colonic mucosa. American Journal of Proctology, 22,308-312.

Karlsson, V. (1966) Three dimensional studies of neurons in the lateral geniculate nucleus of the rat. 1. Organelle organisation in the perikaryon and its proximal branches. Journal of Ultrastructure Research, 16,429-481.

Kaye, G.I., Fenoglio, C.M., Pascal, R.R. & Lane, N. (1973) Comparative electron microscopic features of normal, hyperplastic and adenomatous human colonic epithelium. Gastroenterology, 64,926-945.

Kierszenbaum, A.L. (1969) Relationship between nucleolus and nuclear bodies in human mixed salivary tumours. Journal of Ultrastructure Research, 29, 459-469.

Kiistala, U. & Mustakallio, K.K. (1968) The presence of Langerhans cells in human dermis with special reference to their potential mesenchymal origin. Acta Dermato-Venereologica, 48,115-122.

Klug, H. & Gunther, W. (1972) Ultrastructural differences in human malignant melanomata. An electron microscopical study. British Journal of Dermatology, 86,395-407.

Kobayasi, T. (1969) Dermo-epidermal junction in invasive squamous cell carcinomæ. An electron microscopic study. Acta Dermato-Venereologica, 49,445- 457.

Konodo,, Y. (1969) Macrophage containing Langerhans cell granules in lymph nodes of rabbit. Zeitschrift fur Zellforschung Mikroskopische Anatomie, 98,506-511.

Konodo,, K., Tamura, H. & Tangiuchi, H. (1970) Intracellular microcyst in gastric cancer cells. Journal of Electron Microscopy, 19,41-49.

Krawczyk, W.S. & Wilgram, G.F. (1973) Hemidesmosome and desmosome morphogenesis during epidermal wound healing. Journal of Ultrastructure Research, 45,93-101.

Krishan, A., Uzman, B.G. & Hedley-Whyte, E.T. (1967) Nuclear bodies: a component of cell nuclei in hamster tissues and human tumours. Journal of Ultrastructure Research, 19,563-572.

Lev, R. (1965) The mucin histochemistry of normal and neoplastic gastric mucosa. Laboratory Investigation, 14, 2080-2100.

Lillibridge, C.B. (1964) The fine structure of normal human gastric mucosa, Gastroenterology, 47,269-290.

Lin, H., Lin, C., Yeh, S. & Tu, S. (1969) Fine structure of nasopharyngeal carcinoma with special reference to the anaplastic type. Cancer, 23,390-405.

Lipkin, M. (1971) Proliferation and differentiation of normal and neoplastic cells in the colon of man . Cancer, 28,38-40.

Lorenzsonn, V. & Trier, J.S. (1968) The fine structure of human rectal mucosa. The epithelial lining of the base of the crypt. Gastroenterology, 55,88-101.

Luibel, F.J., Sanders, E. & Ashworth, C.T. (1960) An electron microscopic study of carcinoma in situ and invasive carcinoma of cervix uteri. Cancer Research, 20,357-361.

Lynn, J.A., Martin, J.H. & Kingsley, W.B. (1967) Electron microscopy of surgical specimens from the cryostat. American Journal of Clinical Pathology, 49,232-236.

Makela, V., Korhonen, L.K. & Lilius, G. (1971) Carbohydrate-rich compounds in the colonic mucosa of man. 1. Histochemical characteristics of normal and adenomatous colonic mucosa. Cancer, 27, 120-127.

Martinez-Palomo, A. (1970) Ultrastructural modification of intercellular junction in some epithelial tumours. Laboratory Investigation, 22,605-614.

Masson, P. (1926) Les nevi pigmentaries, tumeurs nerveuses. Annales d' Anatomie Pathologique, 3,417-453.

Masson, P. (1951) My conception of cellular nevi. Cancer, 4,9-38.

Masurousky, E.B., Benitez, H.H. & Murray, M. (1970) Origin, development and nature of intranuclear rodlets and associated bodies in chicken sympathetic neurons. Journal of Cell Biology, 44,172-191.

Matoltsy, A.G. & Parakkal, P.F. (1965) Membrane-coating granules of keratinizing epithelium. Journal of Cell Biology, 24,297-307.

McGavran, M.H. (1965) The ultrastructure of papillary cystadenoma lymphomatosum of the parotid gland. Virchows Archiv fur Pathologische Anatomie, 338,195-202.

Mercer, E.H. (1961) The electron microscopy of normal and neoplastic cells. Proceedings of the Royal Socicty of Medicine, 54,1057-1064.

Mishima, Y. & Pinkus, H. (1968) Electron microscopy of keratin layer stripped human epidermis. Journal of Investigative Dermatology, 50,89-102.

Morales, A.R., Fine, G., Horn, R.C. & Watson, J.H. (1969) Langerhans cells in localized lesions of the eosinophilic granuloma type. Laboratory Investigation, 20,412-423.

Morson, B.C. (1968)Precancerous and early malignant lesions of the large intestine. British Journalof Surgery, 55,725-731.

Mueller, C.B., Menefee, M. & Ivler, D. (1960) Intracytoplasmic inclusions in colon carcinoma. Surgery, 48,261-270.

Mugnaini, E. (1964) Filamentous inclusions in the matrix of mitochondria from human livers. Journal of Ultrastructure Research, 11,525-544.

Nagl, W. (1973) Intranuclear microtubules in Trophocytes of Dytiscus. Journal of Ultrastructure Research, 42,283-286.

Niebauer, G., Krawczyk, W.S., Kidd, L. & Wilgram, G.F. (1969) Osmium zinc iodide reactive sites in epidermal Langerhans cells. Journal of Cell Biology, 43,80-89.

Norton, W.L. (1969) Endothelial inclusions in active lesions of systemic lupus erythematosus. Journal of Laboratory and Clinical Medicine, 74,369-379.

Onoe, T. (1962) Electron microscopic studies of human carcinoma. Journal of Electron Microscopy, 11,70-84.

Overton, J. (1973) Experimental manipulation of desmosome formation. Journal of Cell Biology, 56,636-646.

Ozzello, L. (1971) Ultrastructure of intraepithelial carcinoma of the breast. Cancer, 28,1508-1515.

Patrizi, G. & Middlekamp, J.N. (1969) In vivo and vitro demonstration of nuclear bodies in vaccinia infected cells. Journal of Ultrastructure Research, 28, 275-287.

Pearse, A.G. (1972) Histochemistry, theoretical and applied. Volume 2. London: Churchill

Perier, O. & Vanderhaeghem, J.J. (1967) Subacute sclerosing leuco-encephalitis. Electron microscopic finding in two cases with inclusion bodies. Acta Neuropathologica, 8,362-380.

Pinkus, T., Blacklow, N.R., Grimley, P.M. & Bellanti, J.A. (1970) Glomerular microtubules of systemic lupus erythematosus. Lancent, 2, 1058-1061.

Pittman, F.E. & Pittman, J.C. (1966) An electron microscopic study of the epithelium of normal human sigmoid colonic mucosa. Gut, 4, 644-661.

Polack, F.M., Kanai, A. & Hood, C.I. (1971) Light and electron microscopic studies of orbital rhabdomyosarcoma. American Journalof Ophthalmology, 71, 75-83.

Popoff, N. & Stewart, S. (1968) The fine structure of nuclear inclusions in the brain of experimental golden hamster. Journal of Ultrastructure Research, 23, 347-361.

Prunieras, M. (1969) Interaction between keratinocytes and denderitic cells. Journal of Investigative Dermatology, 52, 1-17.

Reams, W.M. (1973) Ectodermal origin of epidermal Langerhans cells. Anatomical Record, 175, 421.

Rickson, F.R. (1968) Nuclear and cytoplasmic tubules in cortical cells of leaf Beltian bodies. Journal of Cell Biology, 38, 471-474.

Robertson, D.M. (1964) Electren microscopic studies of nuclear inclusions in meningiomas. American Journal of Pathology, 45, 835-848.

Robertson, D.M. & Maclean, J.D. (1965) Nuclear inclusions in malignant gliomas. Archives of Neurology, 13, 287-296.

Rambourg, A. & Leblond, C.P. (1967) Electron microscope observations on the carbohydrate-rich cell coat present at the surface of cells in the rat. Journal of Cell Biology, 32, 27-53.

Rosai, J. & Rodriguez, H.A. (1968) Application of electron microscopy to the differential diagnosis of tumours. American Journal of Clinical Pathology, 50,555-562.

Roth, S.I., Olen, E. & Hansen, L.S. (1962) The eosinophilic cells of the parathyroid(oxyphil cells), slivary(oncocytes) and thyroid(Hurthle cells) glands. Laboratory Investigation, 11,933-941.

Rowden, G. (1966) Membrane-coating granules of mouse oesophageal and gastric epithelium. Journal of Investigative Dermatology, 47,359-362.

Rubin, W., Ross, L.L., Sleisenger, M.H. & Jeffries, G.H. (1968) The normal human gastric epithelium. A fine structural study. Laboratory Investigation, 19,598-626.

Sagebiel, R.W. (1973) In vivo and in vitro uptake of ferritin by Langerhans cells of the epidermis. Journal of Investigative Dermatology, 58,47-54.

Sasano, N., Nakamura, K., Arai, M. & Akazaki, K. (1969) Ultrastructural cell pattern in human gastric carcinoma compared with non neoplastic gastric mucosa. Histologic analysis of carcinoma by mucin histochemistry. Journal of National Cancer Institute, 43,783-802.

Seiji, M. & Mizuno, F. (1969) Electron microscopic study of Bowen's disease. Archives of Dermatology, 99,3-16.

Seite, R. (1970) Etude ultrastructurale de divers types d' inclusions nucleaires dan les neurones sympathiques du chat. Journal of Ultrastructure Research, 30,152-165.

Seite, R., Escaig, J. & Couineau, S. (1971) Microfilaments et microtubules nucleaires et organisation ultrastructurale des battonnets intranucleaires des neurones sympathiques. Journal of Ultrastructure Research, 37,449-478.

Seljelid, R. & Ericsson, J.L. (1965) An electron microscopic study of mitochondria in renal clear cell carcinoma. Journal de Microscopie, 4,759-770.

Shamoto, M., Kaplan, C. & Katoh, A.K. (1971) Langerhans cell granules in human hyperplastic lymph nodes. Archives of Pathology, 92,46-52.

Shklar, G. & Chauncey, H.H. (1965) Papillary cystadenoma lymphomatosum, a developmental malformation; histochemical evidence. Journal of Oral Surgery, 23,222-230.

Siegesmund, K.A., Dutta, C.R. & Fox, C.A. (1964) The ultrastructure of the intranuclear rodlet in certain nerve cells. Journal of Anatomy, 98,93-97.

Silberberg, I. (1973) Apposition of mononuclear cells to Langerhans cells in contact allergic reactions. Acta Dermato-Venereologica, 53,1-12.

Silberberg, I., Baer, R.L. & Rosenthall, S. (1974) Circulating Langerhans cells in a dermal vessel. Acta Dermato-Venereologica, 54,81-86.

Smetana, K., Gyorkey, F., Gyorkey, P. & Busch, H. (1970) Comparative studies on the ultrastructure of nucleoli in human lymphosarcoma cells and leukemic lymphocytes. Cancer Research, 30,1149-1155.

Smetana, K., Gyorkey, F., Gyorkey, P. & Busch, H. (1971) Compact filamentous bodies of nuclei and nucleoli of human prostate gland. Experimental Cell Research, 664,133-139.

Sobrinho-Somes, M.A. & Goncalves, V. (1974) Nuclear bodies in papillary carcinoma of the human thyroid gland. Archives of Pathology, 98,94-99.

Spjut, H.J. & Smith, M.N. (1967) A comparative electron microscopic study of human and rat colonic polyps and carcinoma. Experimental and Molecular Pathology, 6,11-24.

Springs, A.I. & Jerrome, D.W. (1975) Intracellular mucous inclusions. A feature of malignant cells in effusions in the serous cavities, particularly due to carcinoma of the breast. Journal of Clinical Pathology, 28,929-936.

Straile, W.S., Tipnis, U.R., Mann, S.J. & Clark, W.H. (1975) Lattice and rodlet nuclear inclusions in Merkel cells in rabbit epidermis. Journal of Investigative Dermatology, 64,178-183.

Suzuki, H. & Matsuyama, M. (1971) Ultrastructure of functioning β-cell tumours of the pancreatic islets. Cancer, 28,1302-1313.

Swanbeck, G. & Thyresson, N. (1964) Electron microscopy of intranuclear particles in lichen ruber planus. Acta Dermato-Venereologica, 44,105-106.

Szernobilsky, B. & Tsou, K.C. (1968) Adenocarcinoma, adenomas and polyps of the colon. Histochemical study. Cancer, 21,165-177.

Takaki, Y., Masutani, M. & Kawada, A. (1971) Electron microscopic study of keratoacanthoma. Acta Dermato-Venereologica, 51,21-26.

Tanaka, K. & Mizunaga, T. (1974) Striated and crystalline inclusions in the nuclei and cytoplasm of intact yeast cells and yeast protoplasm. Journal of Ultrastructure Research, 48,124-137.

Tandler, B. (1966a) Warthin's tumour. Electron microscopic studies. Archives of Otolaryngology, 84,91-98.

Tandler, B. (1966b) Fine structure of oncocytes in human salivary gland. Virchows Archiv fur Pathologische Anatomie, 341,317-326.

Tandler, B., Denning, C.R., Mandel, I.D. & Kutscher, A.H. (1969) Ultrastructure of human labial salivary glands. 1. Acinar secretory cells. Journal of Morphology, 127,383-408.

Tandler, B., Denning, C.R., Mandel, I.D. & Kutscher, A.H. (1970) Ultrastructure of human labial salivary glands. 3. Myoepithelium and ducts. Journal of Morphology, 130,227-245.

Tandler, B. & Ross, L.L. (1969) Observations of nerve terminals in human labial salivary glands. Journal of Cell Biology, 42,339-343.

Tandler, B. & Shipkey, F.H. (1964) Ultrastructure of Warthin's tumour. Journal of Ultrastructure Research, 11,292-305.

Tarnowski, W.M. & Hashimoto, K. (1967) Langerhans cell granules in histiocytosis X. The epidermal Langerhans cells as macrophages. Archives of Dermatology, 96,298-304.

Thiery, J.P. (1967) Mise en evidence des polysaccharides sur coupes fines en micrescopie electronique. Journal de Microscopie, 6,987-1018.

Tisher, C.C., Bulger, R.E. & Trump, B.F. (1966) Human renal ultrastructure. 1. Proximal tubule of healthy individuals. Laboratory Investigation, 15,1357-1394.

Toner, P.G. & Ferguson, A. (1971) Intraepithelial cells in human intestinal mucosa. Journal of Ultrastructure Research, 34,329-344.

Uzman, B.G., Saito, H. & Kasac, M. (1971) Tubular arrays in the endoplasmic reticulum in human tumour cells. Laboratory Investigation, 24,492-498.

Vella , A. & Lee, P. (1974) Morphogenesis of wheat striate mosiac virus . The internal nucleoprotein component. Journal of Ultrastructure Research, 47,169-178.

Vernon, M.L., Fountain, L., Krebs, M.M., Horta-Barbosa,L., Fuccillo, D.A. & Sever, J.L. (1973) Birbeck granules (Langerhans granules) in human lymph node. American Journal of Clinical Pathology, 60,771-779.

Voth, D. (1962) Phases of cell structure in papillary cystadenolymphoma and their effect on the tumour form. Frankfurt Zeitschrift fur Pathologische, 71,523-530.

Waterhouse, J.P. & Squire, C.A. (1967) The Langerhans cell in human gingival epithelium. Archives of Oral Biology, 12,341-348.

Watson, J.H. & Swedo, J.L. (1968) The Langerhans granule in histiocytoma. Its structure, location and possible genesis. Journal of Cell Biology, 39,159a-160a.

Wells, C.L., Moron, T.J. & Cooper, W.M. (1962) Villous tumours of the rectosigmoid colon with severe electrolyte imbalance. American Journal of Clinical Pathology, 37,507-514.

Wergin, W.P., Gruber, P.J. & Newcomb, E.H. (1970) Fine structural investigation of nuclear inclusions in plants. Journal of Ultrastructure Research, 30,533-557.

Weinstock, M. & Wilgram, G.F. (1970) Fine structural observation and enzymatic activity of keratinosomes in mouse tongue filiform papillae. Journal of Ultrastructure Research, 30,262-274.

Wolff, K. & Schreiner, E. (1970) Uptake of intracellular transport and degradation of exogenous protein by Langerhans cells. Journal of Investigative Dermatology, 54,37-47.

Wood, E.M. (1967) An ordered complex of filaments surrounding the lipid droplets in developing adipose cells. Anatomical Record, 157,437-448.

Woods, D.A. & Smith, C.J. (1969) Ultrastructure of the dermal-epidermal junction in experimentally induced tumours and human lesions. Journal of Investigative Dermatology, 52,259-263.

Yeh, S., Chen, H.C., How, S.W. & Deng, C.S. (1974) Fine structure of Bowen's disease in chronic arsenicalism. Journal of the National Cancer Institute, 53,31-44.

Younes, M.S., Robertson, E.M. & Bencosme, S.A. (1968) Electron microscopic observation of Langerhans cells in the cervix. American Journal of Obstetrics and Gynecology, 102,397-403.

Zelickson, A.S. (1965) The Langerhans cell. Journal of Investigative Dermatology, 44,201-212.

Zelickson, A.S. & Hartmann, J.F. (1962) An electron microscope study of normal human non keratinizing oral mucosa. Journal of Investigative Dermatology, 38,99-107.

NORMAL HUMAN OESOPHAGUS

Figure 1. Basal cells of squamous mucosa. Notice the distinct intercellular spaces (S) and the nuclear bodies (arrows). The cells are separated by a lamina densa from the underlying stroma.

Magnification 13800.

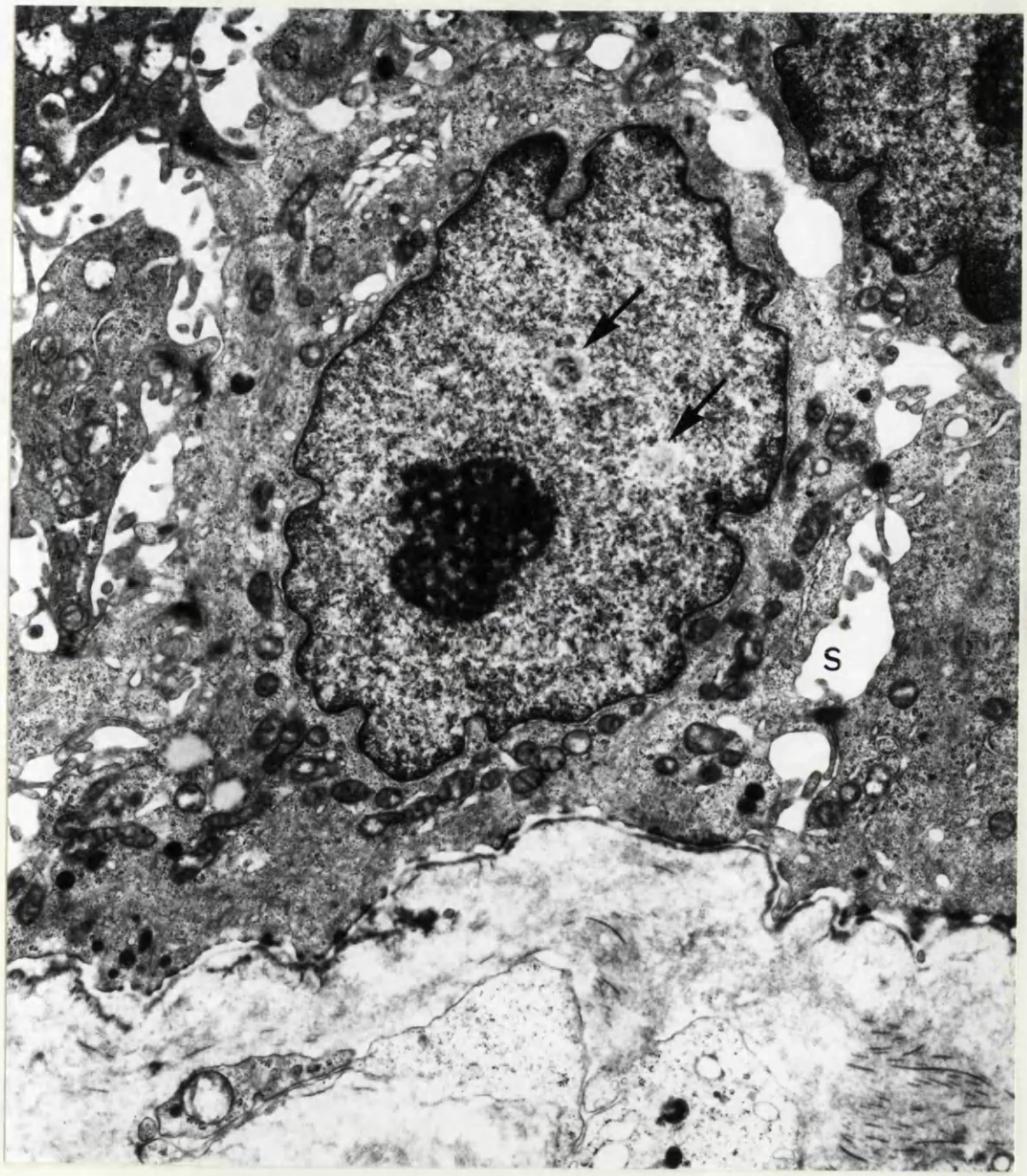

1

NORMAL HUMAN OESOPHAGUS

Figure 2. Base of squamous mucosa, showing basal lamina (B) and hemidesmosomes (H). Numerous free ribosomes are seen in the cytoplasm.

Magnification 40000.

Figure 3. Intermediate zone of squamous mucosa, showing the typical appearance of the cells and their inter-relationships. Prominent desmosomes are seen (D), with associated tonofilaments.

Magnification 11040.

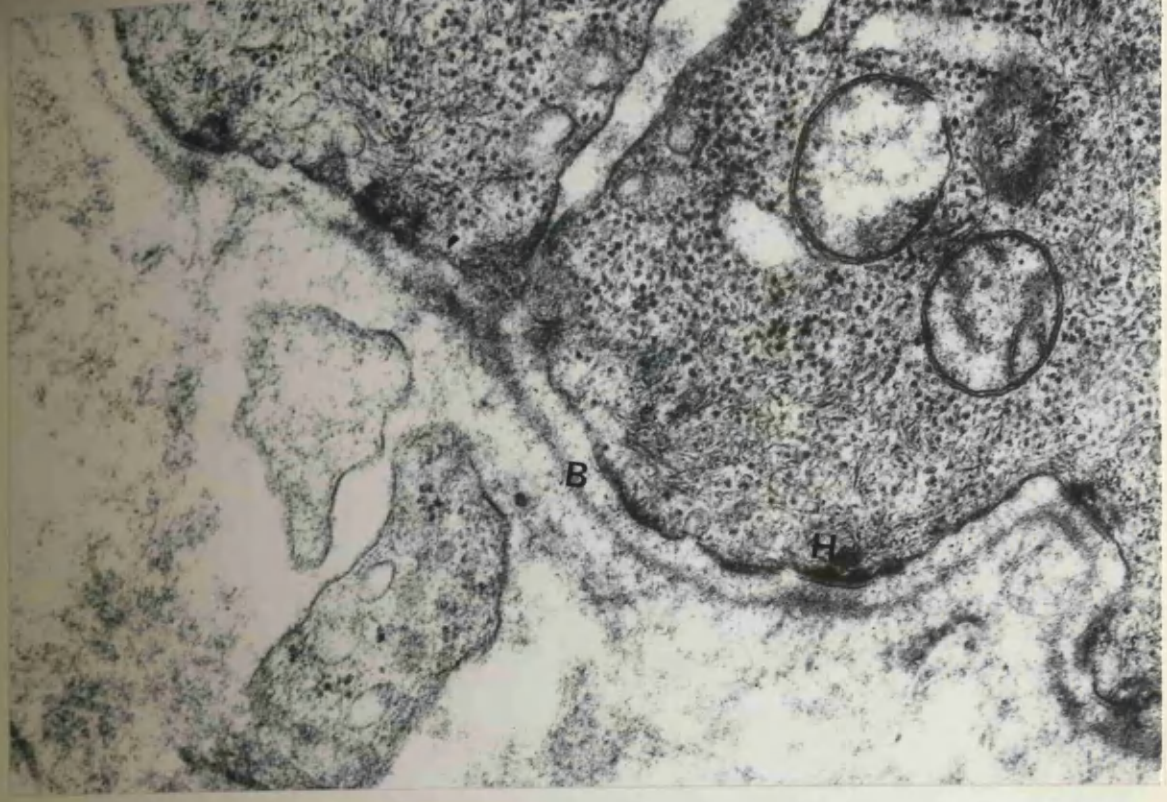

2

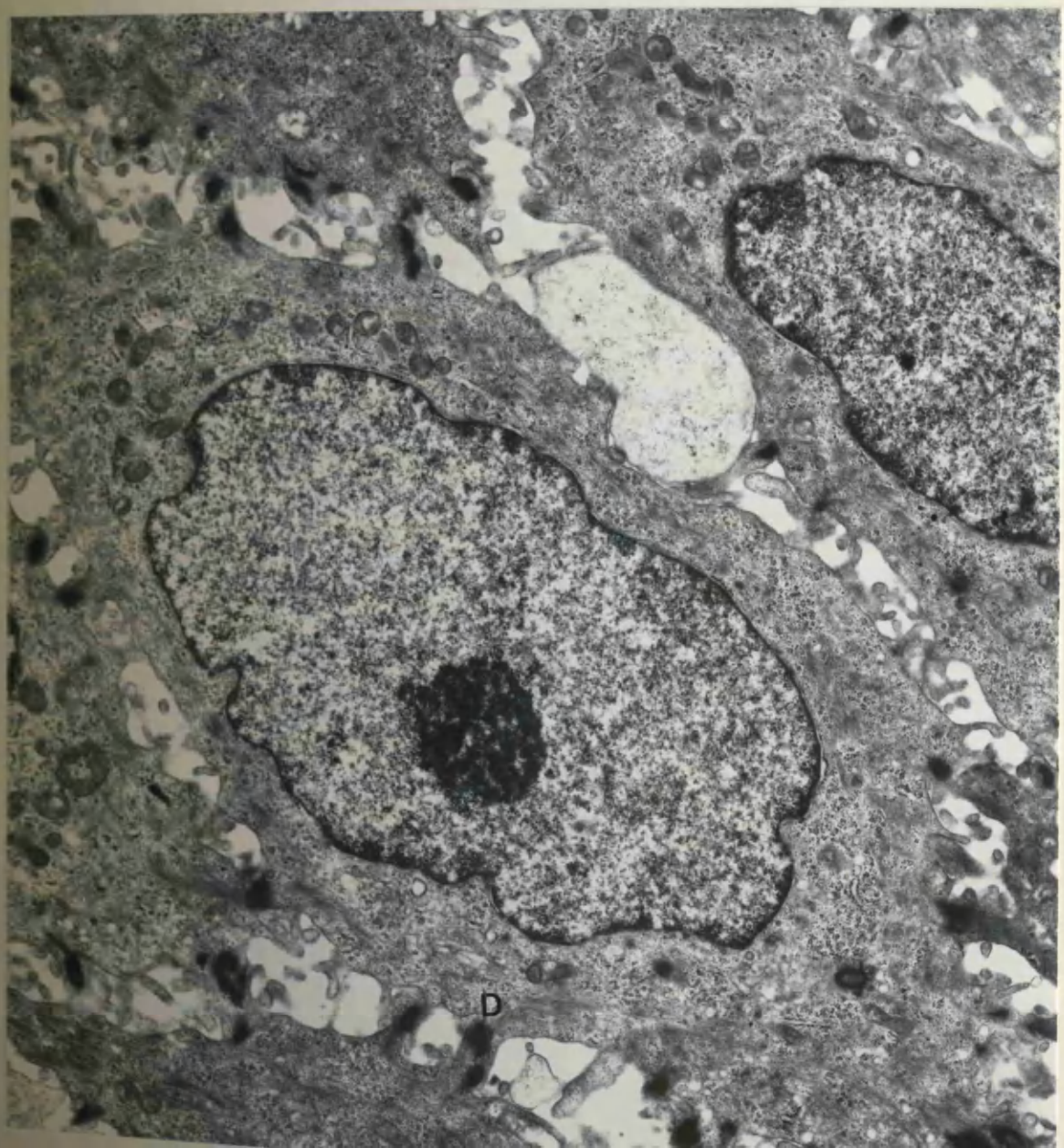

3

Figure 4. Several typical desmosomes (D) with associated tonofilaments. An intracytoplasmic desmosome (arrow) lies in association with other tonofilament aggregates. Notice the Golgi system, (G).

Magnification 39000.

Figure 5. Rudimentary cilium originating in a basal body and projecting into a pocket at the cell surface.

Magnification 67250.

Figure 6. Transverse section of a rudimentary cilium in the intercellular space, between squamous cells. Notice that only six peripheral components are seen instead of the usual nine.

Magnification 84000.

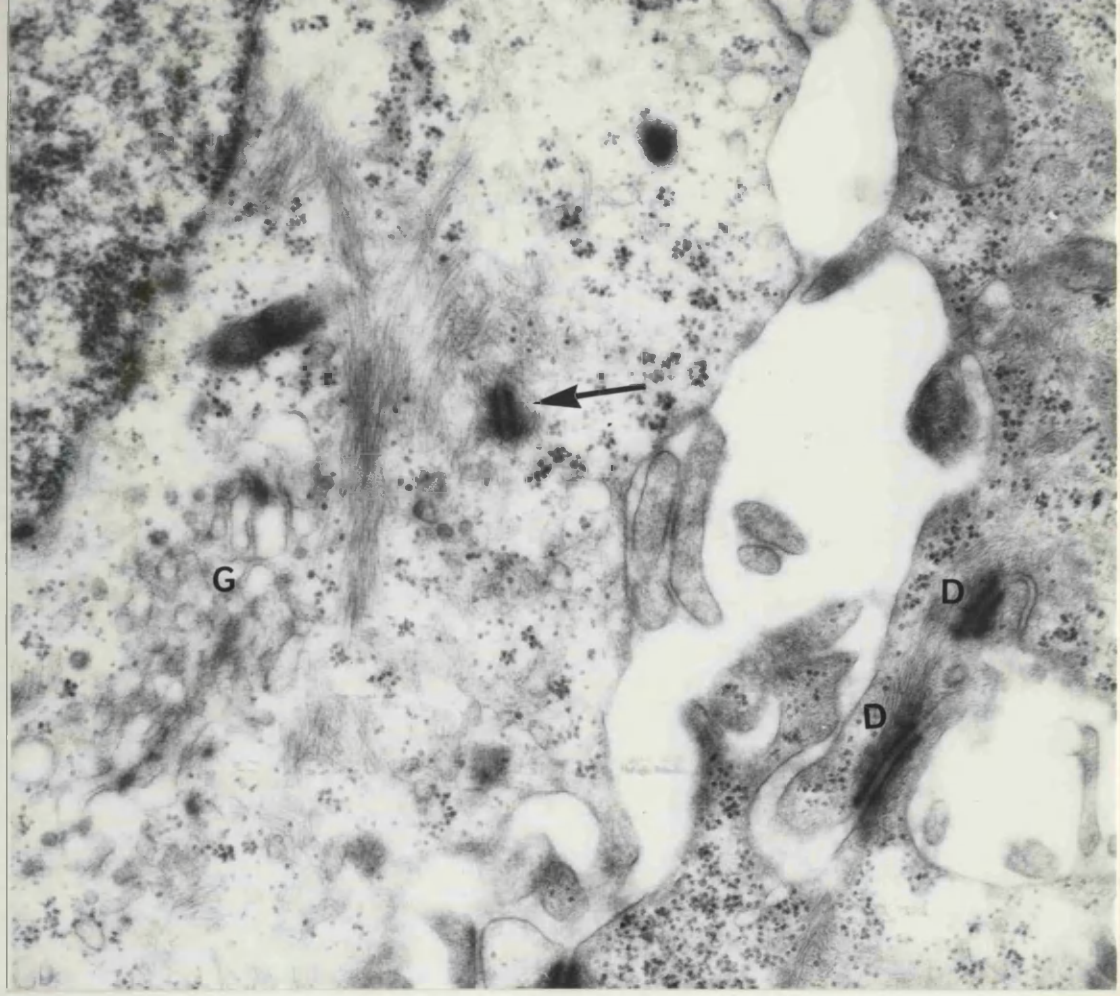

4

5

6

NORMAL HUMAN OESOPHAGUS

Figure 7. Superficial zone of squamous mucosa, showing retained nuclei and diffuse cytoplasmic tonofilaments.

Magnification 10750.

Figure 8. Surface of squamous mucosa, showing flattened cells with diffuse tonofilamentous contents and residual desmosomes (D). Note the prominence of tonofilaments and the asymmetrical thickening of the cell membrane.

Magnification 88250.

Figure 9. High magnification of the cell membrane of the cells of the superficial zone of squamous mucosa. The inner lamina shows a pronounced linear thickening, giving an asymmetrical appearance to the cell surface. Wisps of extracellular cell coat material can be made out, adhering to the outer lamina.

Magnification 199250.

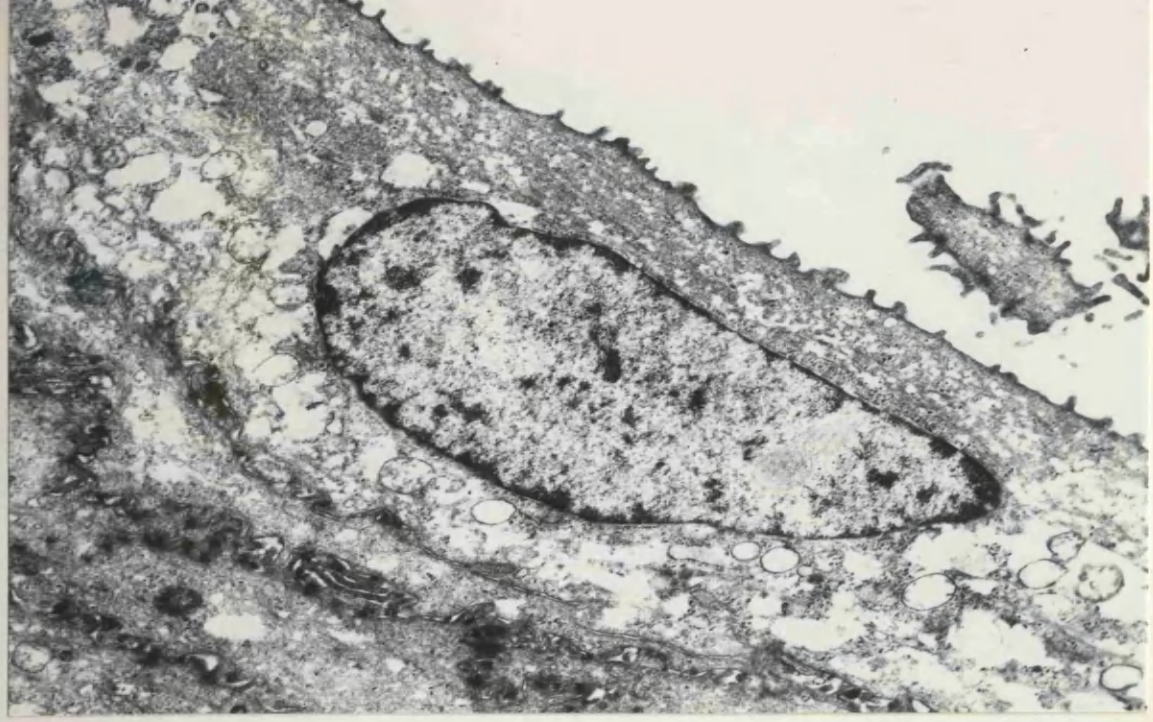

7

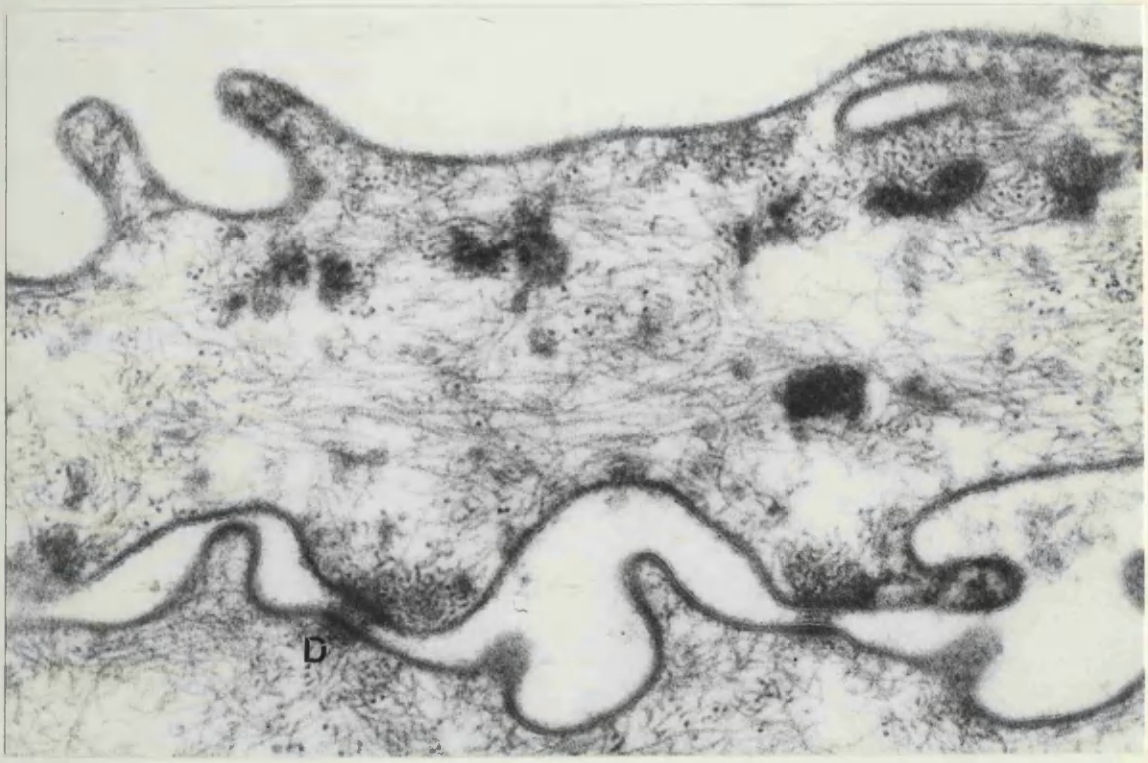

8

9

Figure 10. "Membrane-coating granules" of upper intermediate zone of the mucosa. Notice the trilaminar limiting membrane, pale halo and dense core.

Magnification 143460.

Figure 11. Two membrane-coating granules are seen. Notice the lamellation in the larger one, an appearance reminiscent of the granules of keratinising squamous epithelium.

Magnification 155000.

Figure 12. Membrane-coating granule discharging its dense contents into the intercellular space by a process of exocytosis.

Magnification 155000.

Figure 13. Carbohydrate stain indicates the presence of a positive staining component in the halo of the membrane-coating granules. Note the presence of glycogen granules (arrows).

Magnification 70600.

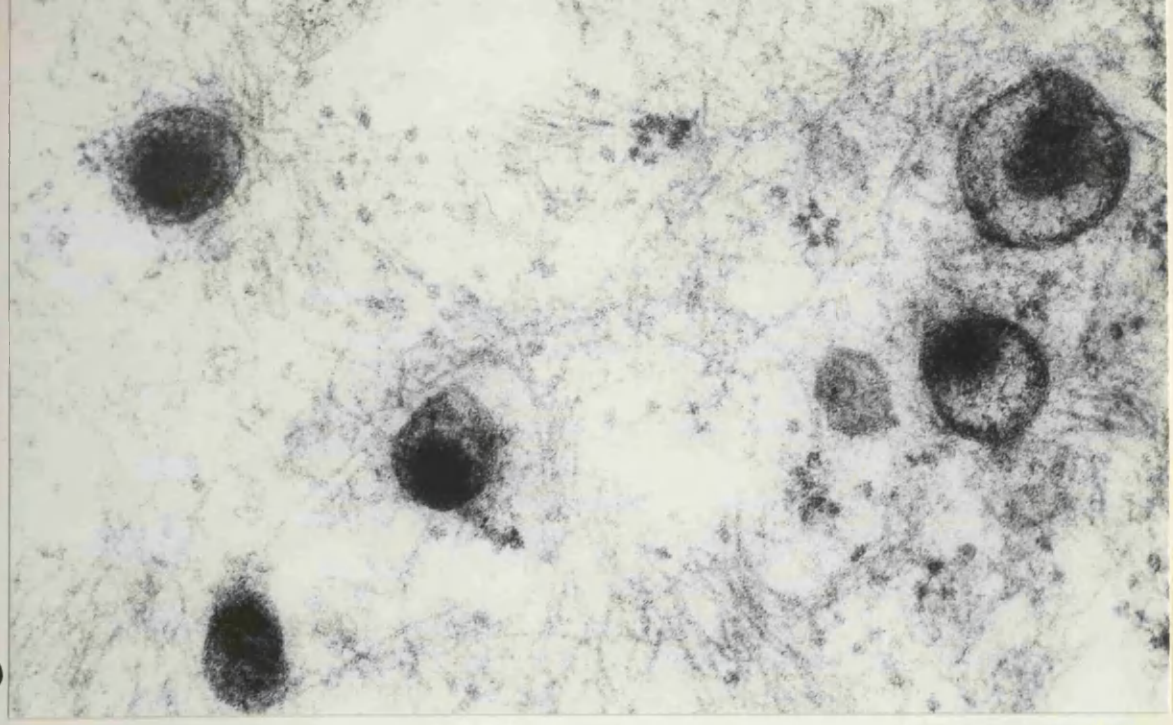

10

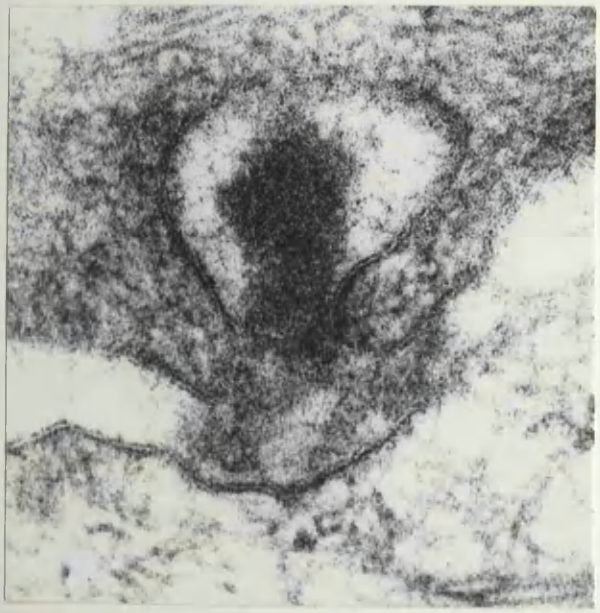

12

11

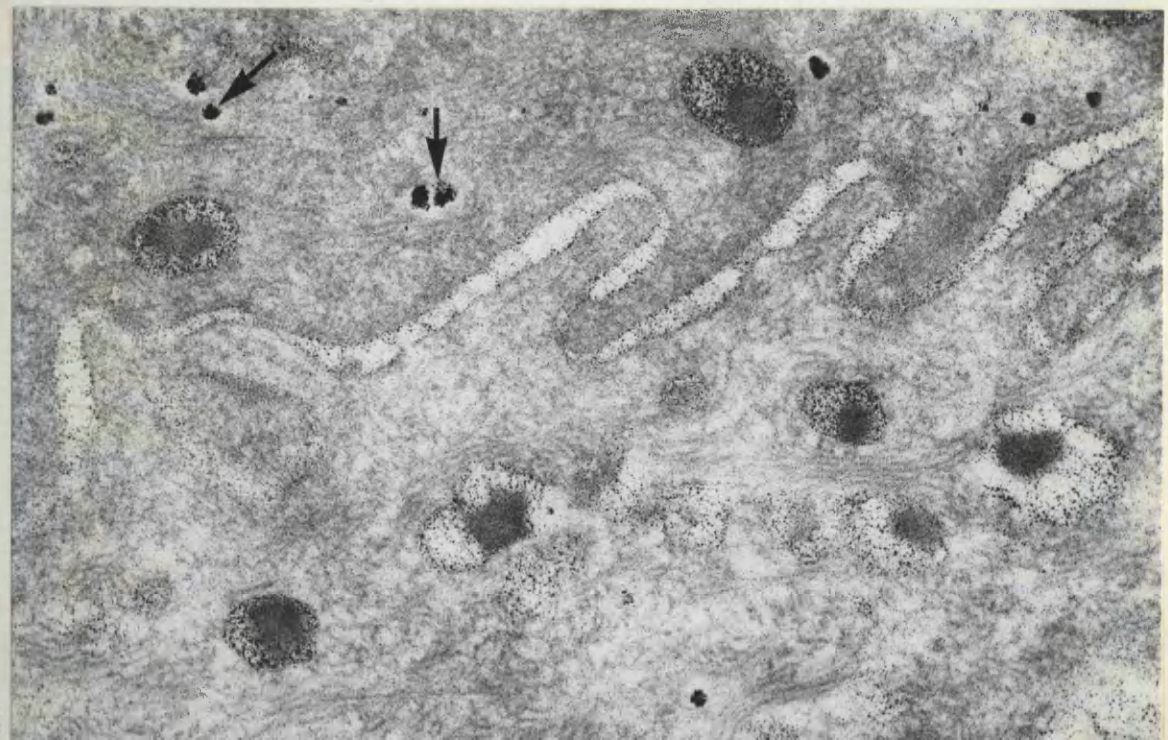

13

NORMAL HUMAN OESOPHAGUS

Figure 14. Carbohydrate stain to demonstrate the cell coat. Note the presence of glycogen granules (arrows).

Magnification 93200.

Figure 15. Carbohydrate stain indicates the presence of masses of glycogen in the cytoplasmic vacuoles of the superficial cells.

Magnification 11040.

Figure 16. Carbohydrate stain to demonstrate glycogen granules in the intracytoplasmic spaces of the superficial cells. Notice unstained nucleus (N) and mitochondria (M).

Magnification 18200.

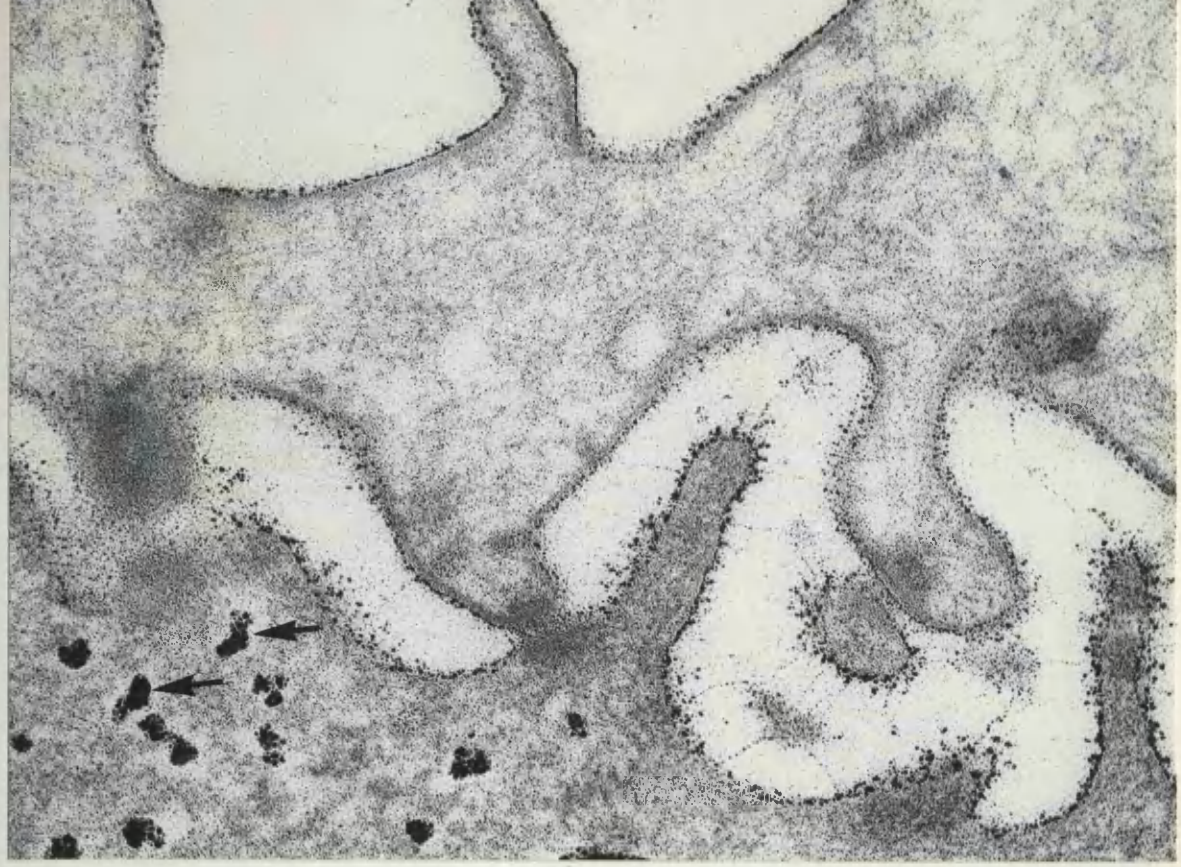

14

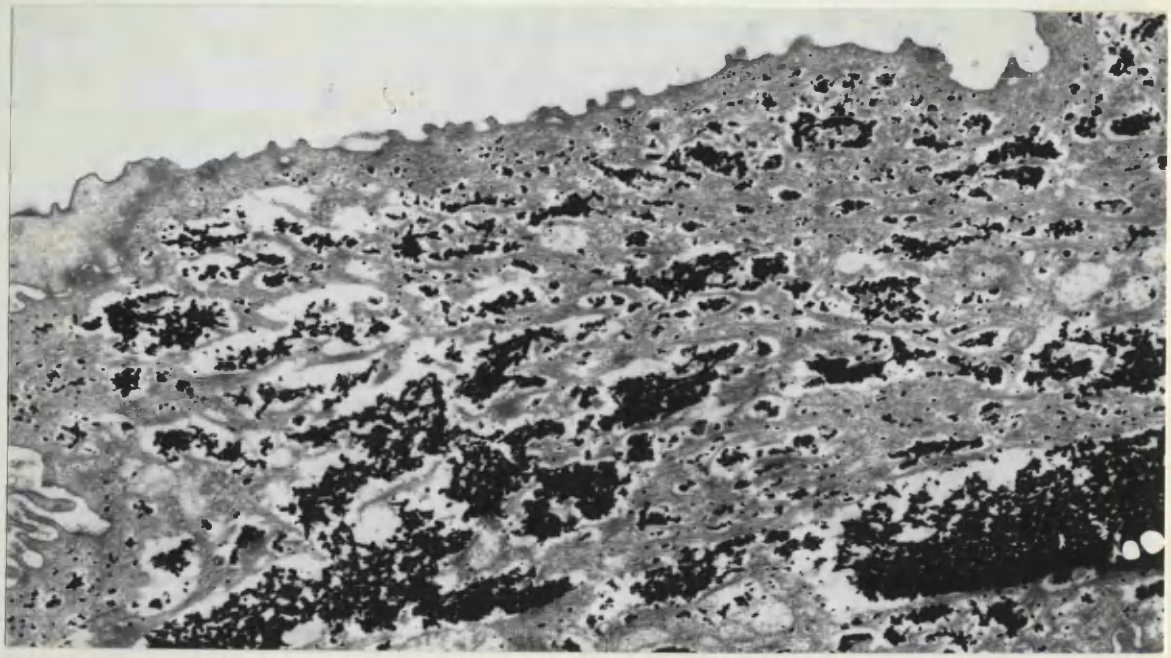

15

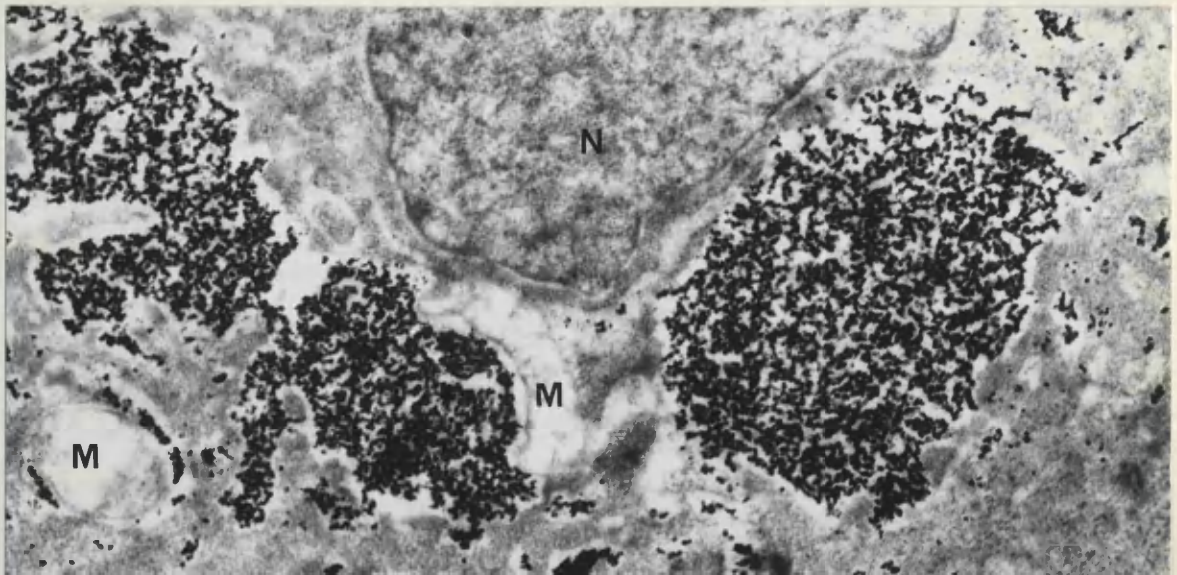

16

NORMAL HUMAN OESOPHAGUS

Figure 17. Acid phosphatase activity. A coarse granular electron dense deposit of lead phosphate lies in the intercellular spaces of the normal squamous mucosa of oesophagus.

Magnification 8400.

Figure 18. Acid phosphatase activity. Dense deposit of lead phosphate on the cell membrane. Note the absence of reaction product from membrane-coating granule (arrow).

Magnification 116500.

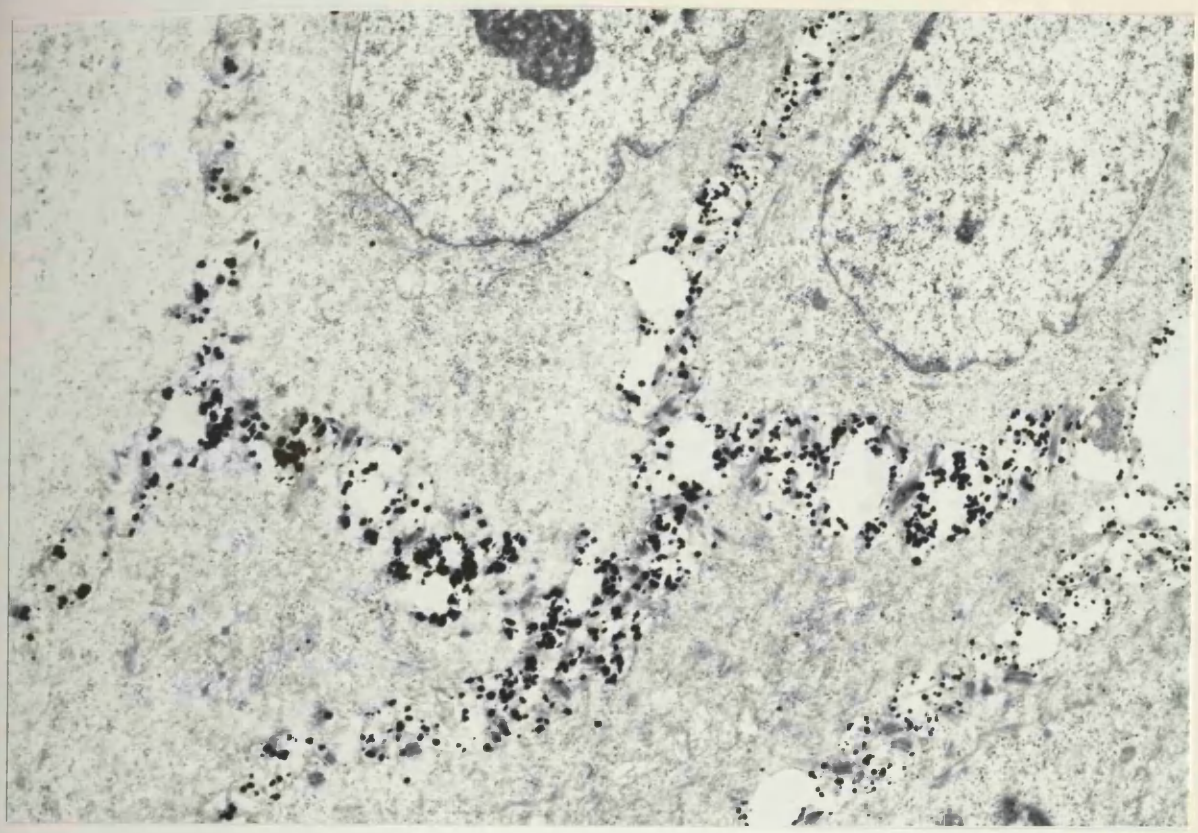

17

18

SUBMUCOSAL GLANDS OF OESOPHAGUS

Figure 19. The typical bulging surface of the principal cells is shown, with two of the pale mucus granules undergoing discharge into the lumen. Only scanty short microvilli are seen.

Magnification 13800.

Figure 20. The bases of two acini are shown with intervening connective tissue. Notice the principal cells with mucous granules (G), elaborate granular endoplasmic reticulum and mitochondria. Notice the "duplex" inclusion (D). Parts of two myoepithelial cells (M) are seen, sandwiched between the principal cells and the basal lamina.

Magnification 17500.

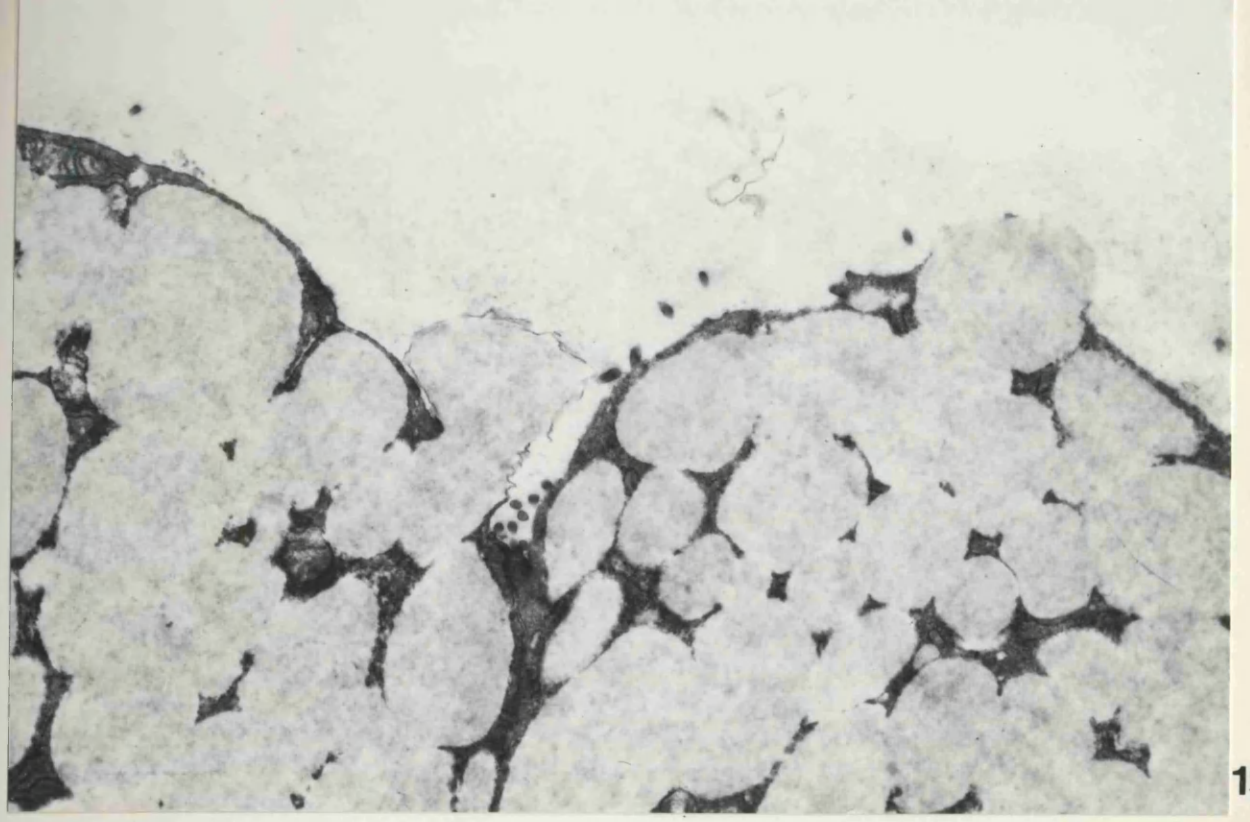

19

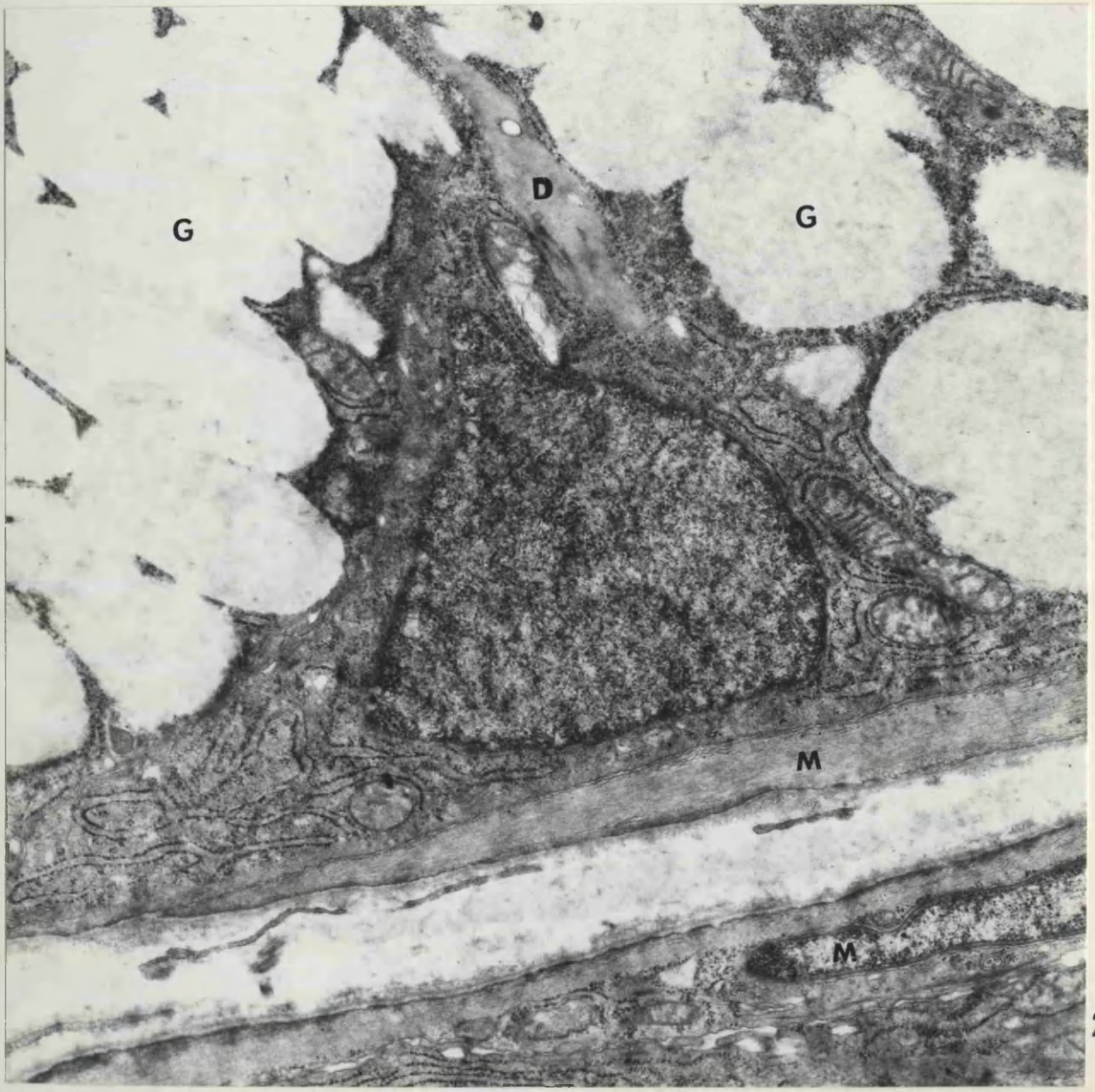

20

SUBMUCOSAL GLANDS OF OESOPHAGUS

Figure 21. Two aggregates of intramitochondrial tubular inclusions are seen in a principal cell. Notice both the longitudinal (L) and transverse sections (T) of these microtubules.

Magnification 39000.

Figure 22. A "duplex" inclusion in a principal cell, consisting of filamentous material with a single vacuole. Note the surrounding granular endoplasmic reticulum.

Magnification 32250.

Figure 23. Principal cells are identified by their empty granules. Two subsidiary cells are seen, one with homogenous granules and one with no granules. The lumen is shown (L).

Magnification 14000.

21

22

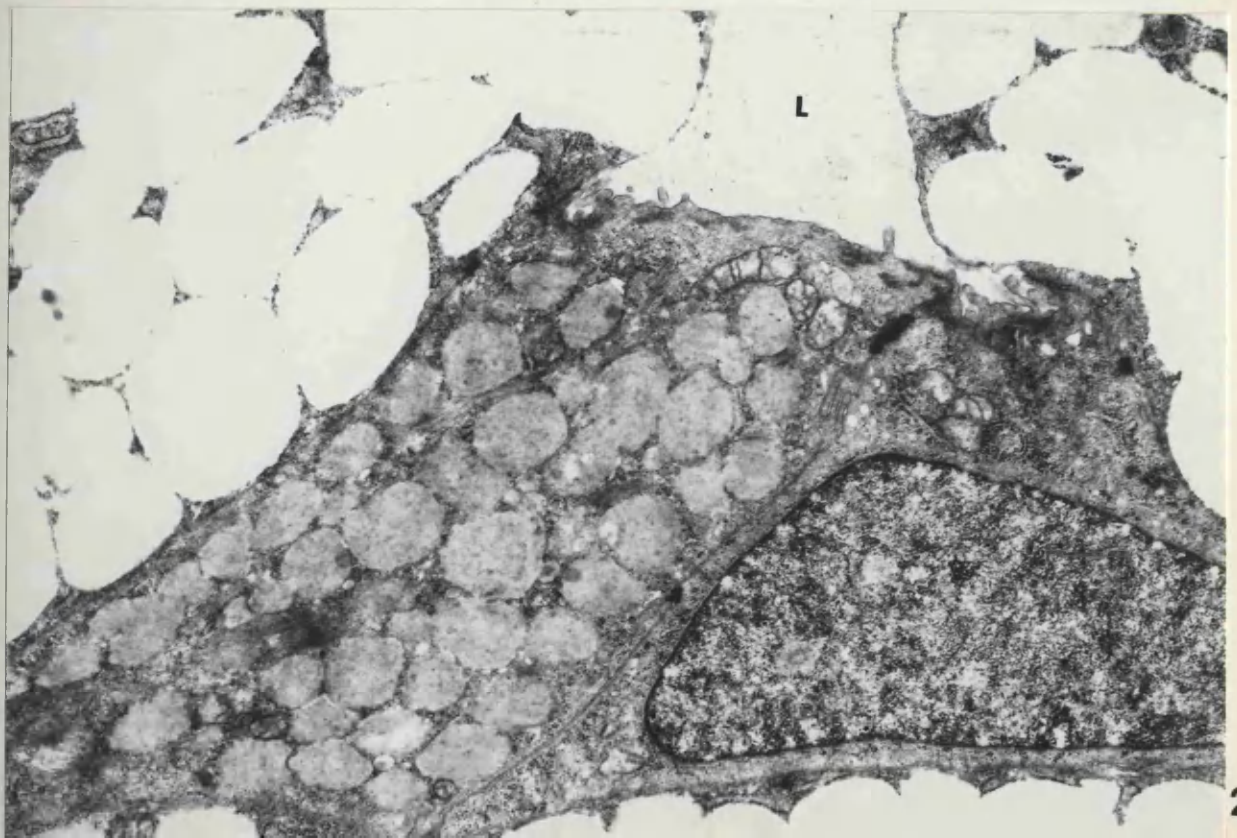

23

SUBMUCOSAL GLANDS OF OESOPHAGUS

Figure 24. A further subsidiary cell type in the submucosal gland is identified by its heterogenous granules and its numerous cytoplasmic filaments.

Magnification 31200.

Figure 25. Two "duplex" inclusions are shown in a principal cell. Notice the absence of vacuoles in one of them.

Magnification 51250.

Figure 26. Another pair of subsidiary cells with no secretion granules. The principal cell is identified by its empty granules. The lumen is shown (L).

Magnification 14000.

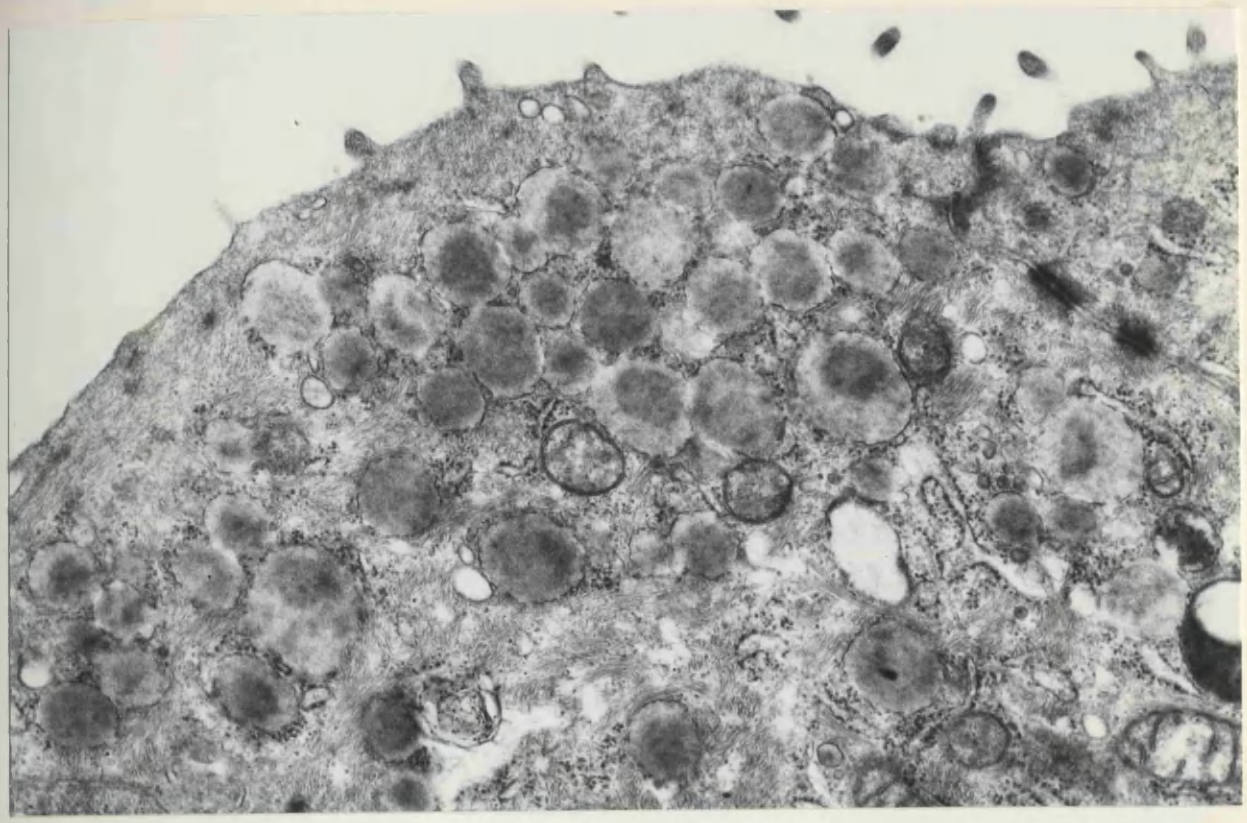

24

25

26

SUBMUCOSAL GLANDS OF OESOPHAGUS

Figure 27. The bases of two gland acini are shown with intervening connective tissue. Note the principal cells with empty granules and elaborate granular endoplasmic reticulum and Golgi system (G). A myo-epithelial cell is seen (M) at the acinar base. One desmosome (arrow) is shown between this cell and the overlying principal cell.

Magnification 11040.

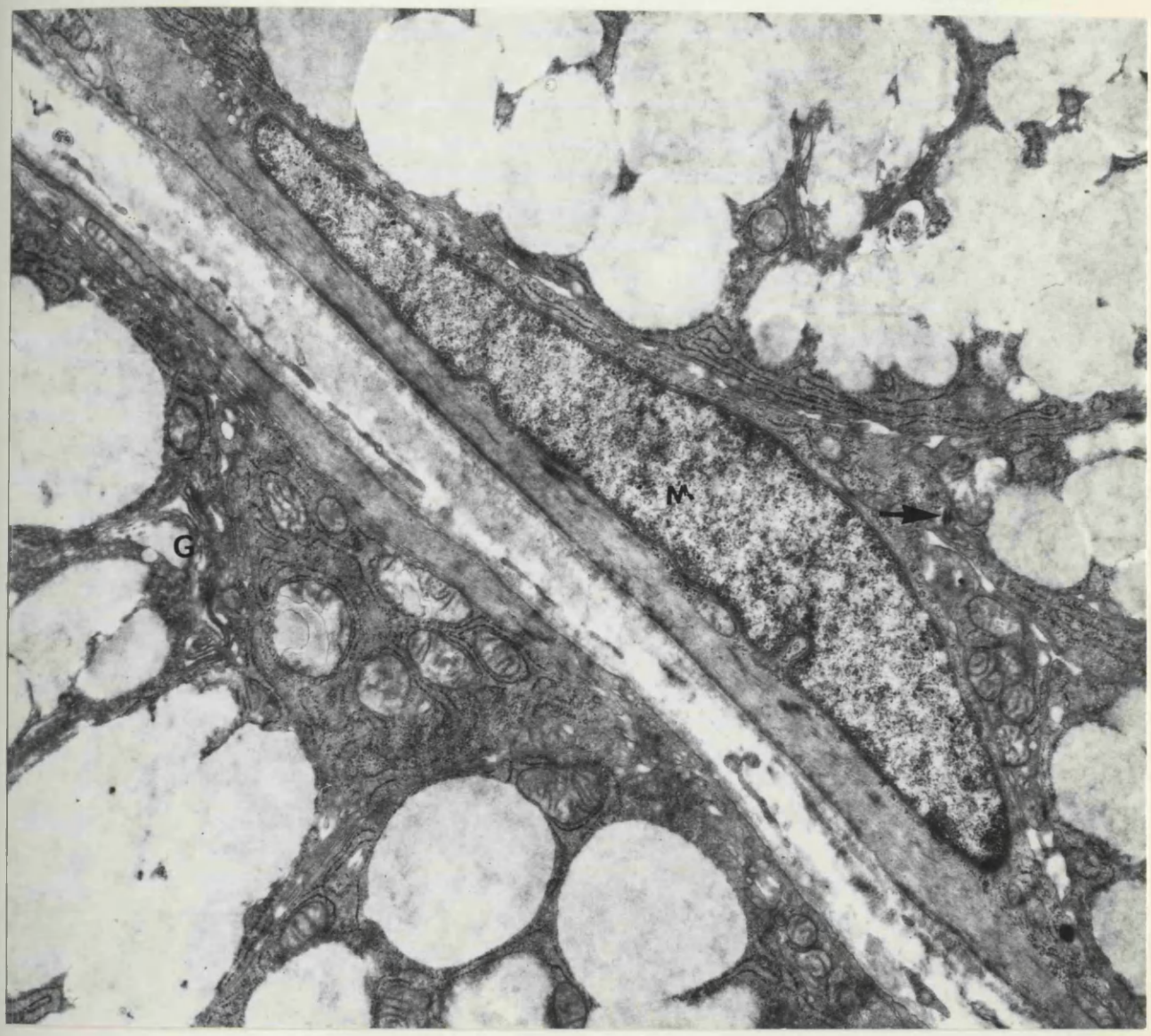

27

SUBMUCOSAL GLANDS OF OESOPHAGUS

Figure 28. Junction of acinus and duct. A principal cell (P), a subsidiary cell (S) and an oncocyte (O) can be identified by their distinctive features.

Magnification 11040.

28

SUBMUCOSAL GLANDS OF OESOPHAGUS

Figure 29. Oncocyte, showing numerous mitochondria and a small Golgi system (G). The adjacent oncocytes are connected by desmosomes.

Magnification 18200.

Figure 30. Unmyelinated nerves in the connective tissue of the submucosal glands. Note the acinar base, (arrow) with its basal lamina.

Magnification 22750.

Figure 31. Part of an oncocyte, showing the structure of the mitochondria and small dense bodies.

Magnification 17500.

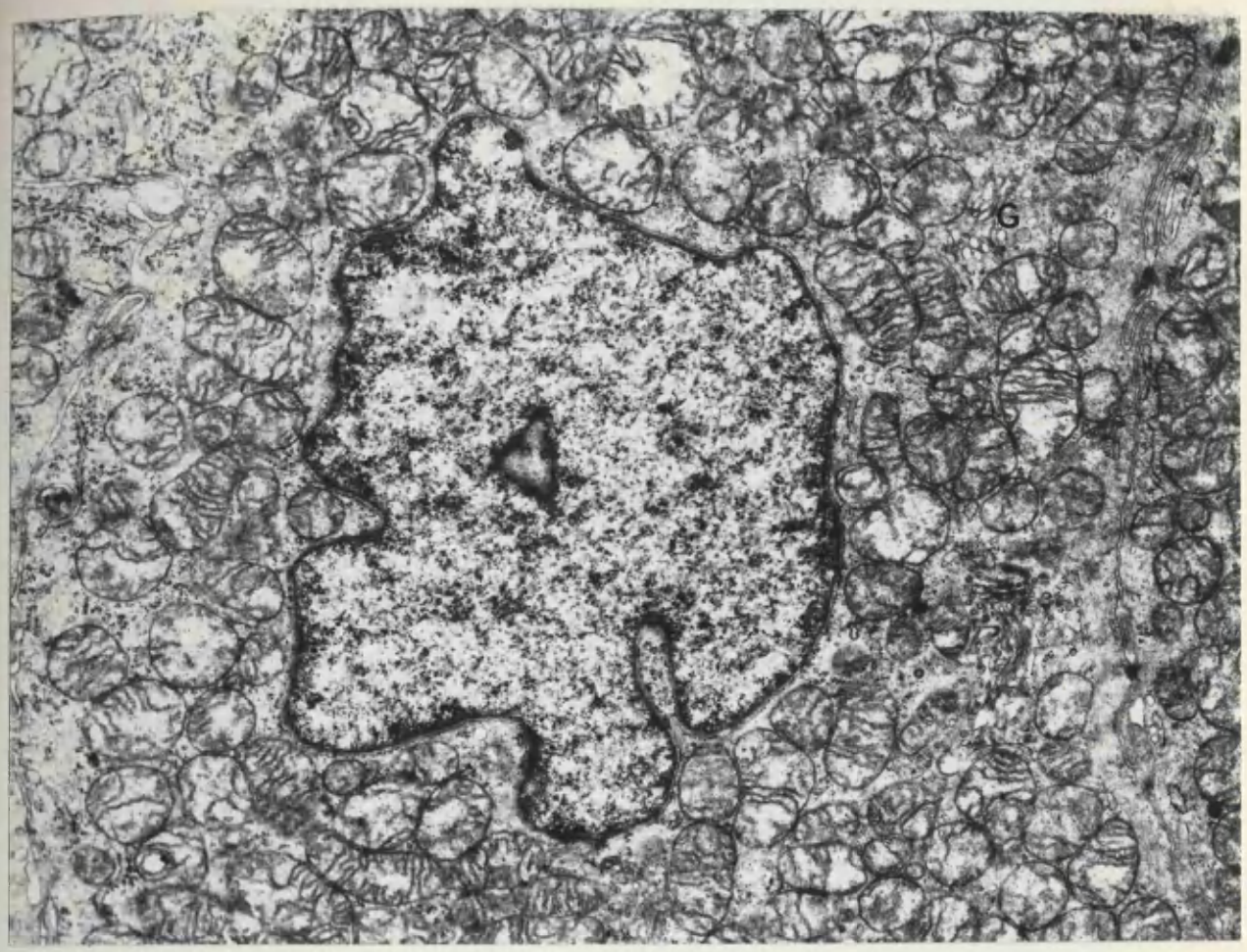

29

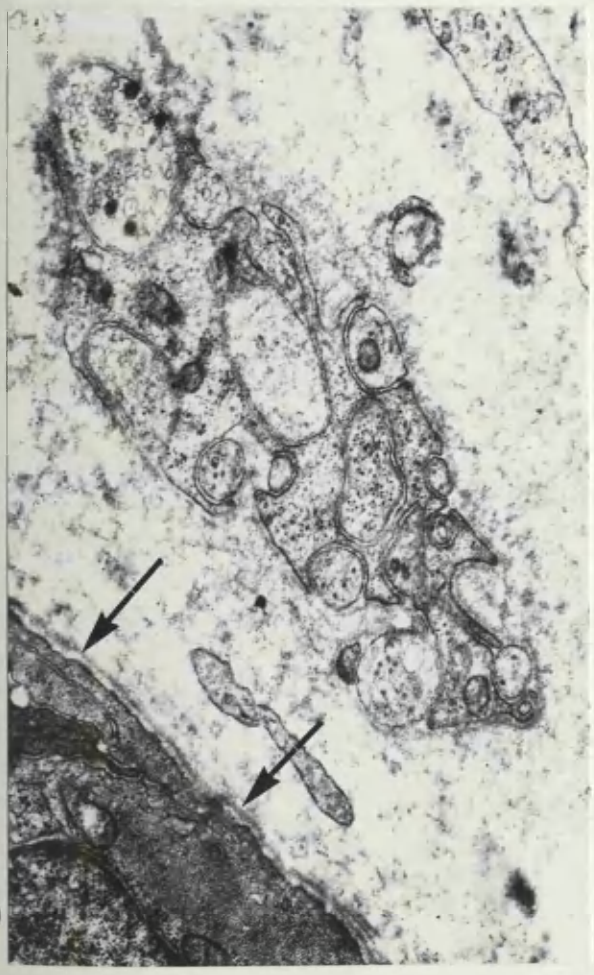

30

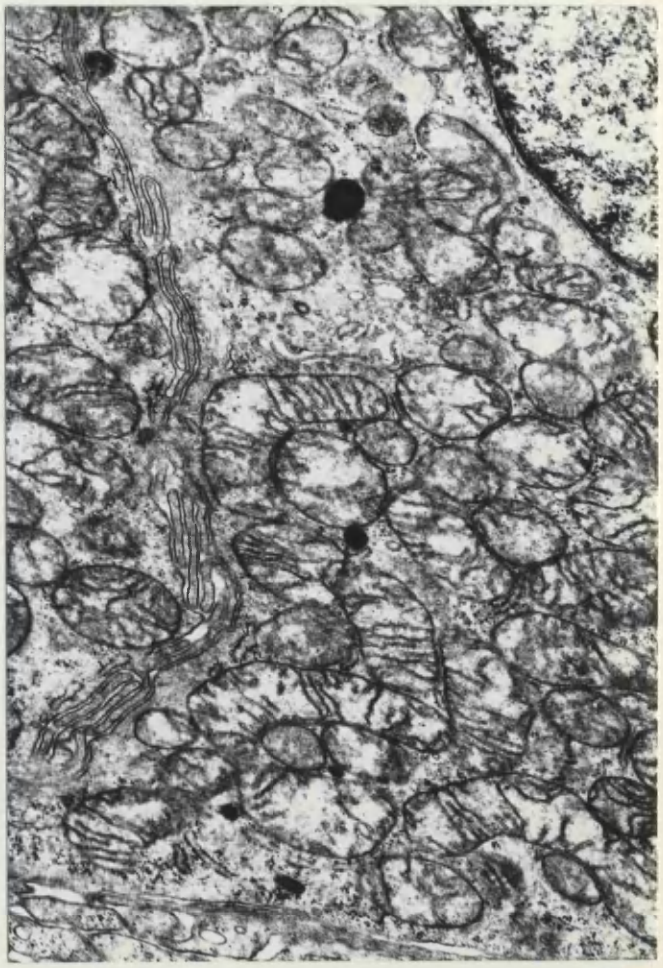

31

SUBMUCOSAL GLANDS OF OESOPHAGUS

Figure 32. Cuboidal epithelium of a small duct, adjacent to an acinus.

Magnification 13000.

Figure 33. Two-layered epithelium of a larger duct. Note the complex inclusions (X) probably lipid-rich.

Magnification 8400.

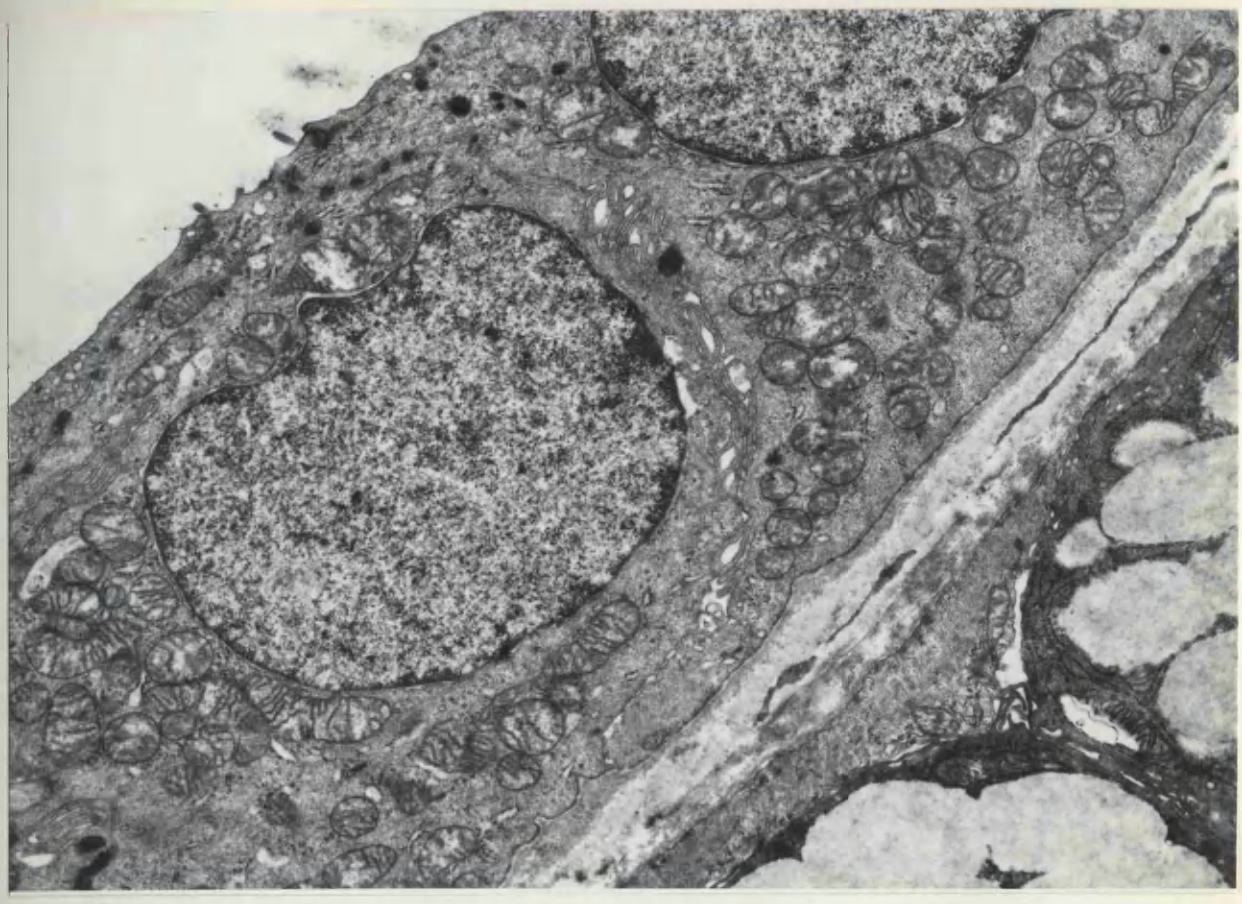

32

33

LANGERHANS CELLS OF OESOPHAGUS

Figure 34. A typical Langerhans cell in the human oesophageal mucosa. Desmosomes are seen between adjacent cells but not between the Langerhans cell and its neighbours. The features of this cell include a centriole and Golgi complex (G), granular endoplasmic reticulum and dense inclusions. The typical Langerhans granules are just detectable at this magnification (arrows).

Magnification 17250.

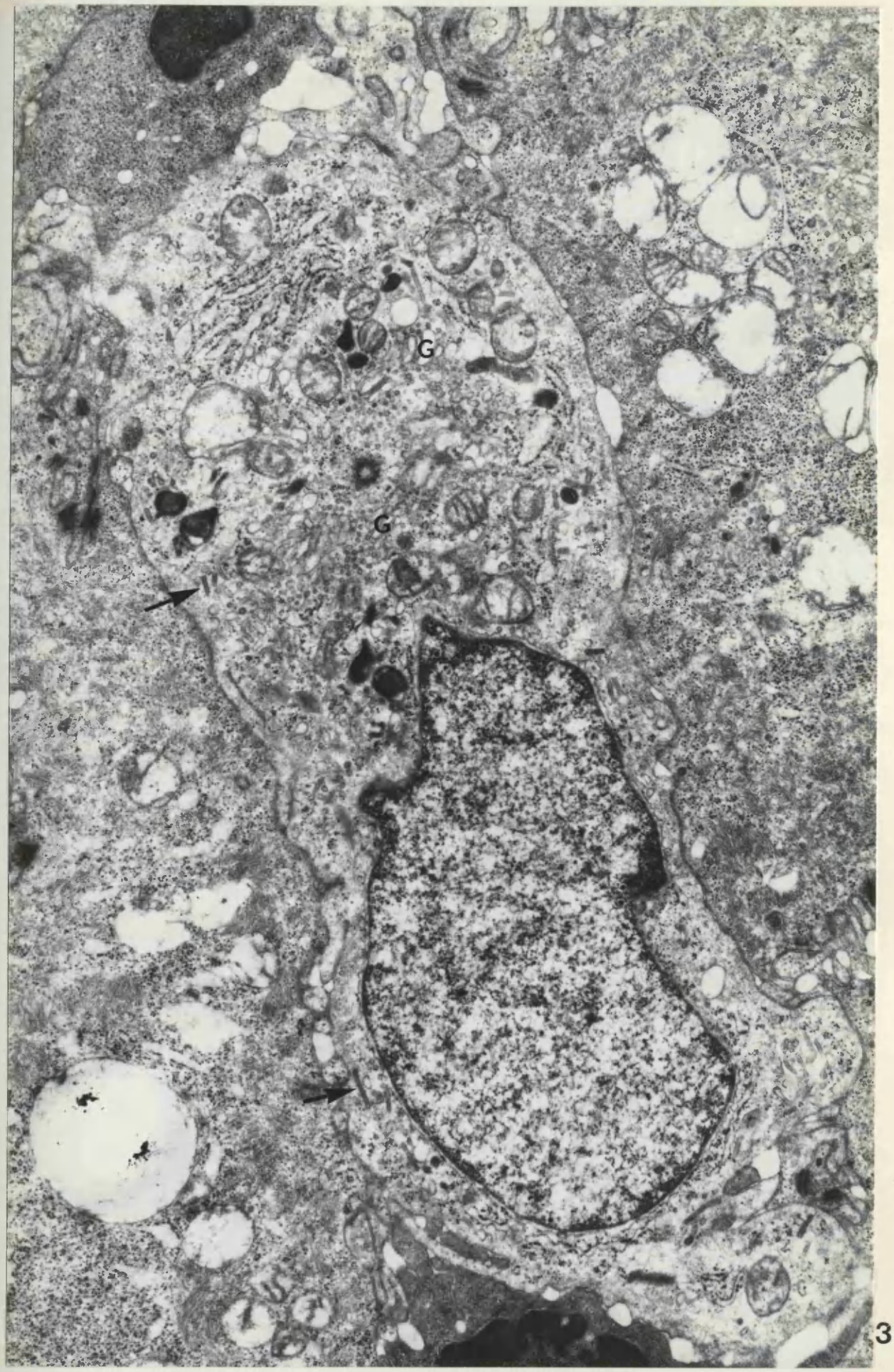

34

LANGERHANS CELLS OF OESOPHAGUS

Figure 35. The typical Langerhans cell granules are barely seen (arrow) at this magnification, which serves, however, to emphasise the dendritic nature of the cell. There are several processes (P) which lie separate from the perikaryon in this plane of section.

Magnification 21000.

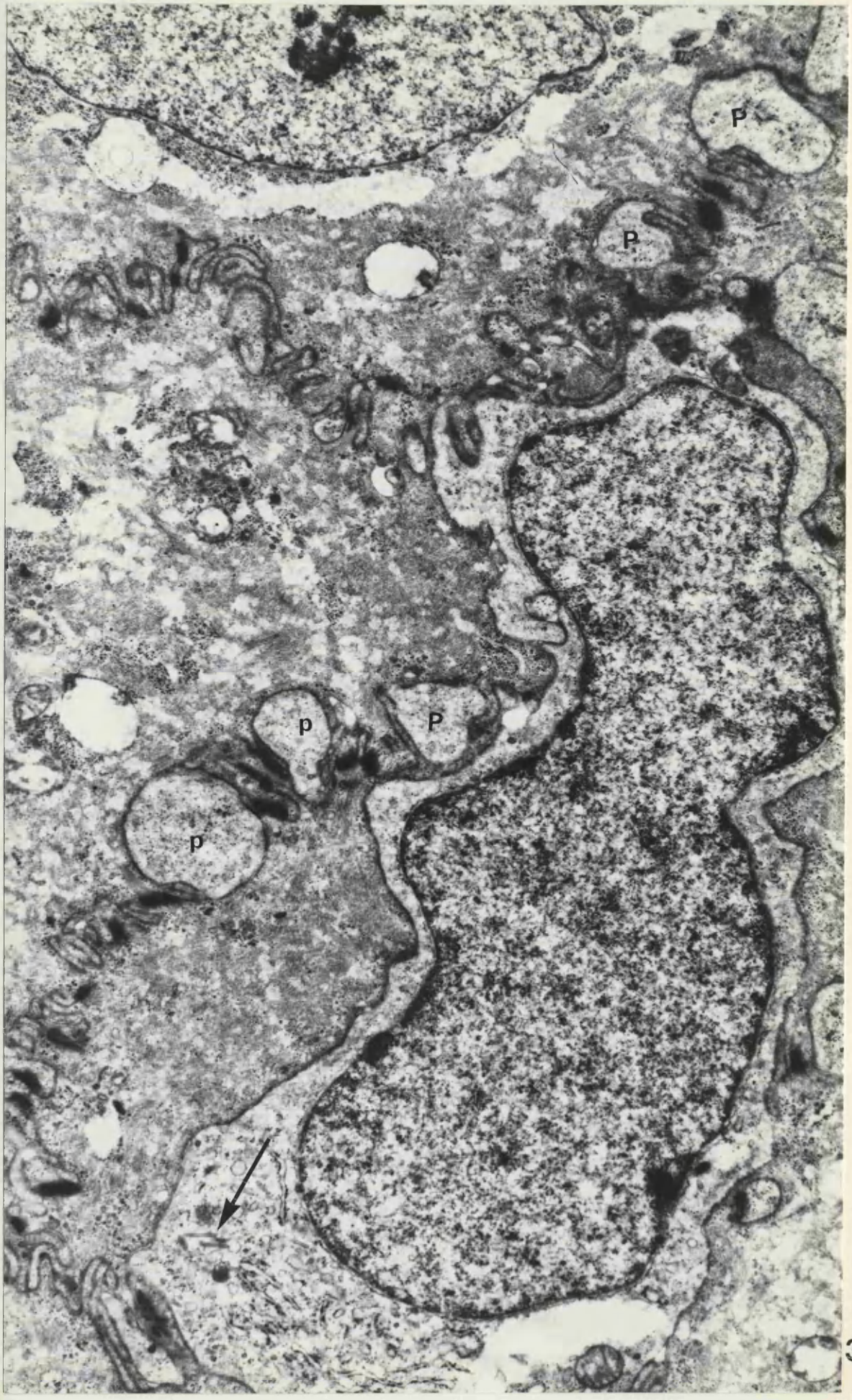

35

Figure 36. High magnification micrograph of Langerhans granules, showing their characteristic internal structure.

Magnification 67250.

Figure 37. Part of a rather poorly differentiated Langerhans cell, showing the continuity of the characteristic granule (arrow) with the cell surface, suggesting an origin by invagination. The desmosome seen links adjacent squamous cells.

Magnification 32250.

Figure 38. This micrograph is a deeper plane of section from the area shown in Figure 39. Notice the variations in the disposition and shape of the Langerhans granules (arrow).

Magnification 39000.

Figure 39. Higher magnification micrograph of the centriolar region from the cell shown in Figure 34. The Golgi complex has numerous associated vesicles. The mitochondria are undistinguished. Several Langerhans granules are present, some showing the terminal vacuolar dilatations which are termed "tennis racket" structures (arrow).

Magnification 39000.

36

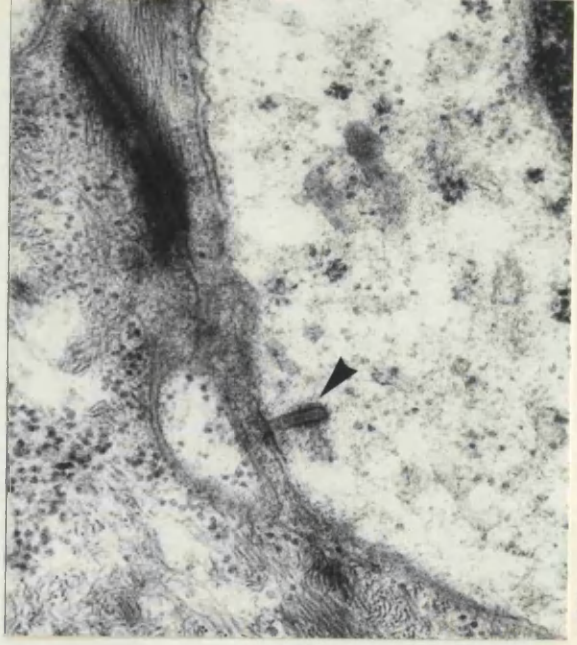

37

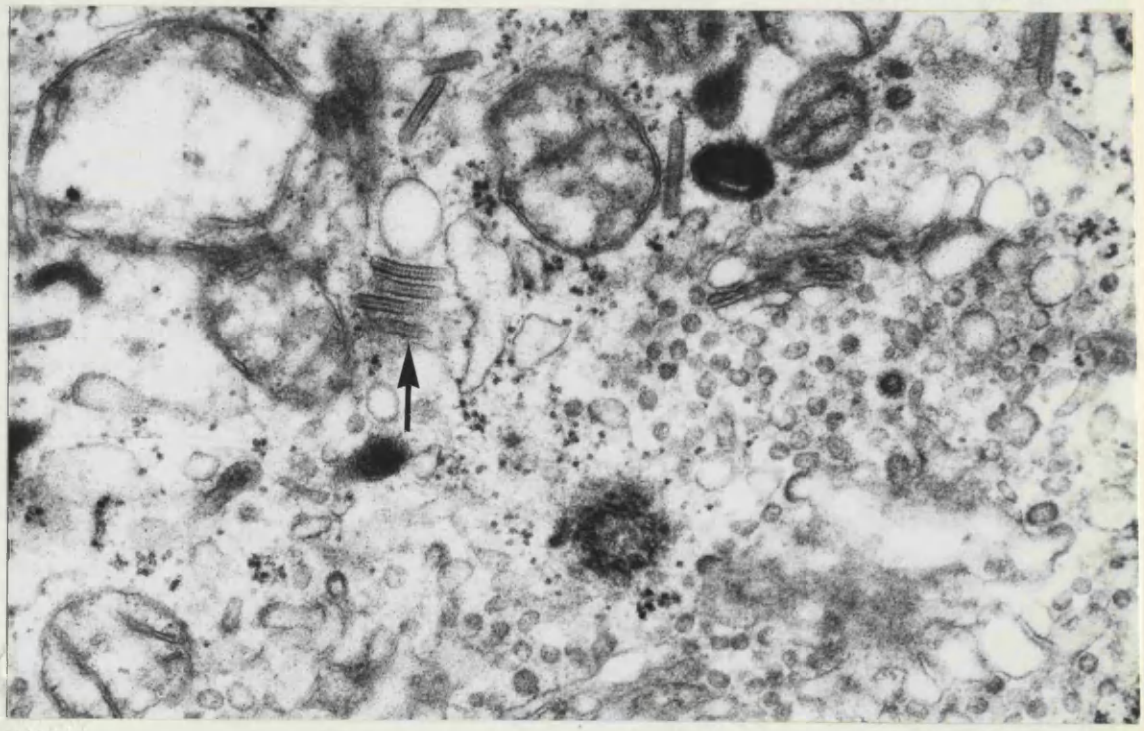

38

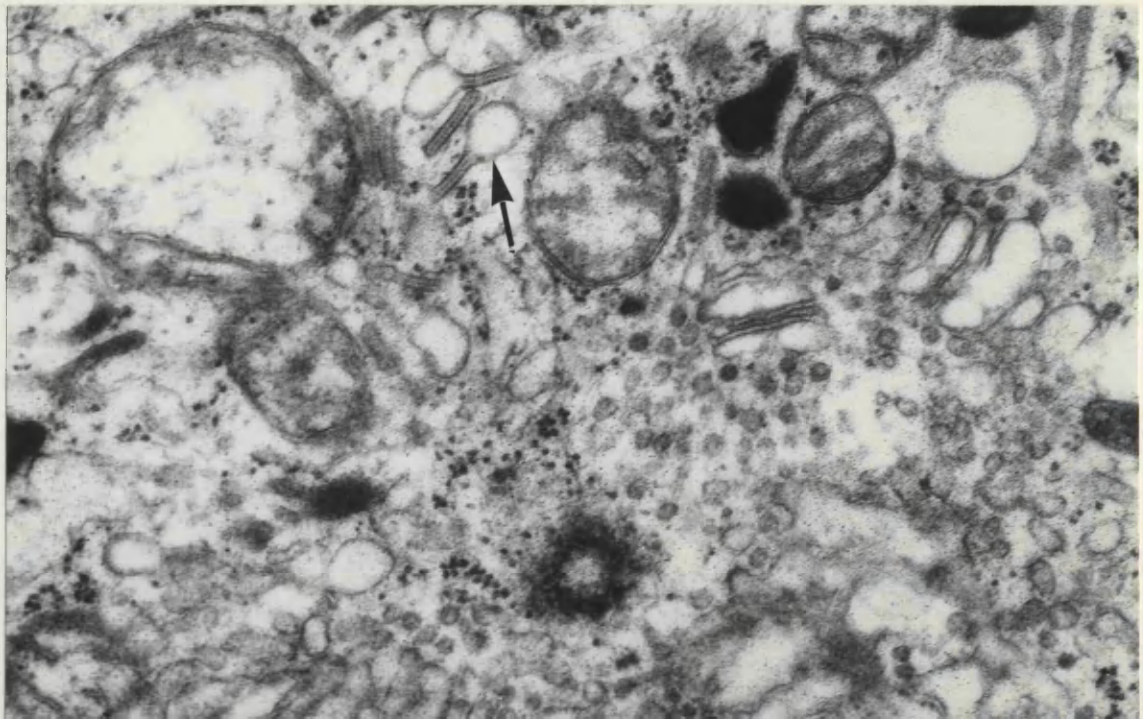

39

LANGERHANS CELLS OF OESOPHAGUS

Figure 40. A relatively poorly differentiated Langerhans cell with a single mitochondrial profile and little cytoplasmic organisation. Two typical Langerhans granules are present (arrows).

Magnification 12900.

Figure 41. A poorly differentiated Langerhans cell with two mitochondrial profiles, a long cytoplasmic process and a segmented nucleus having two nucleoli. One Langerhans granule is barely seen (arrow). Compare this figure with Figure 43.

Magnification 13800.

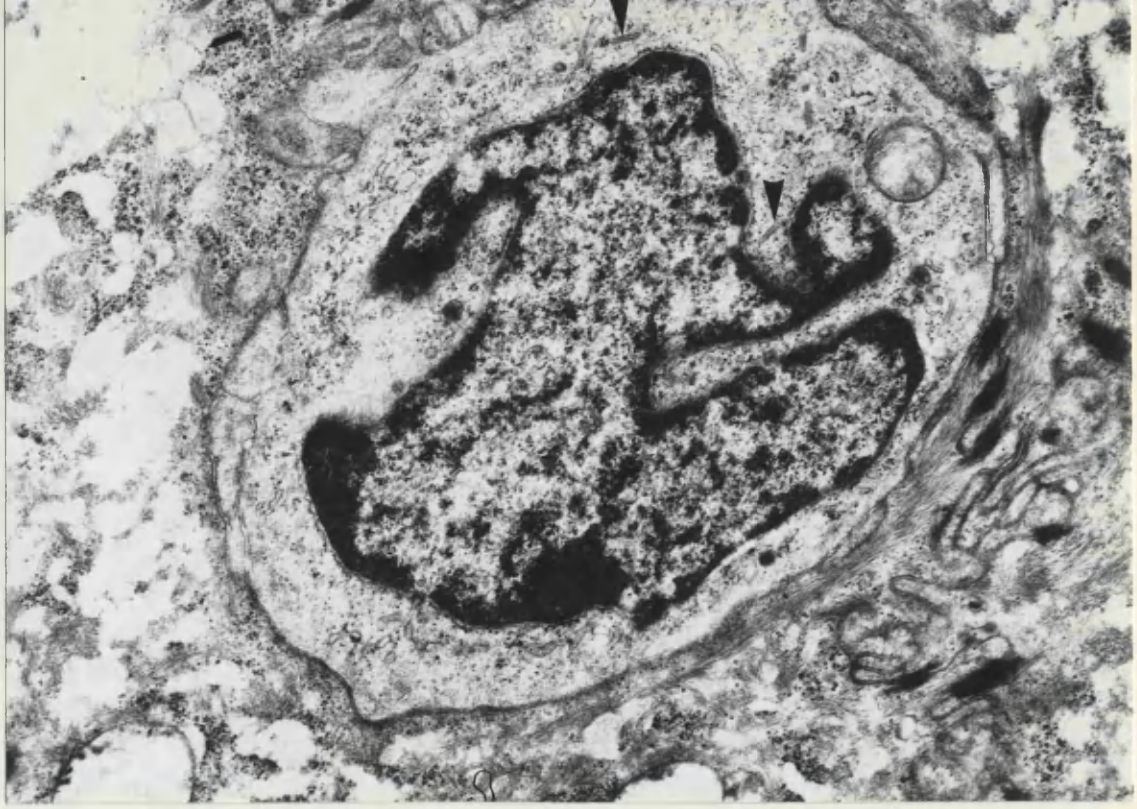

40

41

LANGERHANS CELLS OF OESOPHAGUS

Figure 42. A typical lymphocyte from the oesophageal mucosa, showing the characteristic lack of cytoplasmic organization. Two mitochondria are seen.

Magnification 13800.

Figure 43. In the absence of Langerhans granules, the identity of this cell cannot be confidently established, although its nucleus is suggestive of a Langerhans cell.

Magnification 8400.

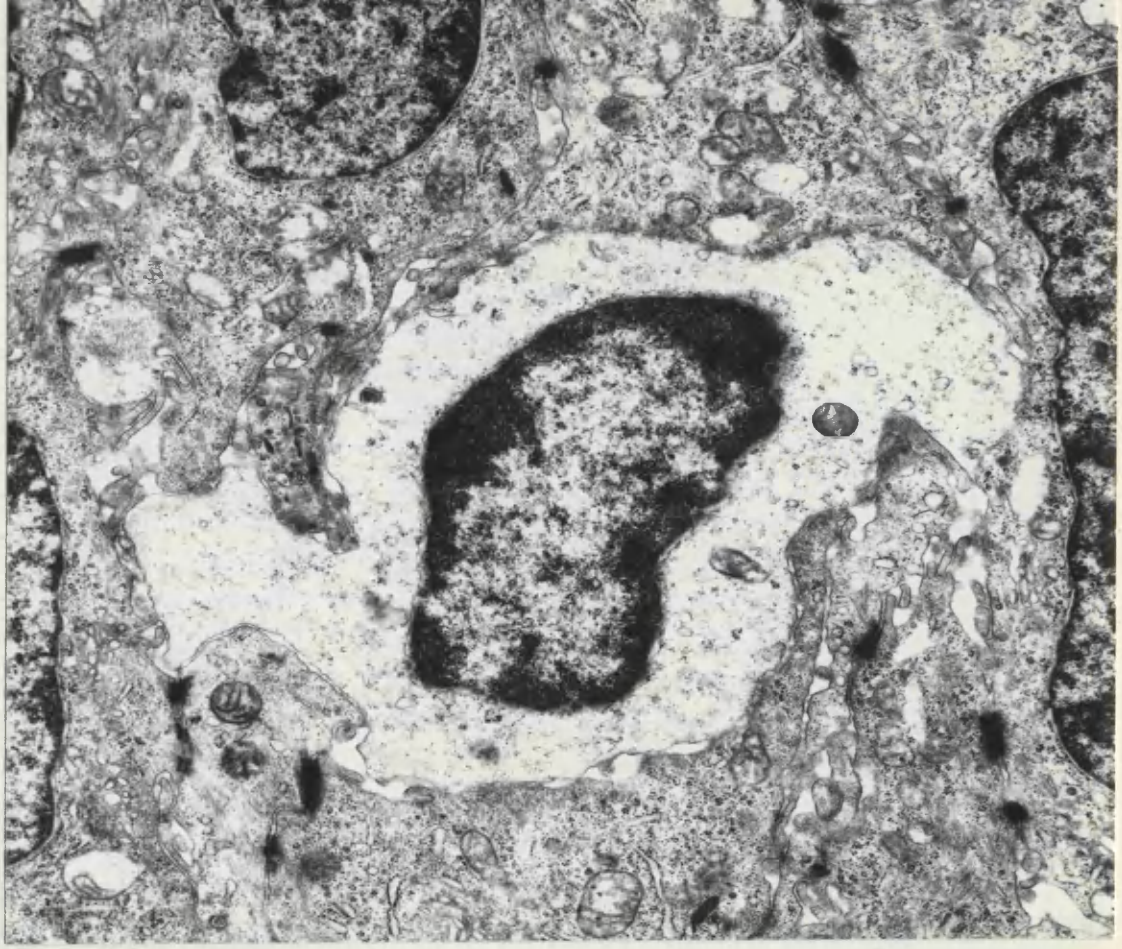

42

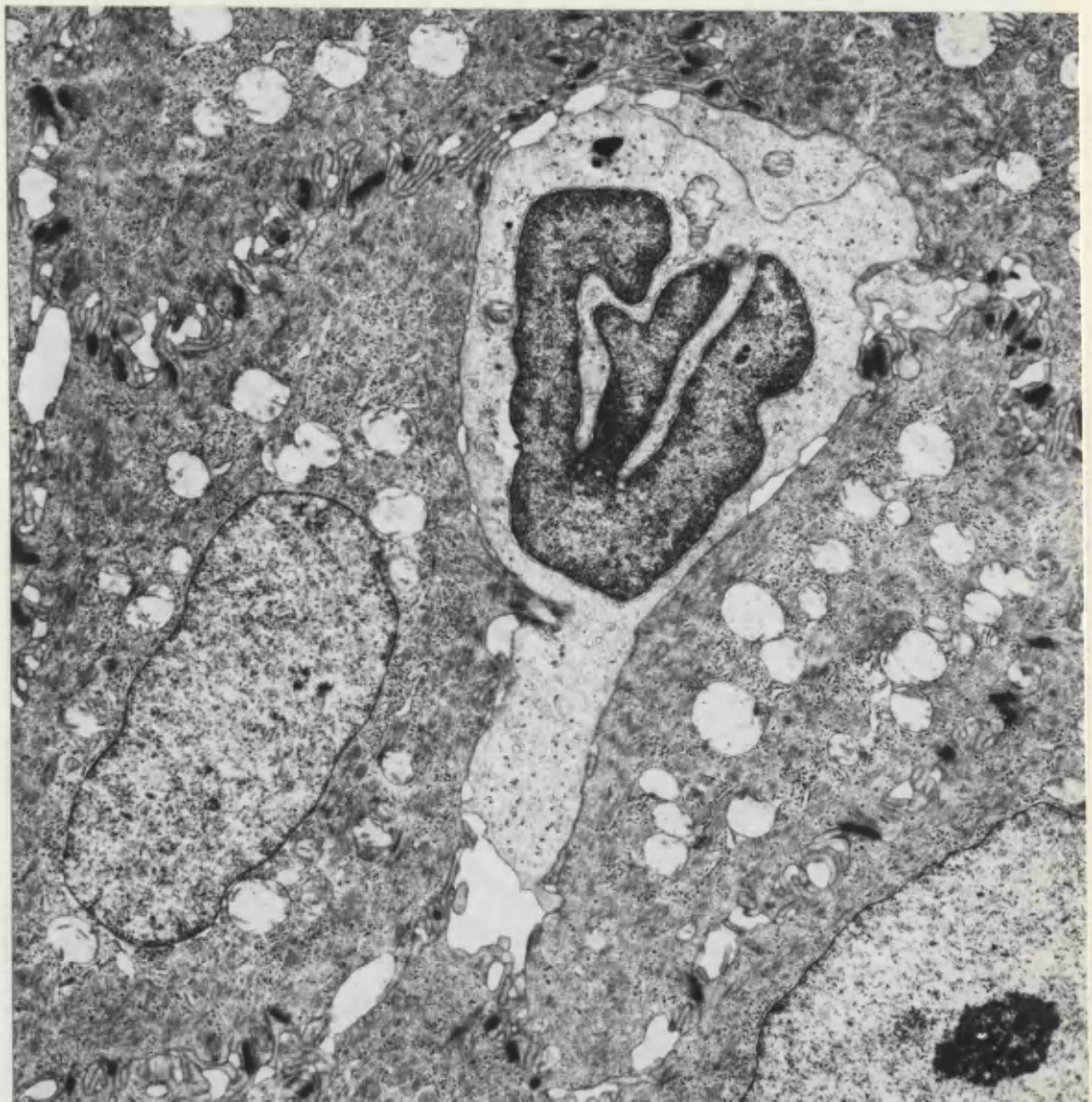

43

NORMAL HUMAN STOMACH

Figure 46. Chief cell, human stomach. The cell has a basally situated nucleus and an apical and supranuclear aggregate of secretion granules.

Magnification 6000

Figure 47. Gastric gland, human stomach. The cytoplasm of the parietal cell shown in this micrograph contains numerous mitochondria, profiles of sections through the canaliculus, tubulvesicles and dense bodies.

Magnification 6720

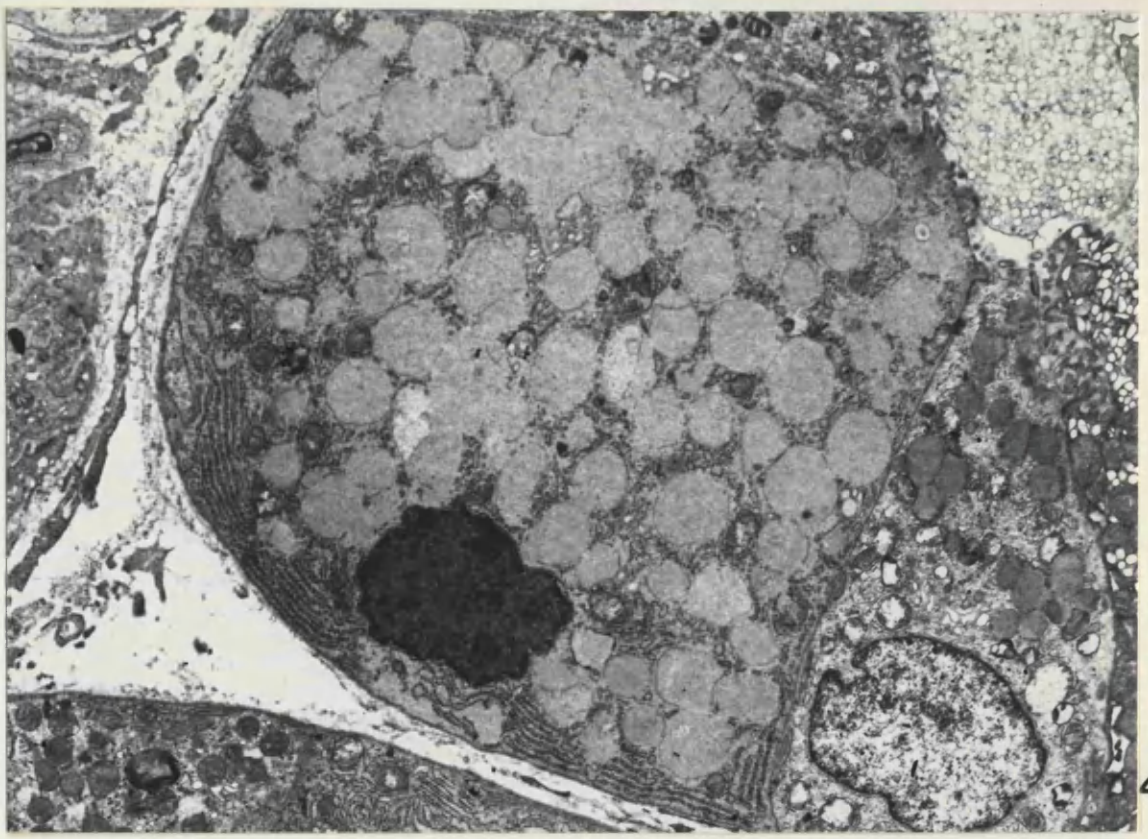

46

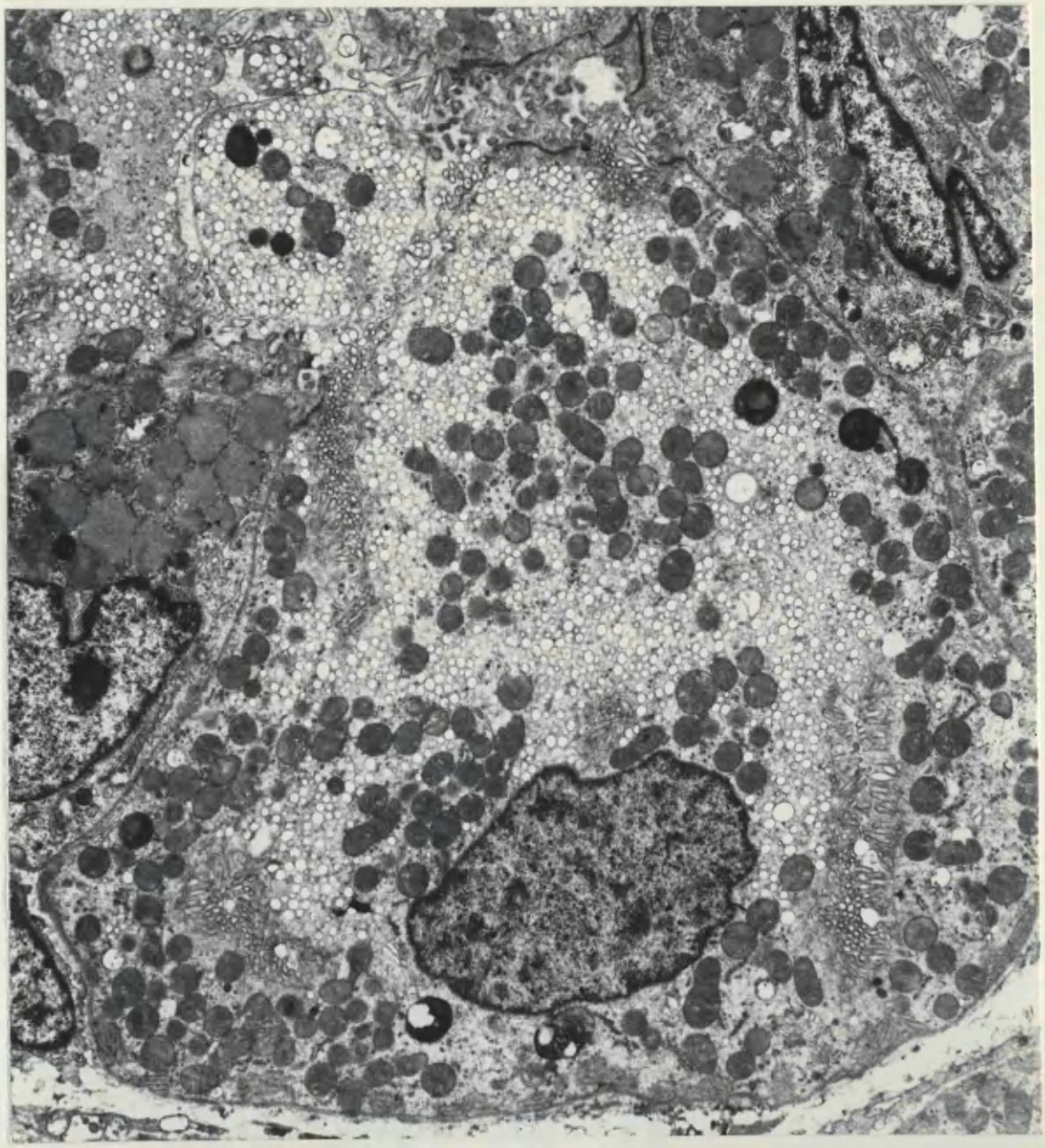

47

NORMAL HUMAN STOMACH

Figure 48. Tubulovesicles of parietal cell, human stomach. The central "inclusion" seen within many of these smooth-walled vesicles appears at two points to be continuous (arrows) with the cytoplasm, being in fact an invagination of cytoplasm into the lumen of the vesicle.

Magnification 27300.

Figure 49. Endocrine cell, human stomach. Basal region of gastric endocrine cell is shown, including the lower pole of the nucleus. Mitochondria, scattered cisternae of granular endoplasmic reticulum, and ribosomes are seen between the round secretion granules.

Magnification 13800.

Figure 50. Mucous neck cells, human stomach. Eccentrically placed dark areas are seen in some secretory granules.

Magnification 13800.

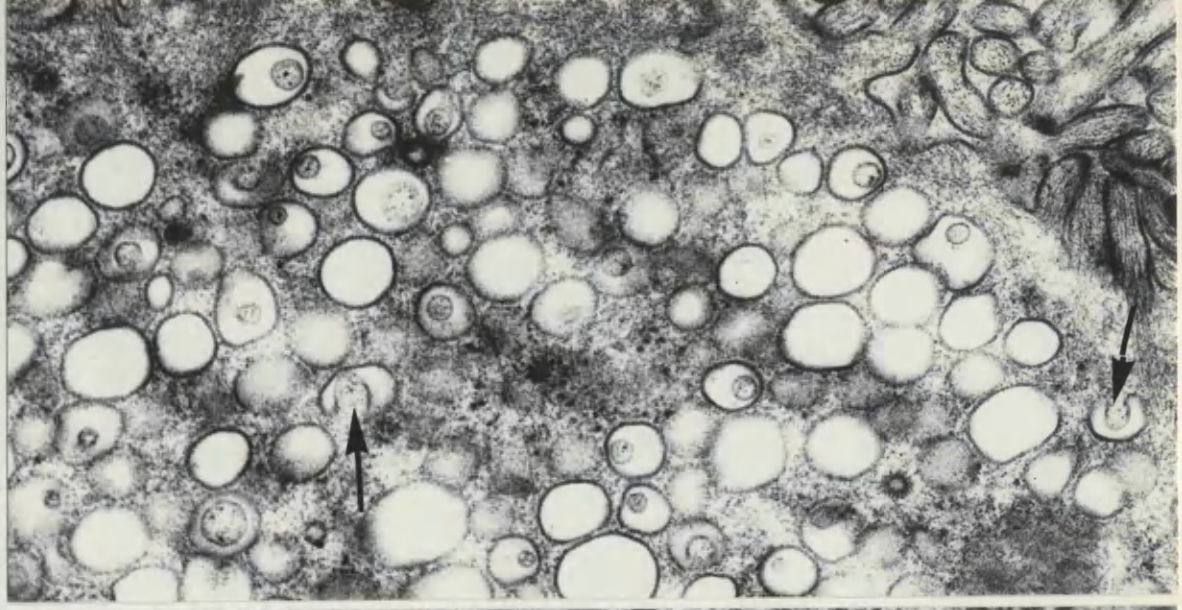

48

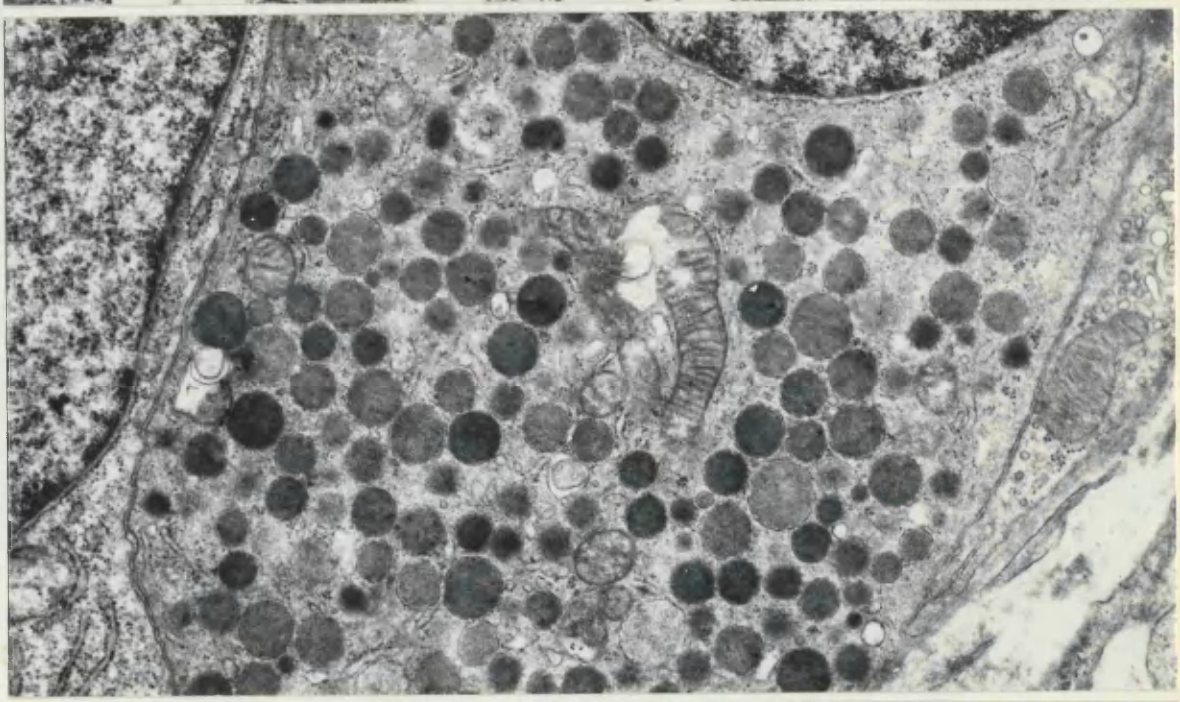

49

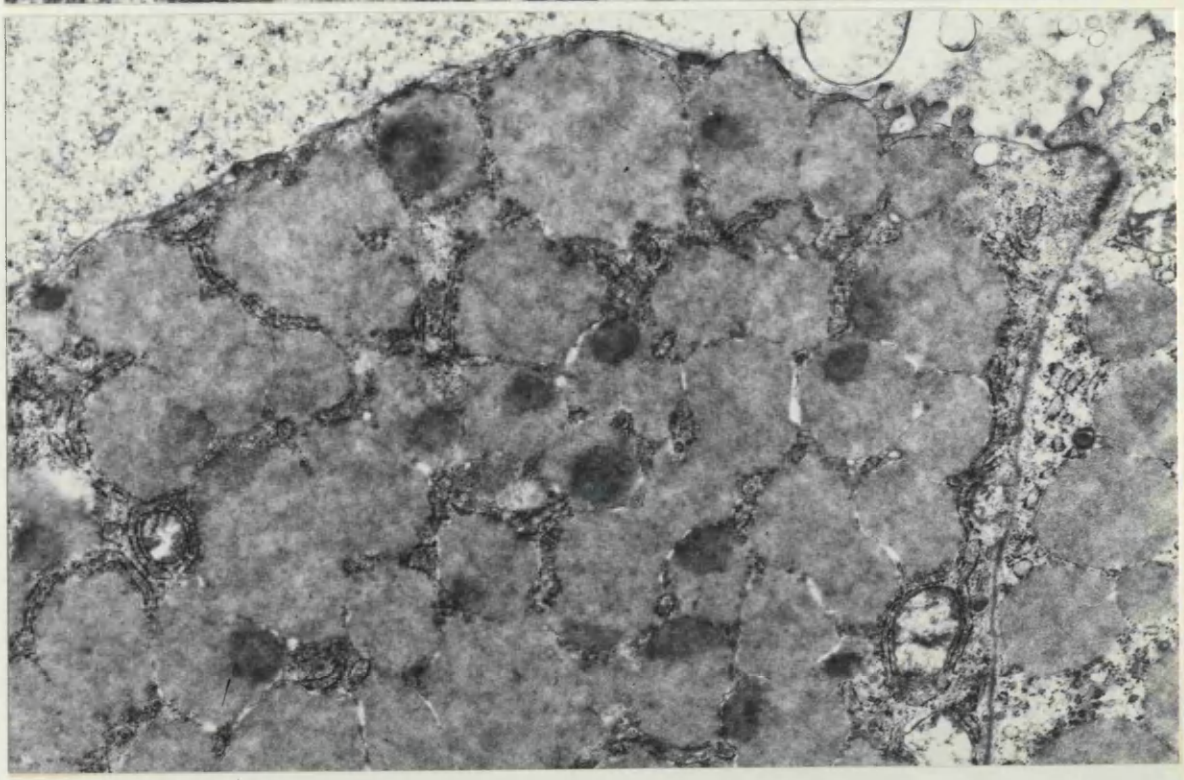

50

NORMAL HUMAN STOMACH

Figure 51. Carbohydrate staining of the gastric mucous cells. The granules are strongly positive.

Magnification 13800

Figure 52. Carbohydrate staining of the gastric mucous cells. Note the fine granular deposits in the lumen(L), the deposit-free zone(F) and the inconspicuous fuzzy coat.

Magnification 22750

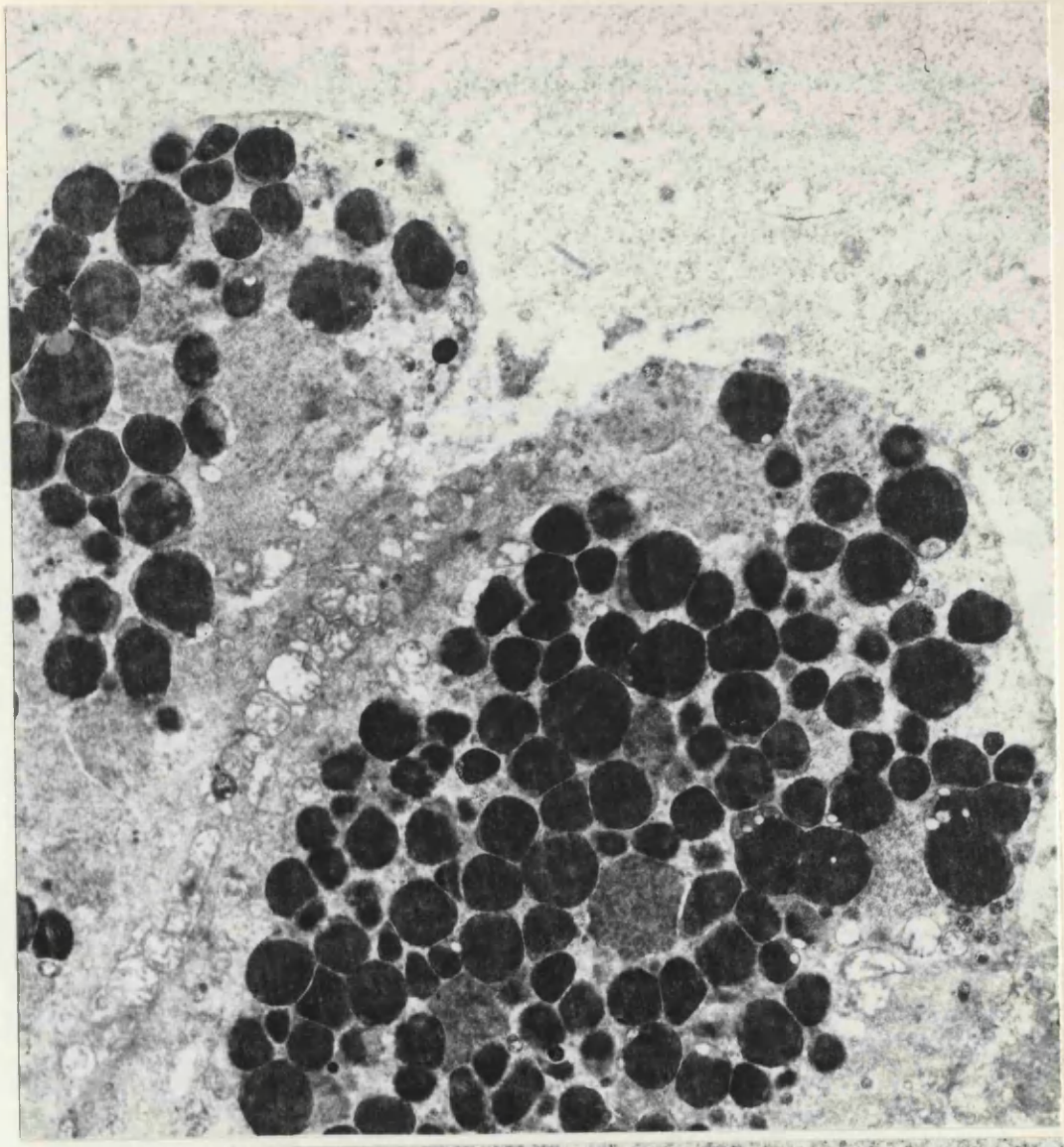

51

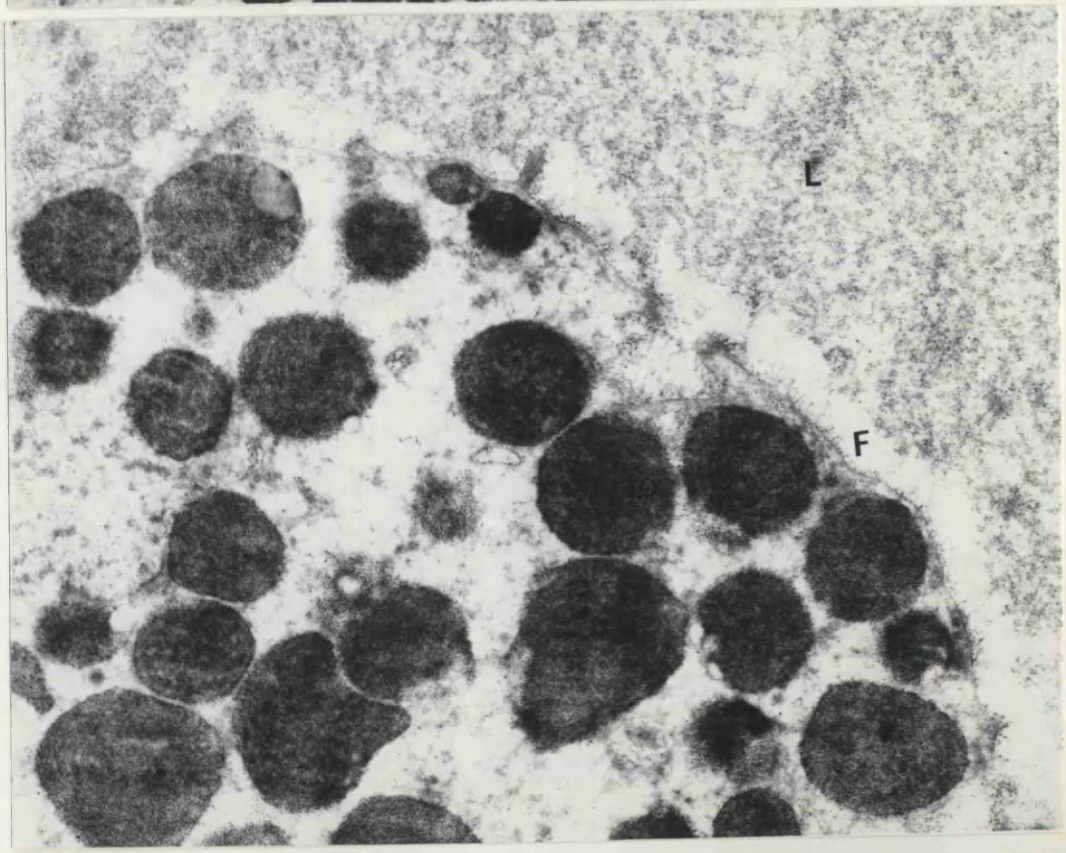

52

NORMAL HUMAN STOMACH

Figure 53. Human stomach. Some of the dense inclusions seen in the cytoplasm of parietal cells show lamellation.

Magnification 13800.

Figure 54. Gastric chief cells, human stomach. Small homogenous and large heterogenous dense inclusions are seen.

Magnification 22750.

Figure 55. Acid phosphatase preparation. Acid phosphatase activity is localised in the small dense bodies and in the periphery of the lamellated inclusions of the parietal cell of human stomach.

Magnification 17500.

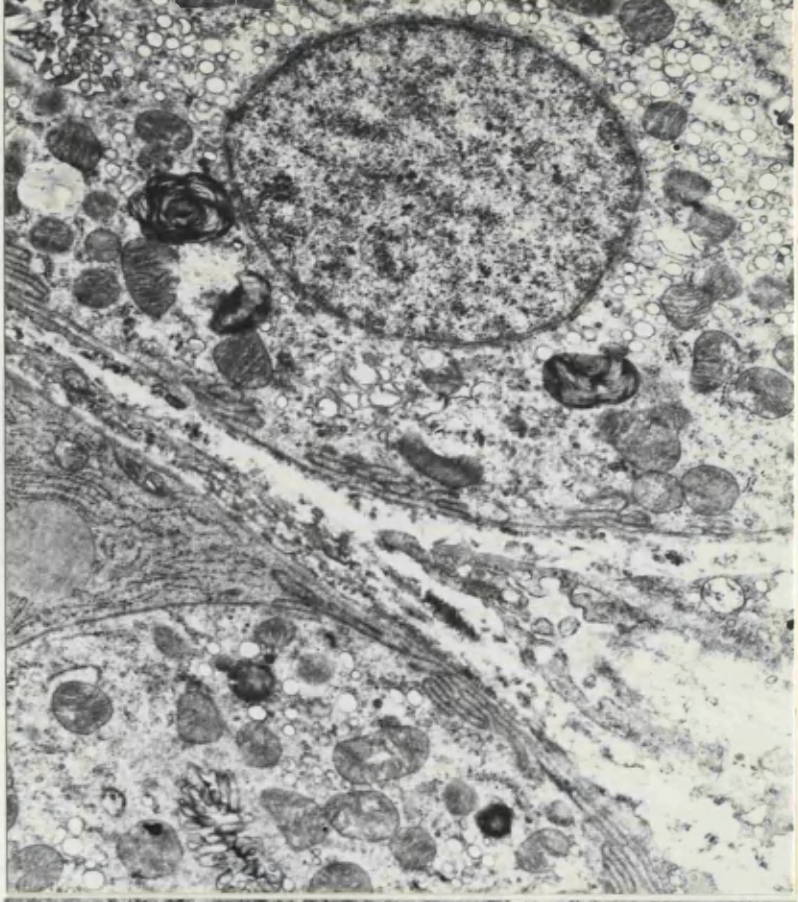

53

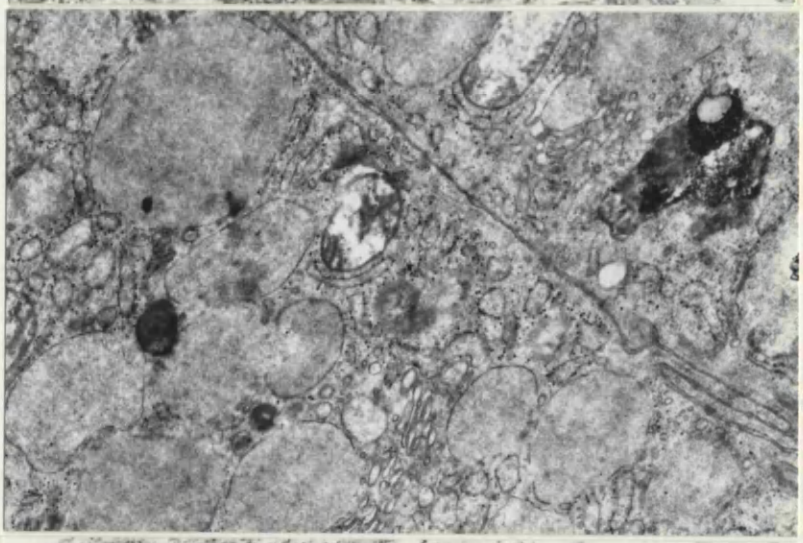

54

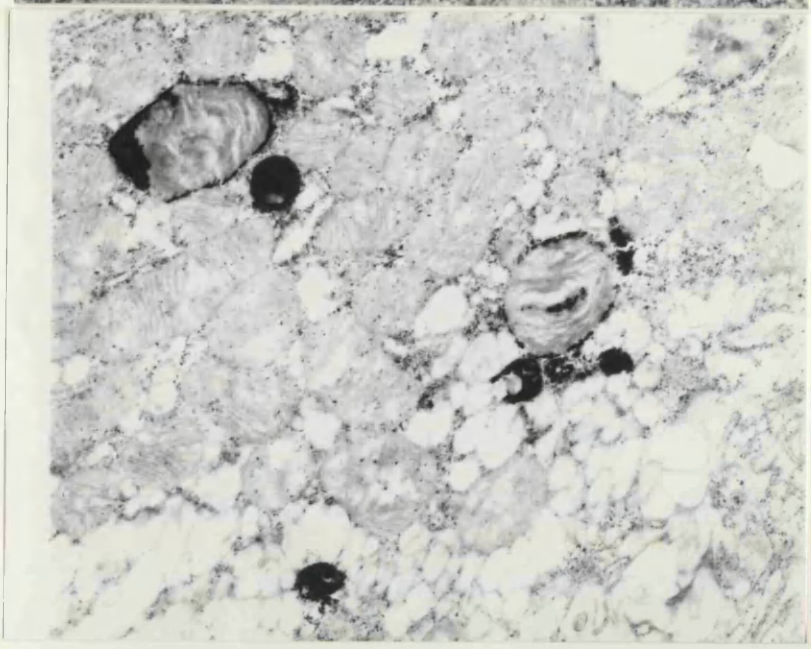

55

NORMAL HUMAN STOMACH

Figure 56. Acid phosphatase activity is seen in the small dense bodies of gastric mucous cells.

Magnification 39000

Figure 57. Acid phosphatase activity is localised in two small bodies of chief cell of gastric mucosa.

Magnification 22750

Figure 58. A large heterogeneous dense body showing acid phosphatase activity, in the gastric chief cell.

Magnification 22750

Figure 59. Acid phosphatase activity in heterogeneous and lamellated inclusions in parietal cell of gastric mucosa.

Magnification 22750

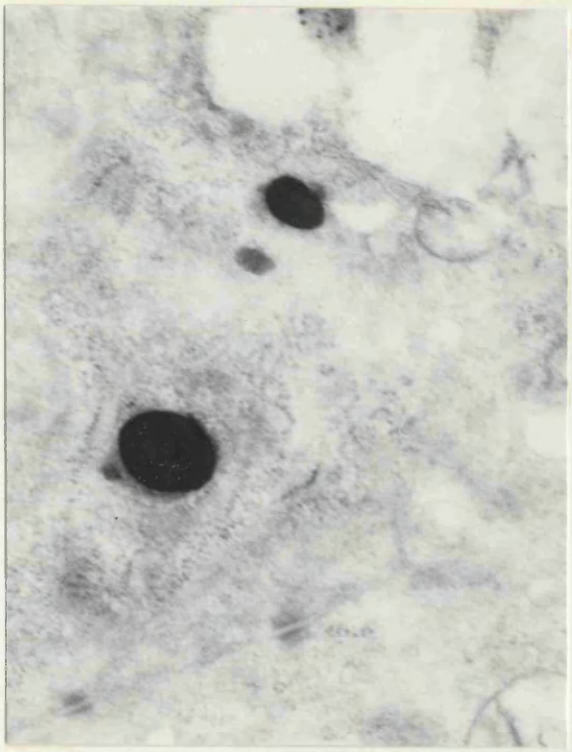

56

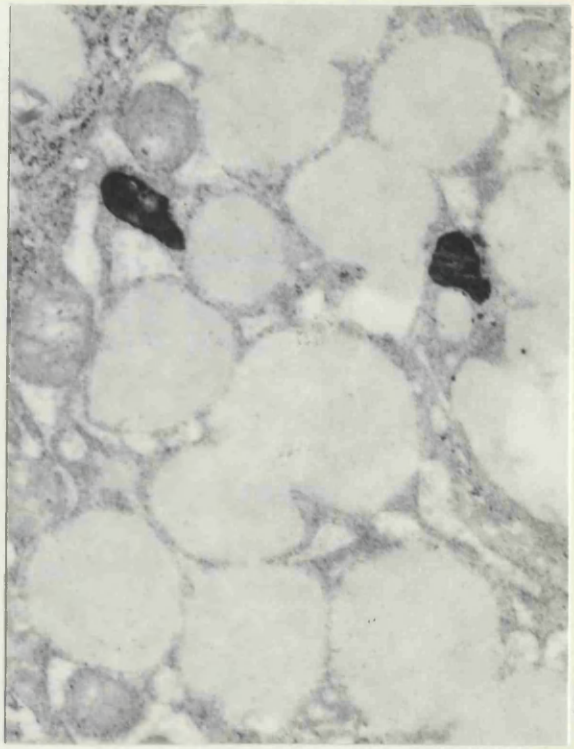

57

58

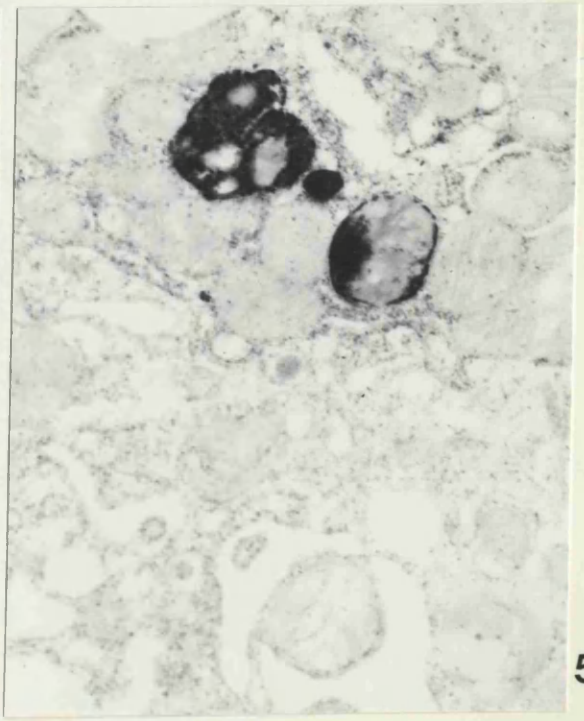

59

NORMAL HUMAN COLON

Figure 60. Colonic epithelium, human colon. The apical region of a goblet and an absorptive cell is seen. There are small vacuoles in the apical cytoplasm of the absorptive cell

Magnification 17250

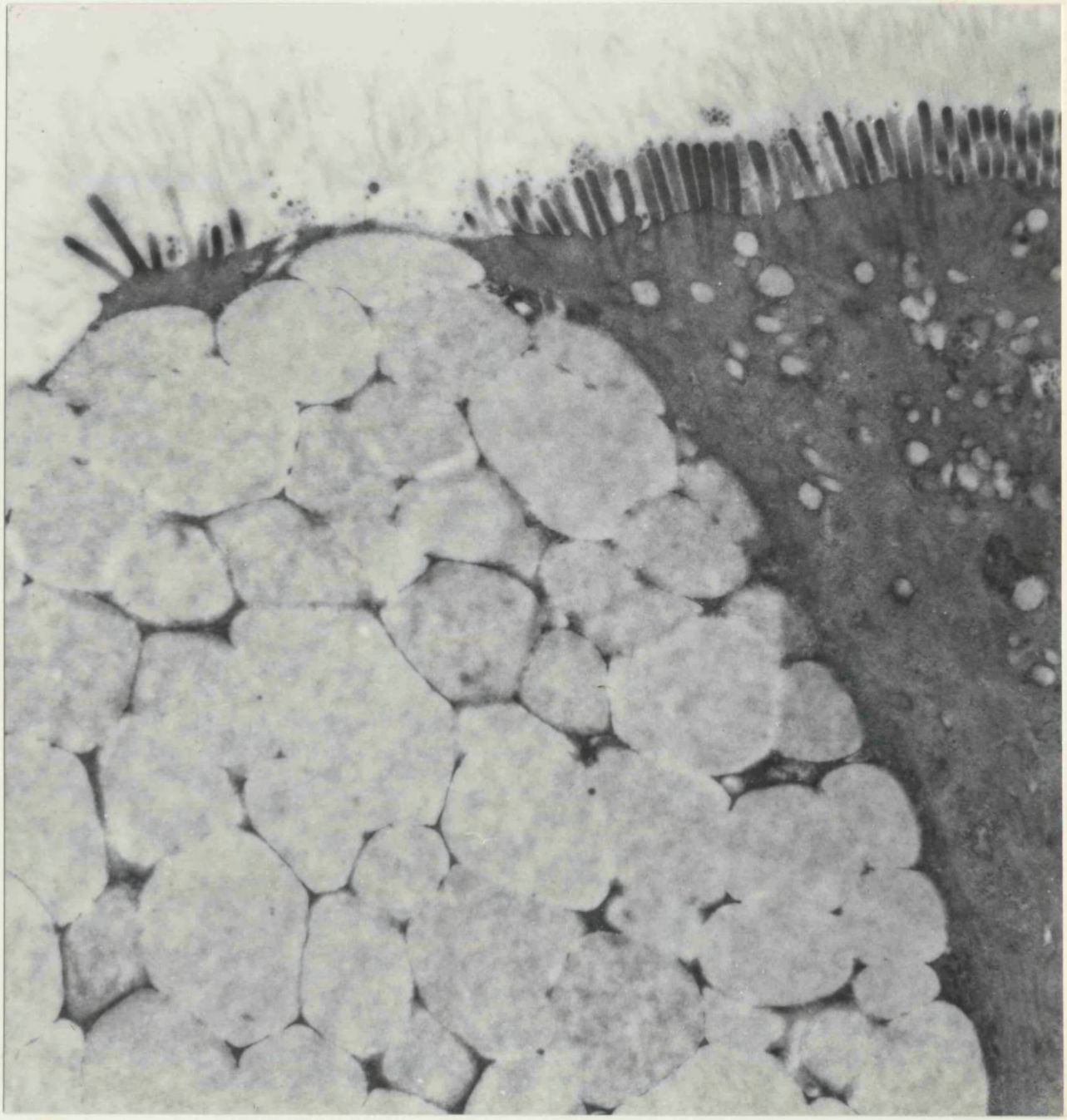

60

NORMAL HUMAN COLON

Figure 61. Colonic epithelium, human colon. Several goblet cells are shown. Note the characteristic features of goblet cells, including the distended apical cytoplasm and the nucleus pushed towards the base by the accumulated mucus mass.

Magnification 3600

Figure 62. Colonic epithelium, human colon. Parts of absorptive and goblet cells are shown. There are small oval and round membrane-limited dense inclusions in the cytoplasm of both cells.

Magnification 17500

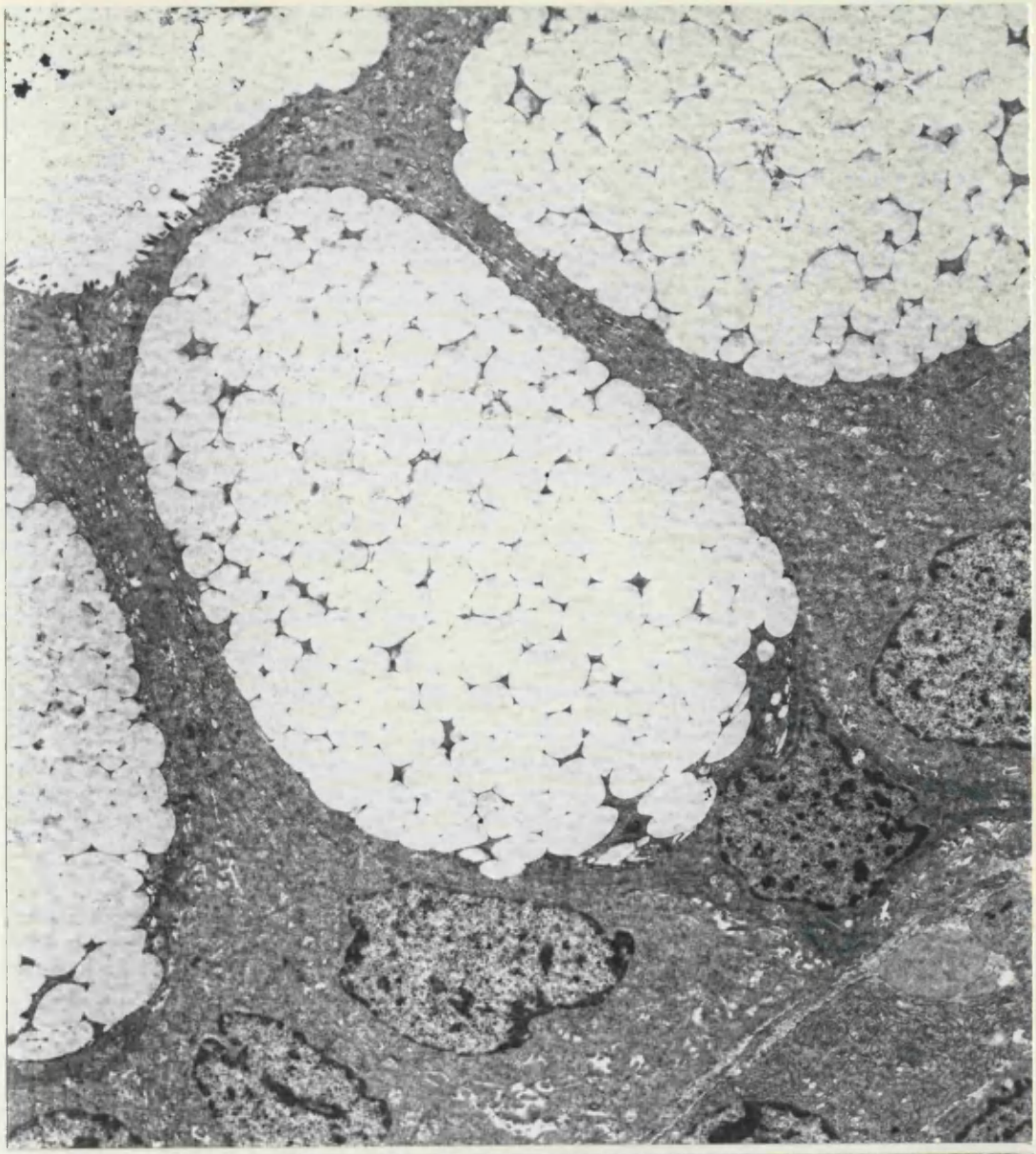

61

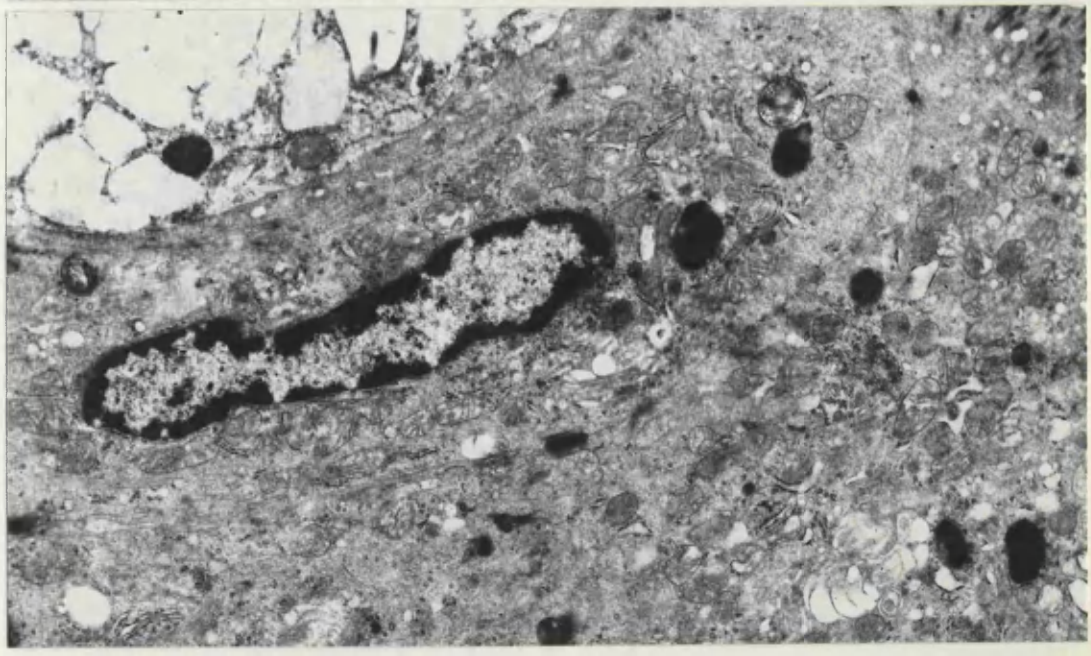

62

NORMAL HUMAN COLON

Figure 63. Colonic crypt, human colon. Apical region of lower one third of the colonic crypt, showing vacuolated apical cytoplasm. There are small round vesicles between and distal to the microvilli.

Magnification 17500

Figure 64. Colonic crypt, human colon. The lower parts of the cells of the colonic crypt, showing the lateral interdigitations and the basal aggregates of mitochondria.

Magnification 10750

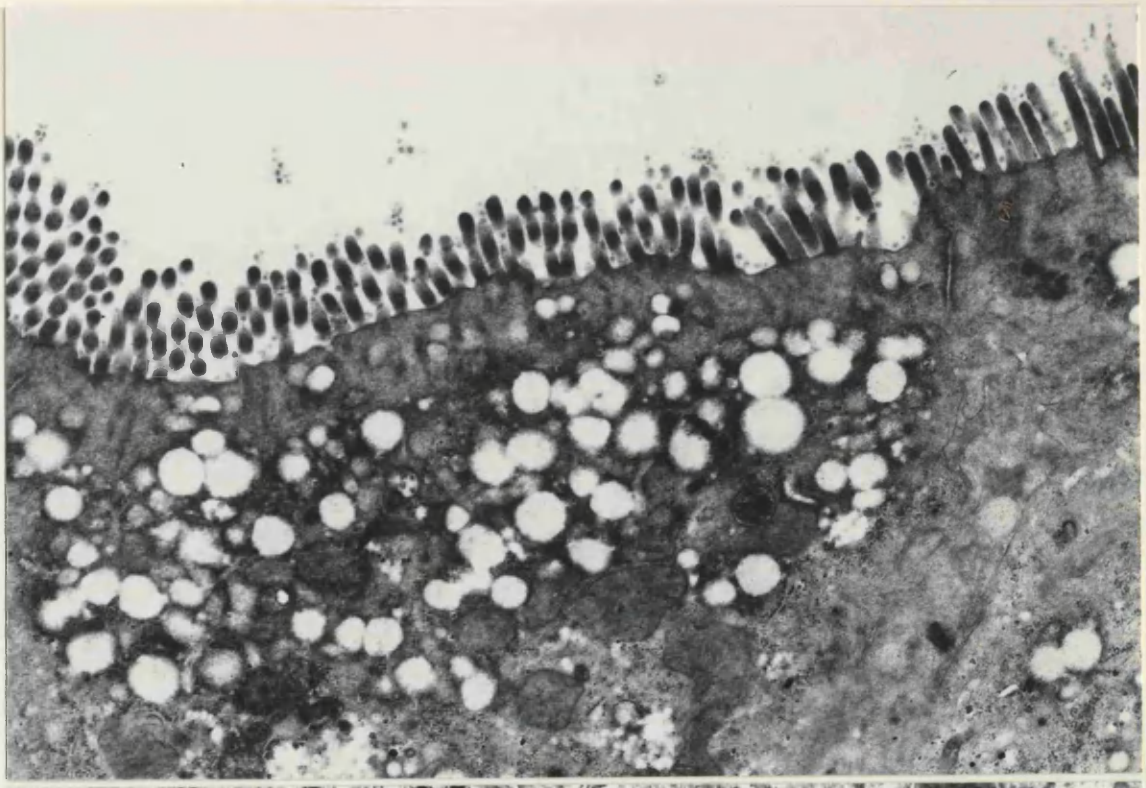

63

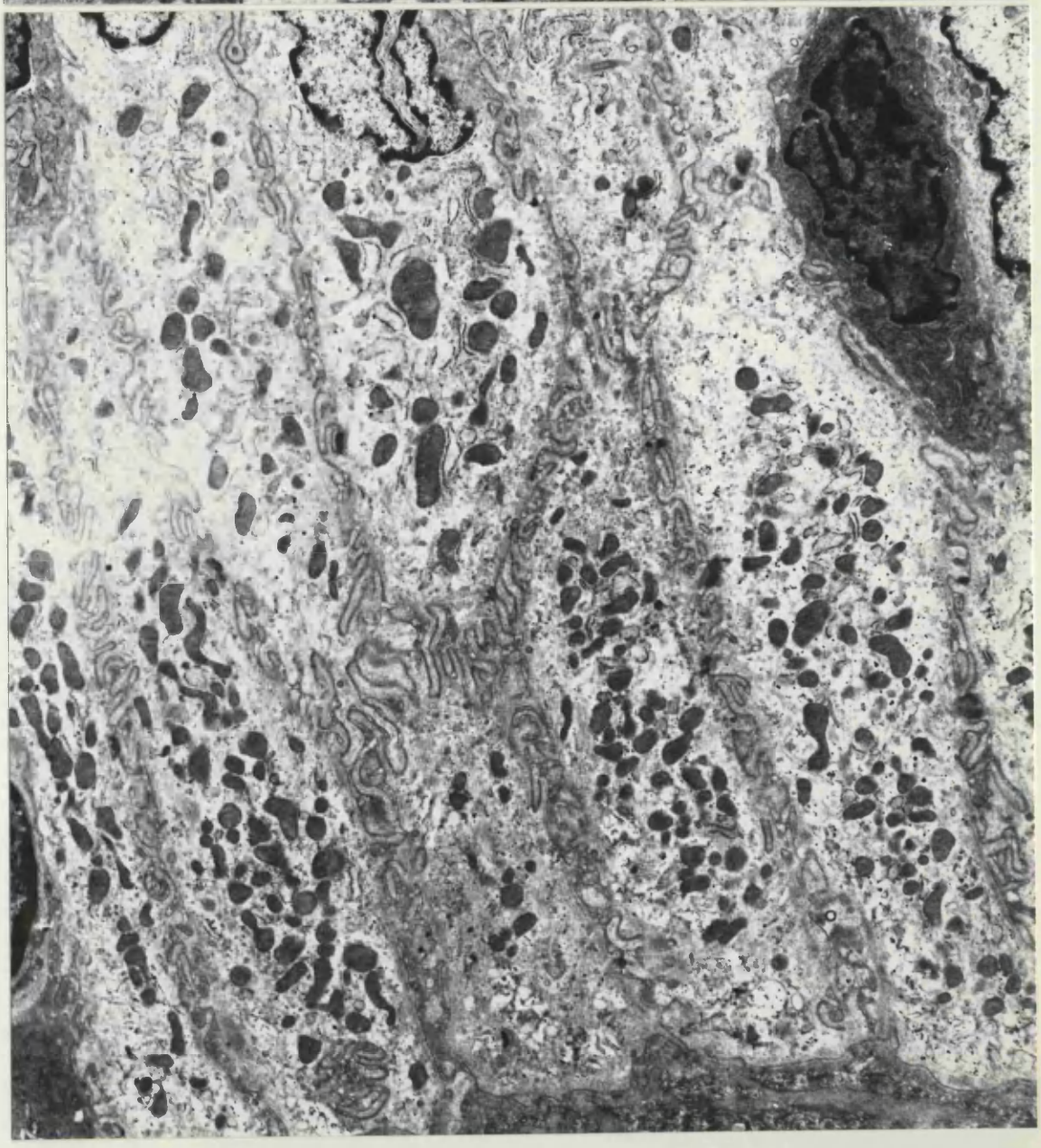

64

NORMAL HUMAN COLON

Figure 65. Colonic crypt, human colon. Immature cells of colonic crypt showing the typical irregular and segmented nucleus.

Magnification 13800

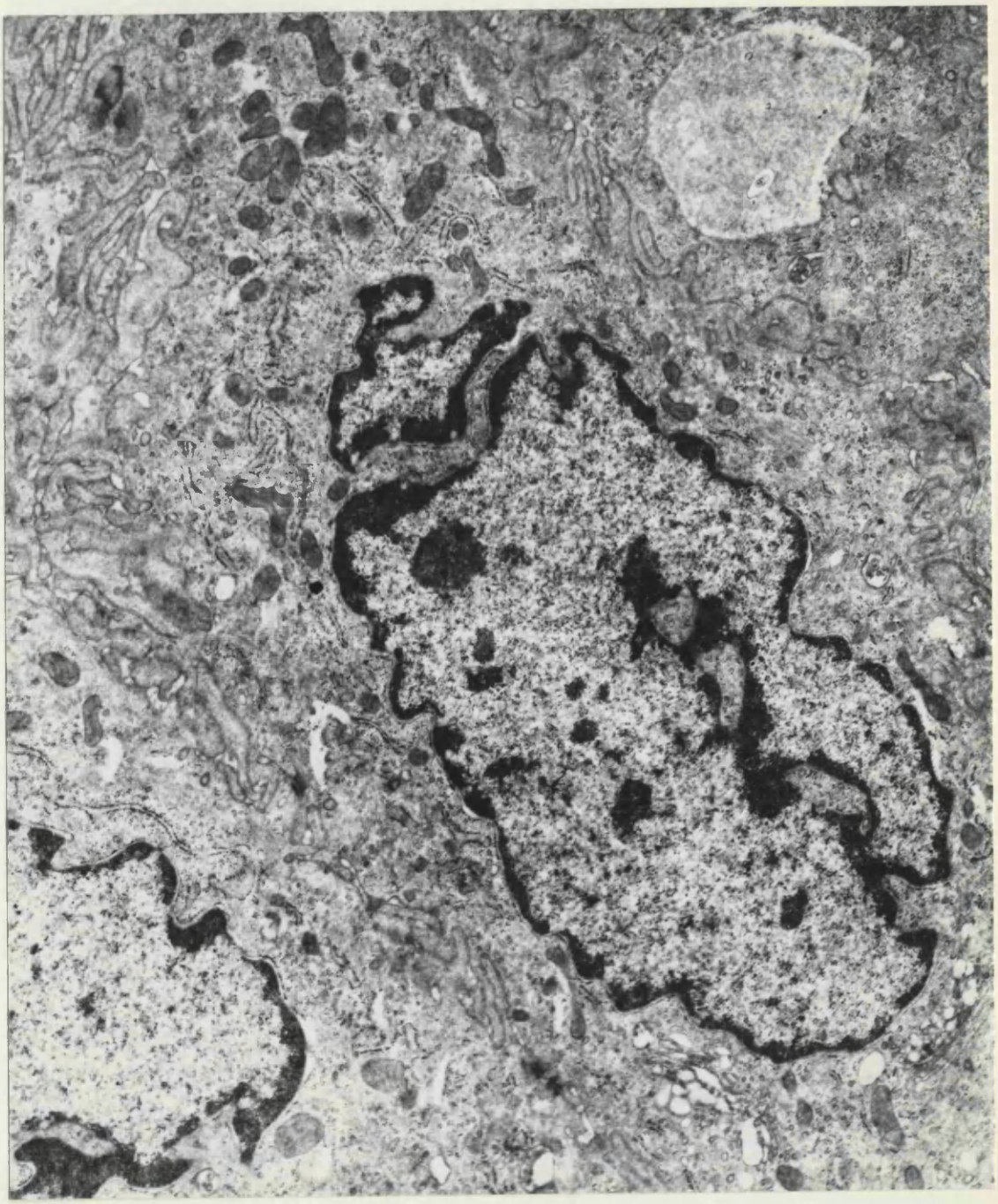

65

NORMAL HUMAN COLON

Figure 66. Acid phosphatase activity is localised in the small dense inclusions of colonic goblet cells.

Magnification 17500.

Figure 67. Acid phosphatase activity in a dense inclusion in the absorptive cell of colon.

Magnification 21000.

Figure 68. Acid phosphatase activity in the small dense bodies in colonic goblet cells.

Magnification 21000.

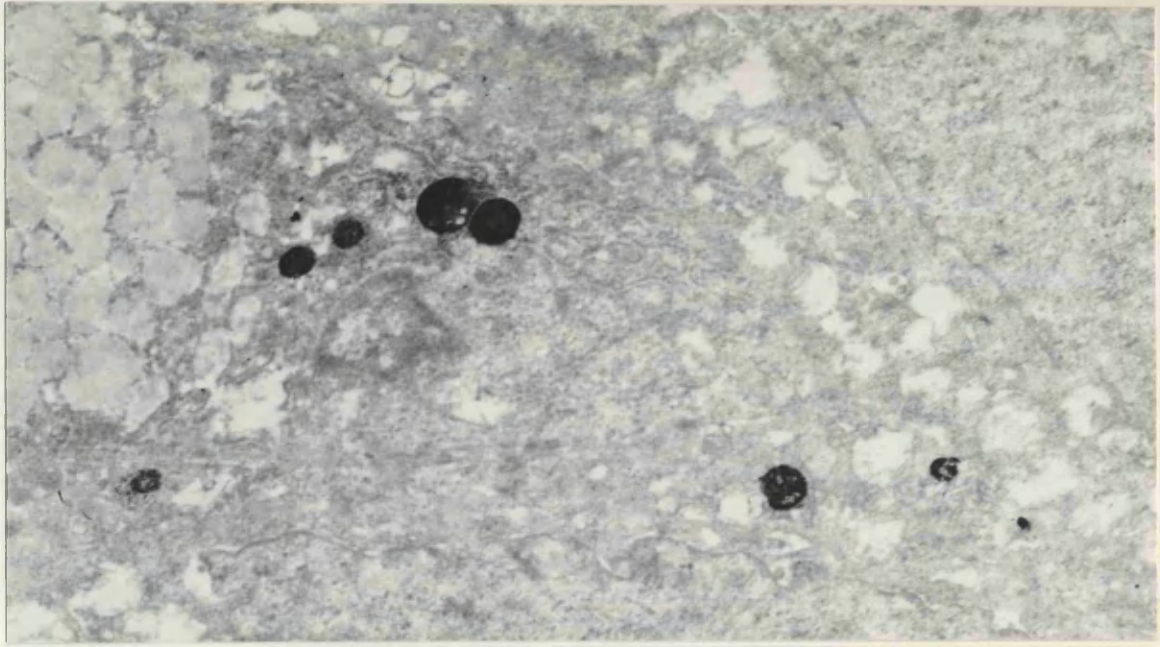

66

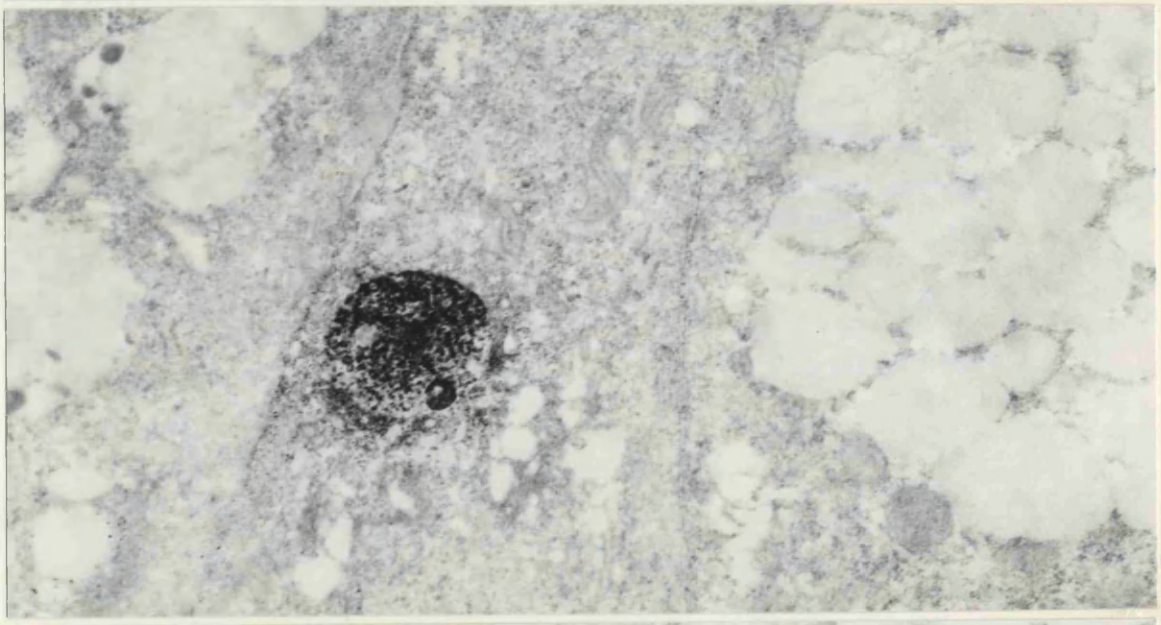

67

68

ULTRASTRUCTURAL PATHOLOGY OF HUMAN GASTROINTESTINAL TUMOURS

Volume Two

Thesis Submitted for the Degree of Ph. D.
of the University of Glasgow

By

Tariq Mohamed Al-Yassin, M. B. Ch. B.

From

The Department of Pathology,

Royal Infirmary, Glasgow

April 1976

SQUAMOUS CARCINOMA OF OESOPHAGUS

Figure 69. The histological pattern of a typical case of well differentiated squamous cell carcinoma of human oesophagus is shown.

Magnification 225

Figure 70. Squamous cell carcinoma, human oesophagus. The cells have a cytoplasmic matrix of moderate density and large nuclei. Note the binucleate cell and the intact basal lamina (arrows).

Magnification 8400

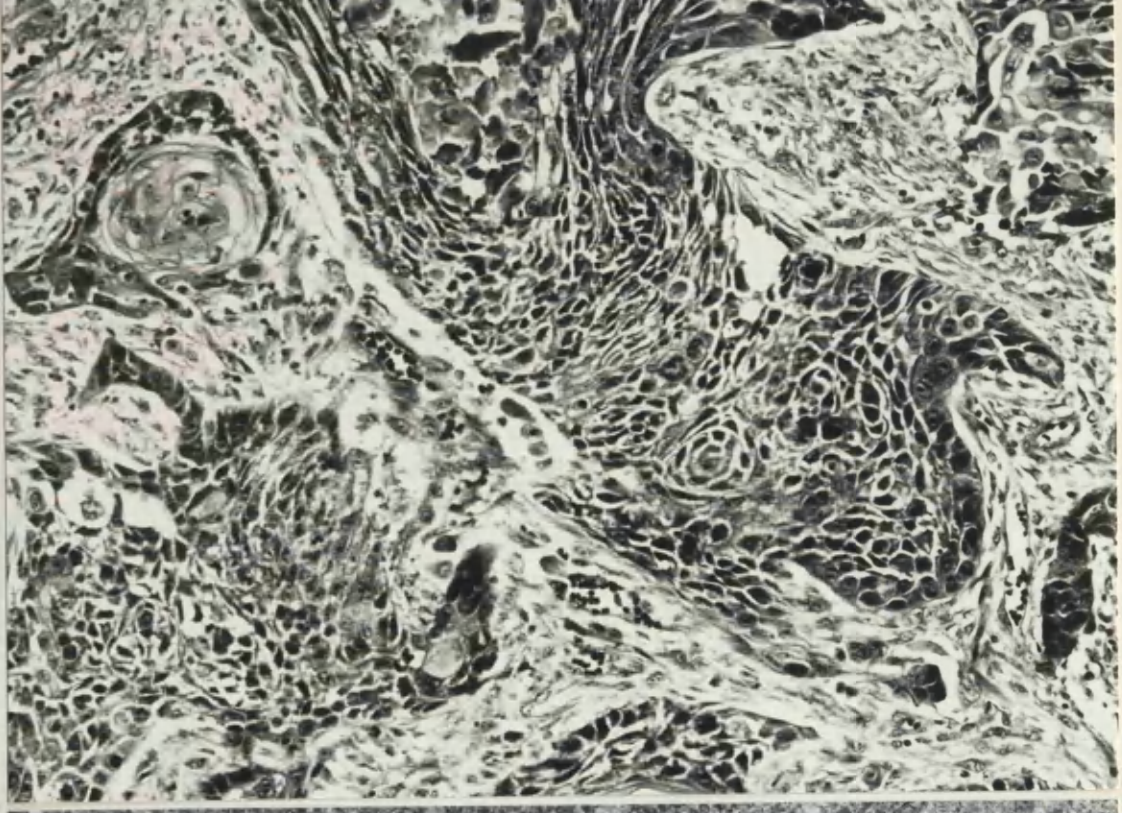

69

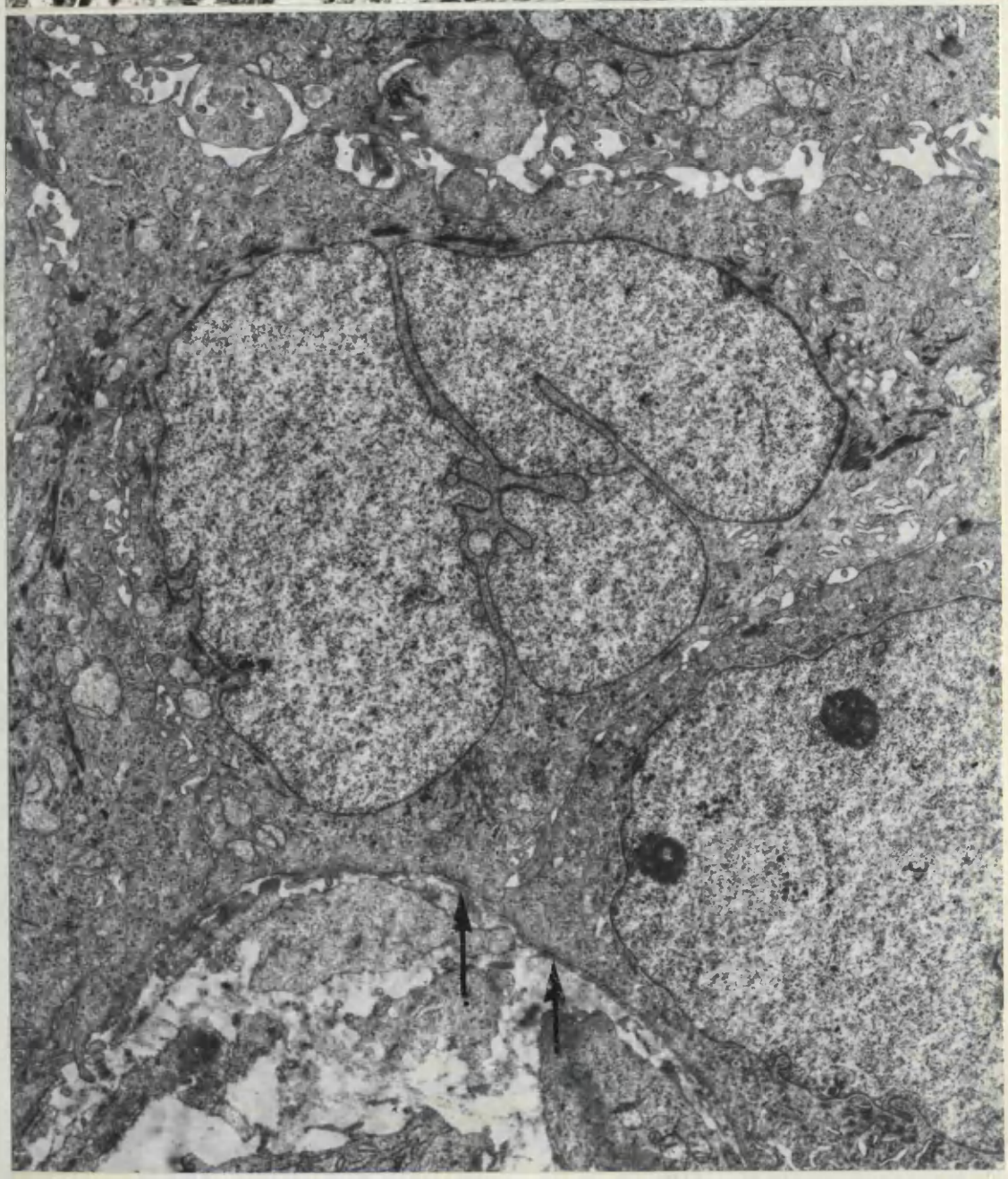

70

SQUAMOUS CARCINOMA OF OESOPHAGUS

Figure 71. "Membrane-coating granule" of squamous cell carcinoma of oesophagus. Note the limiting membrane, pale halo and dense core.

Magnification 124000.

Figure 72. Carbohydrate stain shows the presence of a positive staining component in the membrane-coating granules of squamous cell carcinoma.

Magnification 116500.

Figure 73. Squamous cell carcinoma of oesophagus. The neoplastic cells are irregular in outline and have large nuclei. Notice the peripheral location of the nucleoli and the perinuclear arrangement of the tonofilaments, (arrows).

Magnification 6720.

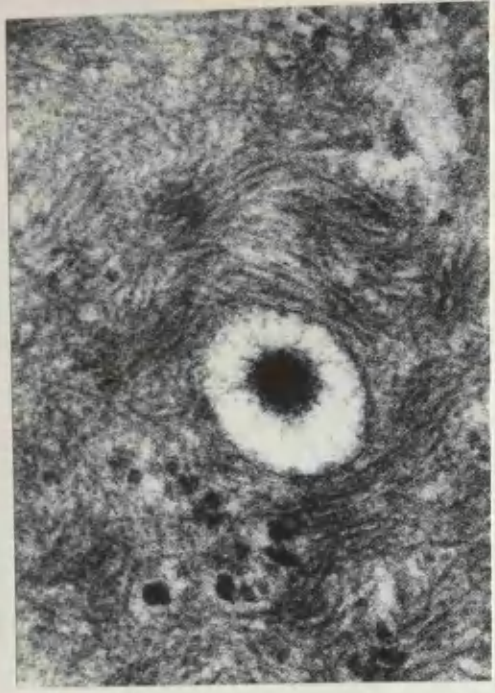

71

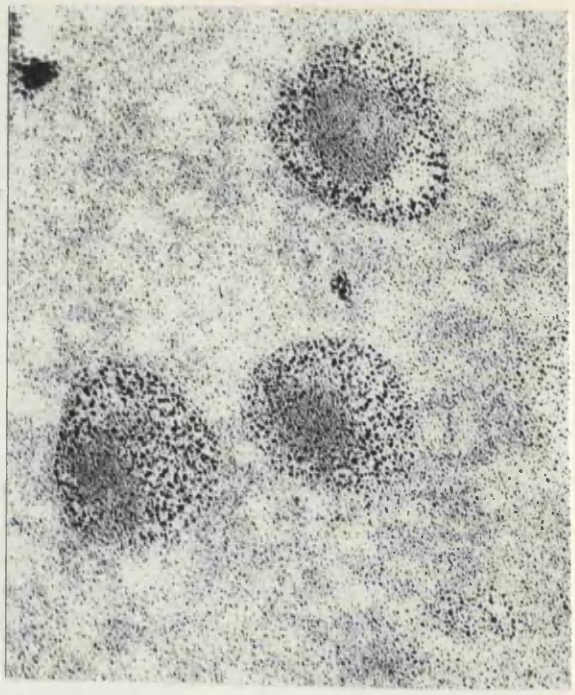

72

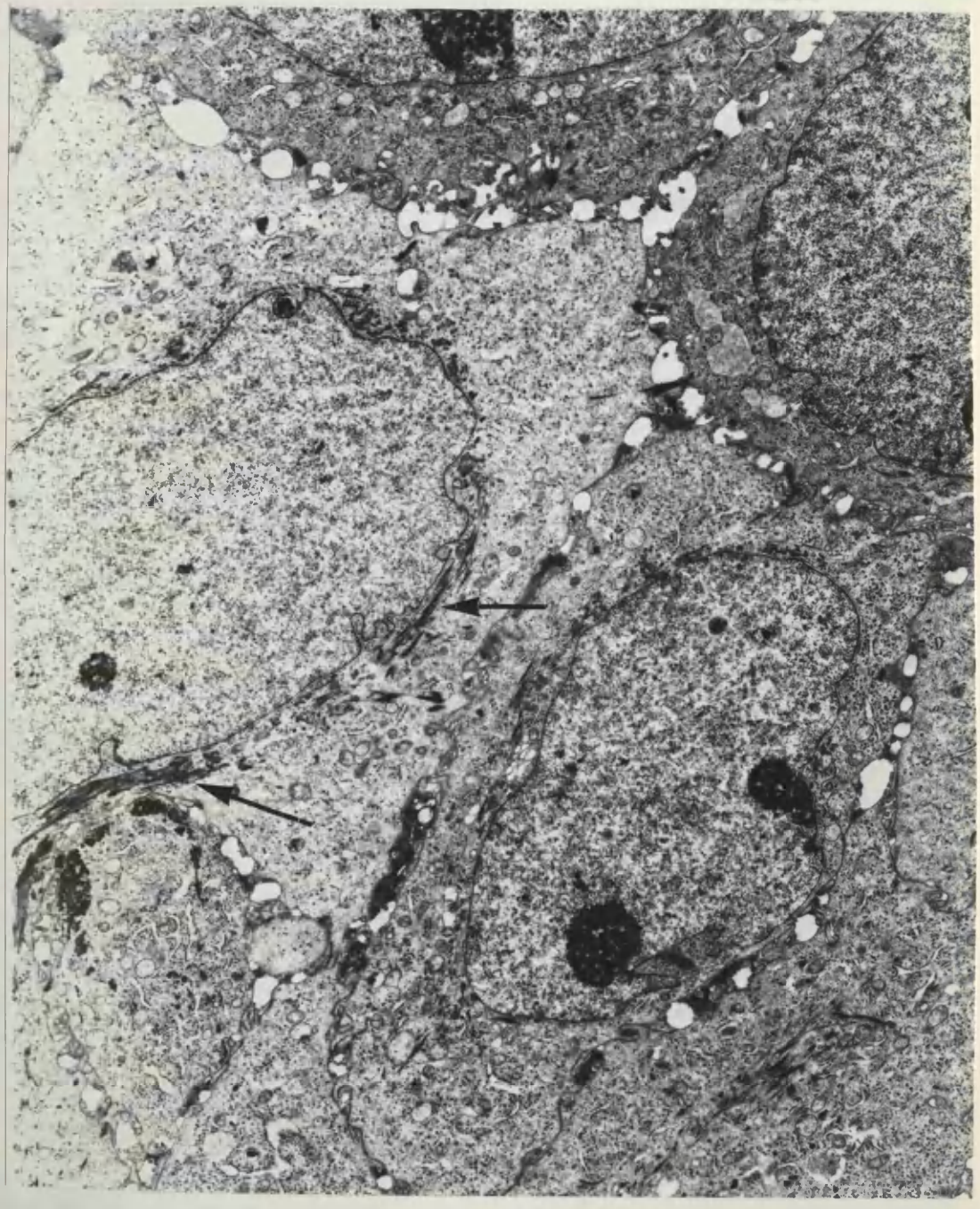

73

SQUAMOUS CARCINOMA OF OESOPHAGUS

Figure 74. Squamous cell carcinoma of oesophagus. Bulbous protrusion is shown, extending from a tumour cell into the intercellular space. This protrusion is devoid of tonofilaments and is not attached by desmosomes to adjacent cells.

Magnification 8600.

Figure 75. The large nucleus of a cancer cell is seen to have two prominent nucleoli which lie in contact with the apices of two invaginating cytoplasmic channels.

Magnification 14000.

Figure 76. Another large nucleus of a cancer cell is shown to contain two prominent nucleoli. Notice the island of cytoplasm which is apparently stranded within the centre of the nucleus, but which no doubt communicates with the nuclear surface at a different level.

Magnification 10750.

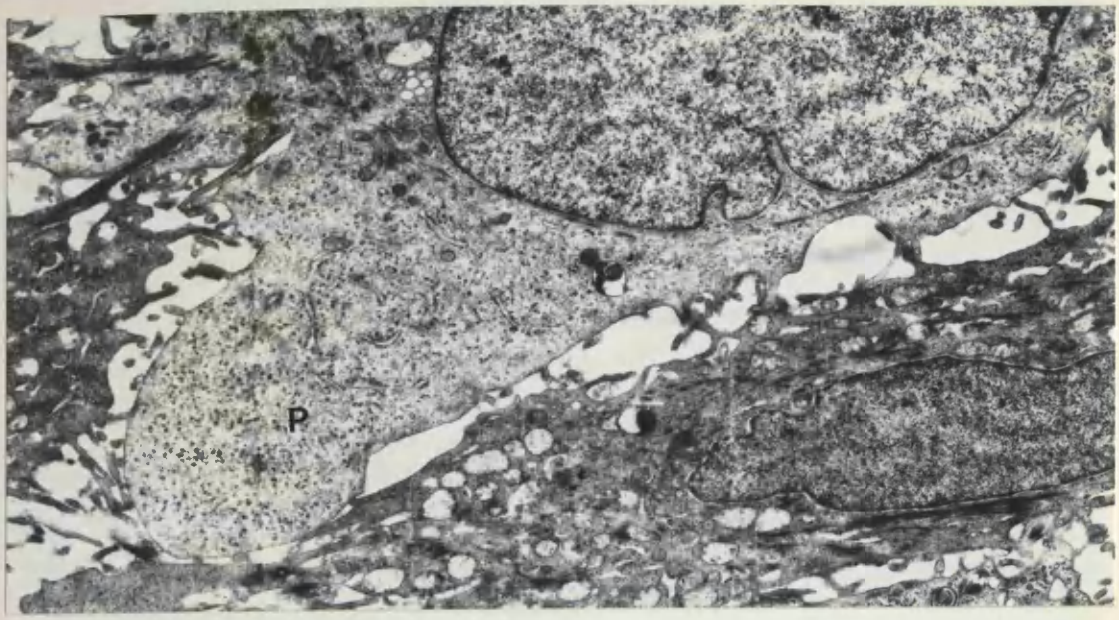

74

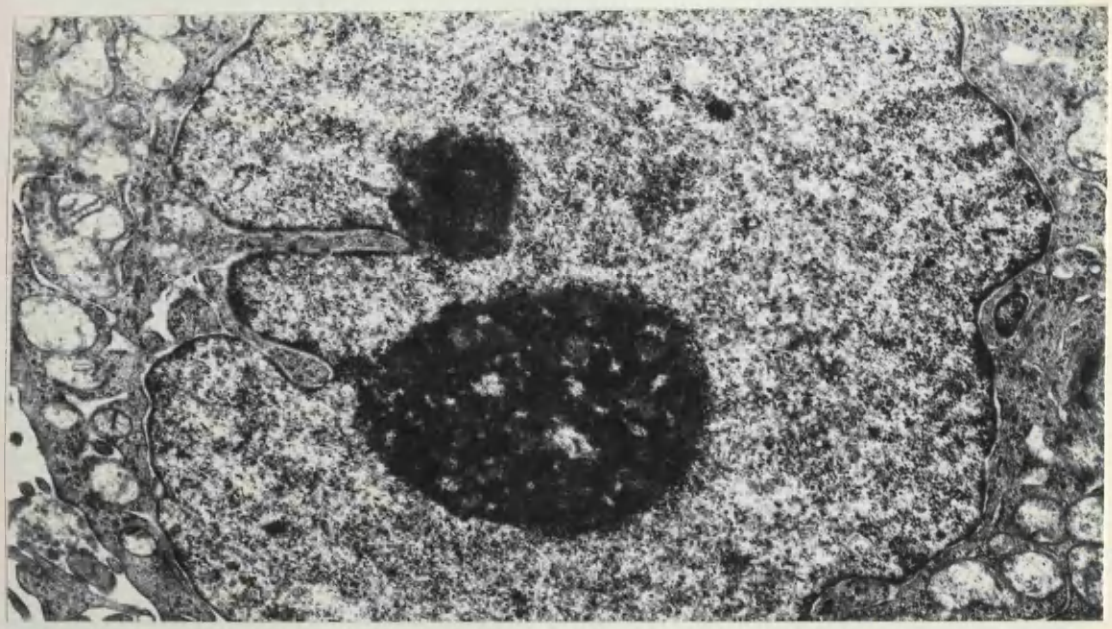

75

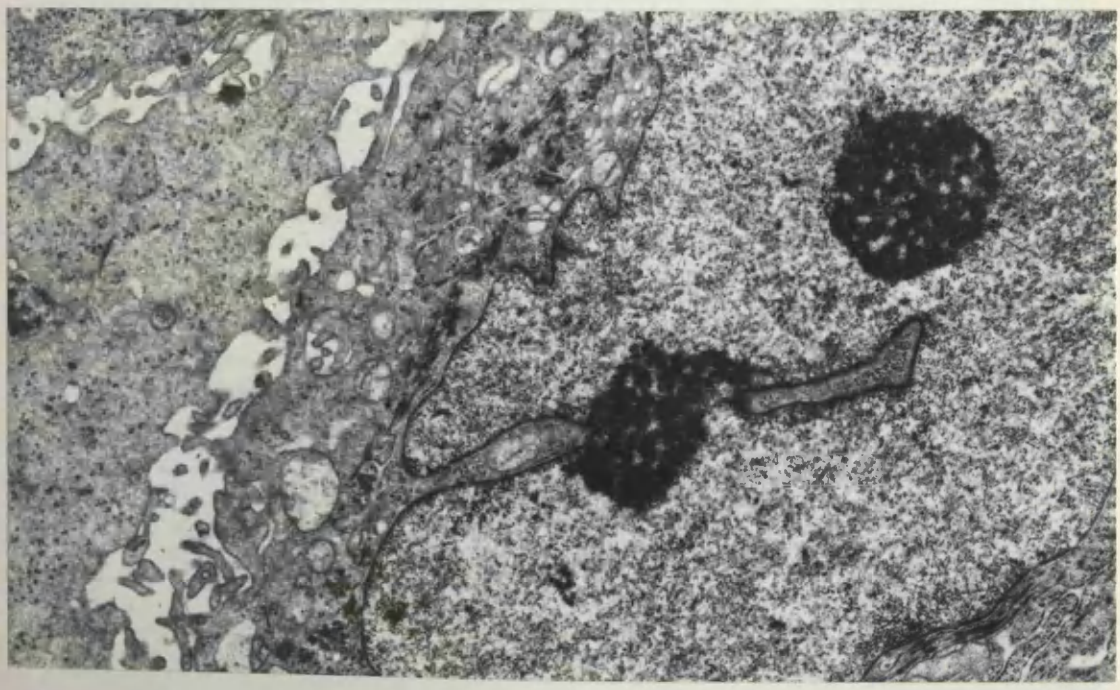

76

SQUAMOUS CARCINOMA OF OESOPHAGUS

Figure 77. The dark and light cells of squamous cell carcinoma of oesophagus are shown. The dark cell has a dark nucleus while the light cell has a much paler nucleus. Notice the more numerous tonofilaments in the dark cell. The increased density, however, is largely due to the more numerous ribosomes as well as to a generally increased density of the cytoplasmic matrix.

Magnification 12900

Figure 78. An intracytoplasmic desmosome(arrow) is shown. Notice the widened intercellular space(S) and the absence of intercellular adhesion at that point. The lamination pattern of the intracytoplasmic desmosome is identical to that of a conventionally situated desmosome. Notice the associated tonofilaments around the desmosome.

Magnification 32500

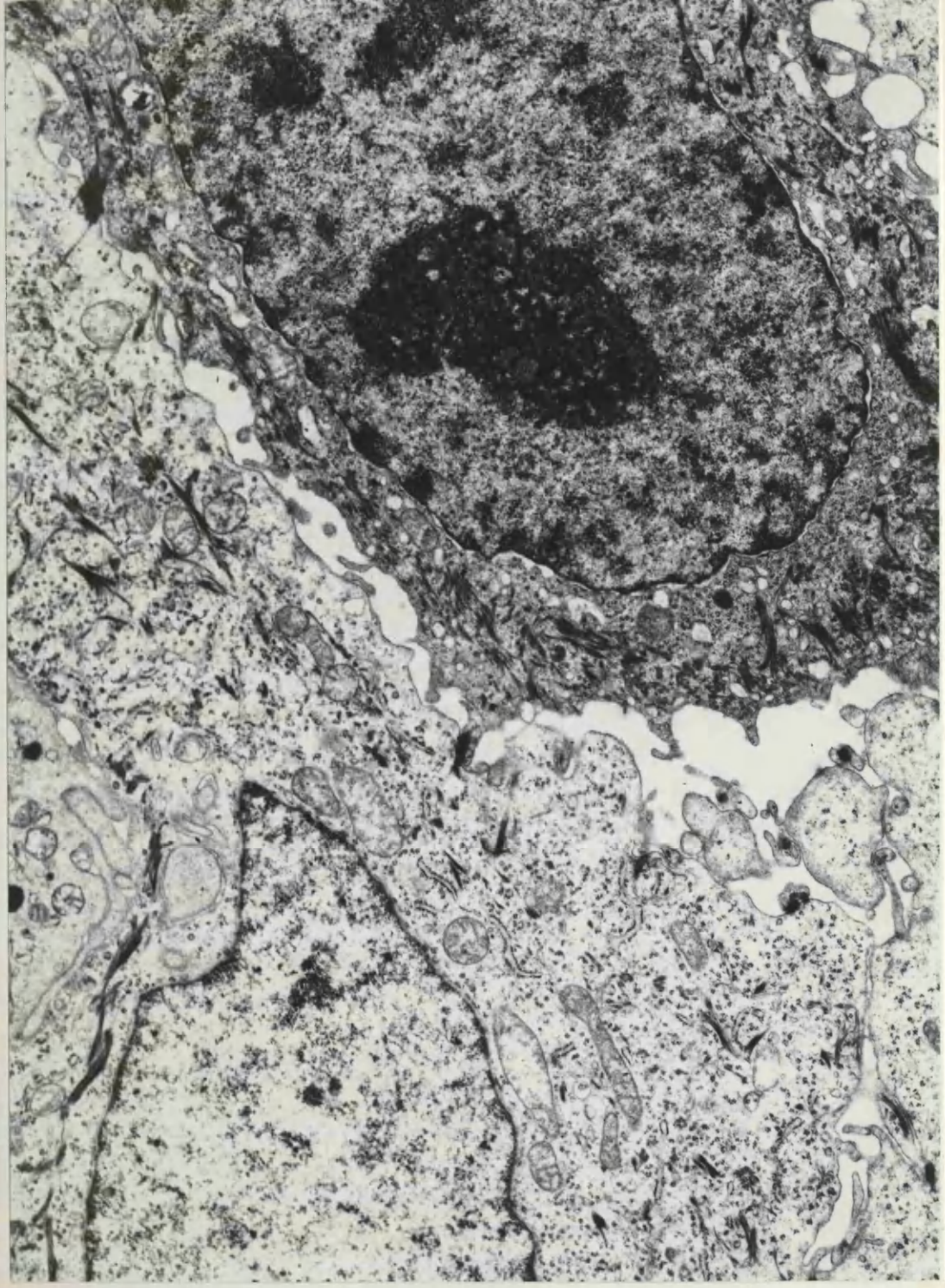

77

78

SQUAMOUS CARCINOMA OF OESOPHAGUS

Figure 79. Squamous cell carcinoma of human oesophagus. Intracytoplasmic desmosomes (C) are seen surrounded by dense masses of tonofilaments in the cells of the epithelial pearl. Notice the intercellular desmosome(D) connecting adjacent cells.

Magnification 39000.

Figure 80. Numerous pseudopodial cytoplasmic protrusions(P) extend from this cancer cell into the adjacent stroma (S). Notice the absence of any coherent basal lamina at the interface.

Magnification 10750.

Figure 81. Cell from the epithelial pearl of squamous cell carcinoma. The cell has a pyknotic nucleus. Randomly oriented tonofilaments form large cytoplasmic bundles and also appear within the nucleus.

Magnification 26000.

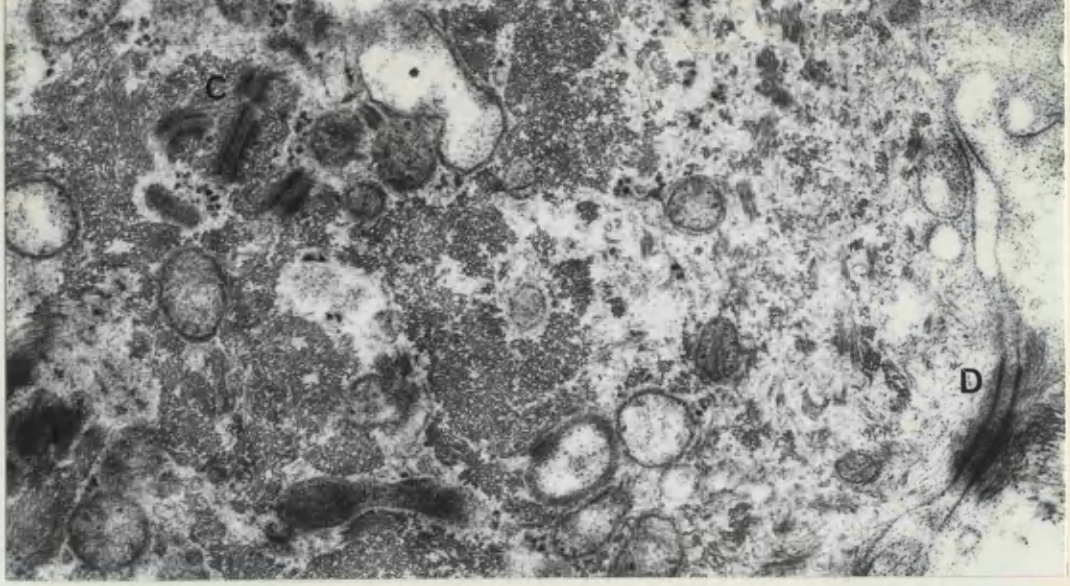

79

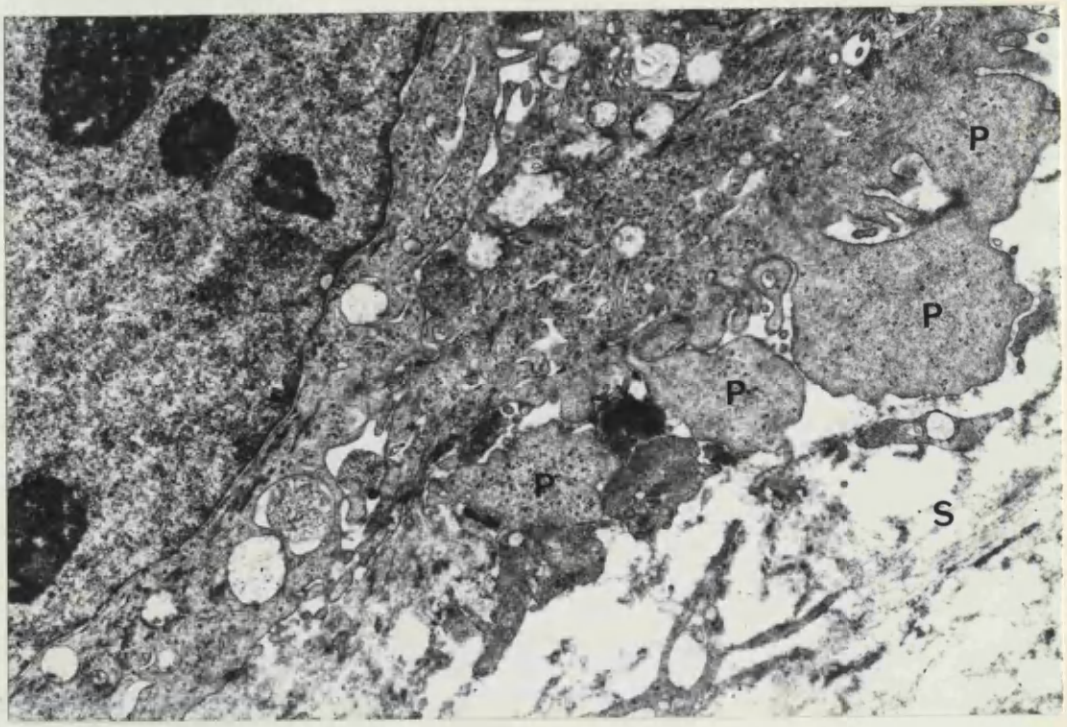

80

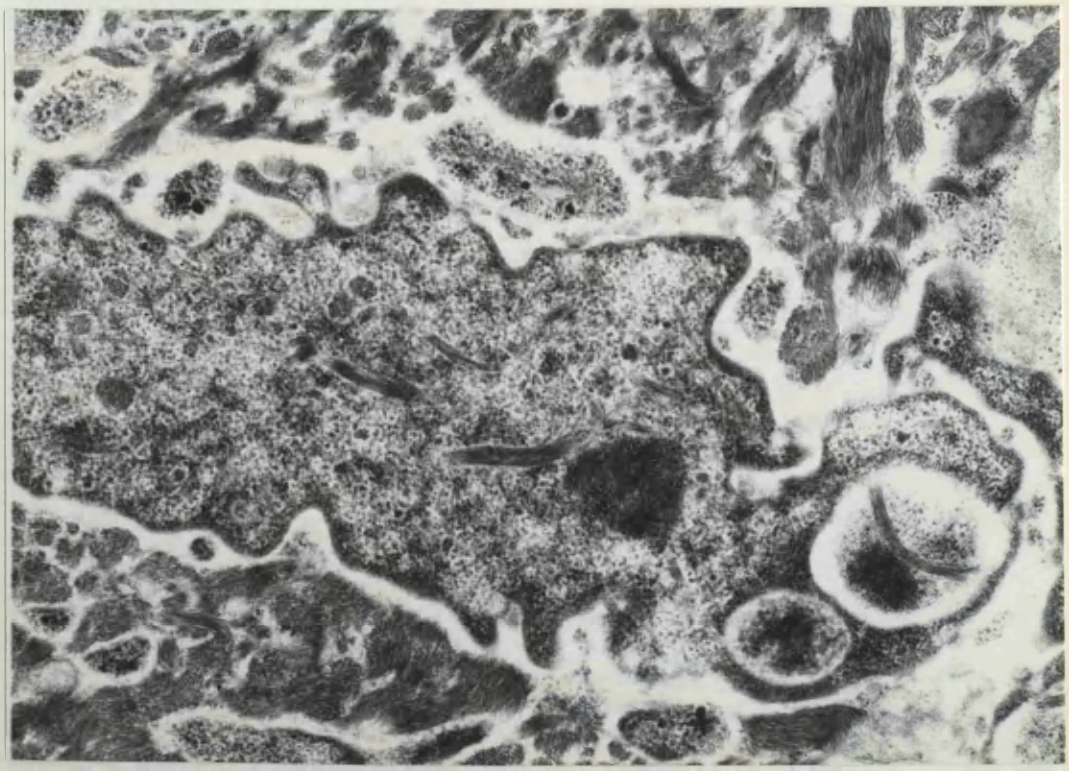

81

SQUAMOUS CARCINOMA OF OESOPHAGUS

Figure 82. Two intracytoplasmic desmosomes of squamous cell carcinoma of oesophagus, tilted +45°. They are not continuous with the cell surface or any extensive membranes.

Magnification 107500.

Figure 83. The same intracytoplasmic desmosomes in Figure 82 untilted.

Magnification 107500.

Figure 84. The intracytoplasmic desmosomes of Figure 82 tilted - 45°. Again no continuity with cell surface is seen.

Magnification 107500.

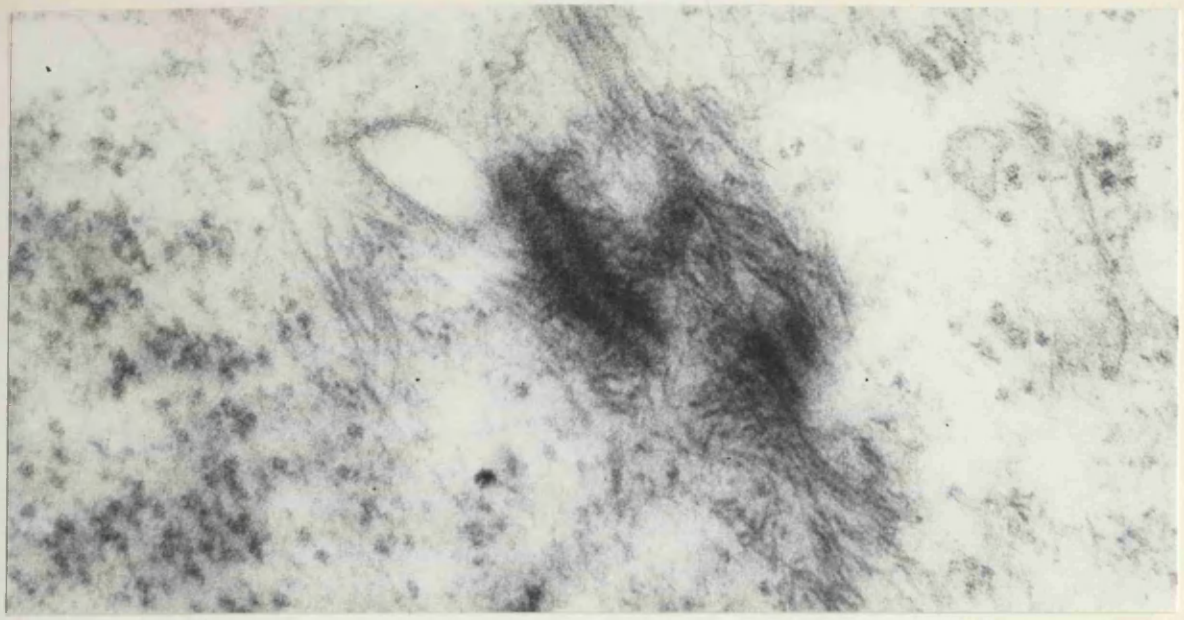

82

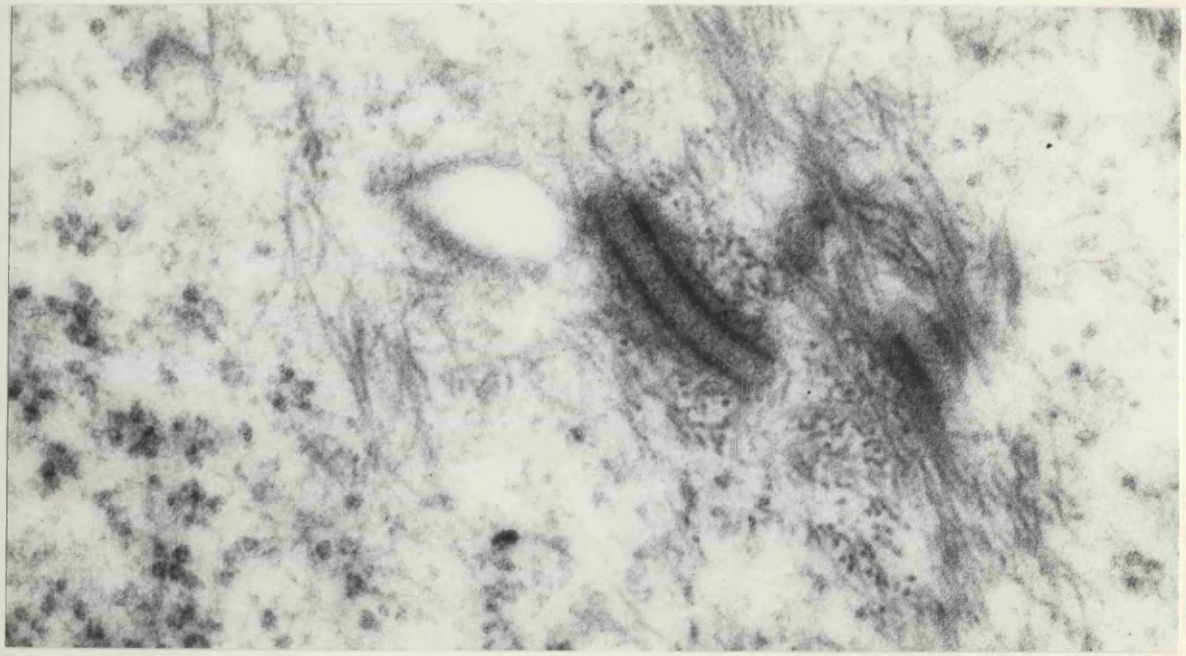

83

84

SQUAMOUS CARCINOMA OF OESOPHAGUS

Figure 85. Tonofilaments within the nucleus of a cell of the epithelial pearl of squamous cell carcinoma. The cytoplasm on the left upper corner of the micrograph is crowded with tonofilaments.

Magnification 32500.

Figure 86. A typical keratohyalin granule from the epithelial pearl of squamous carcinoma.

Magnification 88250.

Figure 87. A round thick-walled vesicle is seen in the cytoplasm of a cell from the epithelial pearl.

Magnification 93200.

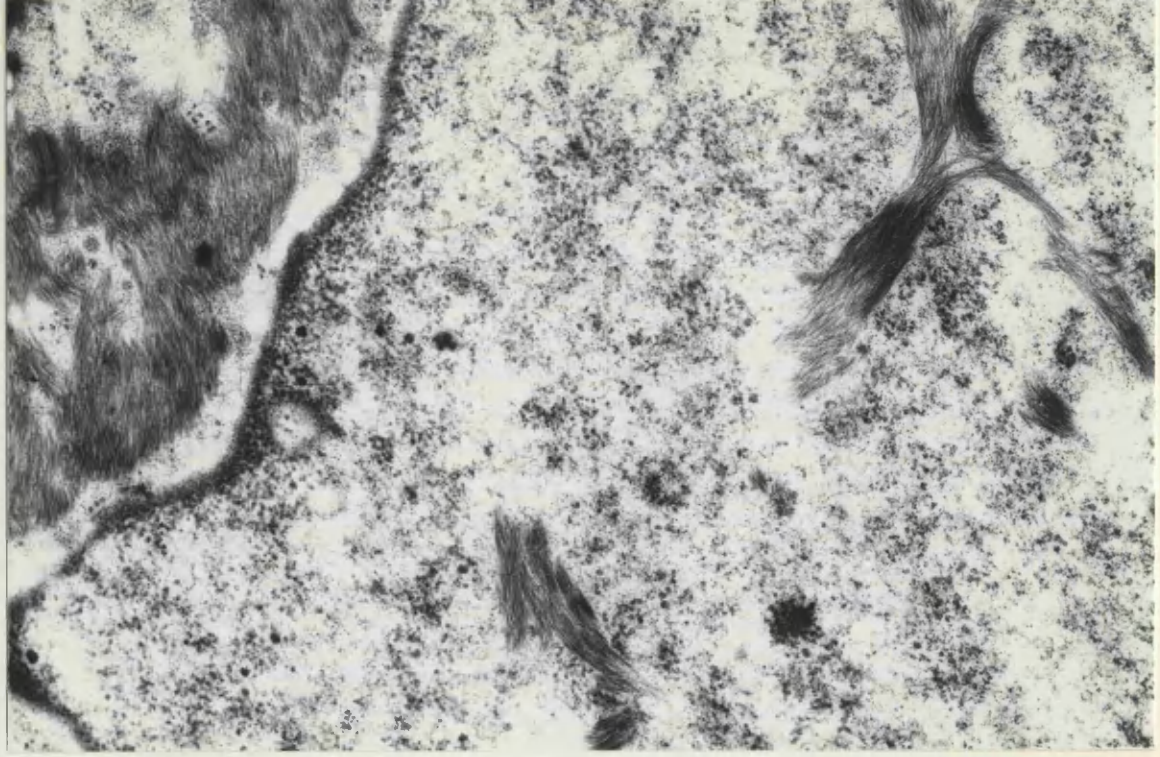

85

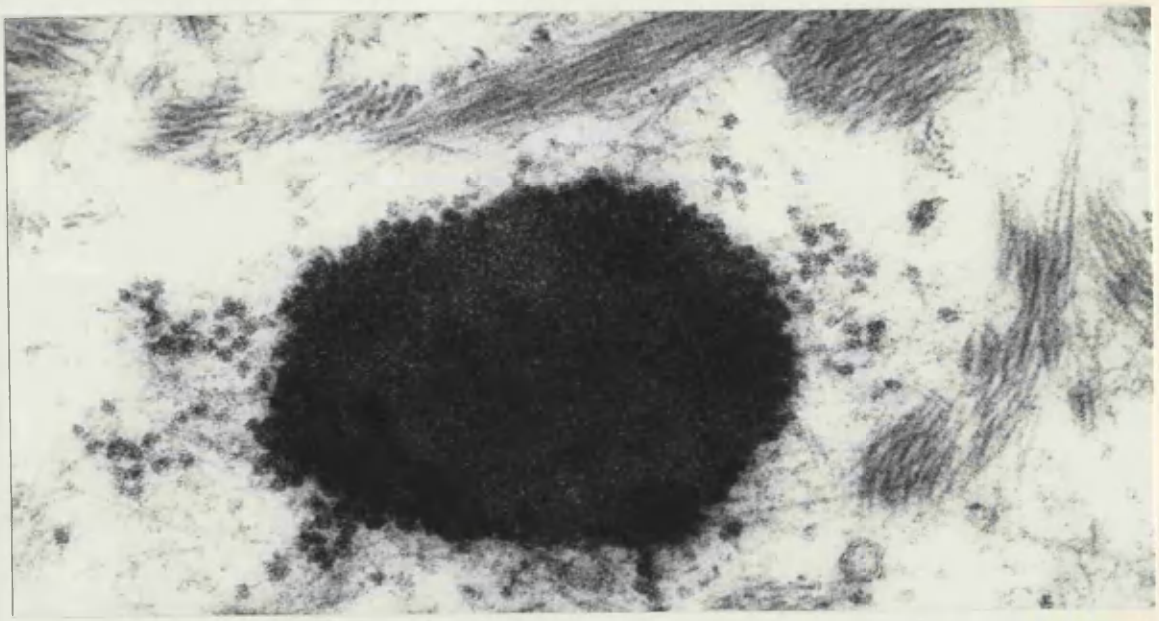

86

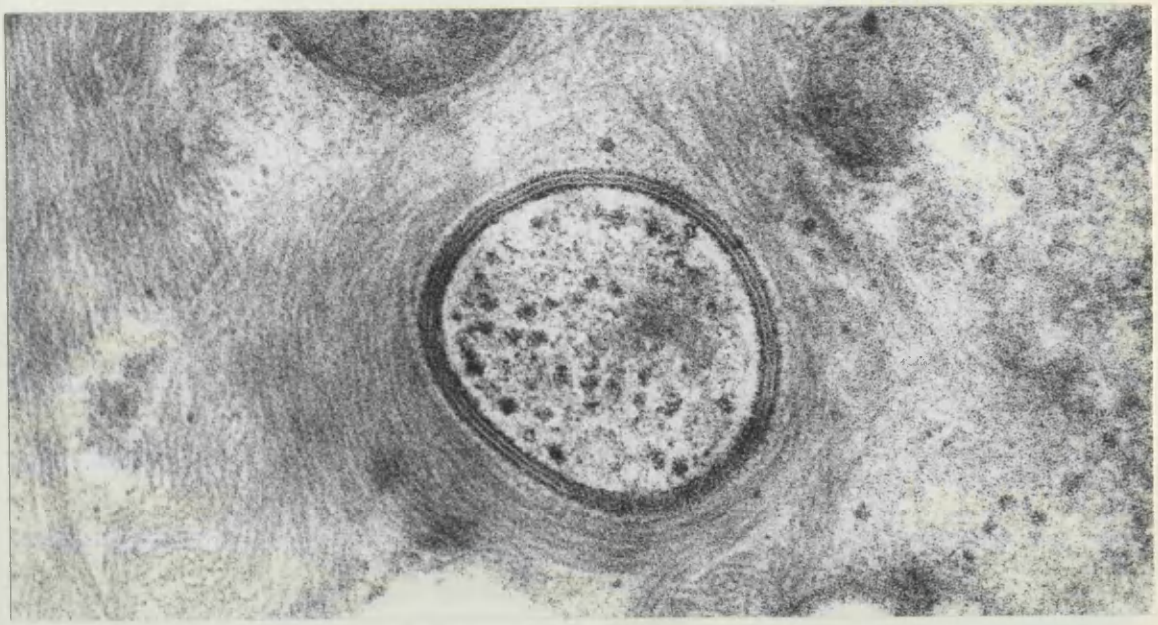

87

SQUAMOUS CARCINOMA OF OESOPHAGUS

Figure 88. An oval thick-walled vesicle of the epithelial pearl of squamous cell carcinoma showing an invaginated wall.

Magnification 116500.

Figure 89. A Langerhans cell from a case of squamous carcinoma of oesophagus is recognised by its distinctive granules.

Magnification 70600.

Figure 90. Acid phosphatase activity in the intercellular spaces and on the cell membrane of squamous cell carcinoma of oesophagus. Notice the absence of reaction product from the membrane-coating granules (G). The appearances are identical to those seen in normal oesophageal squamous mucosa.

Magnification 93200.

88

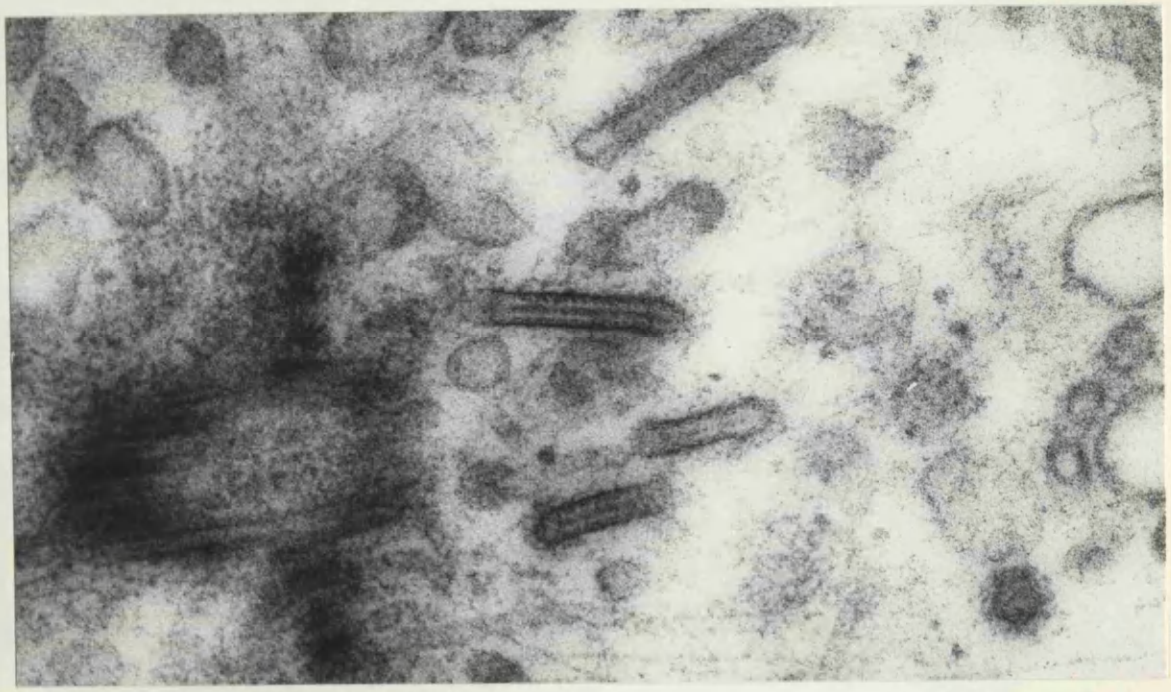

89

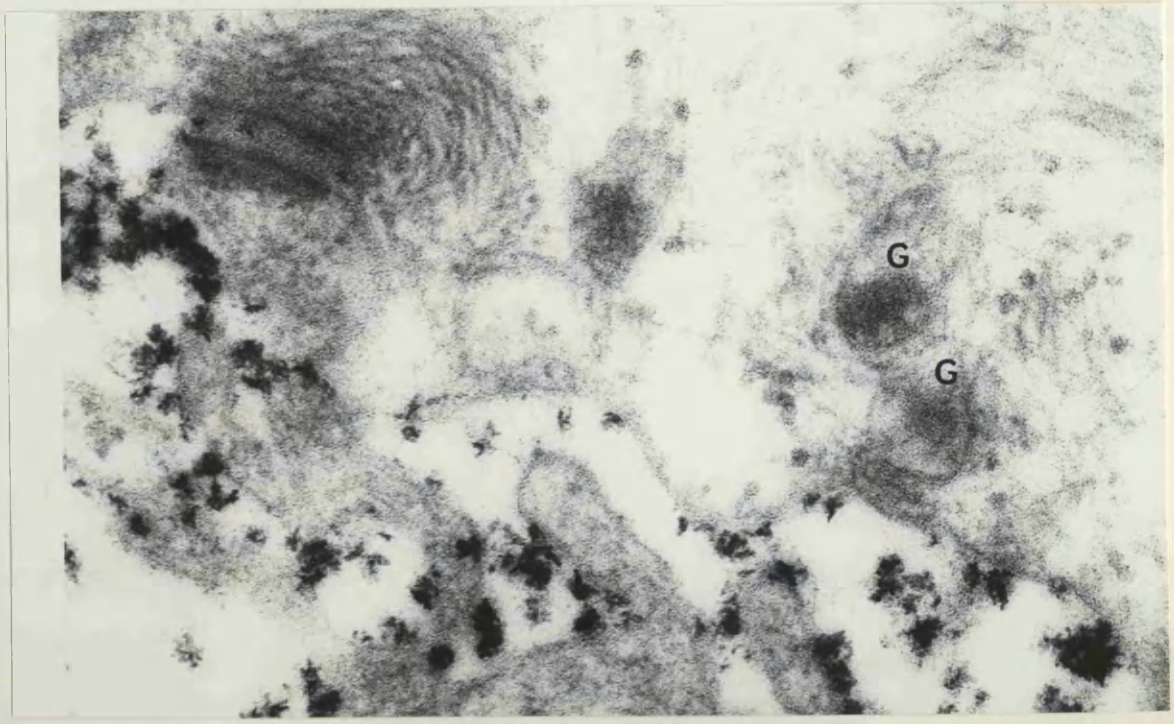

90

SQUAMOUS CARCINOMA OF OESOPHAGUS

Figure 91. Acid phosphatase activity in the intercellular spaces of squamous cell carcinoma of human oesophagus. The dense small granules inside the cytoplasm are ribosomes.

Magnification 14000

Figure 92. Acid phosphatase activity in large heterogeneous inclusions of squamous carcinoma.

Magnification 52950

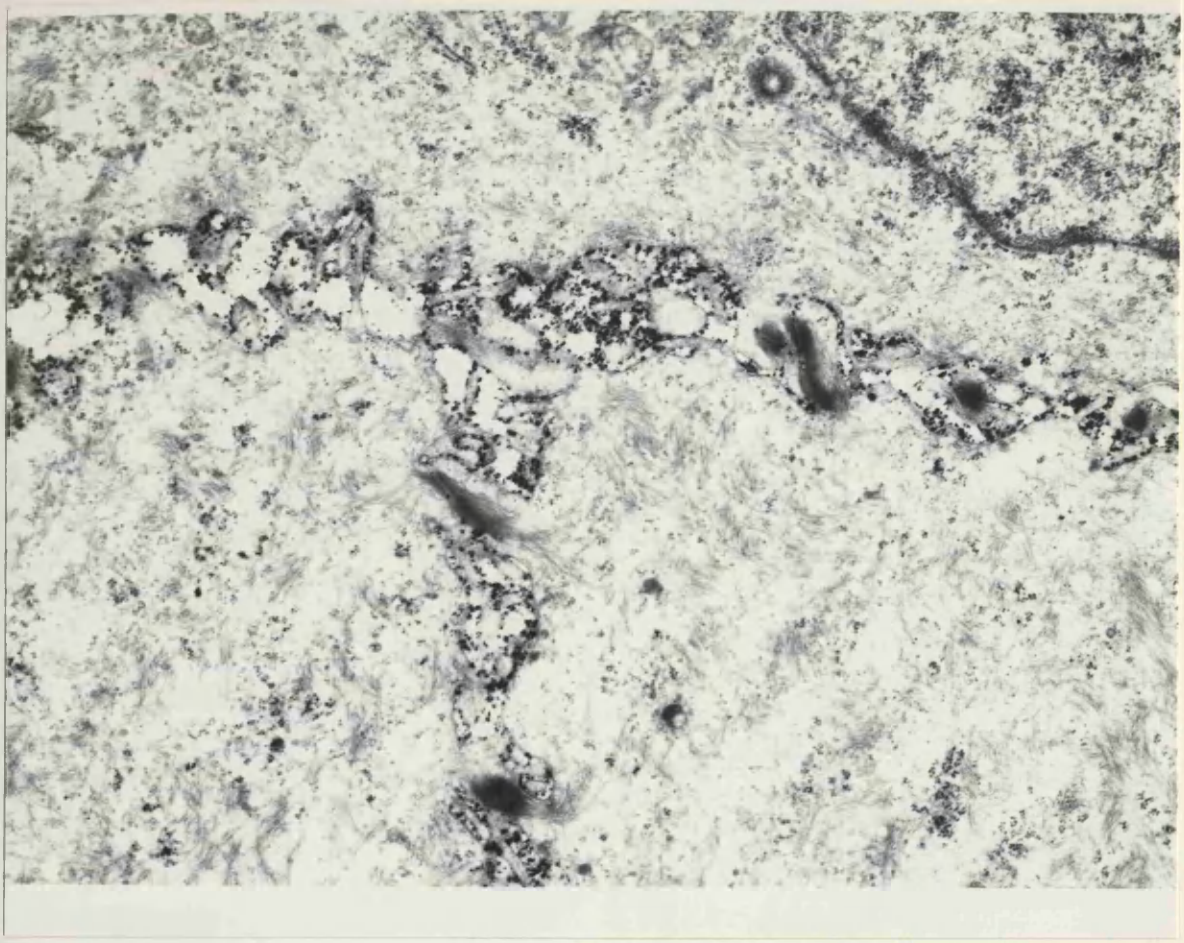

91

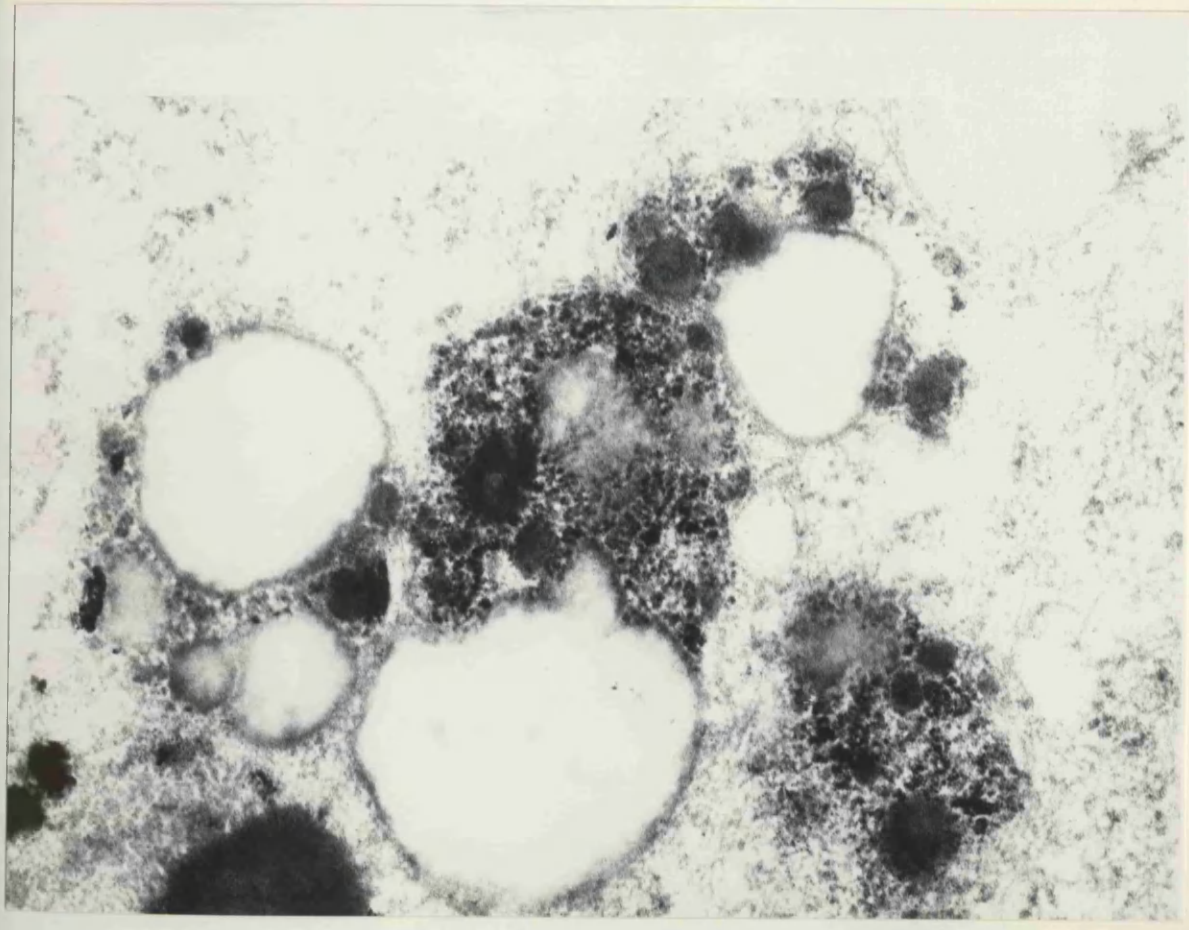

92

SQUAMOUS CARCINOMA OF OESOPHAGUS

Figure 93. Squamous cell carcinoma of oesophagus. There are heterogeneous membrane-limited dense inclusions in the cytoplasm. The large nucleus of the cancer cell contains a ring-shaped nucleolus.

Magnification 10750

Figure 94. Acid phosphatase activity is seen in a round dense inclusion of squamous cell carcinoma.

Magnification 17500

93

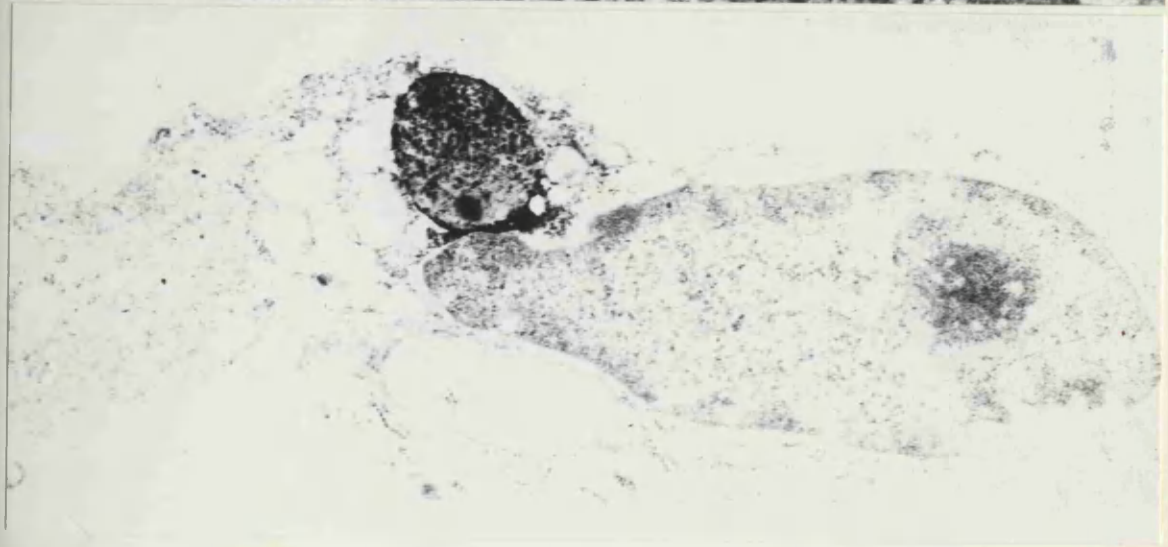

94

GASTRIC TUMOURS

Figure95. The histology of primary well differentiated gastric carcinoma is shown. This case is typical of those in which mucous secretion granules occur.

Magnification 225

Figure 96. Electron micrograph from the case shown in figure 95. The columnar cells are closely packed and havebasally situated nuclei. The most distinctive feature of these cells is the occurrence of dark mucous secretion granules in their apical cytoplasm. Note the lumen(L) of the gland.

Magnification 4800

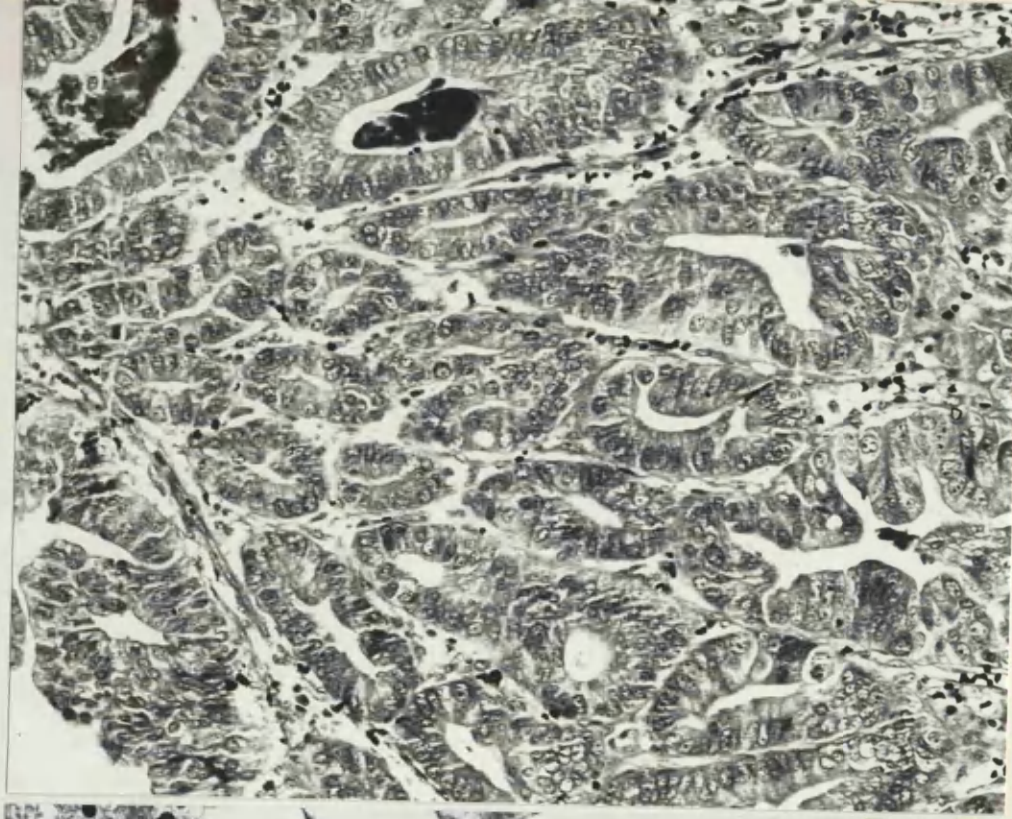

95

96

GASTRIC TUMOURS

Figure 97. Apical cytoplasm of cancer cells of gastric cell type of adenocarcinoma. The mucous granules are similar to those of normal gastric mucous cells(Fig.44).

Magnification 32500

Figure 98. Mucous secretion granules of the gastric cell type of carcinoma. The granules have a closely applied limiting membrane similar to that of the mucous granules of gastric mucous cells.

Magnification 51250

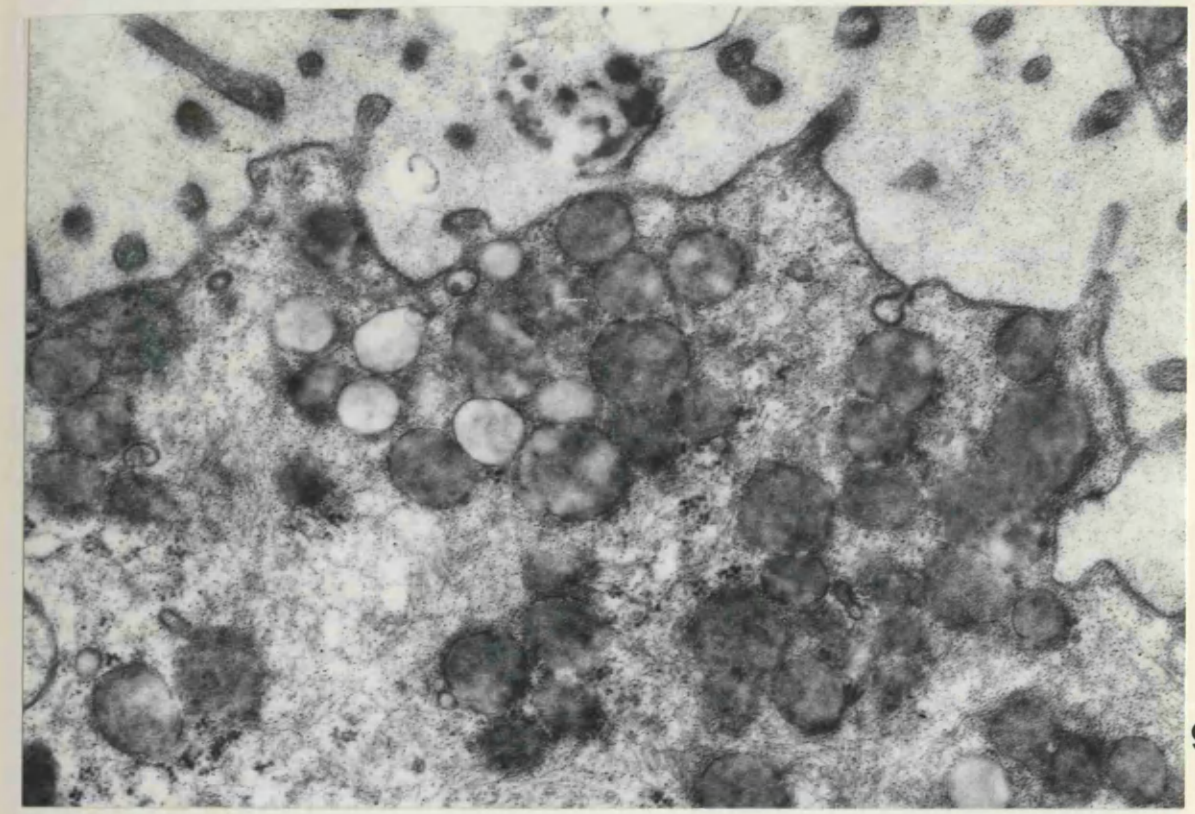

97

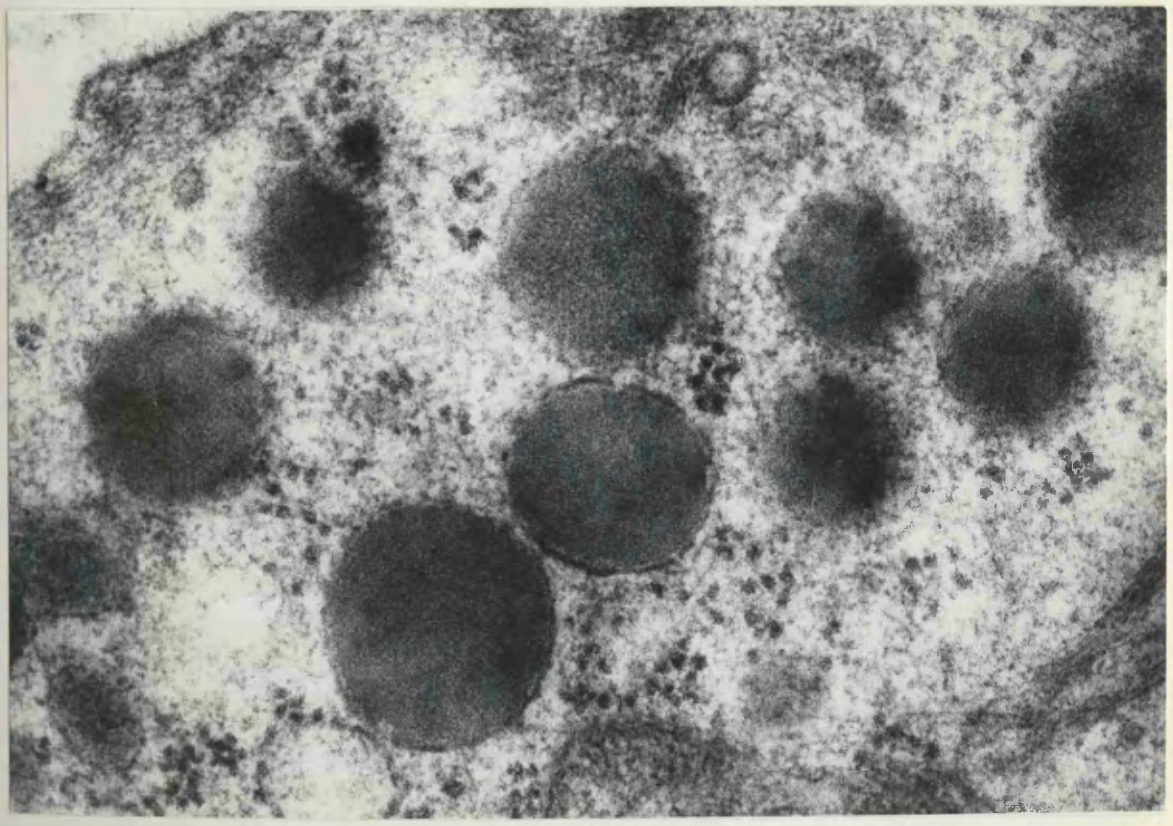

98

GASTRIC TUMOURS

Figure 99. Gastric cell type of adenocarcinoma . Mitochondria(M) with tubular and vesicular cristae are seen. Notice the nucleus(N) of the cancer cell.

Magnification 21000

Figure 100. Gastric cell type of adenocarcinoma showing a large mitochondrion containing rod-shaped inclusions. Another mitochondrion(M) contains obliquely sectioned inclusions. Notice the distinct periodicity in the longitudinally sectioned profiles.

Magnification 32000

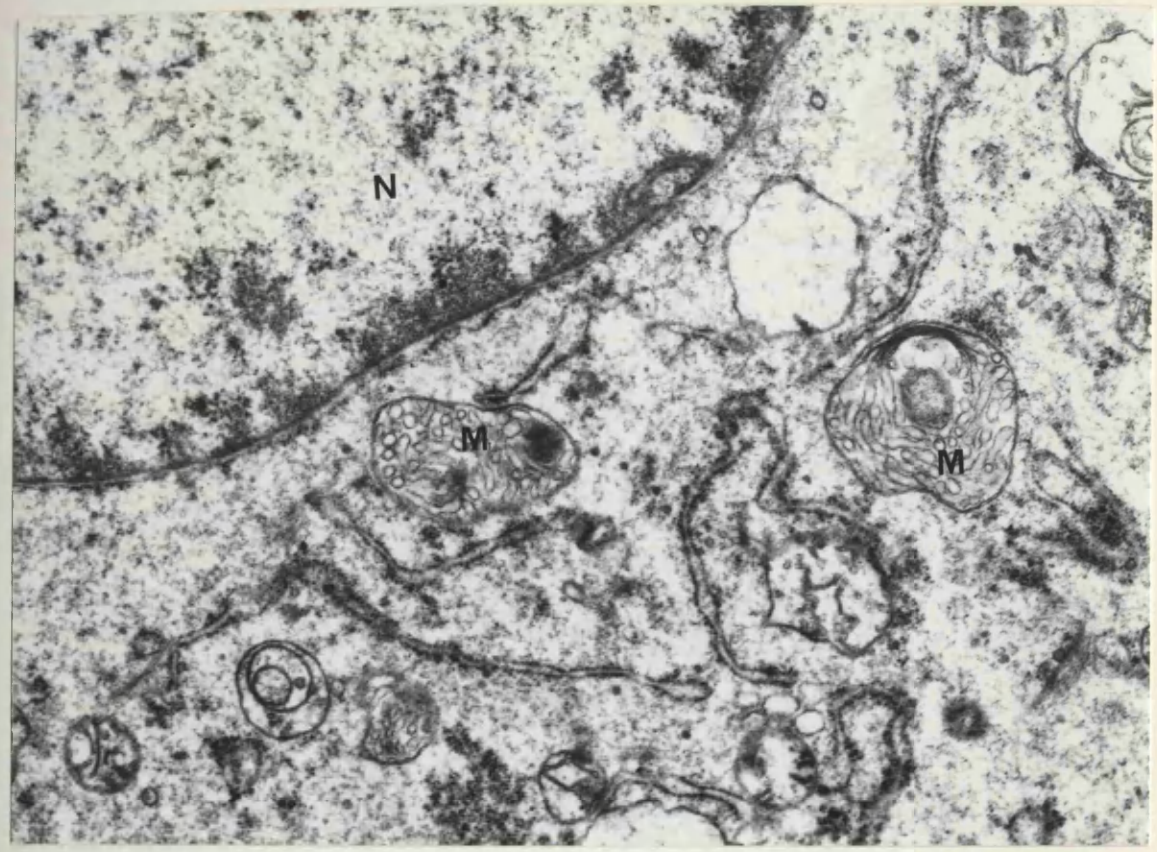

99

100

GASTRIC TUMOURS

Figure 101. Gastric cell type of adenocarcinoma, showing a mitochondrion with concentric cristae.

Magnification 88250

Figure 102. Gastric cell type of adenocarcinoma. The dilated cisternae of granular endoplasmic reticulum contain rod-shaped inclusions.

Magnification 70000

Figure 103. Gastric cell type of adenocarcinoma. The membranous inclusion shown consists of concentrically arranged membranes which enclose granular material of moderate density.

Magnification 92000

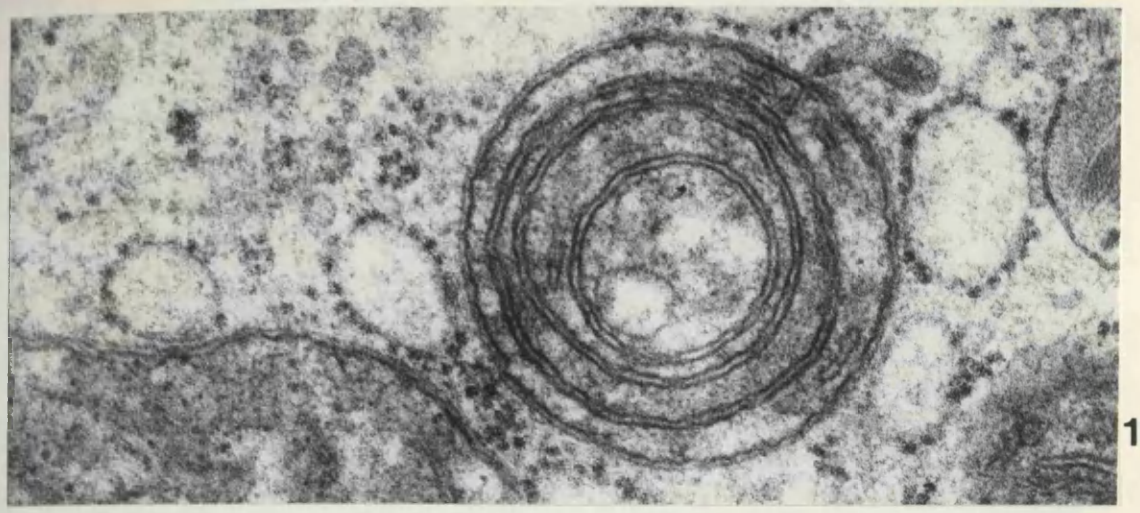

101

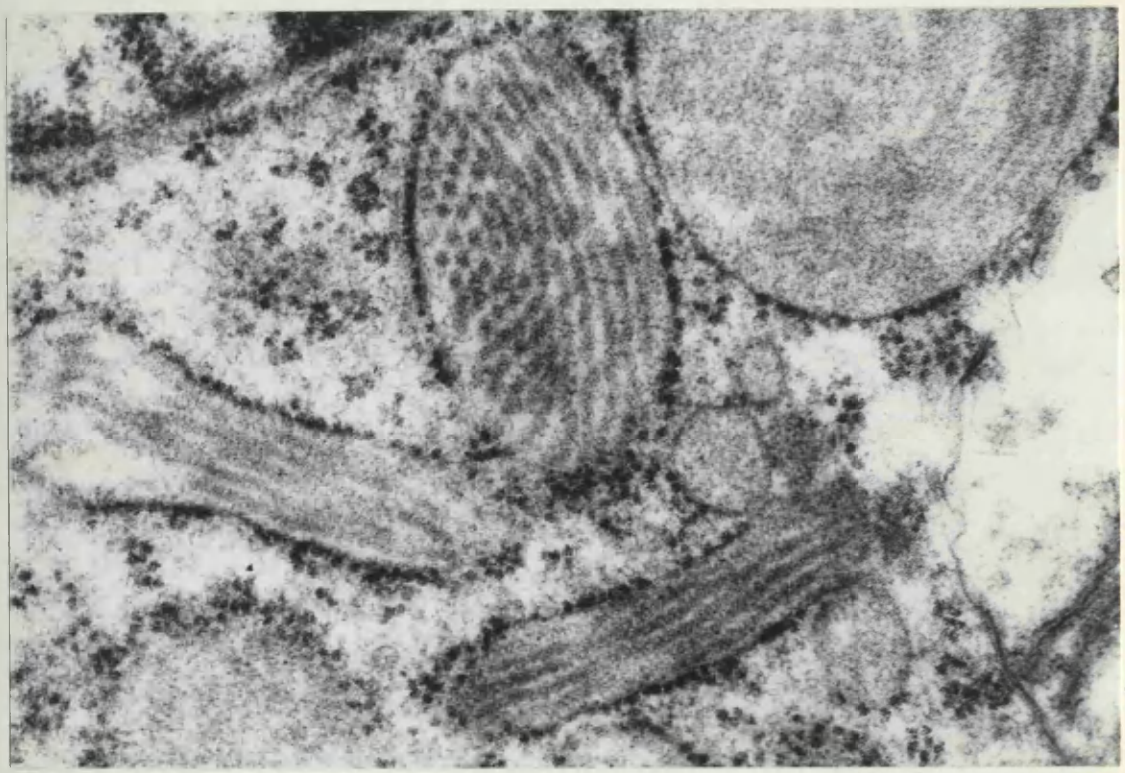

102

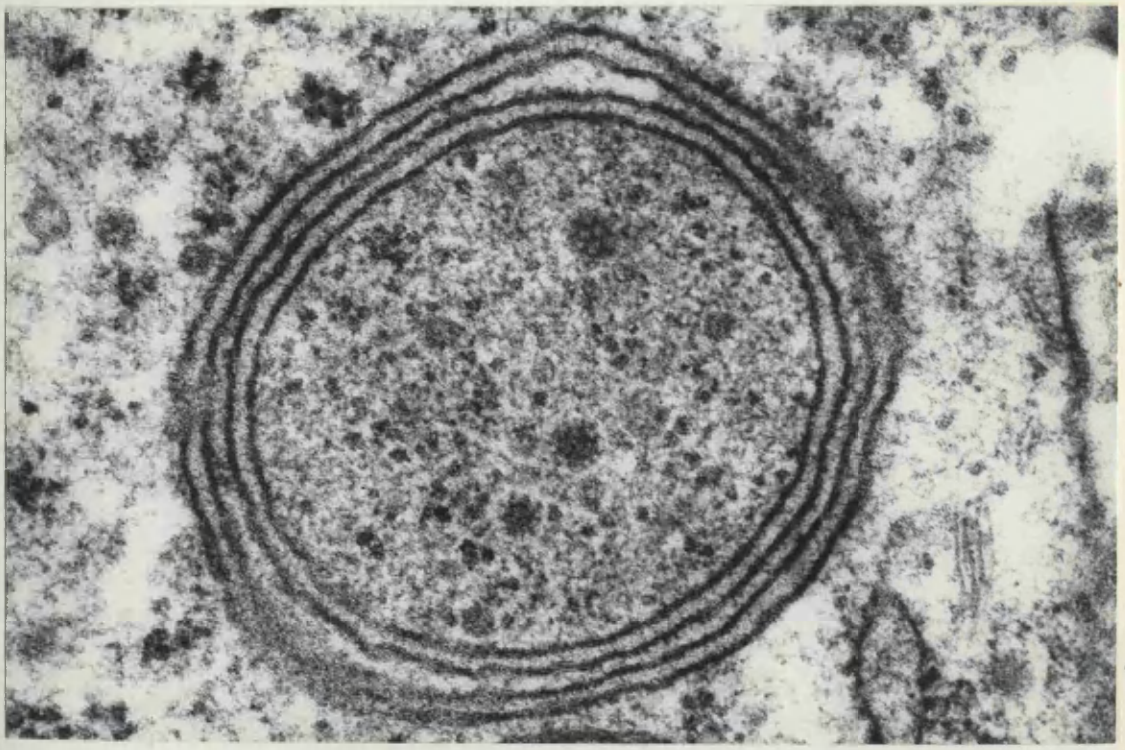

103

GASTRIC TUMOURS

Figure 104. The histology of a typical case of primary well differentiated gastric carcinoma which did not contain mucous secretion granules.

Magnification 225

Figure 105. Intestinal type of gastric carcinoma as shown above. The neoplastic cells arranged around an acinar space have long microvilli but no mucous secretion granules. Notice the moderately dense material within the lumen of the gland which may represent accumulated cell debris.

Magnification 6000

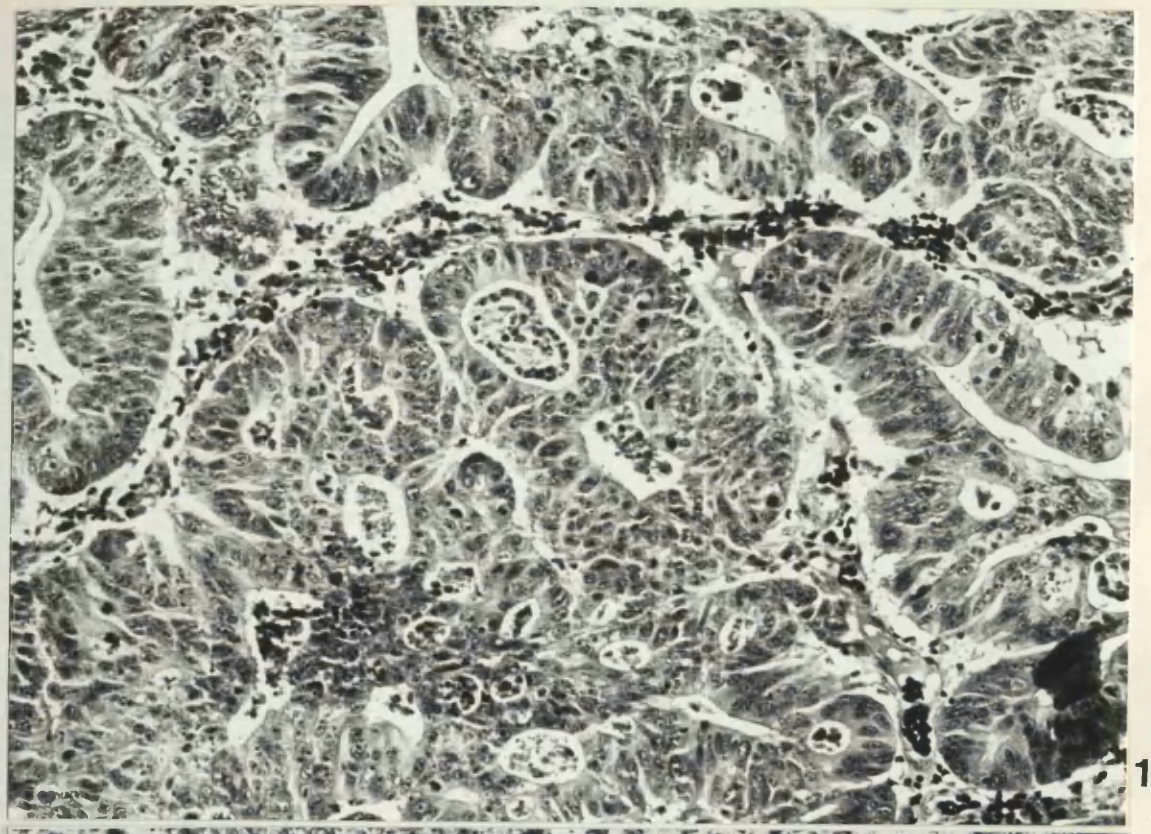

104

105

GASTRIC TUMOURS

Figure 106. Intestinal type of gastric carcinoma. The apical surface of the cancer cell bears long microvilli and a prominent fuzzy coat.

Magnification 13800

Figure 107. Intestinal type of gastric carcinoma . The basal parts of several cancer cells rest on a continous basal lamina and have conspicuous lateral interdigitations. The large nuclei are basally located.

Magnification 8400

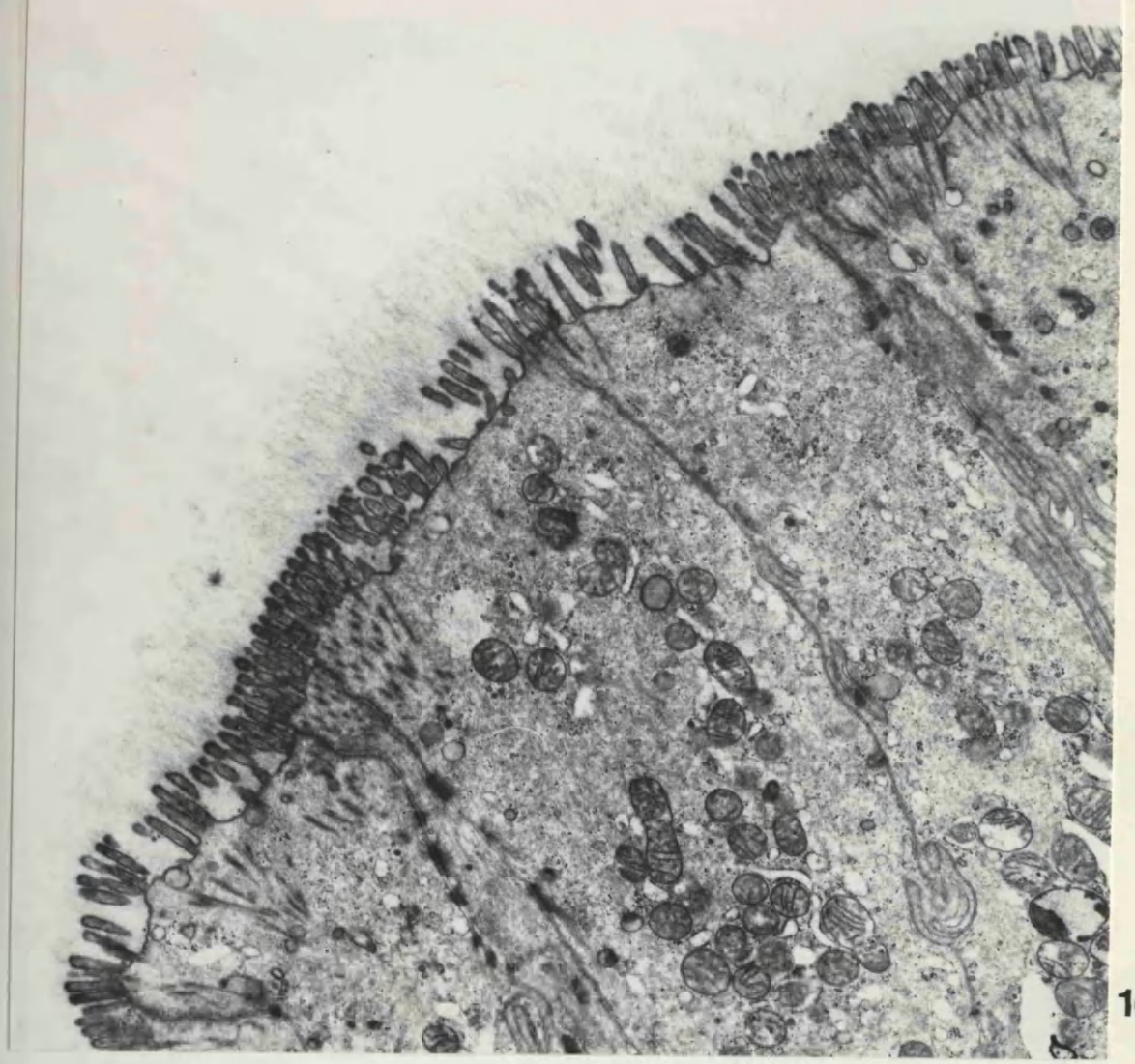

106

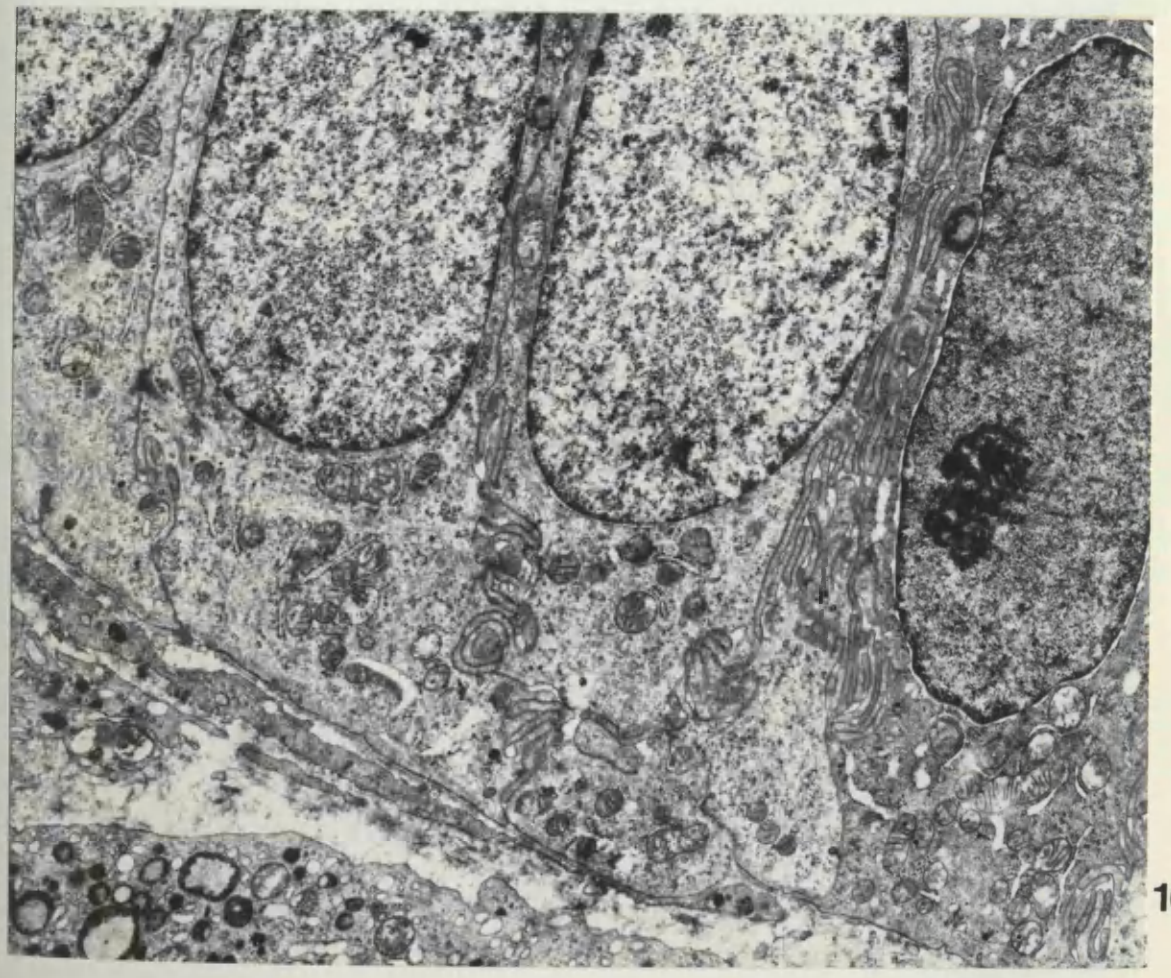

107

GASTRIC TUMOURS

Figure 108. Intestinal type of gastric carcinoma. The microvilli of this type of carcinoma are long and have a microfiamentous core extending to the apical ctoplasm. Notice the presence of intermicrovillous vesicles.

Magnification 70000

Figure 109. Intestinal type of gastric carcinoma. The cytoplasm of a cancer cell contains typical mitochondria, Golgi system, free ribosomes and scattered cisternae of granular endoplasmic reticulum. Notice the dense intramitochondrial particles.

Magnification 67250

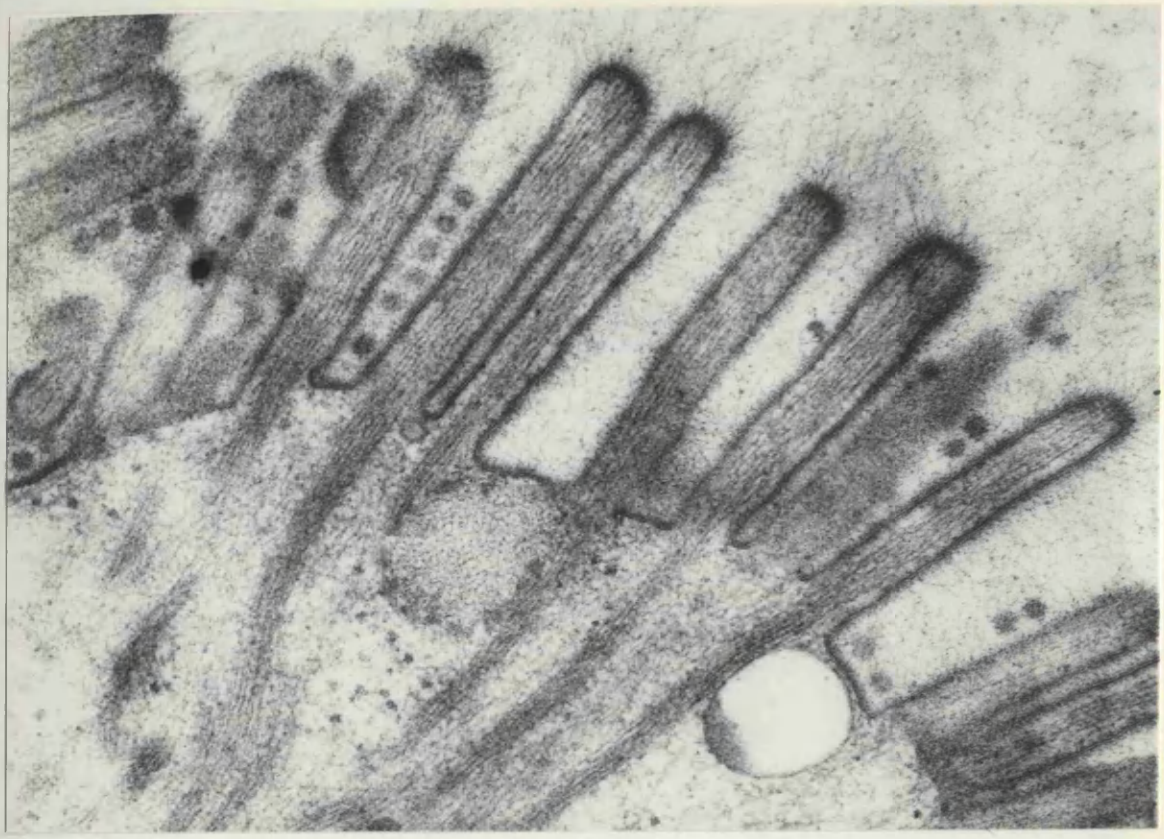

108

109

GASTRIC TUMOURS

Figure 110. Intestinal type of gastric carcinoma. A goblet cell(G) is interposed between less differentiated cancer cells. The dark nucleus of the goblet cell is pushed basally by the accumulated mass of mucous granules. Notice the lumen (L) and the microvilli.

Magnification 8400

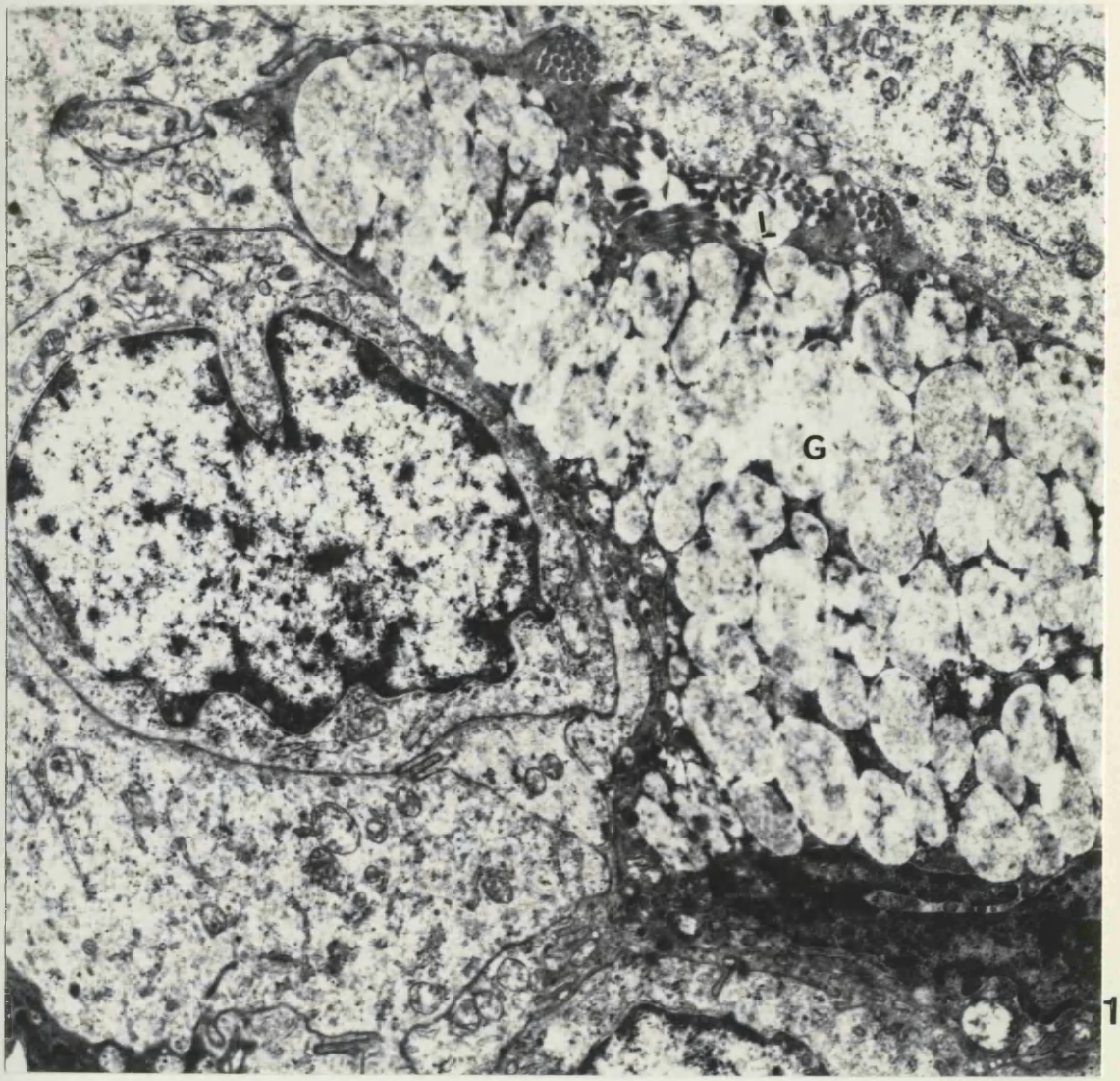

110

GASTRIC TUMOURS

Figure 111. Gastric carcinoma. Invagination of the nuclear envelope results in the formation of a channel of cytoplasm leading to the prominent nucleolus.

Magnification 21000

Figure 112. Gastric carcinoma. The two prominent and compact nucleoli are located near an island of cytoplasm(S) which is stranded within the nucleus.

Magnification 24000

Figure 113. Gastric carcinoma. An island of cytoplasm containing a mitochondrion is seen within the nucleus.

Magnification 28500

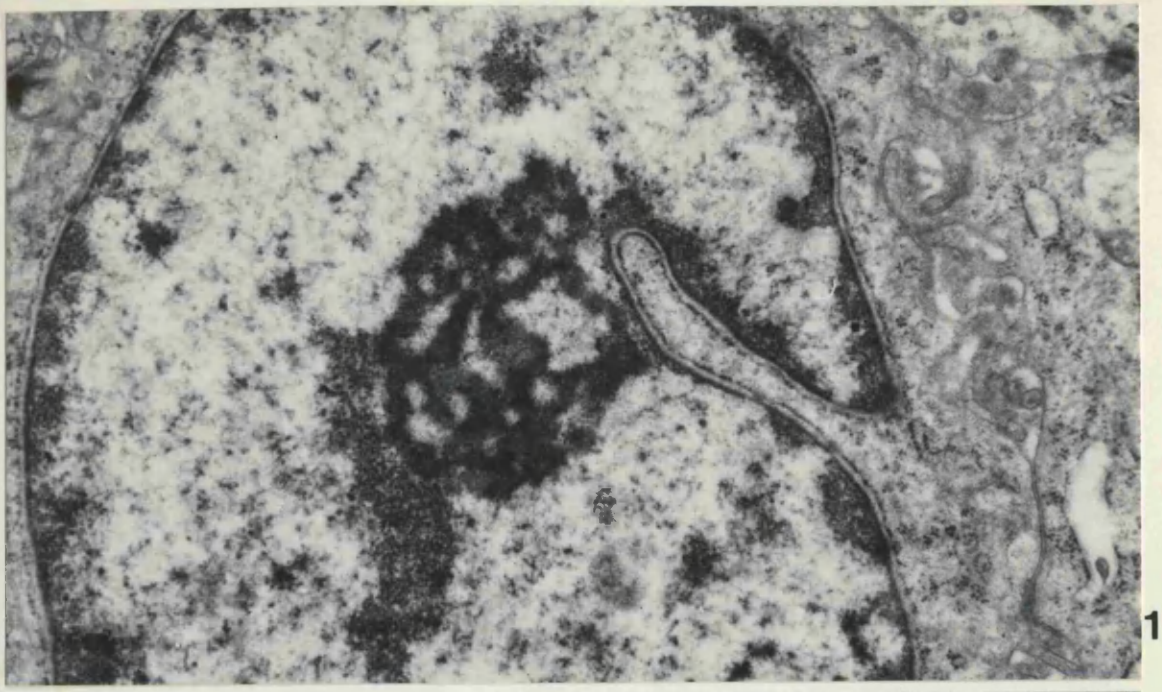

111

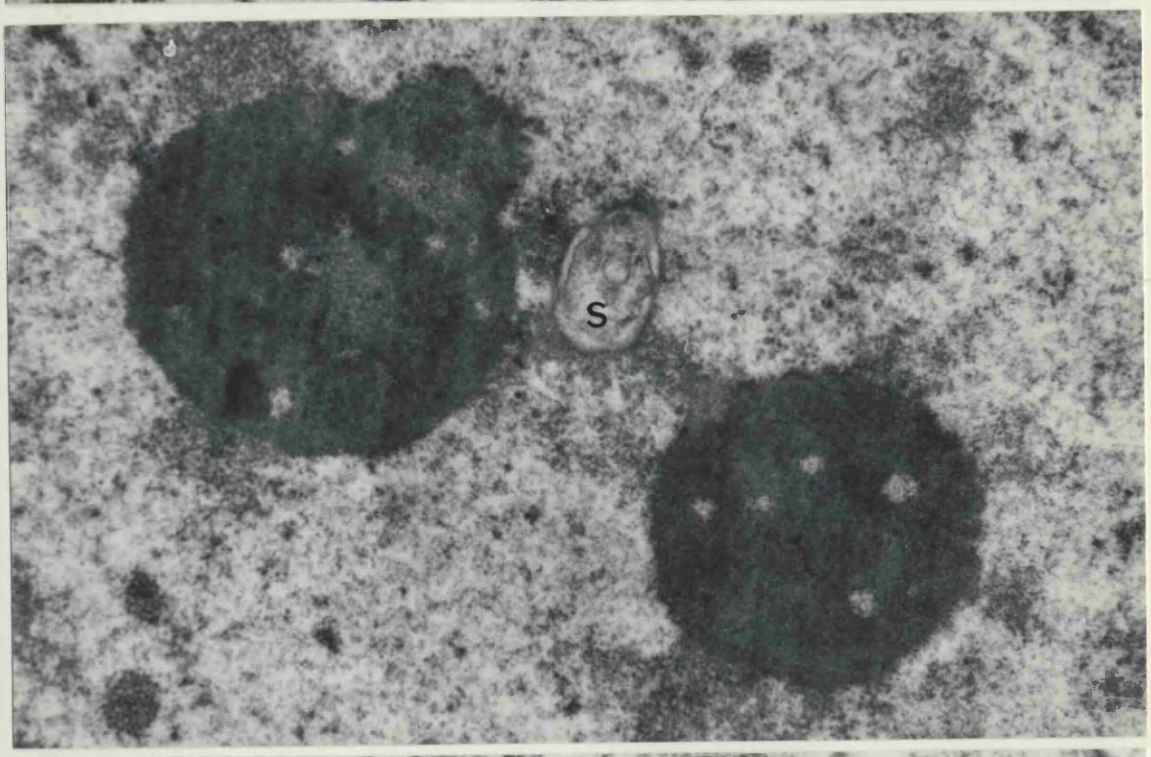

112

113

GASTRIC TUMOURS

Figure 114. Intestinal type of gastric carcinoma. There are some membrane-limited cytoplasmic vesicles, some of which contain dense material.

Magnification 22750

Figure 115. Gastric carcinoma. Small homogeneous dense bodies are seen in the cytoplasm of cancer cells.

Magnification 17500

Figure 116. Gastric carcinoma. A large heterogeneous dense inclusion is seen in a tumour cell.

Magnification 32500

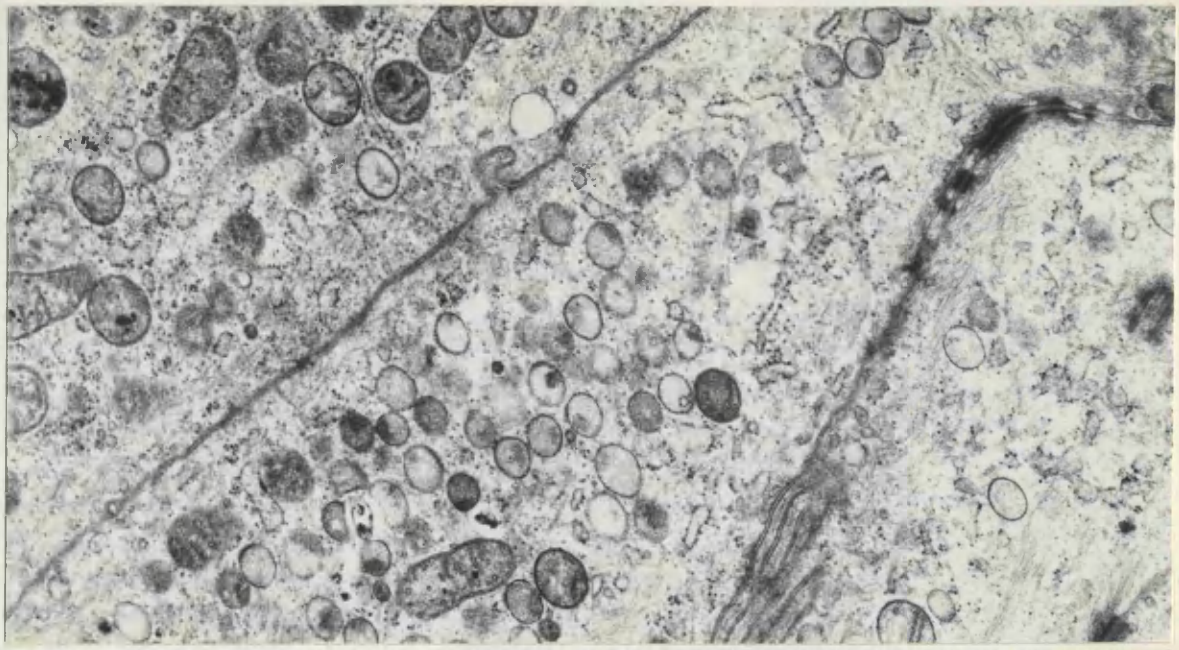

114

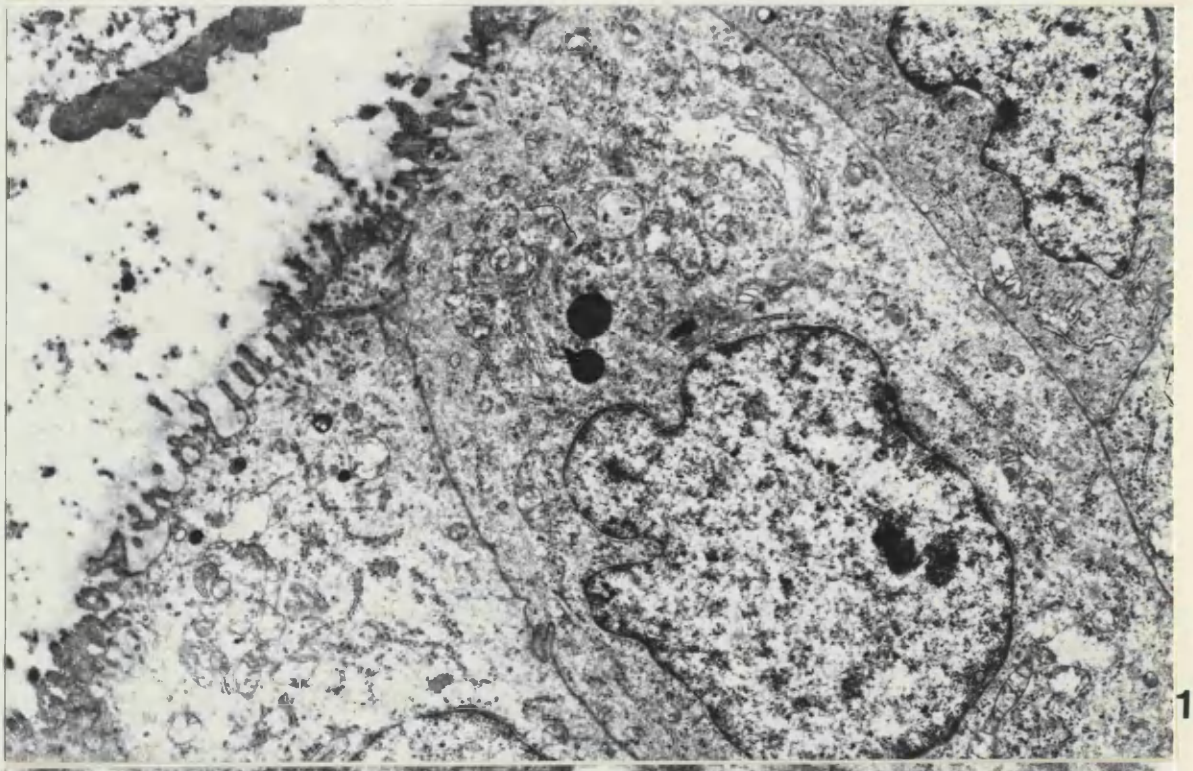

115

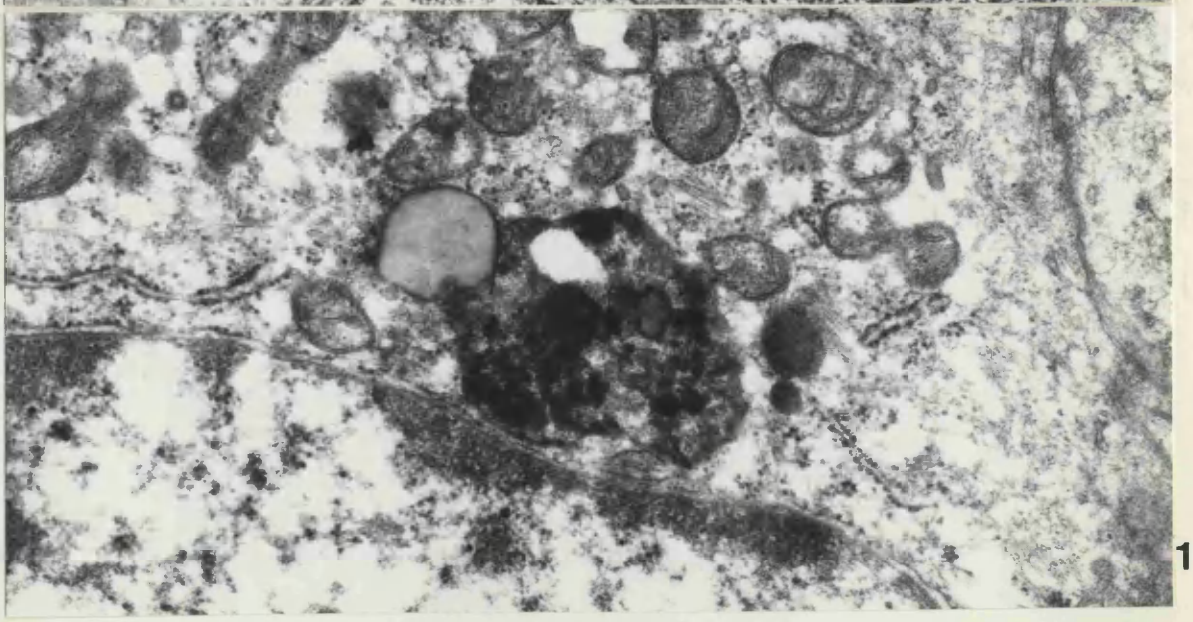

116

GASTRIC TUMOURS

Figure 117. Poorly differentiated primary gastric carcinoma.

Cancer cells arranged around an acinar space (L) contain mucous secretion granules identical to those of gastric mucous cells (Fig. 50). Note the cytoplasmic projections from cancer cells into the lumen (L). There are no true microvilli.

Magnification 32500

Figure 118. Poorly differentiated primary gastric carcinoma.

The cells rest on a continous basal lamina .

Magnification 17500

Figure 119. Poorly differentiated primary gastric carcinoma.

The cancer cell contains mucous granules identical to those of gastric mucous cells (Fig.50).

Magnification 32500

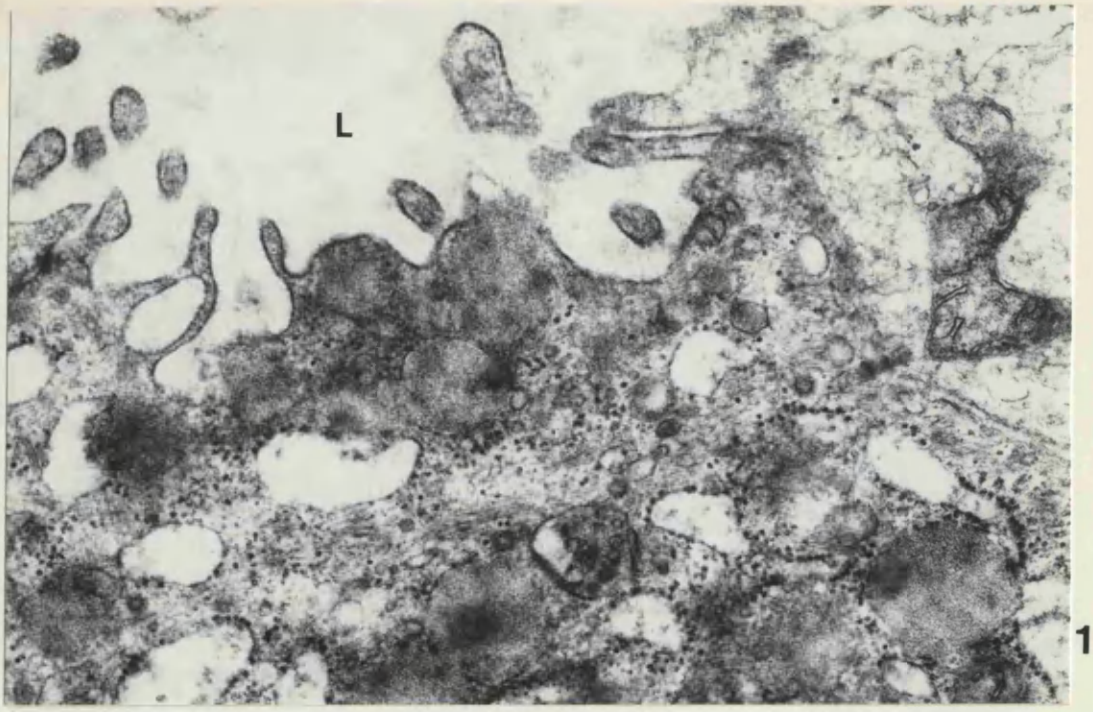

117

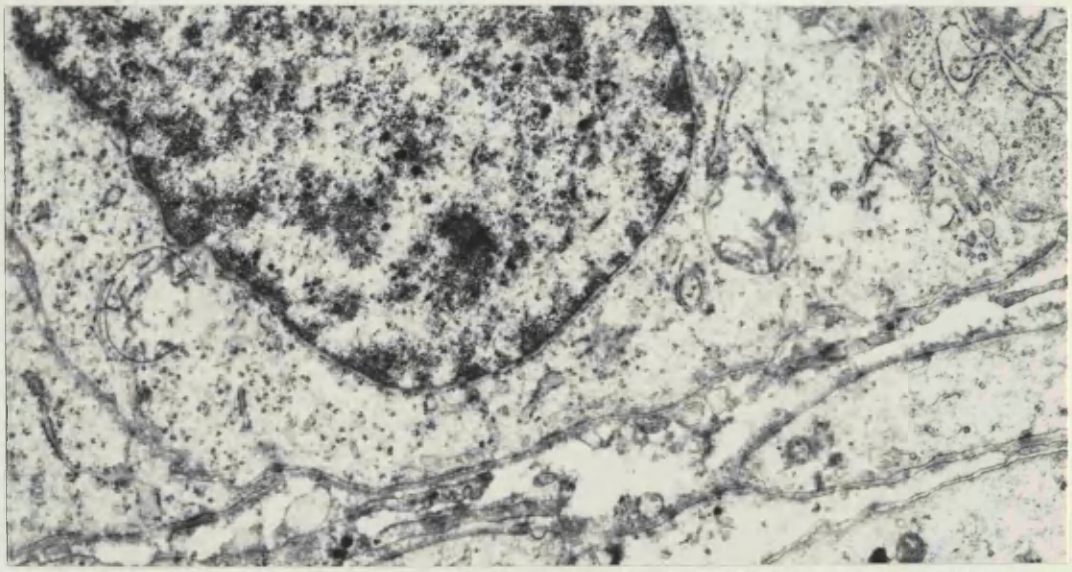

118

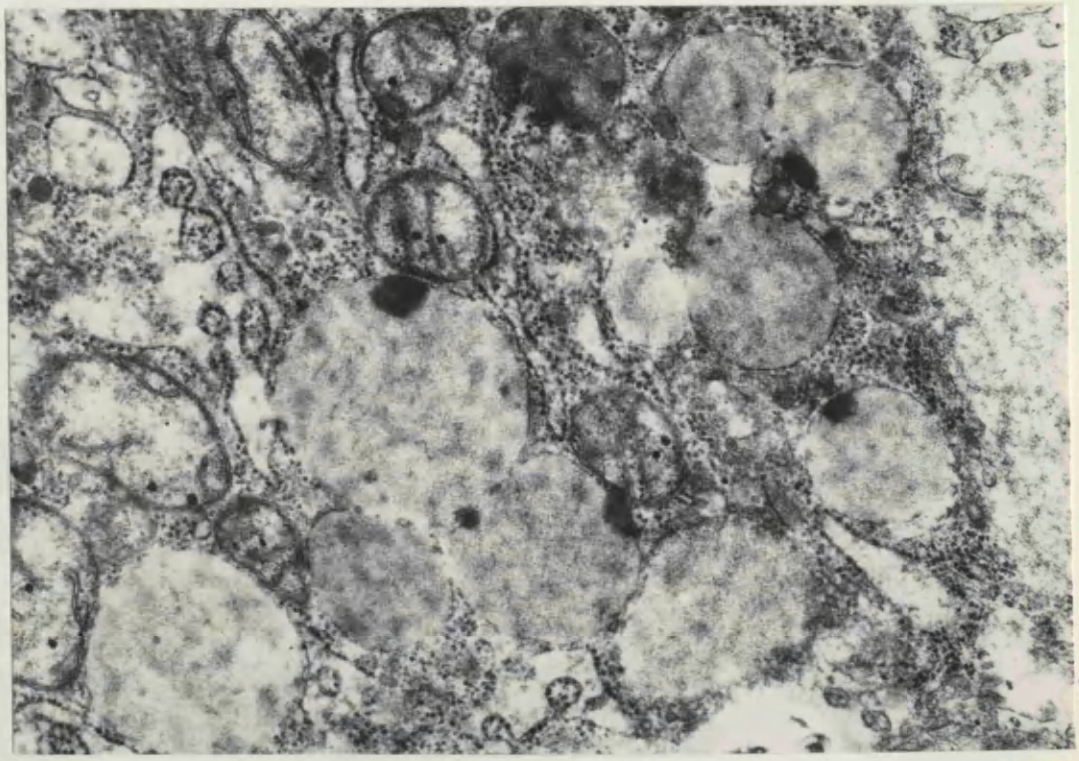

119

GASTRIC TUMOURS

Figure 120. Poorly differentiated primary gastric carcinoma. The neoplastic cells have typical mitochondria and Golgi system, large irregular nuclei, and are connected by desmosomes(D). There are no secretion granules.

Magnification 18200

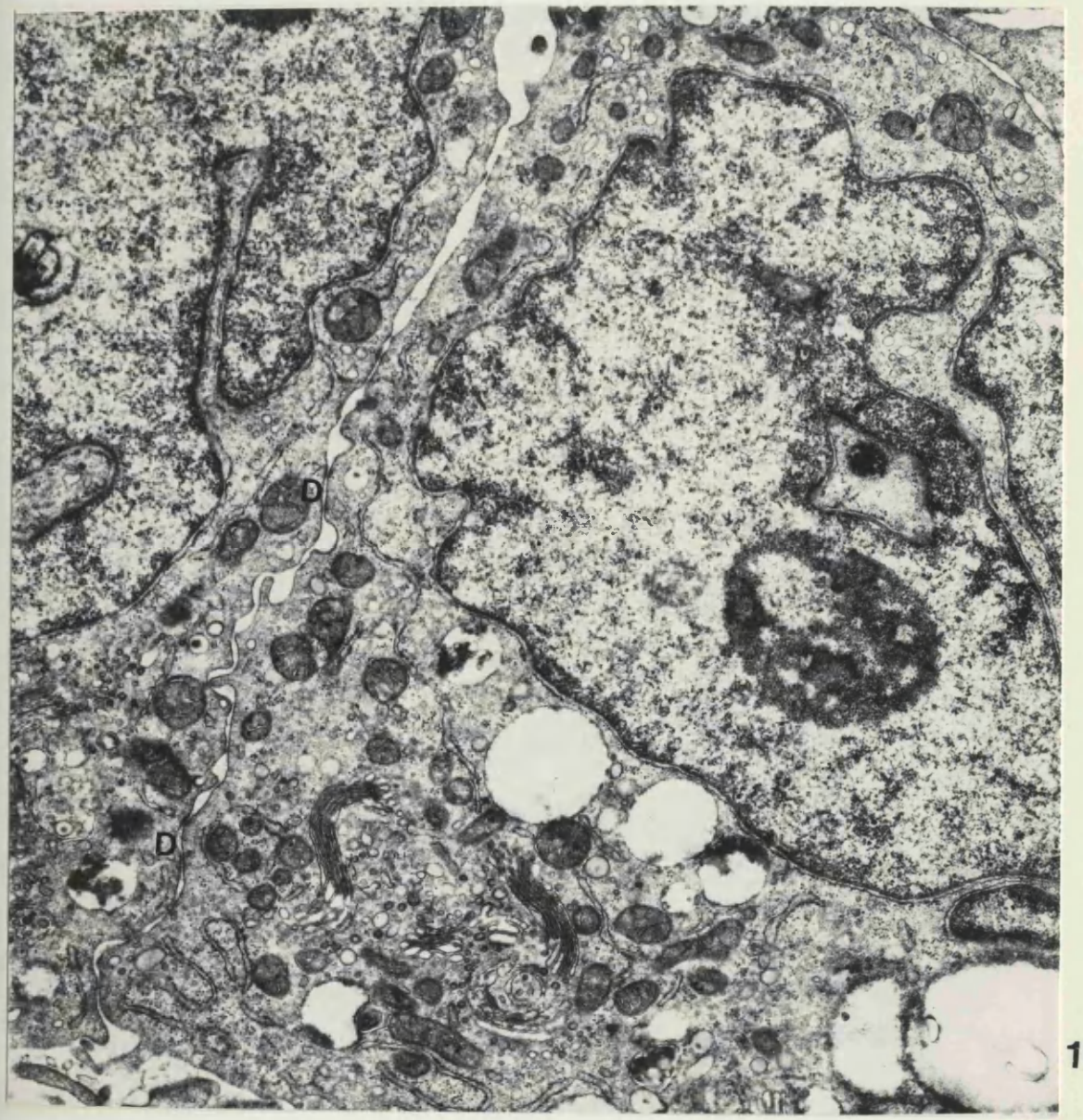

120

GASTRIC TUMOURS

Figure 121. Primary gastric lymphoma. The compact cells are closely packed and have large irregular nuclei. There are no epithelial adhesion specialisations. The resemblance to lymphoid tissue is close.

Magnification 6000

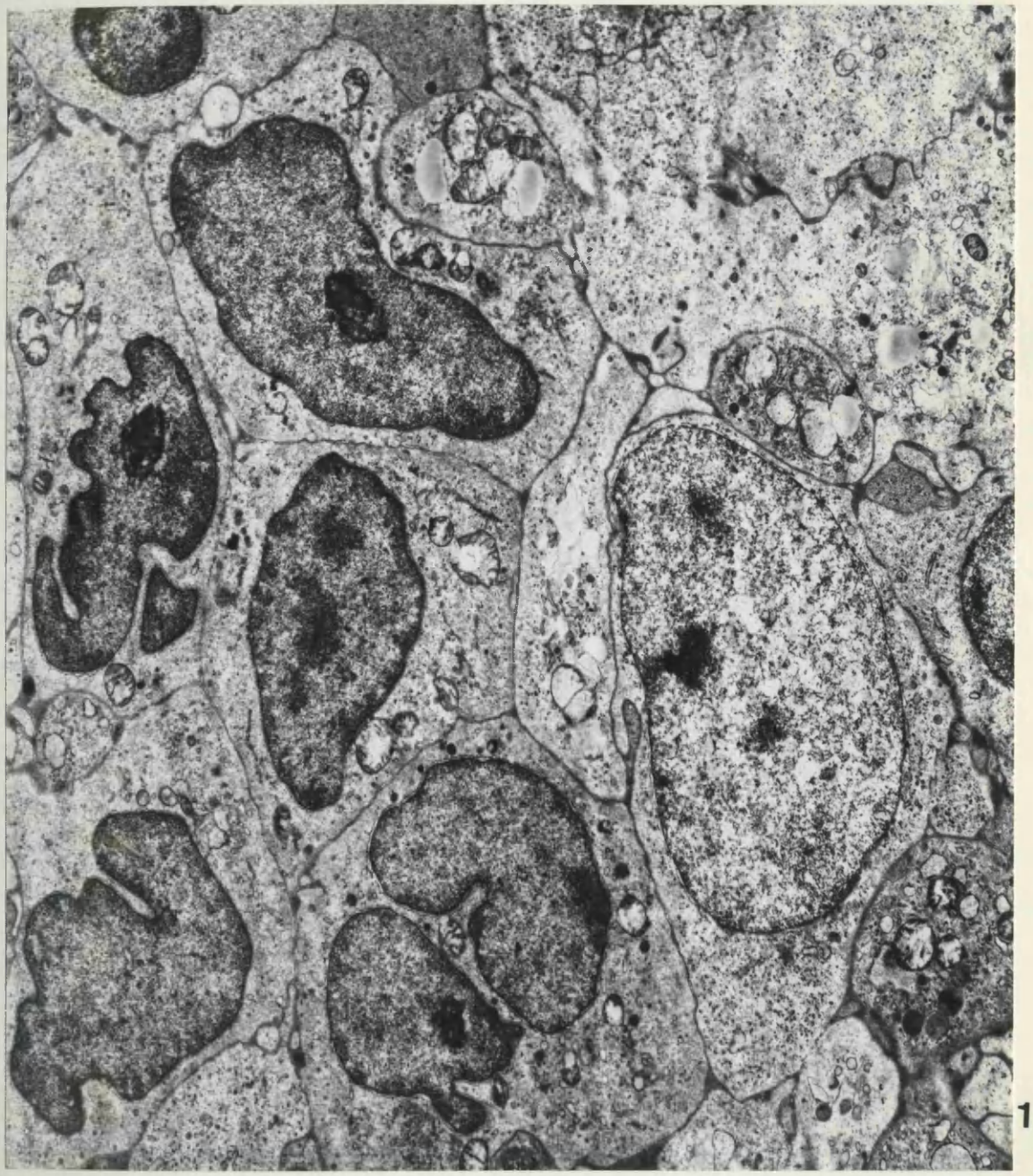

121

GASTRIC TUMOURS

Figure 122. Primary gastric lymphoma. The neoplastic cells are not connected by epithelial adhesion specialisations. This large neoplastic cell has large nucleus and minimal cytoplasmic organisation.

Magnification 8600

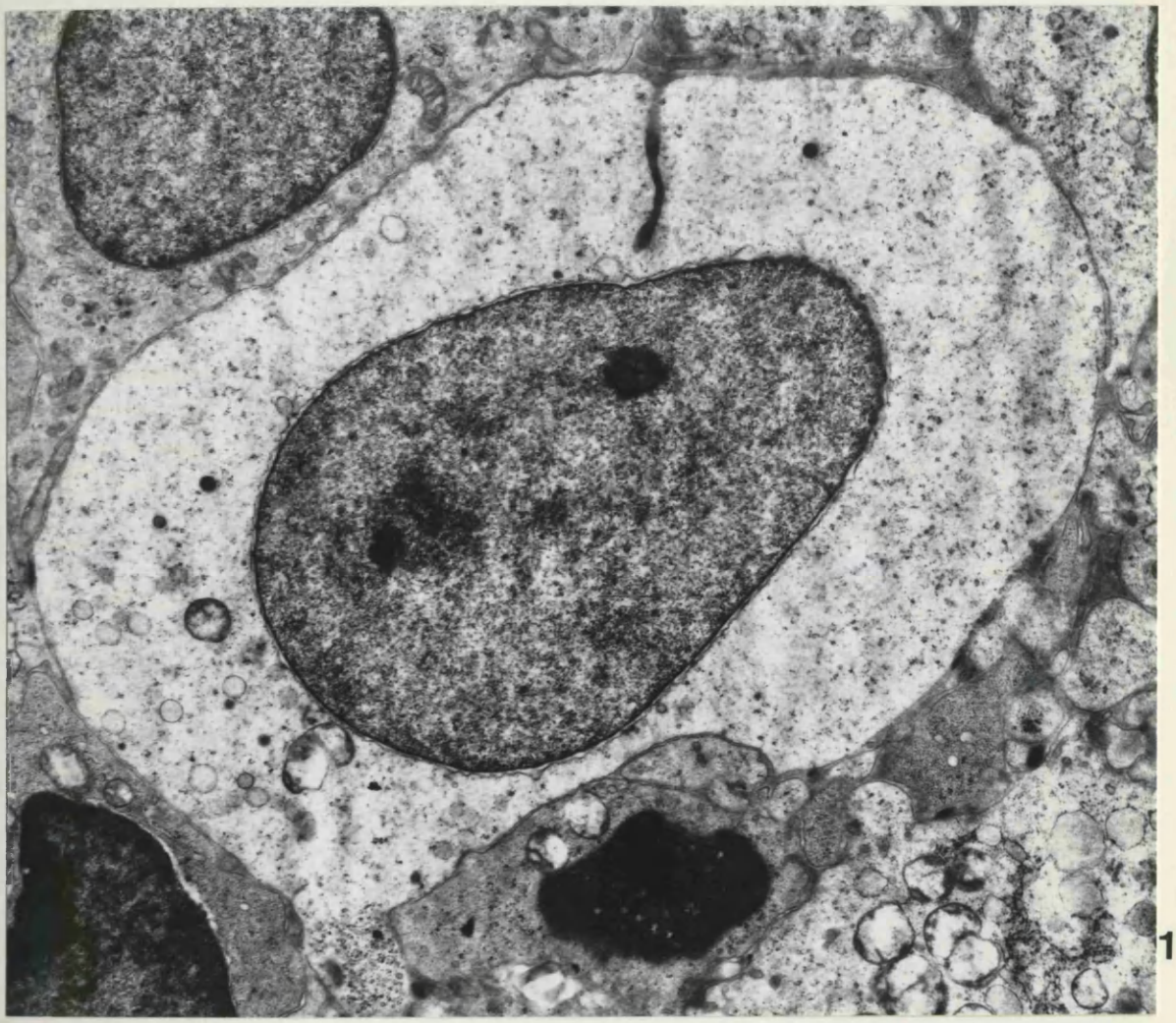

122

GASTRIC TUMOURS

Figure 123. Gastric cell type of adenocarcinoma. Periodic acid thiocarbohydrazide silver proteinate staining, showing the distribution of carbohydrates in the neoplastic cells. The surface coat and the mucous granules are positively stained.

Magnification 18200

Figure. 124. Gastric cell type of adenocarcinoma. Positive carbohydrate staining is seen in the mucous secretion granules.

Magnification 51250

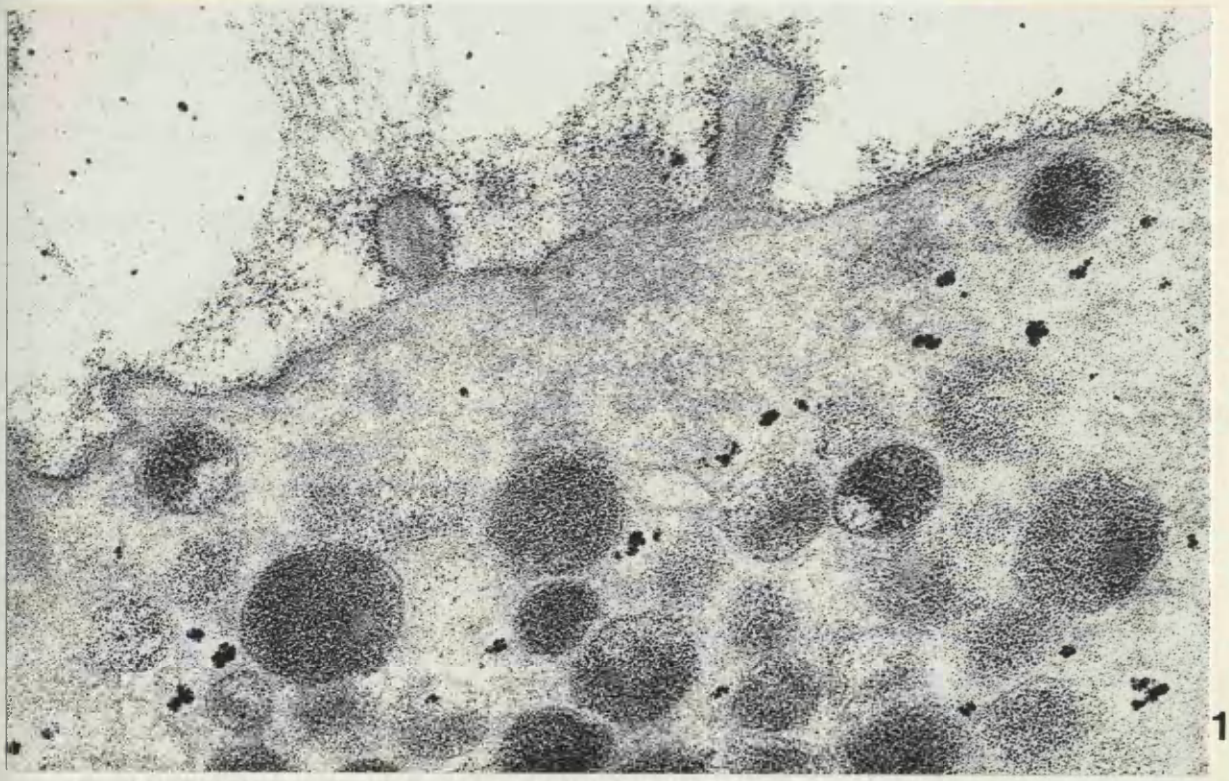

123

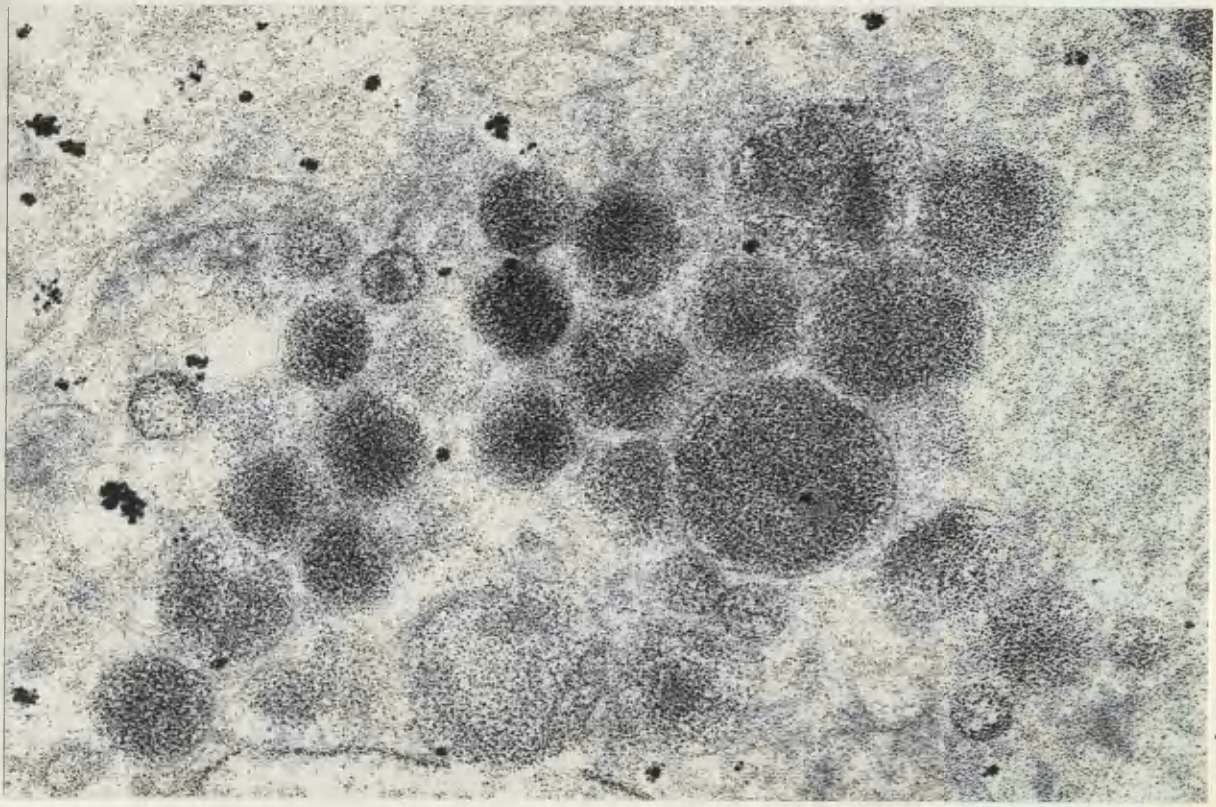

124

GASTRIC TUMOURS

Figure 125. Intestinal type of gastric carcinoma. Positive carbohydrate-staining is seen in the fuzzy coat and the membrane-limited vesicles.

Magnification 70000

Figure 126. Intestinal type of gastric carcinoma. Positive carbohydrate-staining is seen in the membrane-limited vesicles.

Magnification 70000

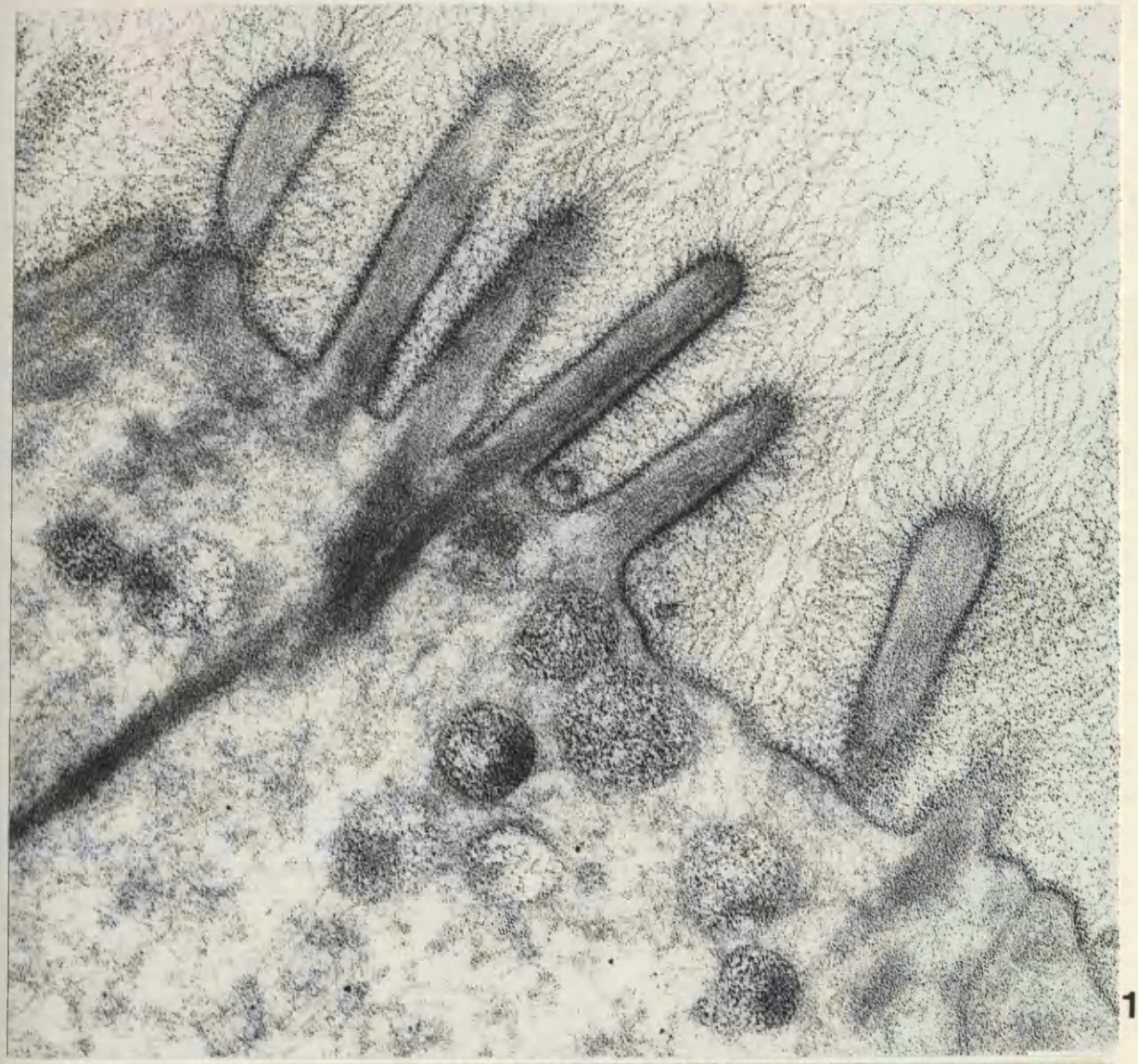

125

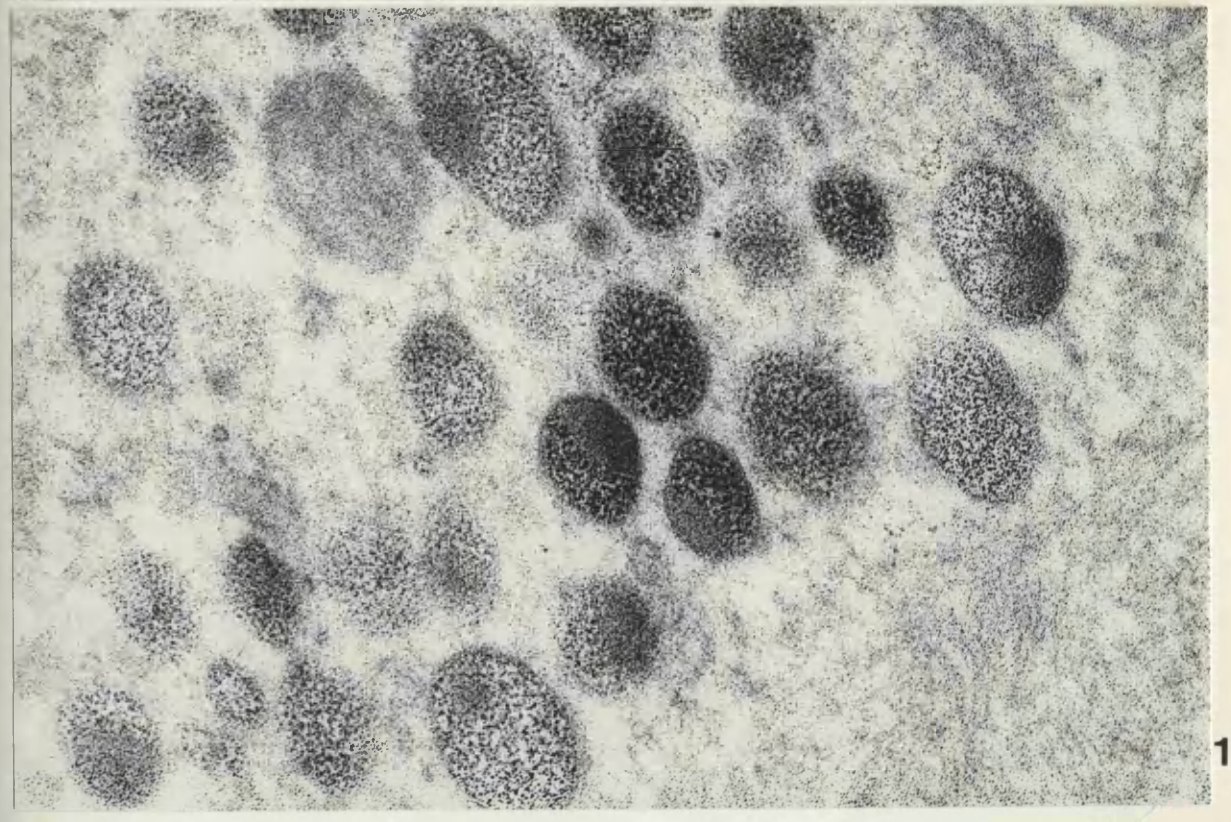

126

GASTRIC TUMOURS

Figure 127. Gastric carcinoma. Acid phosphatase activity in the smallcytoplasmic inclusions indicates their lysosomal nature.

Magnification 13800

Figure 128. Gastric carcinoma. Positive acid phosphatase activity is seen in these two inclusions, indicating their lysosomal identity.

Magnification 39000

Figure 129. Gastric carcinoma. Acid phosphatase activity is shown in a large heterogeneous inclusion, again indicating its lysosomal nature.

Magnification 22750

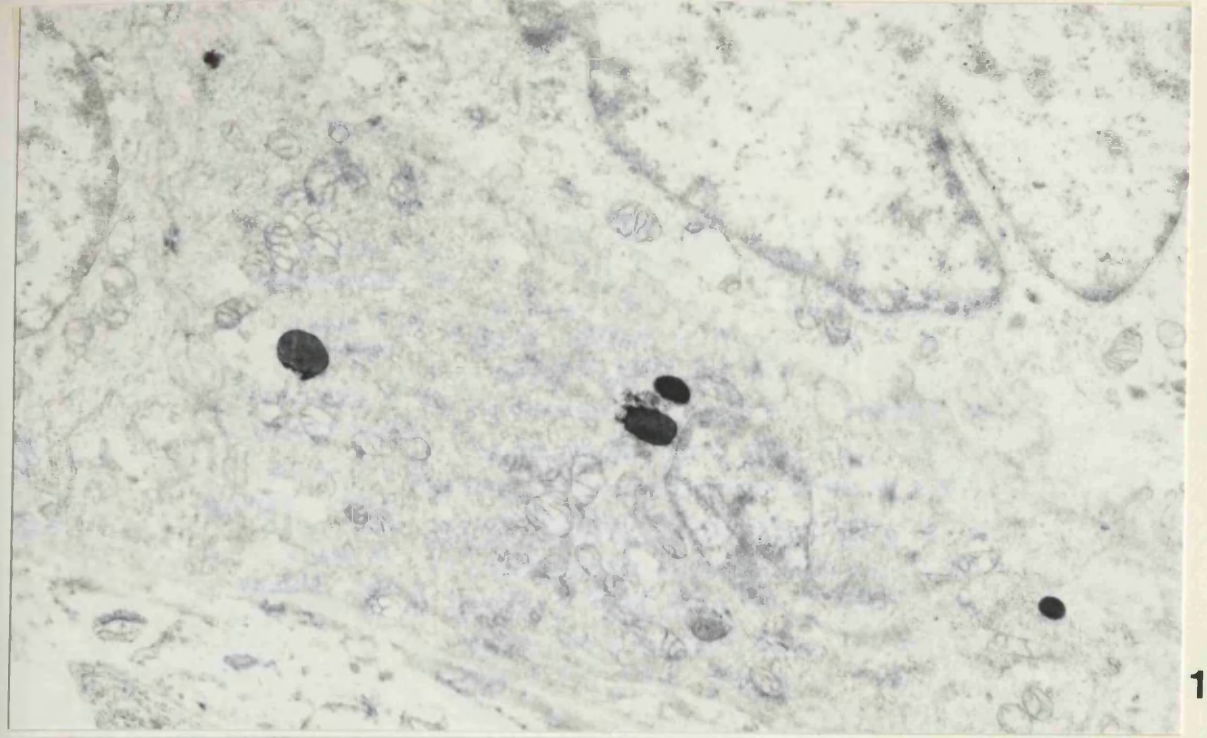

127

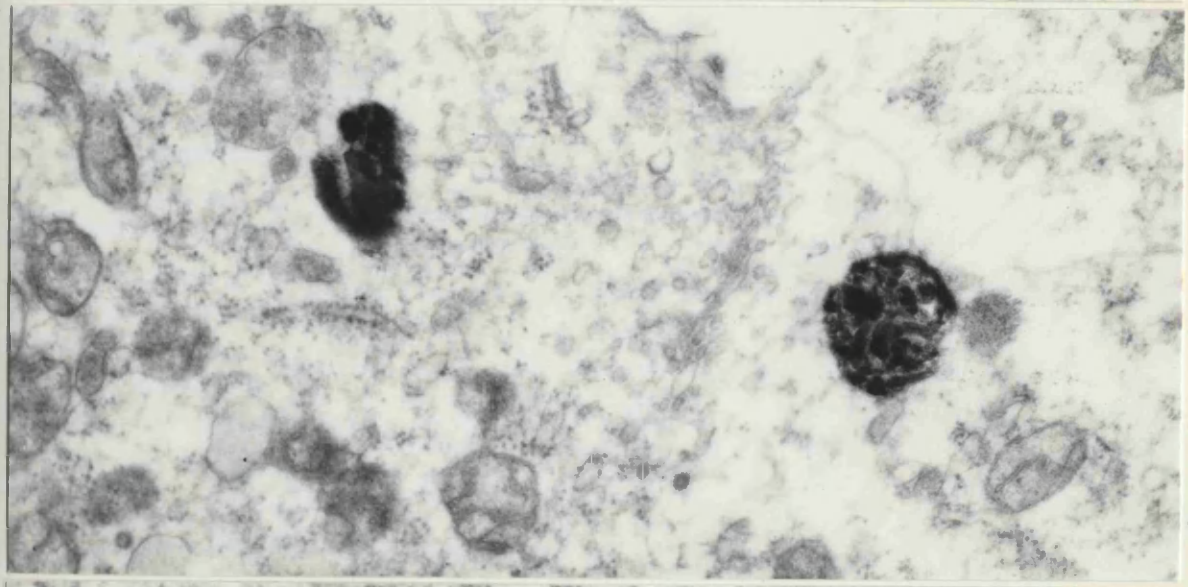

128

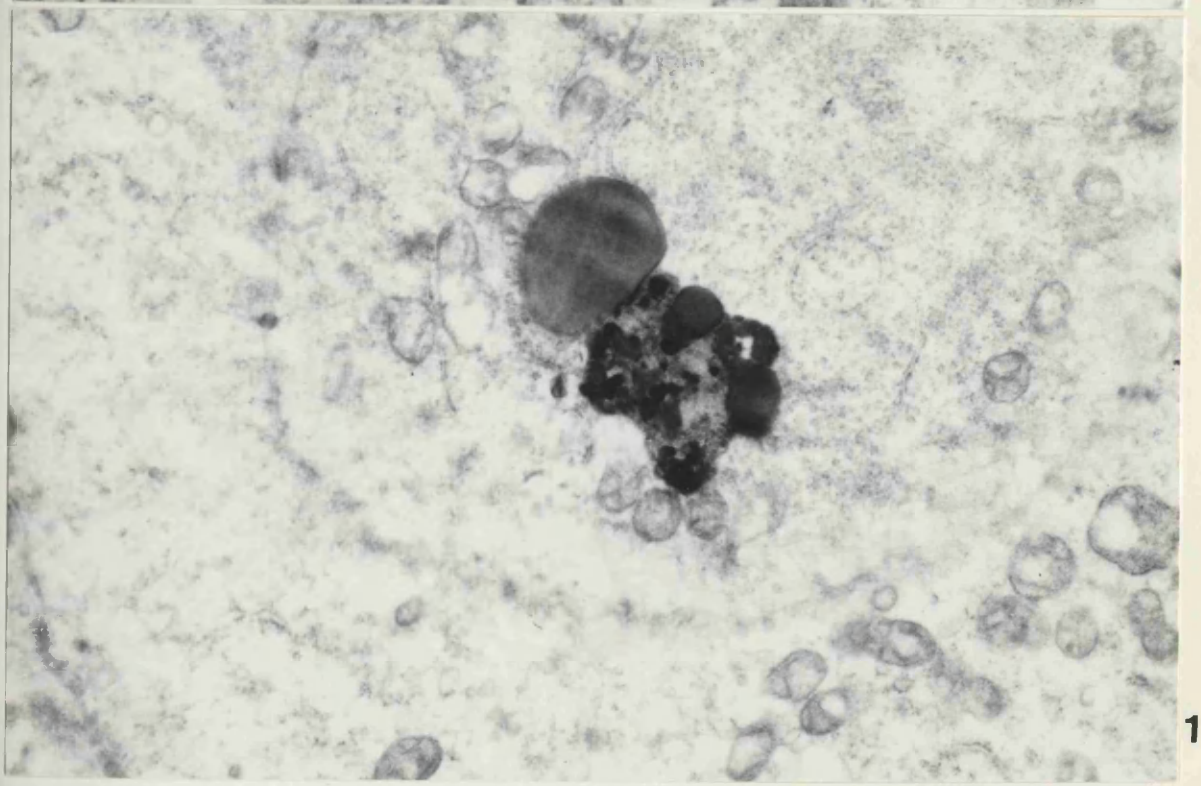

129

GASTRIC TUMOURS

Figure 130. The histology of a typical case of well differentiated metastatic gastric carcinoma is shown.

Magnification 225

Figure 131. Well differentiated metastatic gastric carcinoma. The apical cytoplasm of cancer cells contains numerous mucous secretion granules identical to those of gastric mucous cells(Figs.45,50). The microvilli seen here are more sparse than in the intestinal cell type of tumour (Figs.106,108).

Magnification 32500

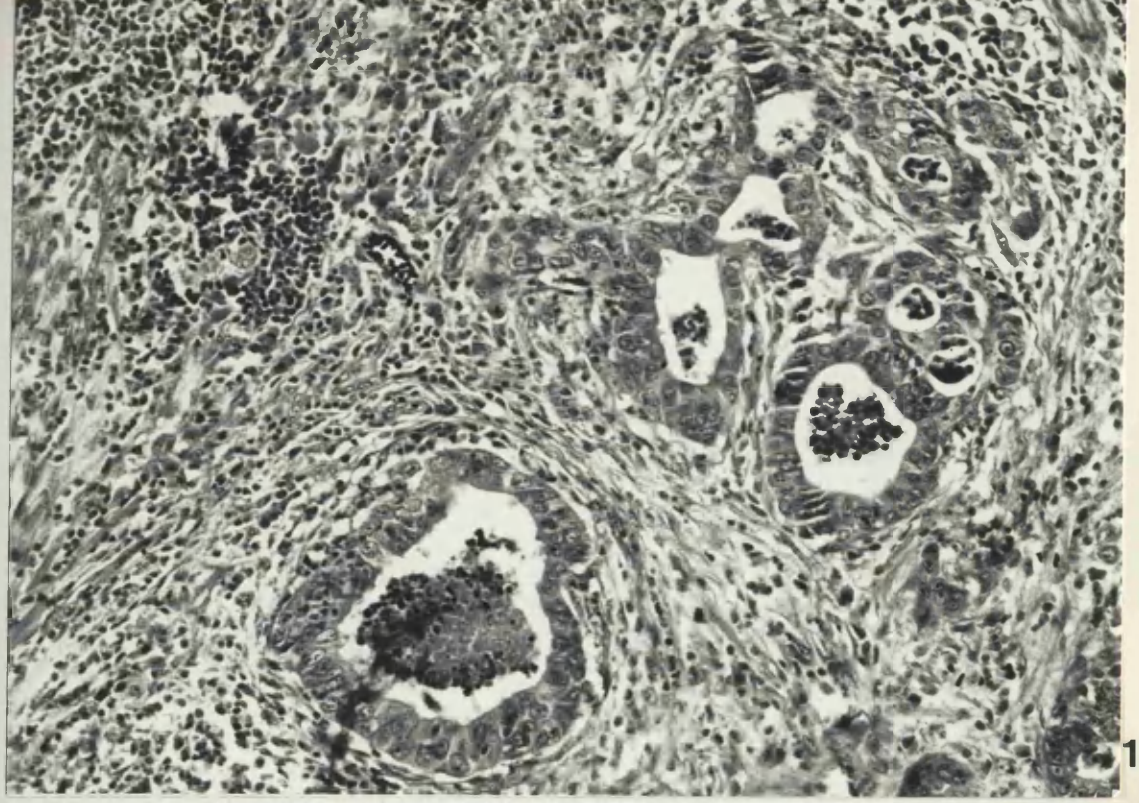

130

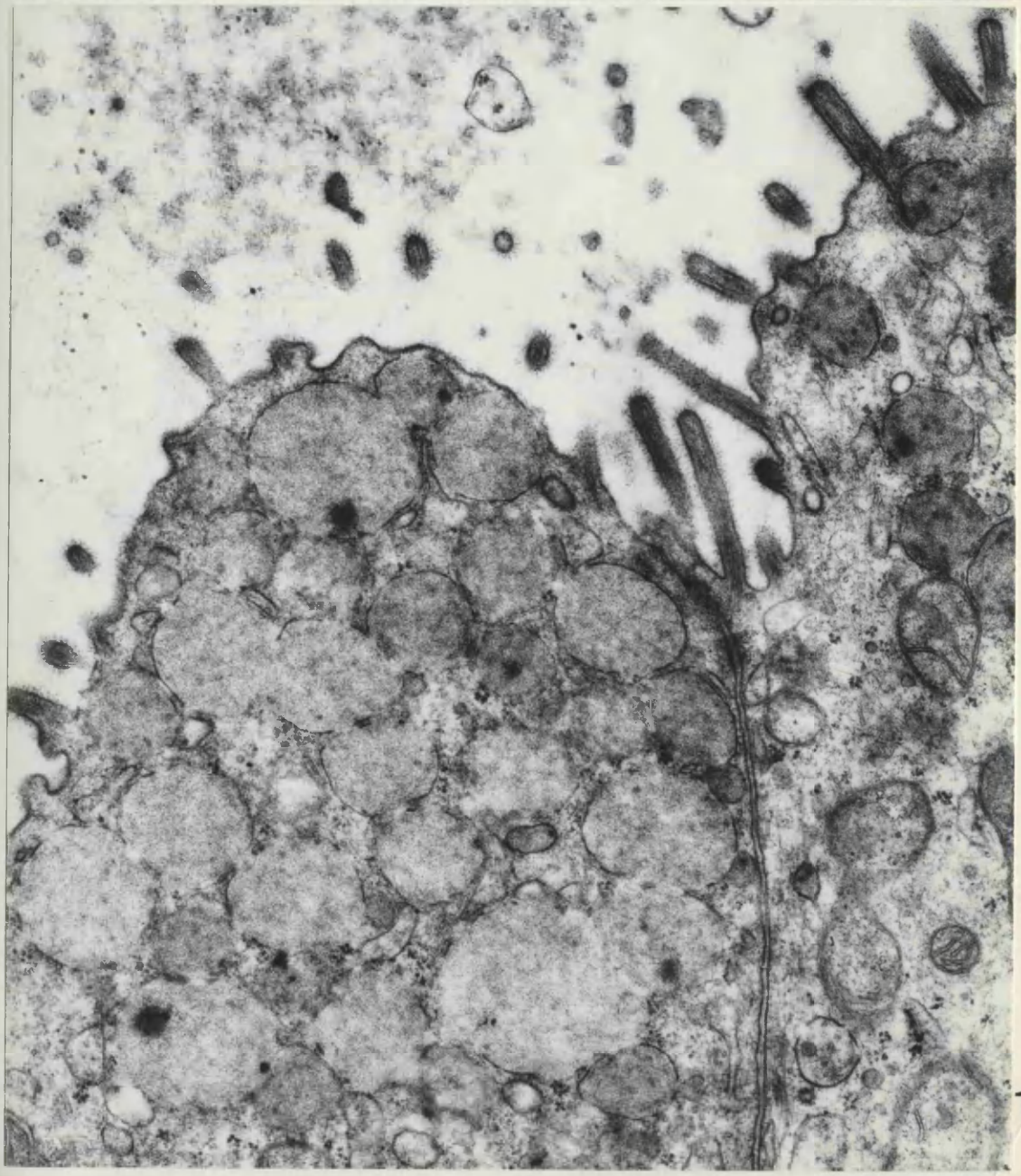

131

GASTRIC TUMOURS

Figure 132. Well differentiated metastatic gastric carcinoma.

The dense mucous granules are identical to those of gastric mucous cells(Fig.44). The microvilli are short and covered by a scanty fuzzy coat.

Magnification 51250

Figure 133. Well differentiated metastatic gastric carcinoma.

The columnar neoplastic cell contains a large basally situated nucleus and only a few mucous granules(G). Notice the intracytoplasmic vacuoles(V) and the nuclear body(arrow).

Magnification 13800

132

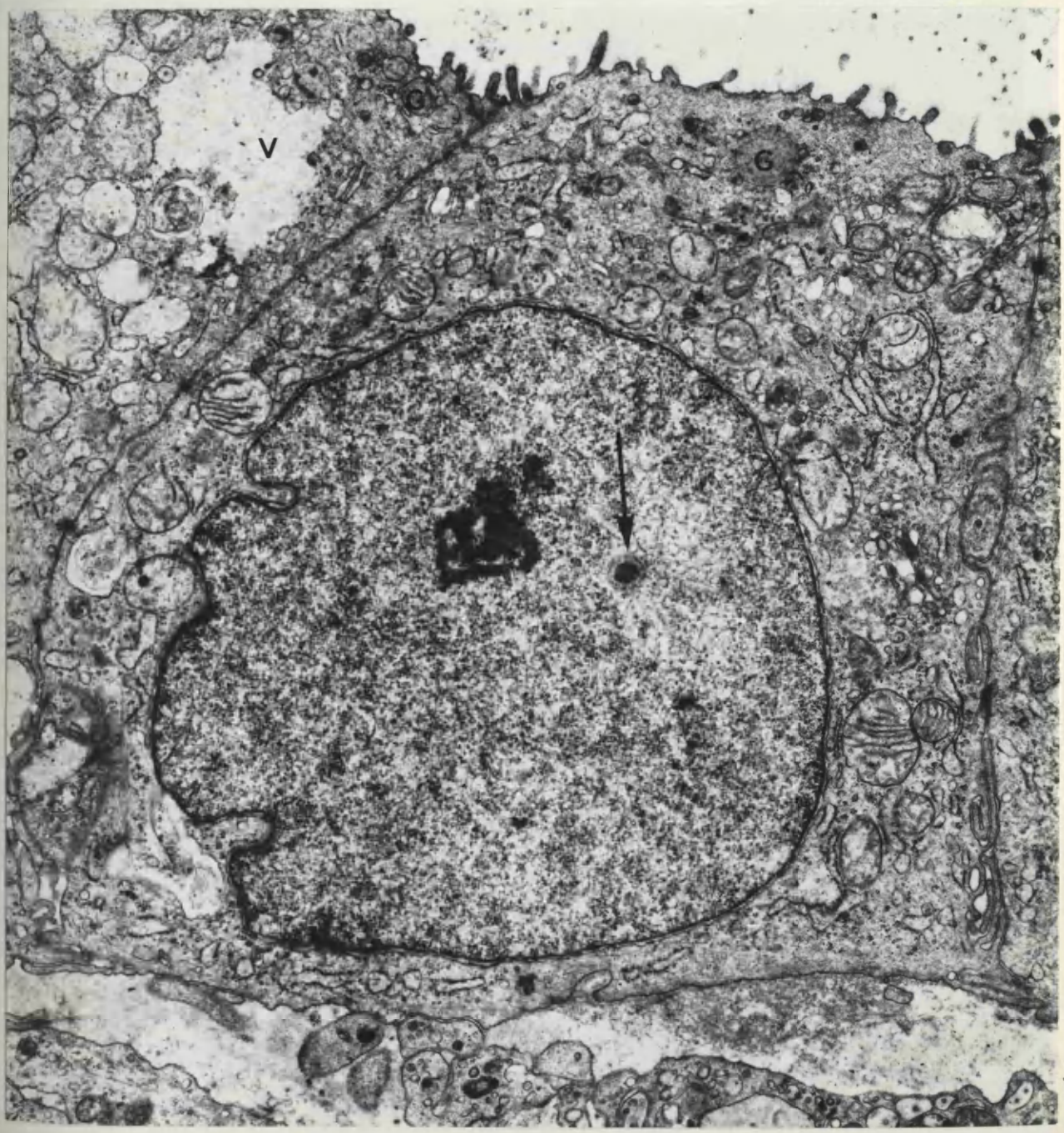

133

GASTRIC TUMOURS

Figure 134. Well differentiated metastatic gastric carcinoma.

A dense ring-shaped nucleolus is shown.

Magnification 22750

Figure 135. Well differentiated metastatic gastric carcinoma.

Another dense ring-shaped nucleolus is seen.

Magnification 22750

Figure 136. Well differentiated metastatic gastric carcinoma.

The large mitochondrion has tubular and vesicular cristae.

Magnification 88250

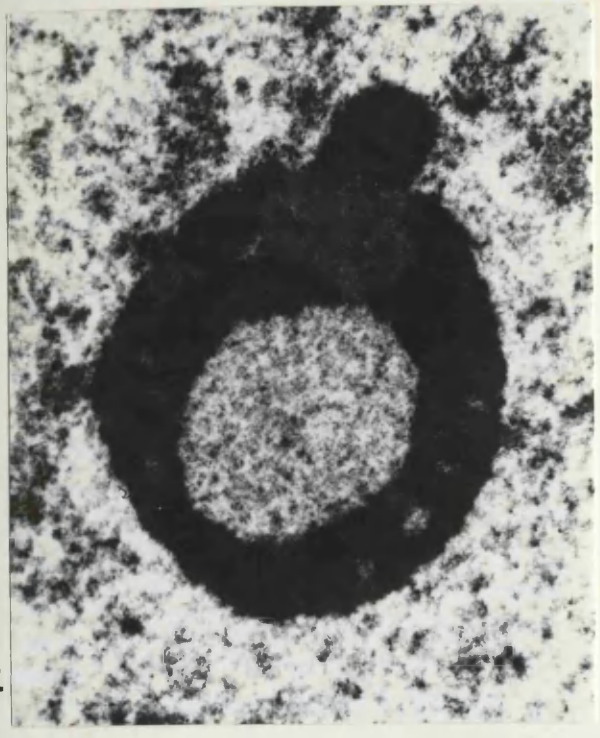

134

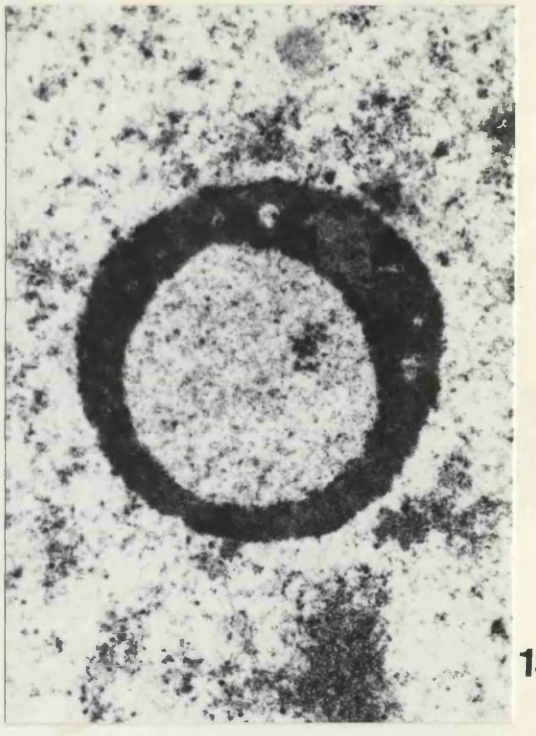

135

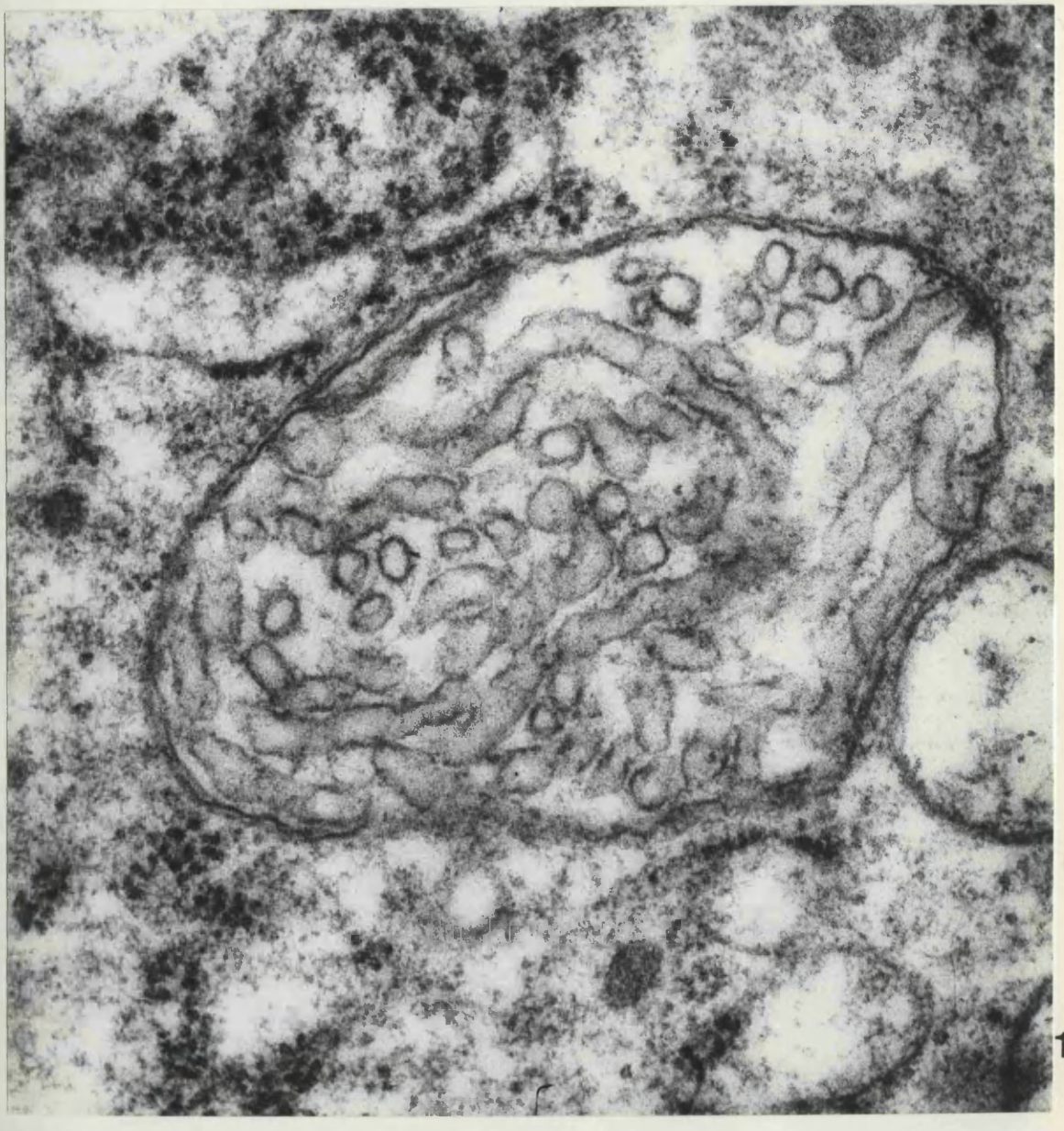

136

GASTRIC TUMOURS

Figure 137. Well differentiated metastatic gastric carcinoma.

A mitochondrion with tubular and vesicular cristae is seen.

Magnification 88250

Figure 138. Well differentiated metastatic gastric carcinoma.

A ring-shaped mitochondrion is shown, with tubular cristae.

Magnification 69900

Figure 139. Well differentiated metastatic gastric carcinoma.

Two ring-shaped mitochondria are seen.

Magnification 93200

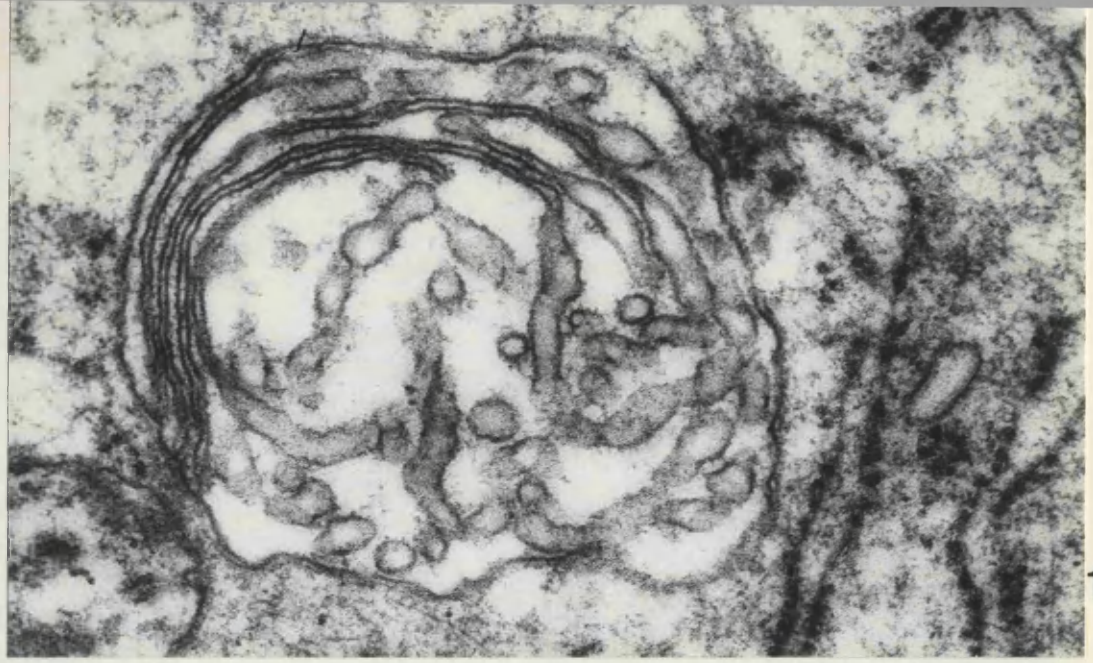

137

138

139

Figure 140. Well differentiated metastatic gastric carcinoma.

A large mitochondrion contains concentric cristae.

Magnification 88250

Figure 141. Well differentiated metastatic gastric carcinoma.

A mitochondrion is shown with a less organised concentric arrangement of cristae.

Magnification 88250

Figure 142. Well differentiated metastatic gastric carcinoma.

The mitochondrion shown contains a central inclusion, of uncertain identity.

Magnification 93200

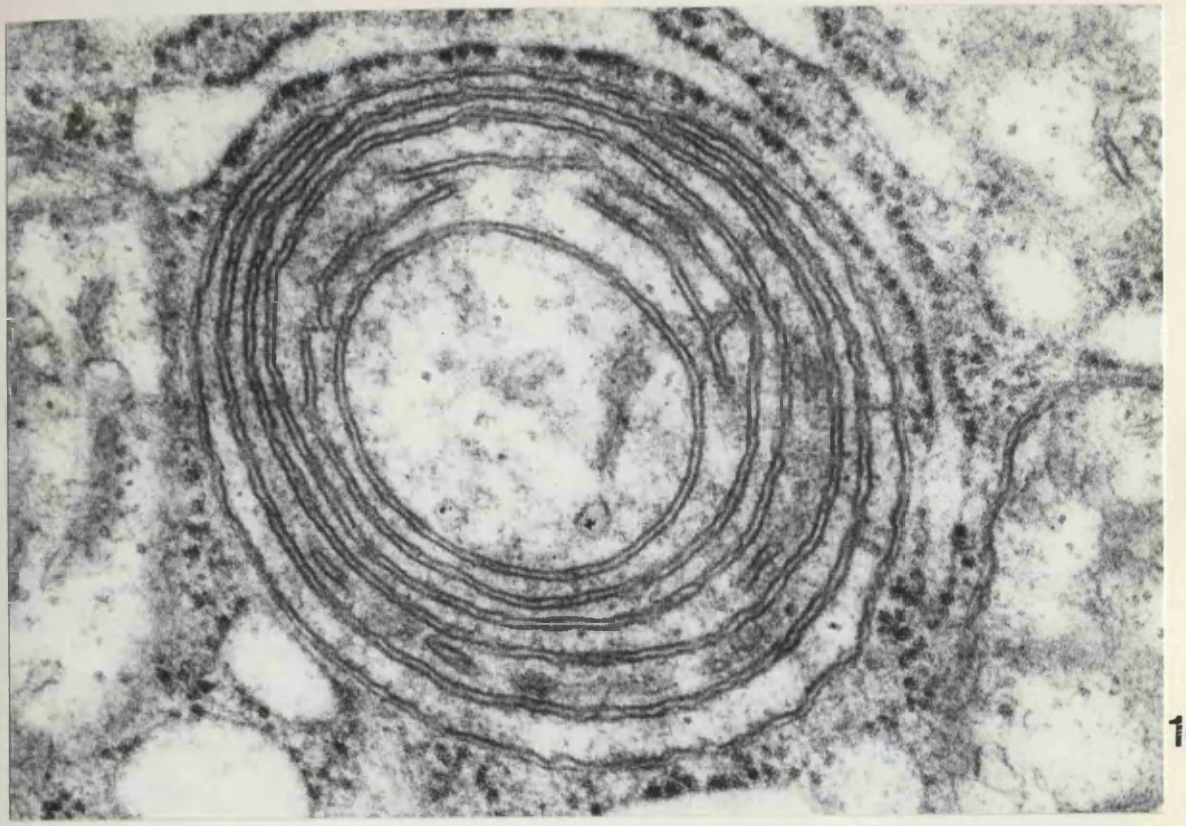

140

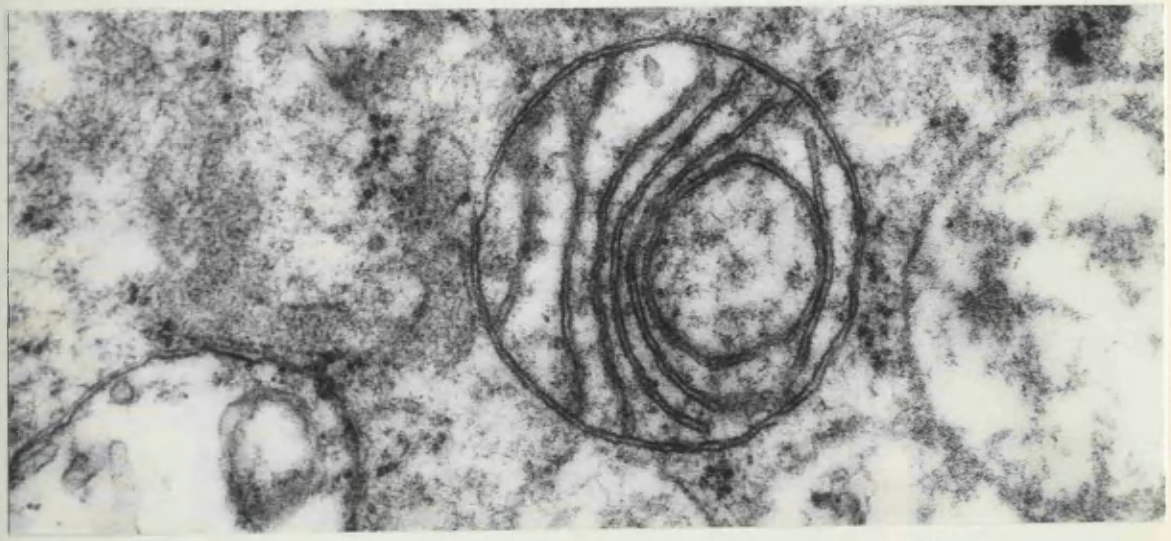

141

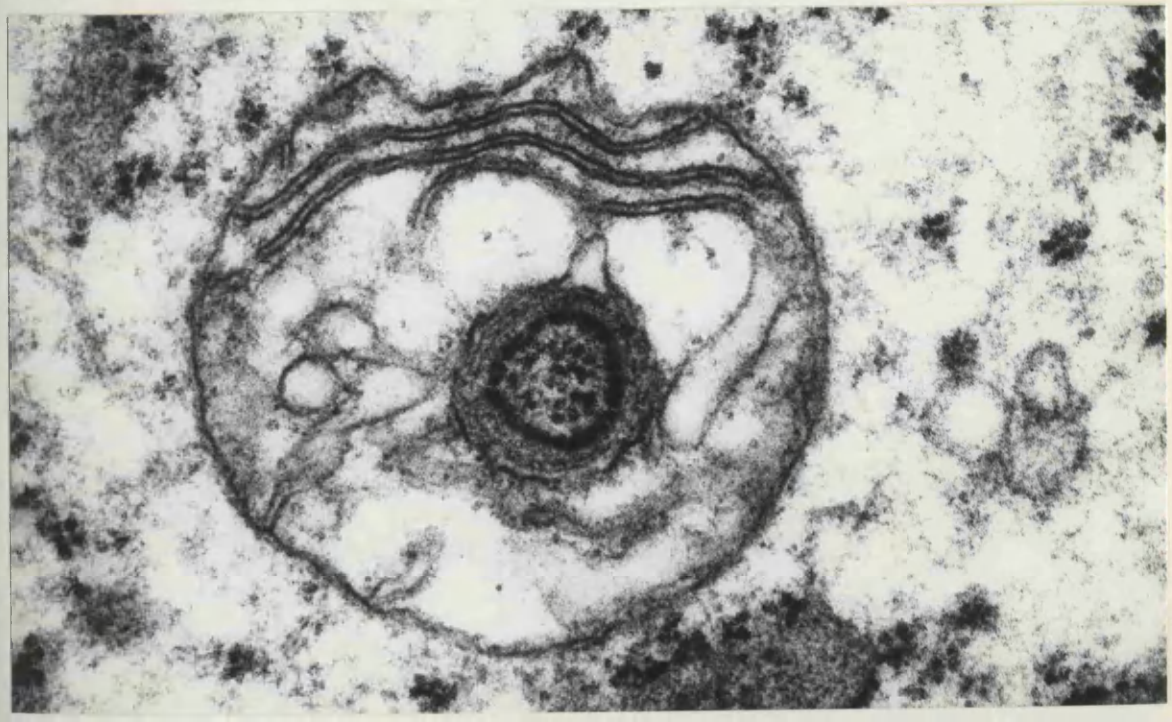

142

Figure 143. Well differentiated metastatic gastric carcinoma.

The mitochondrion shown has concentric cristae and contains central material similar to that seen in the surrounding cytoplasm.

Magnification 93200

Figure 144. Well differentiated metastatic gastric carcinoma.

An invaginated "cup-shaped" mitochondrion contains inconspicuous cristae. The cytoplasmic peg which projects into the mitochondrion is similar to the central "inclusions" seen in figures 142, 143.

Magnification 51250

Figure 145. Well differentiated metastatic gastric carcinoma.

Intracisternal convoluted tubules are seen.

Magnification 88250

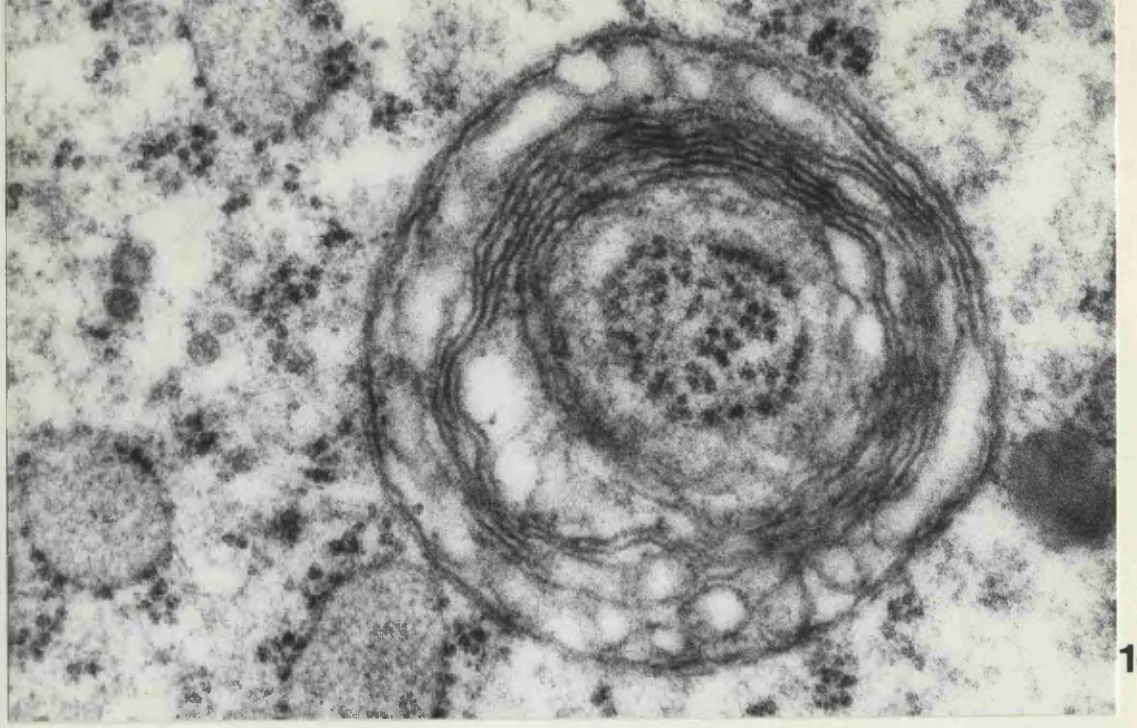

143

144

145

GASTRIC TUMOURS

Figure 146. Well differentiated metastatic gastric carcinoma.

A dilated cisterna of endoplasmic reticulum contains tubular structures.

Magnification 67250

Figure 147. Well differentiated metastatic gastric carcinoma.

A network of convoluted membraneus structures is shown.

Magnification 93200

146

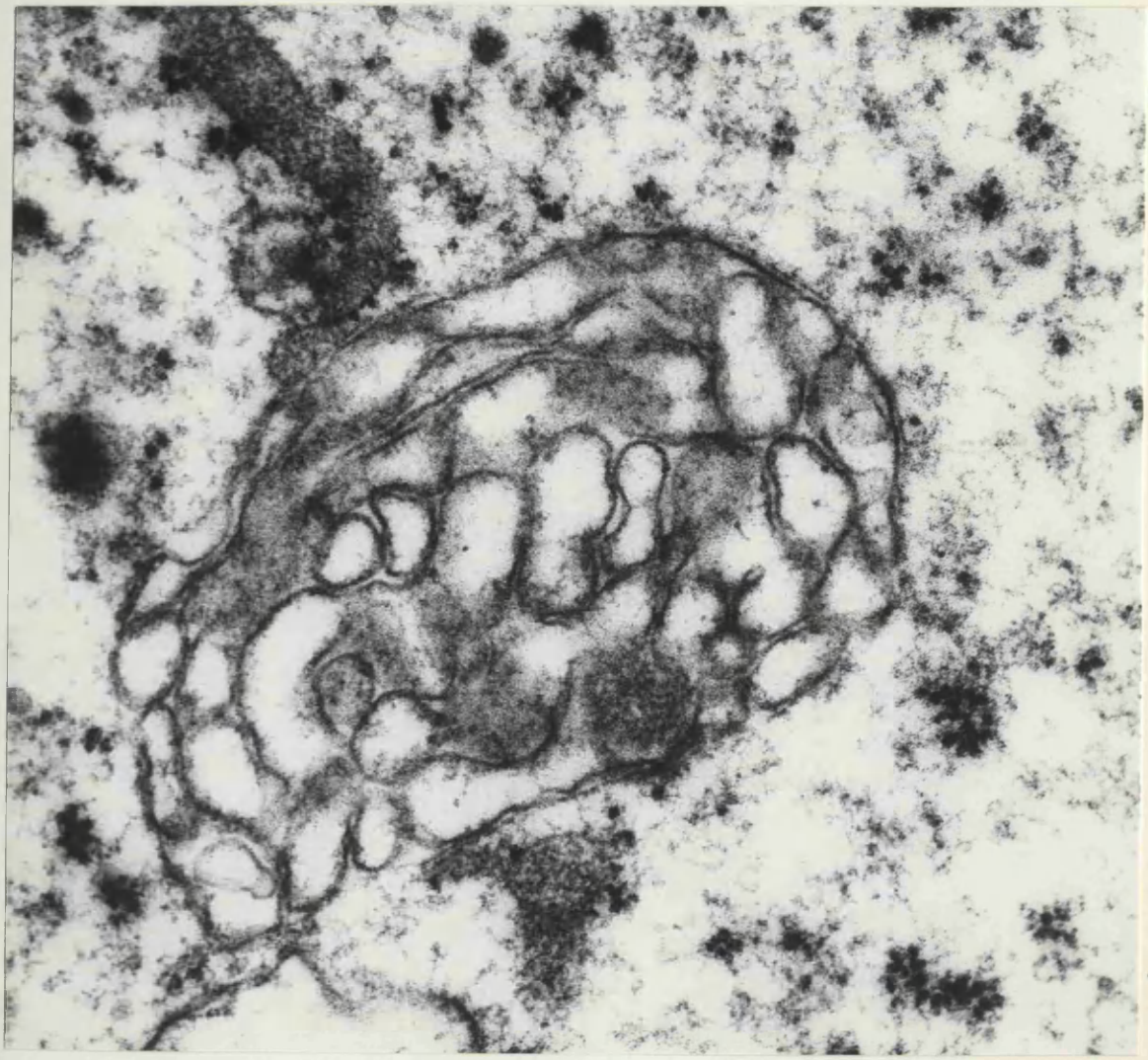

147

GASTRIC TUMOURS

Figure 148. Well differentiated metastatic gastric carcinoma.

A curious arrangement of granular and smooth endoplasmic reticulum is seen. The presence of several clearly defined 'pore' structures(arrows) indicates that this is a stack of annulate lamellae.

Magnification 88250

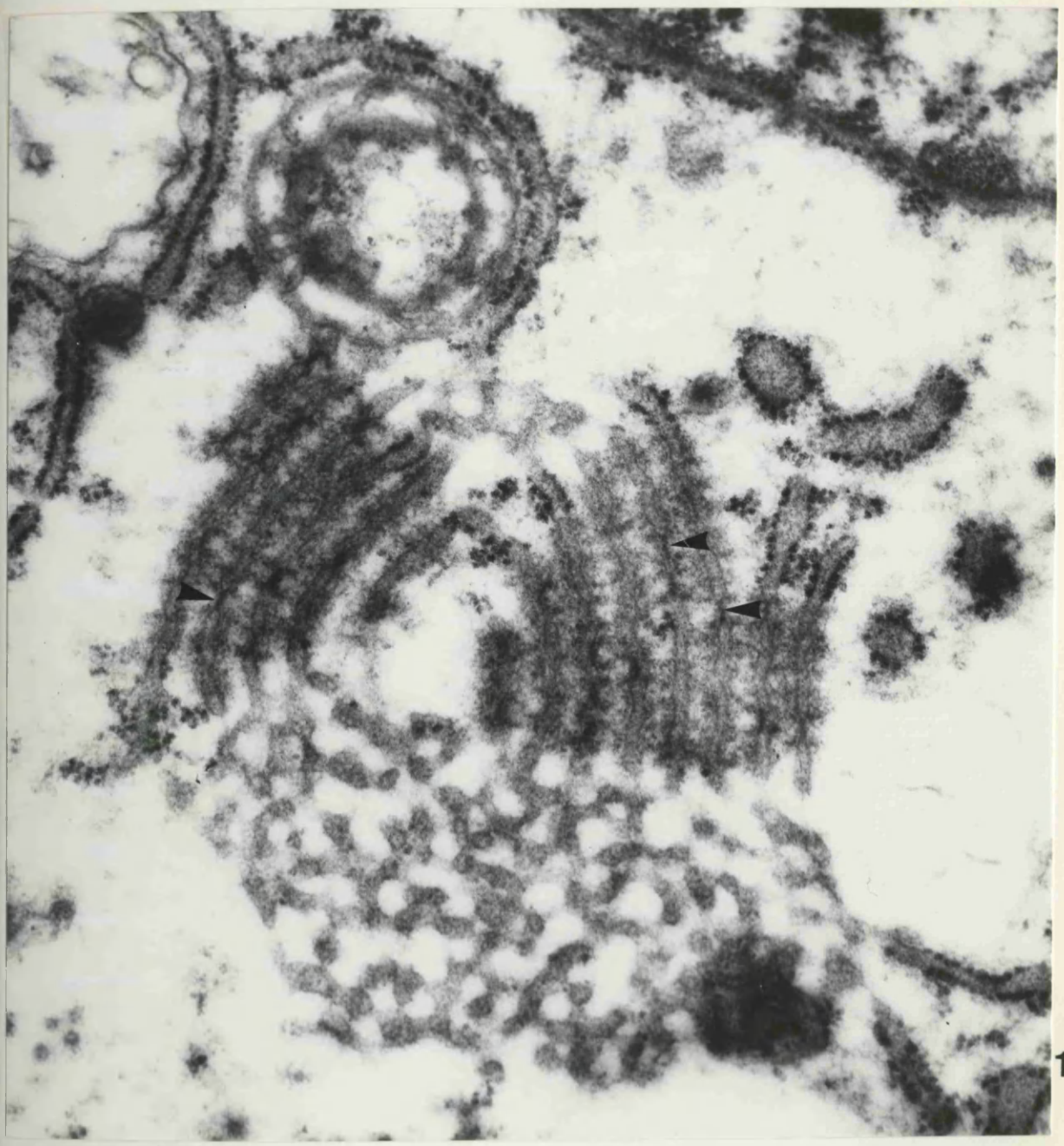

148

GASTRIC TUMOURS

Figure 149. Carbohydrate-staining of well differentiated metastatic gastric carcinoma. Fine granular deposits are seen in the lumen (L) and in the mucous secretion granules.

Magnification 39000

Figure 150. Carbohydrate-staining of well differentiated metastatic gastric carcinoma. Dense granular deposits are seen in the fuzzy coat and mucous granules.

Magnification 88250

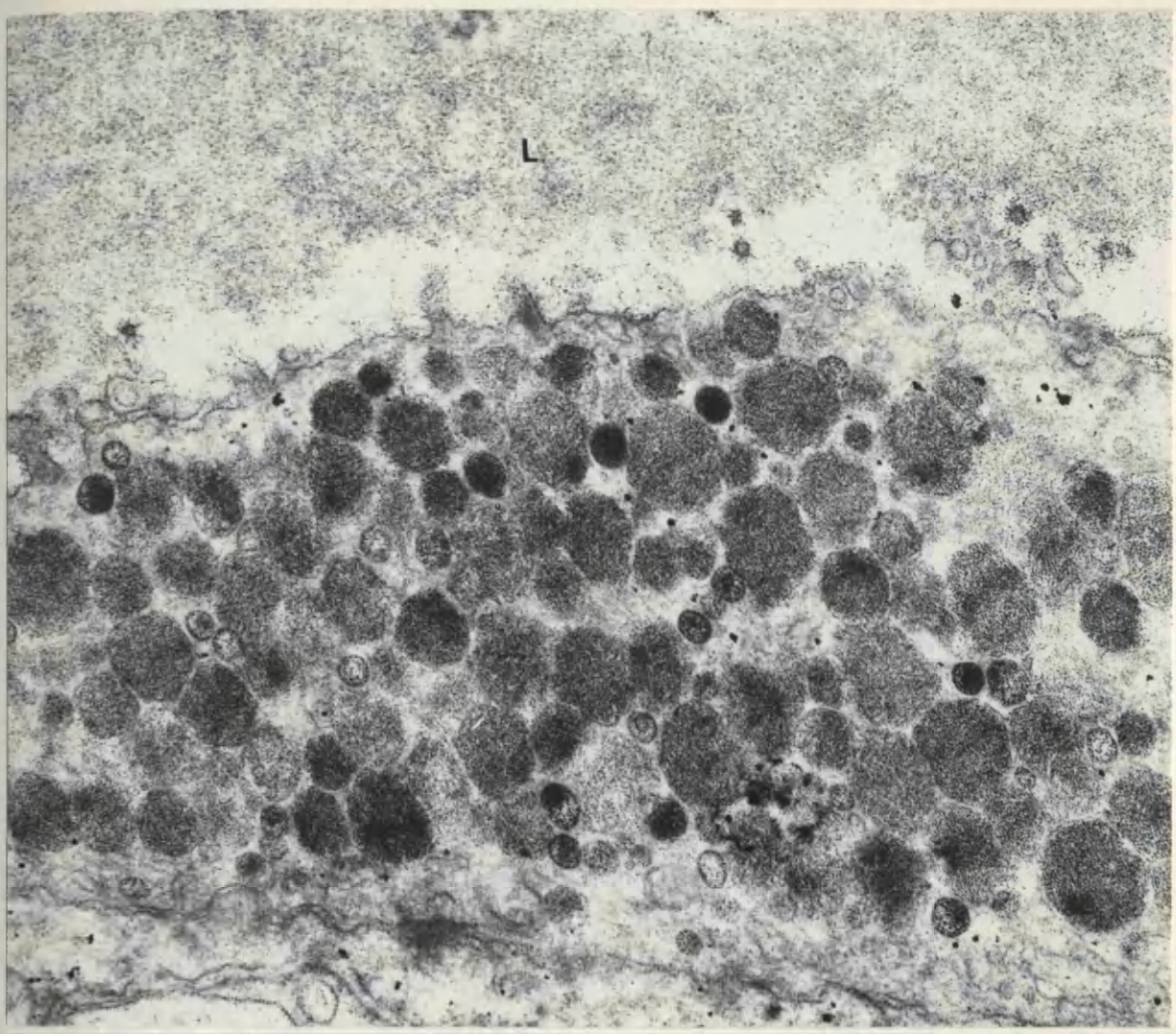

149

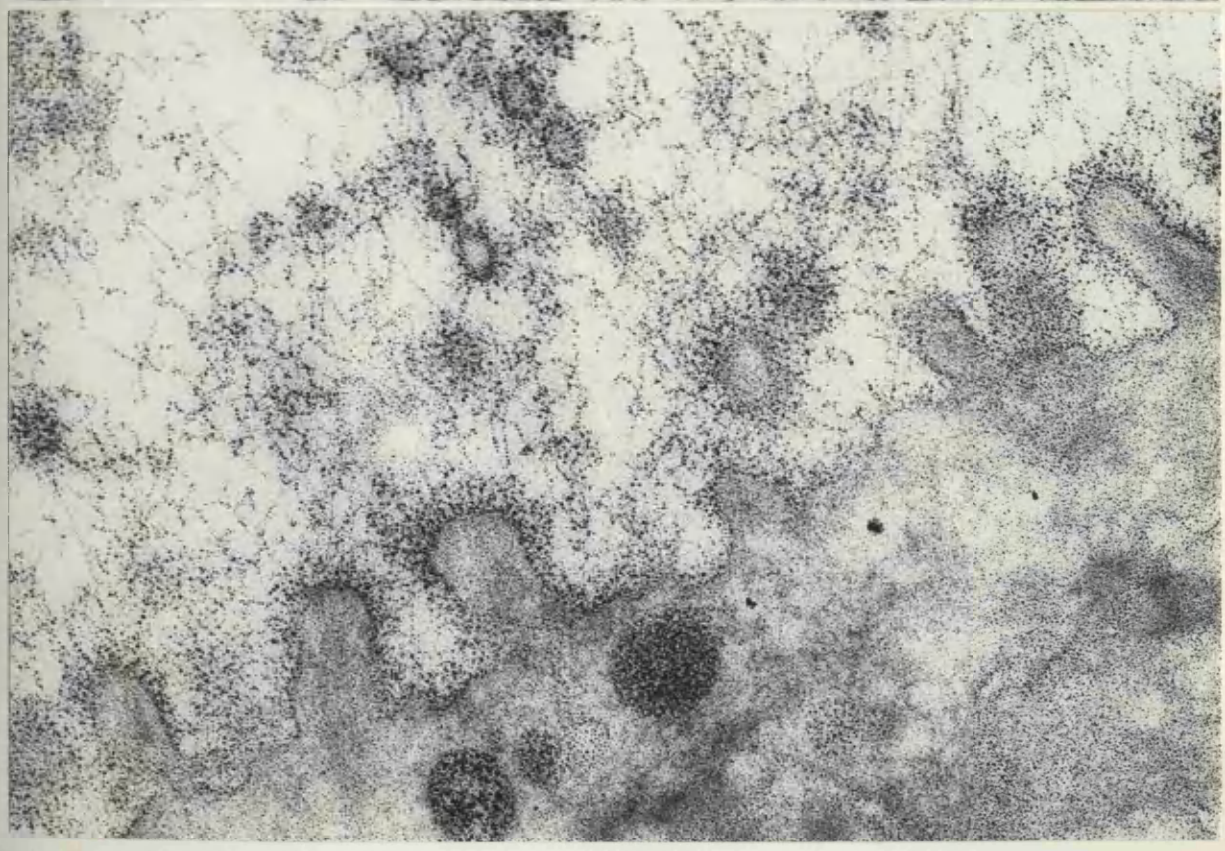

150

GASTRIC TUMOURS

Figure 151. Carbohydrate-staining of well differentiated metastatic gastric carcinoma. Coarse granular deposits, possibly glycogen, are seen in the intracytoplasmic vacuoles. These vacuoles appeared empty in conventional micrographs (Fig. 133). Notice the lumen(L) of the gland and the large nucleus(N) which is free of the reaction product.

Magnification 14000

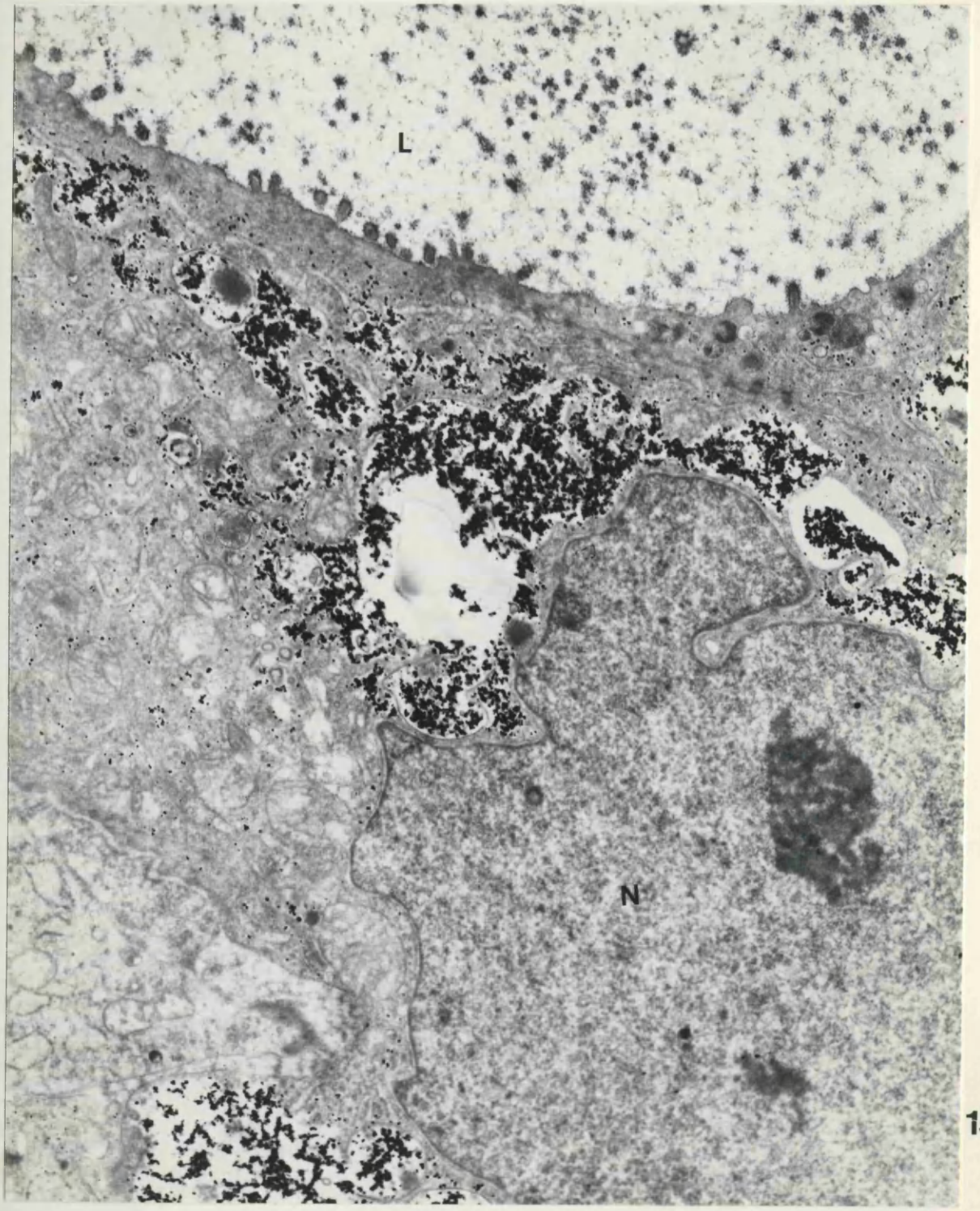

151

Figure 152. The histology of a typical case of poorly differentiated metastatic gastric carcinoma is shown.

Magnification 225

Figure 153. Poorly differentiated metastatic gastric carcinoma. The neoplastic cells are closely packed and have large nuclei. The desmosomes connecting the cells are barely seen(arrows).

Magnification 6720

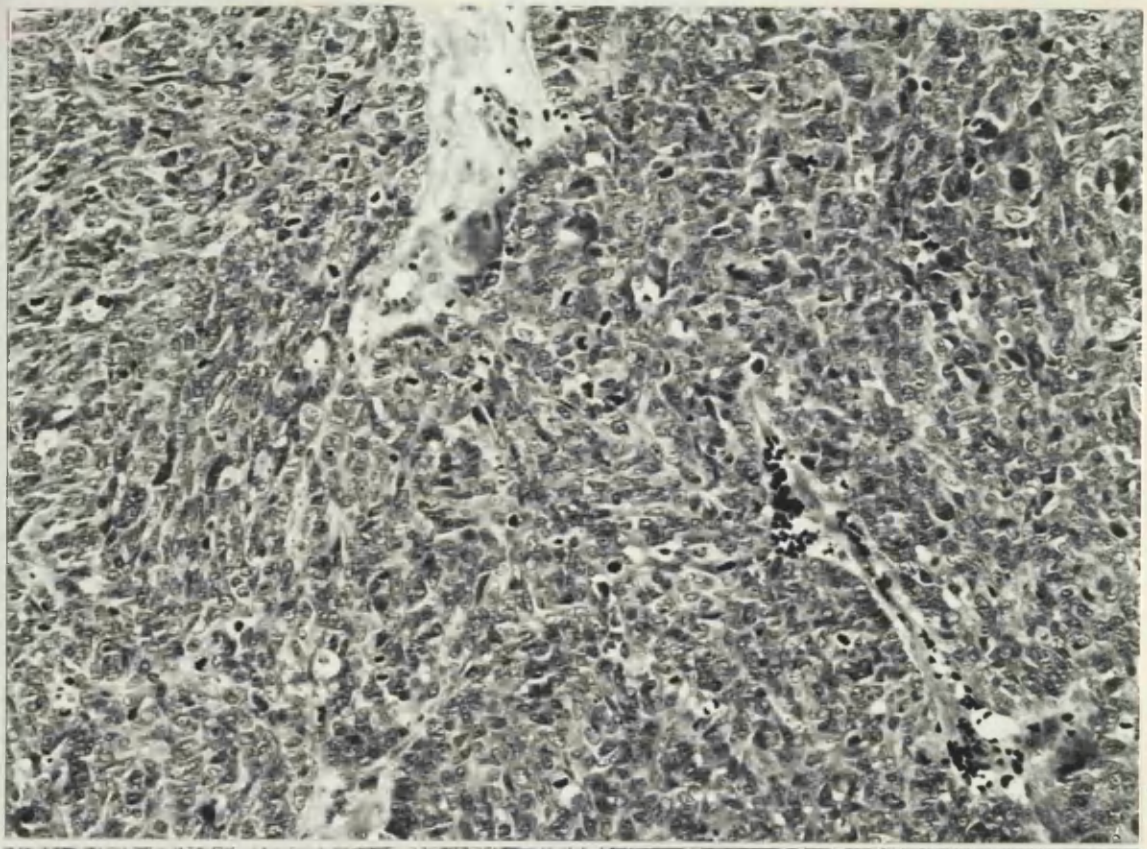

152

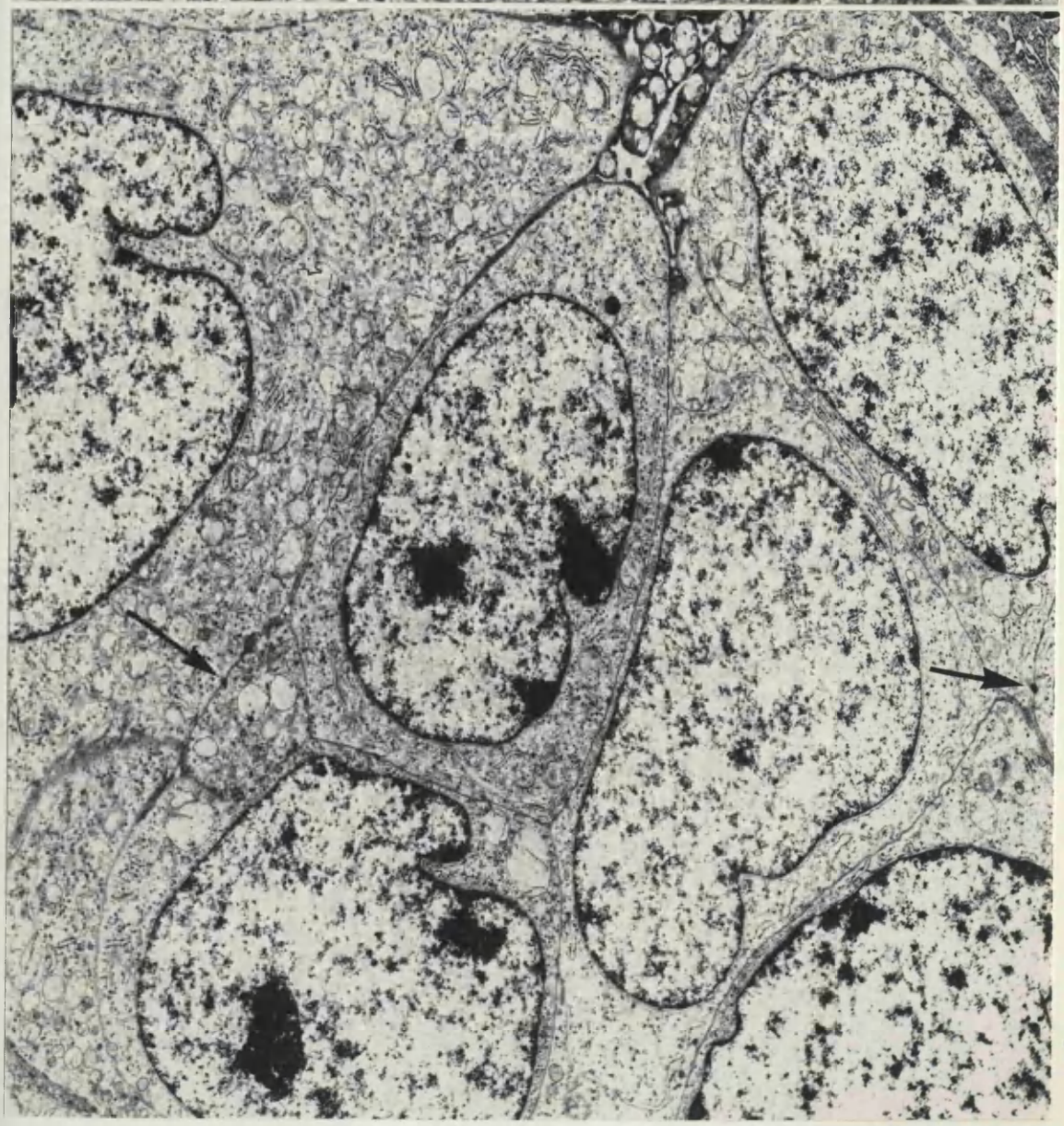

153

Figure 154. Poorly differentiated metastatic gastric carcinoma.

neoplastic cells having typical microvilli(M) are seen.

Magnification 22750

Figure 155. Poorly differentiated metastatic gastric carcinoma.

The neoplastic cells are seen to rest on a typical basal lamina(B). Note the pale nucleus(N).

Magnification 22750

Figure 156. Poorly differentiated metastatic gastric carcinoma.

There are numerous microvilli and vacuolated mitochondria seen in this micrograph.

Magnification 13800

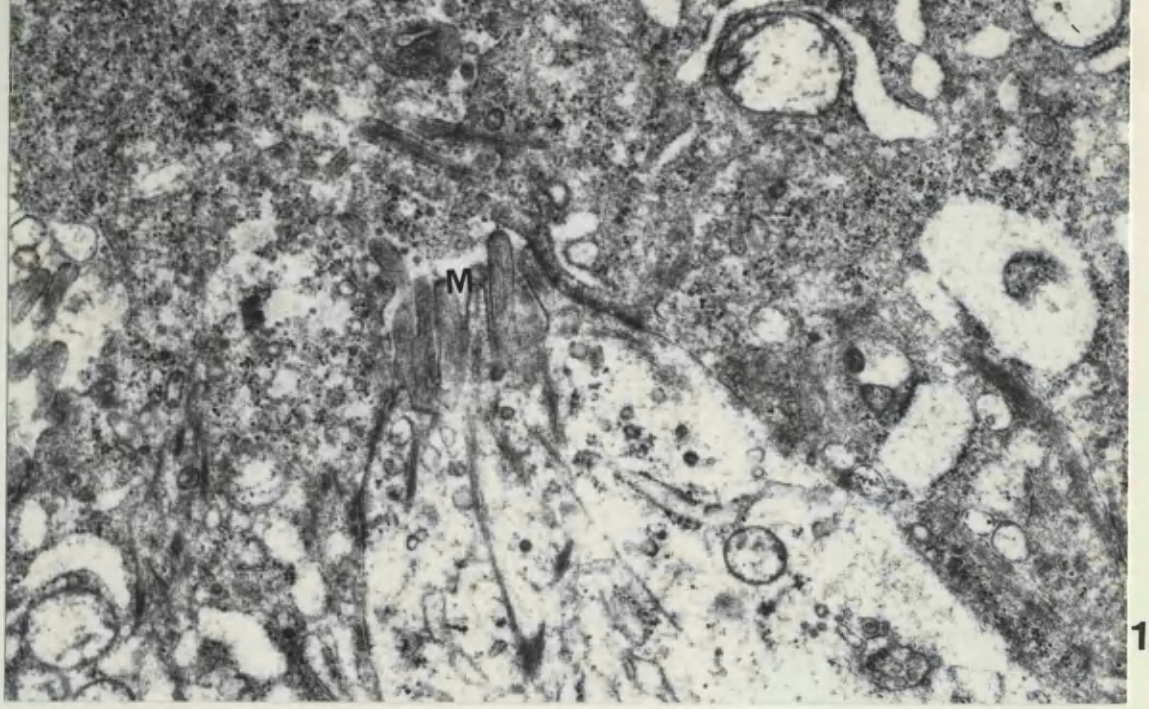

154

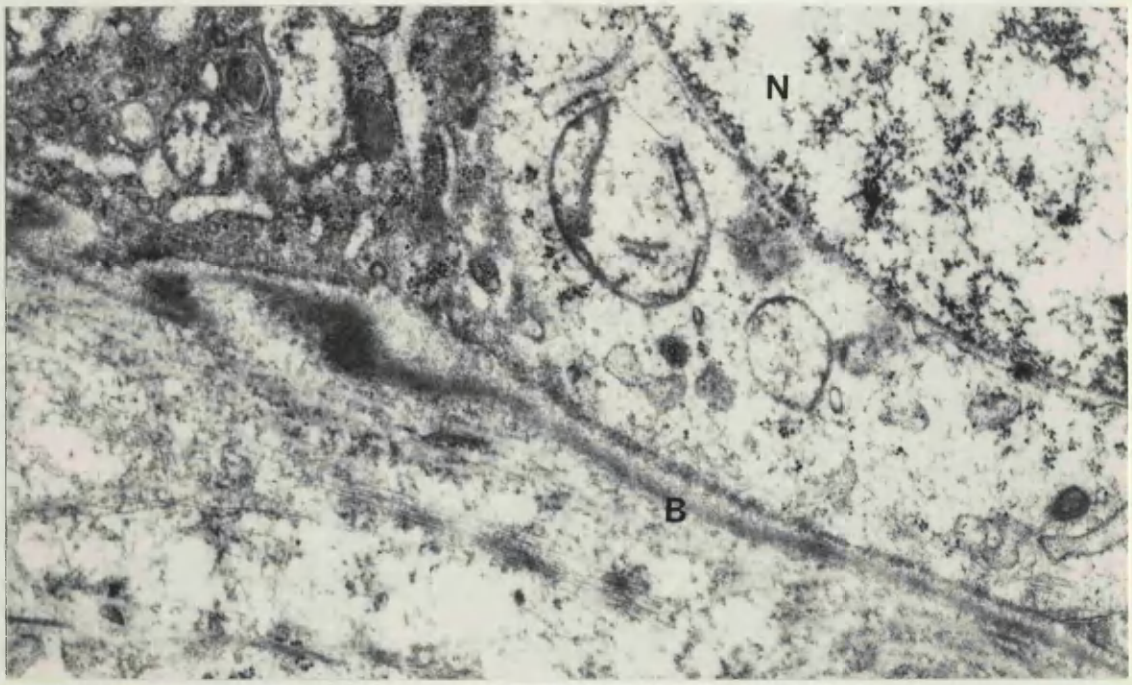

155

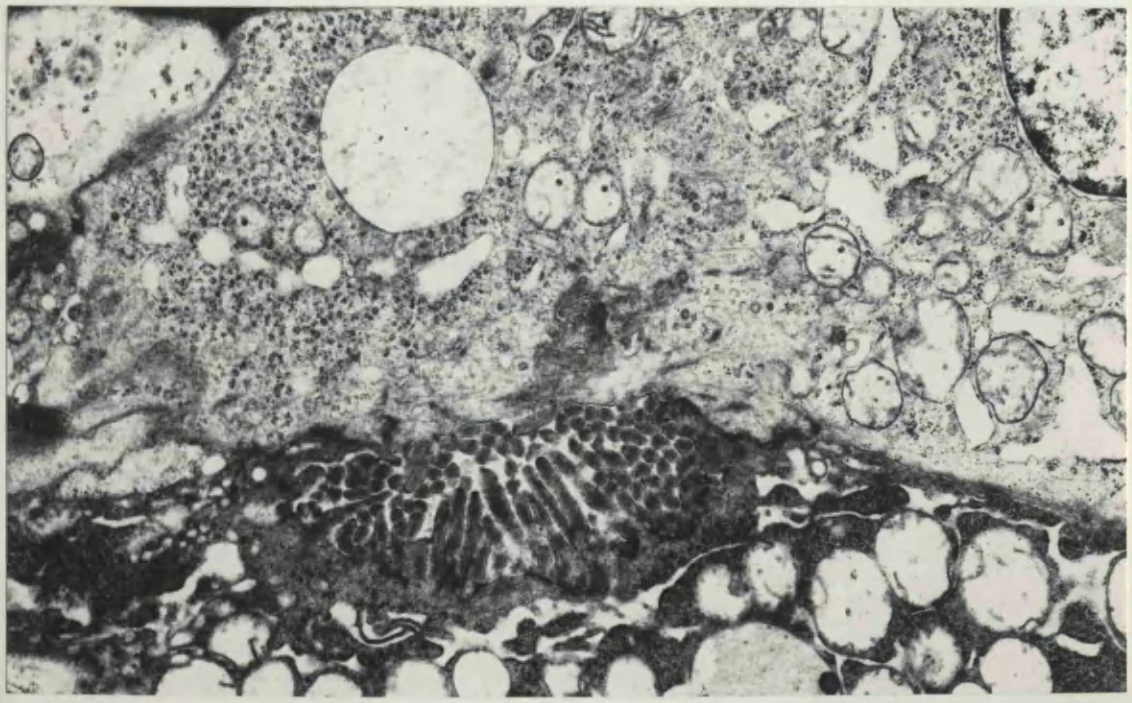

156

GASTRIC TUMOURS

Figure 157. Poorly differentiated metastatic gastric carcinoma. The neoplastic cells are connected by typical epithelial adhesion specialisations (D).

Magnification 17500

Figure 158. Metastatic gastric lymphoma. The neoplastic cells closely packed but are not connected by the adhesion specialisations seen in figure 157. Notice the pyknotic vacuolated cell with dark shrunken nucleus.

Magnification 8400

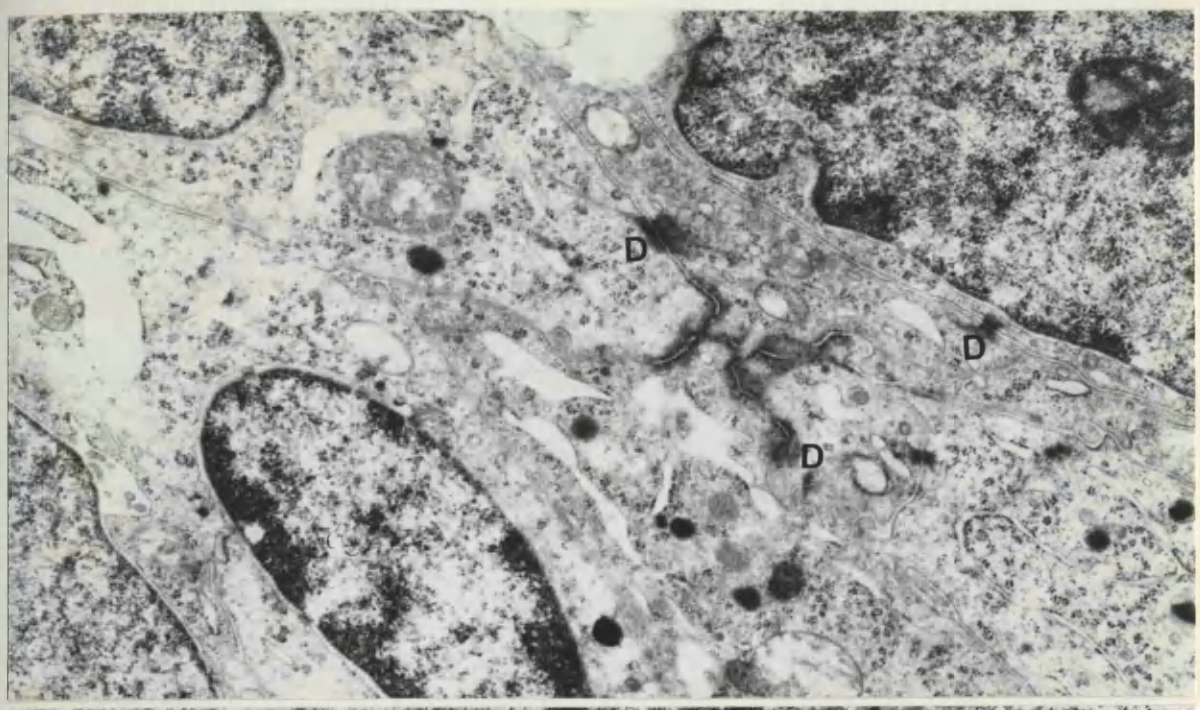

157

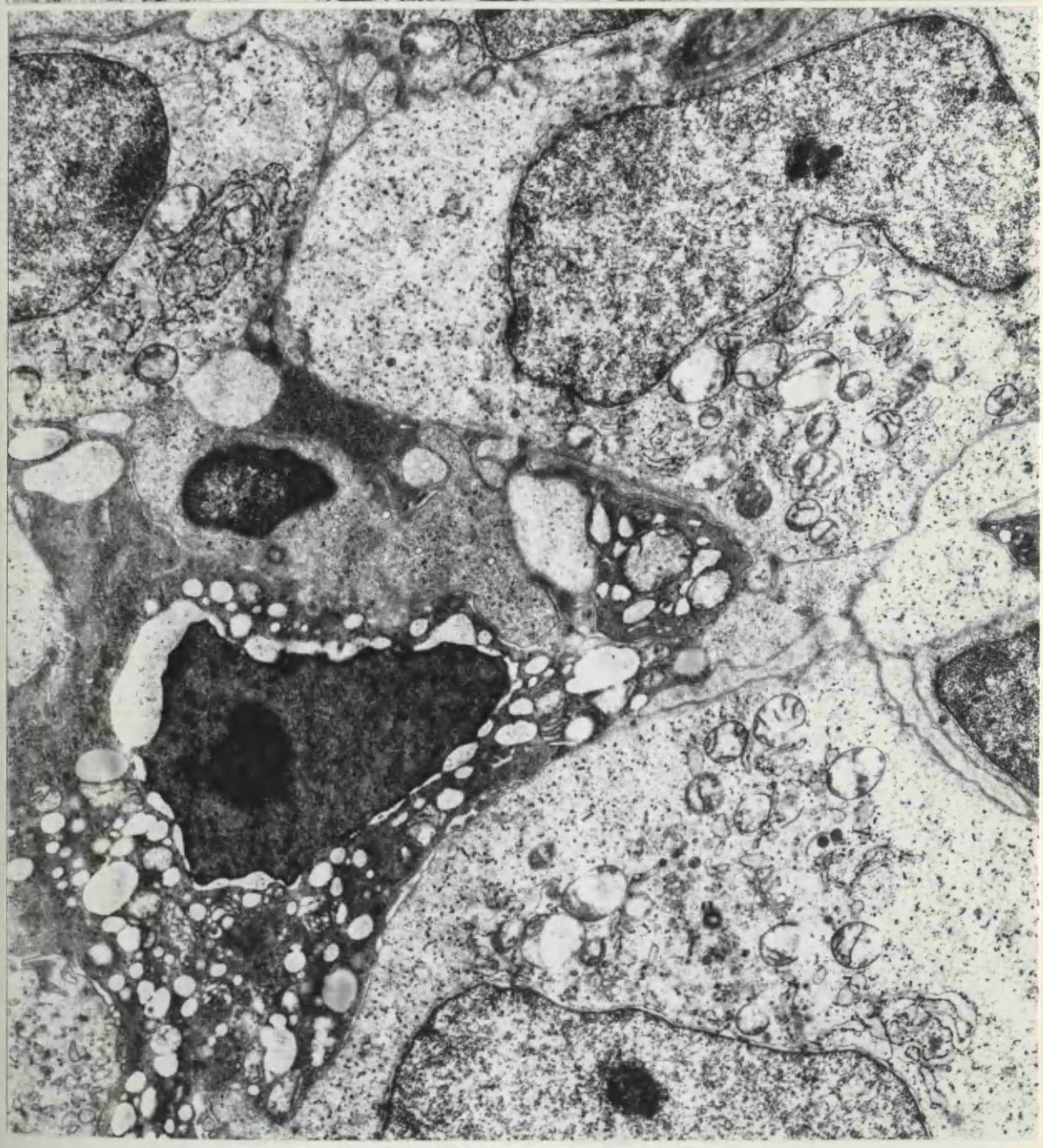

158

GASTRIC TUMOURS

Figure 159. The histology of a typical case of metastatic signet ring cell gastric carcinoma is shown.

Magnification 225

Figure 160. Metastatic signet ring cell gastric carcinoma. The neoplastic cells within lymphatic vessels are seen to have a highly irregular outline. The centrally located nucleus is compressed by pale mucous granules.

Magnification 8400

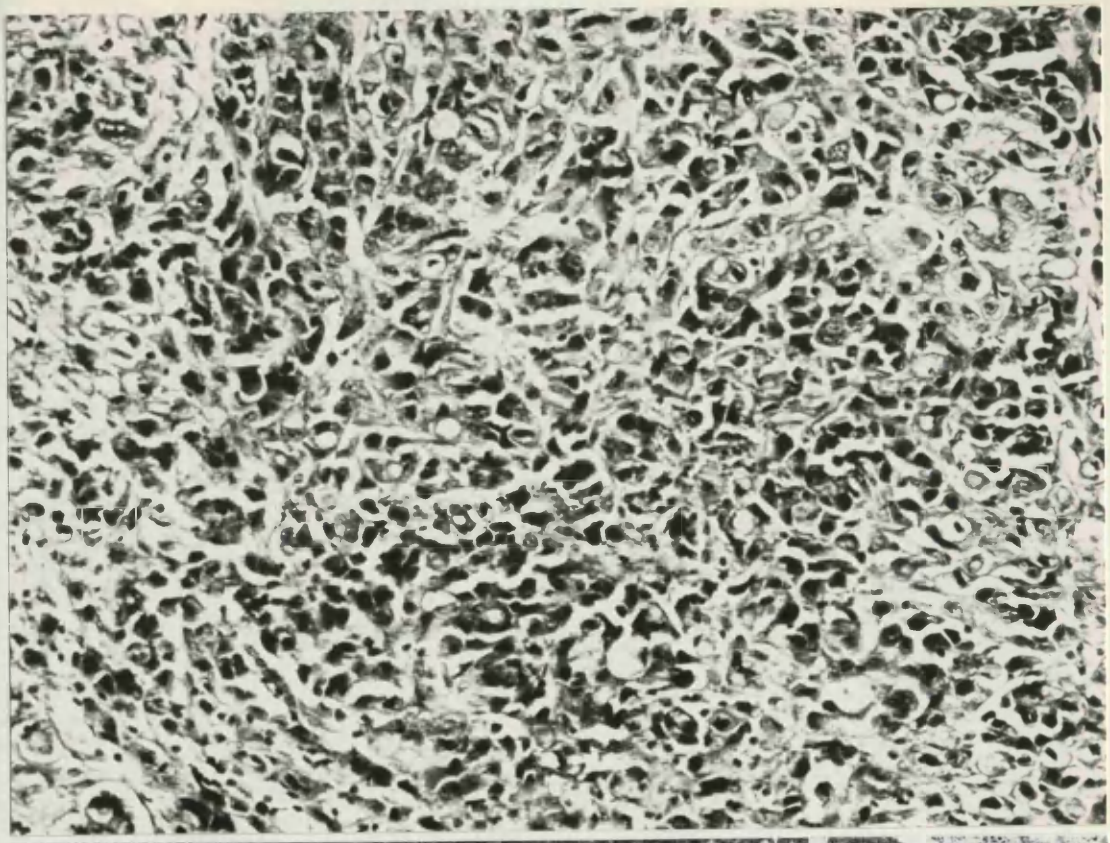

159

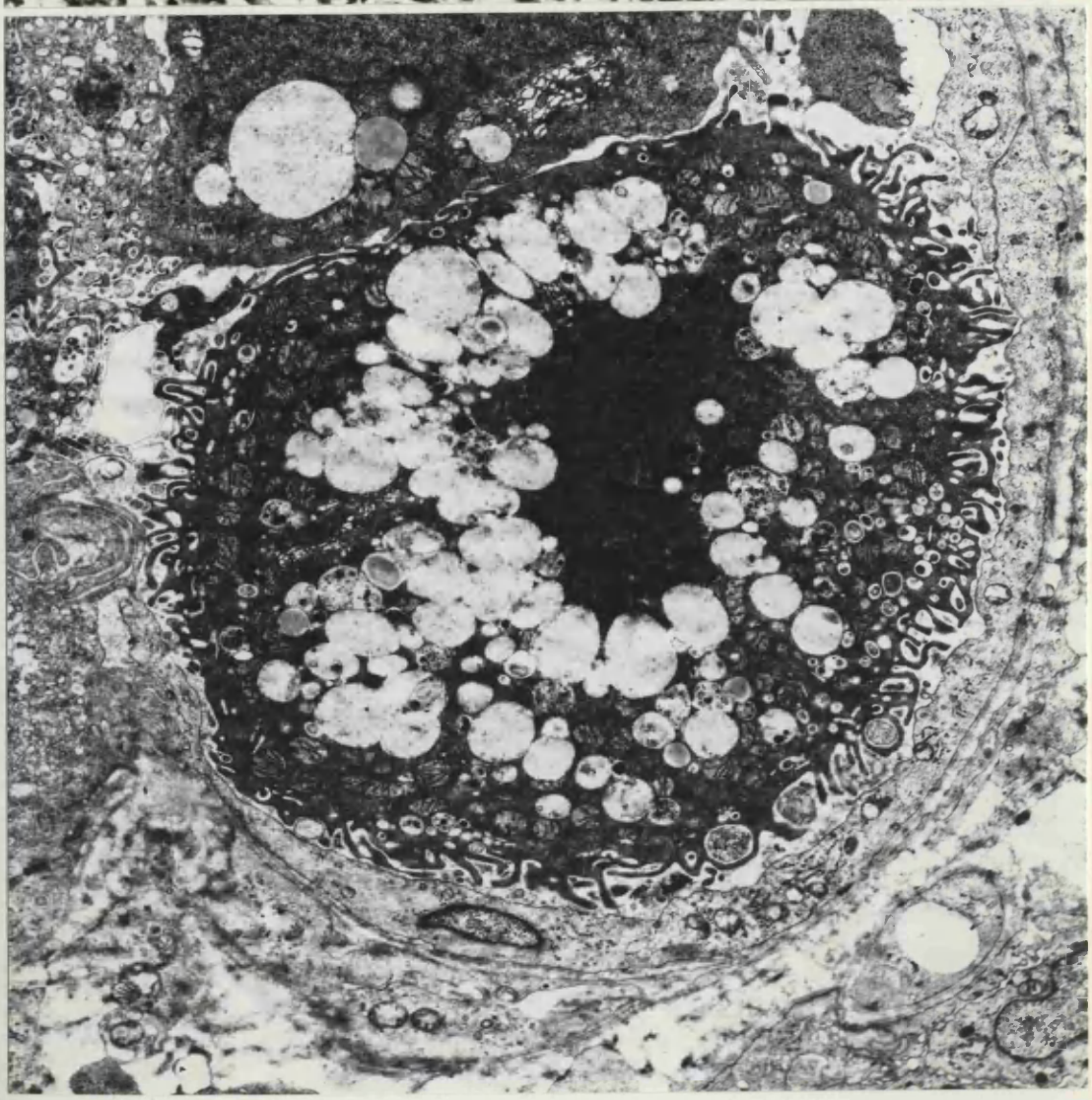

160

Figure 161. Metastatic signet ring cell gastric carcinoma. The neoplastic cells have numerous finger-like projections and are separated by distinct intercellular spaces. Their cytoplasm contains numerous tubulovesicular structures(T) and pale mucous granules. Note that some residual cell-to-cell adhesion persists, with clearly defined desmosomes(D).

Magnification 6000

Figure 162. Metastatic signet ring gastric carcinoma. This neoplastic cell rests on a basal lamina(B).

Magnification 88250

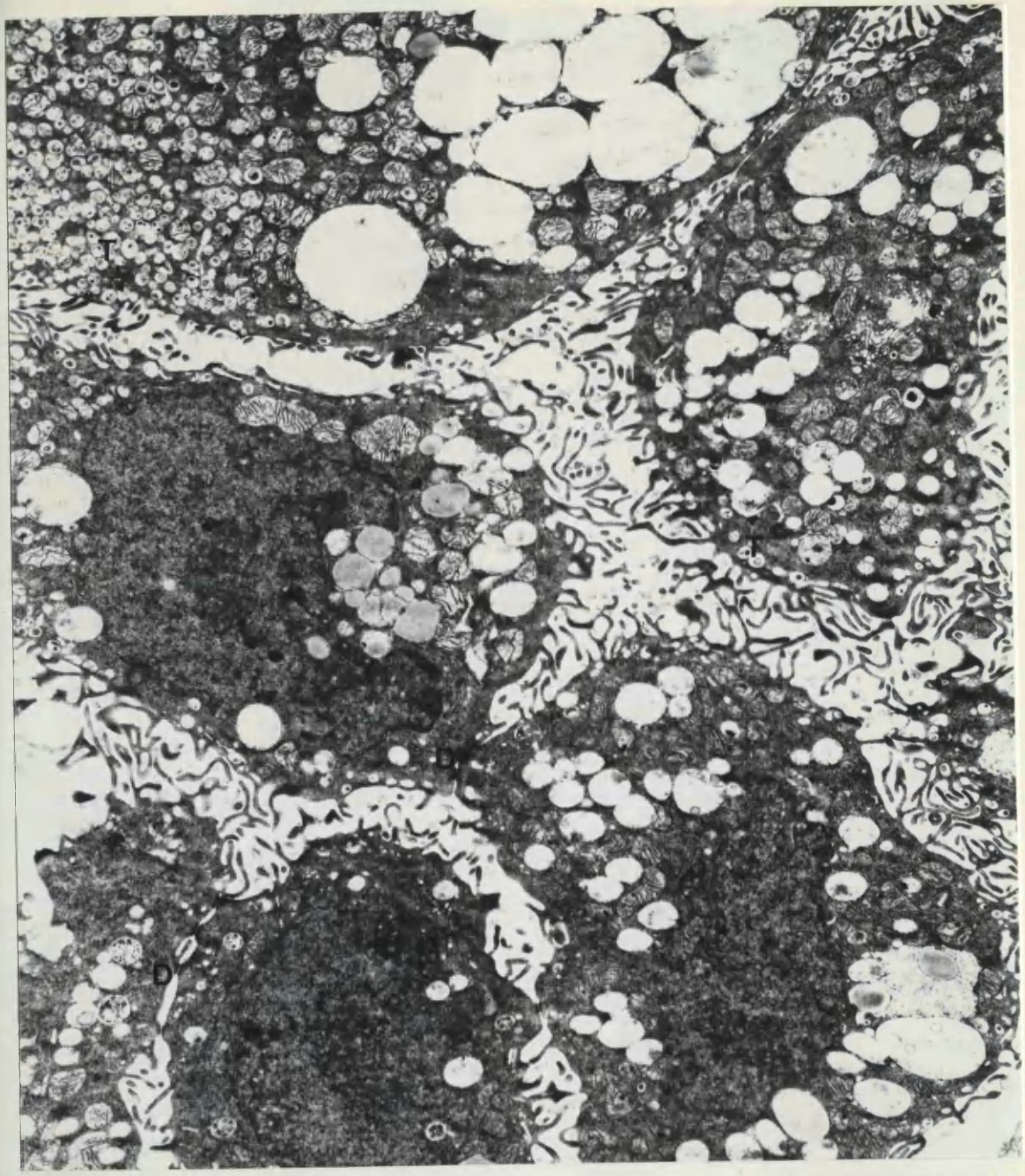

161

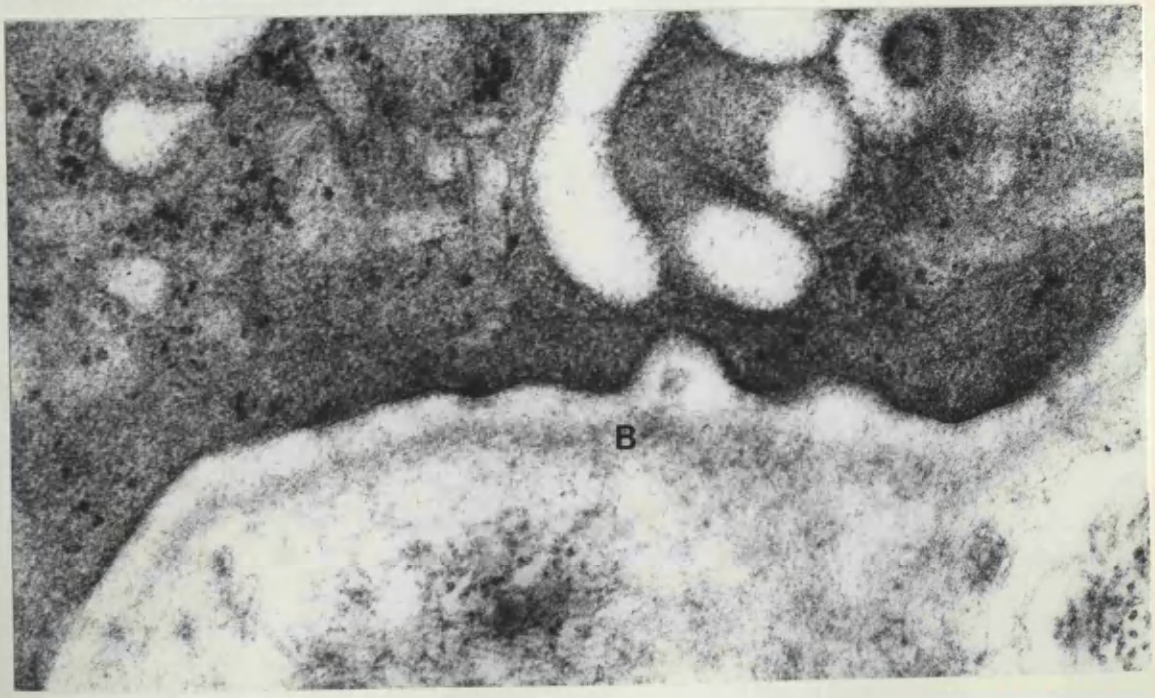

162

Figure 163. Metastatic signet ring cell gastric carcinoma. The intracytoplasmic desmosomes typical of this type of metastatic gastric carcinoma are shown. Notice the "tennis racket" desmosomes(T).

Magnification 116500

Figure 164. Metastatic signet ring cell gastric carcinoma. Vesicle formations(V) and "tennis racket" desmosome(T) are seen.

Magnification 116500

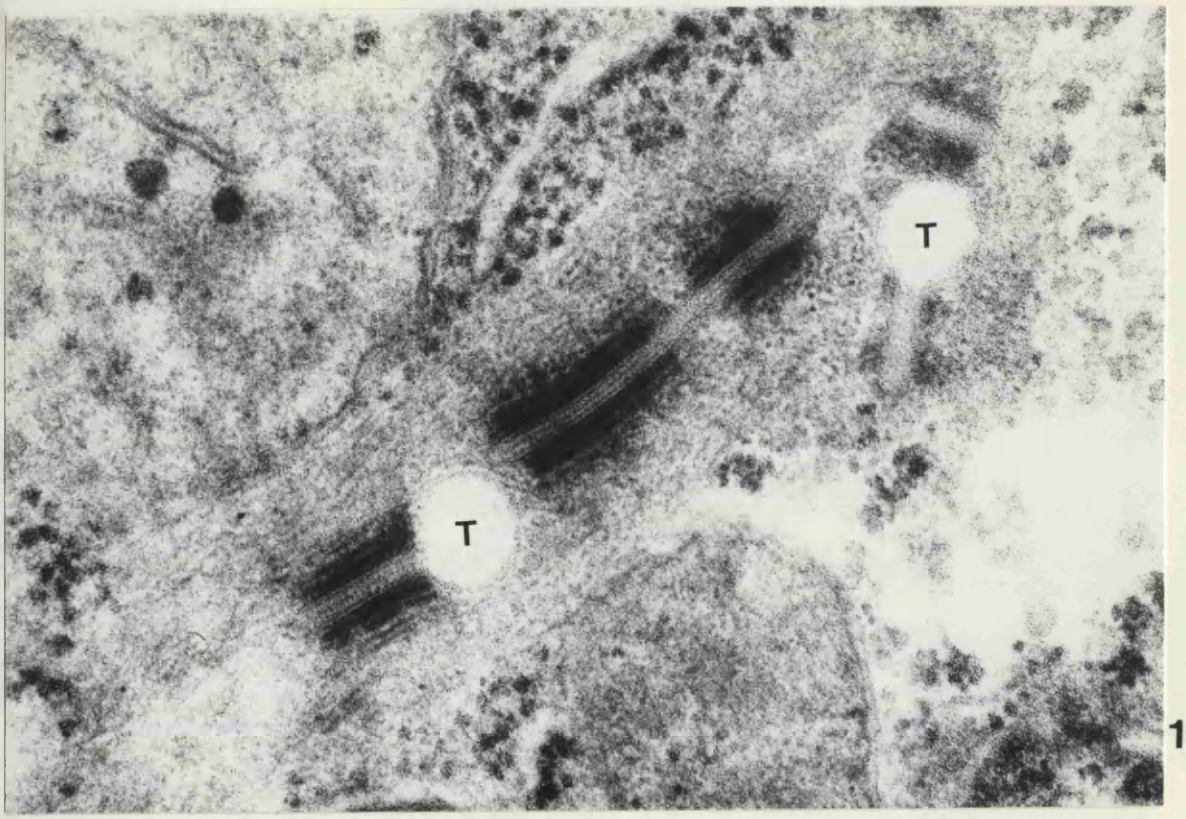

163

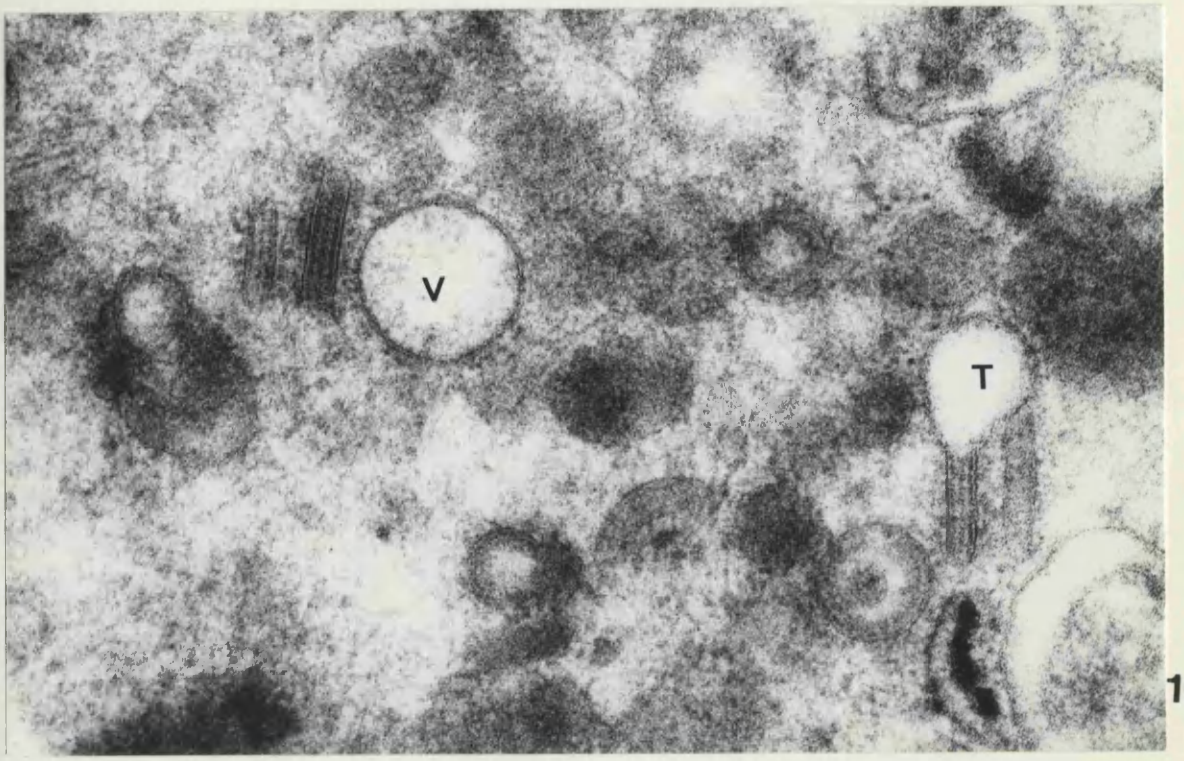

164

GASTRIC TUMOURS

Figure 165. Metastatic signet ring cell gastric carcinoma.

The neoplastic cell contains an intracytoplasmic saccular inclusion. The inclusion is lined by numerous microvilli.

Magnification 22750

Figure 166. Metastatic signet ring gastric carcinoma.

Multiple intracytoplasmic saccular inclusions are seen.

Magnification 22750

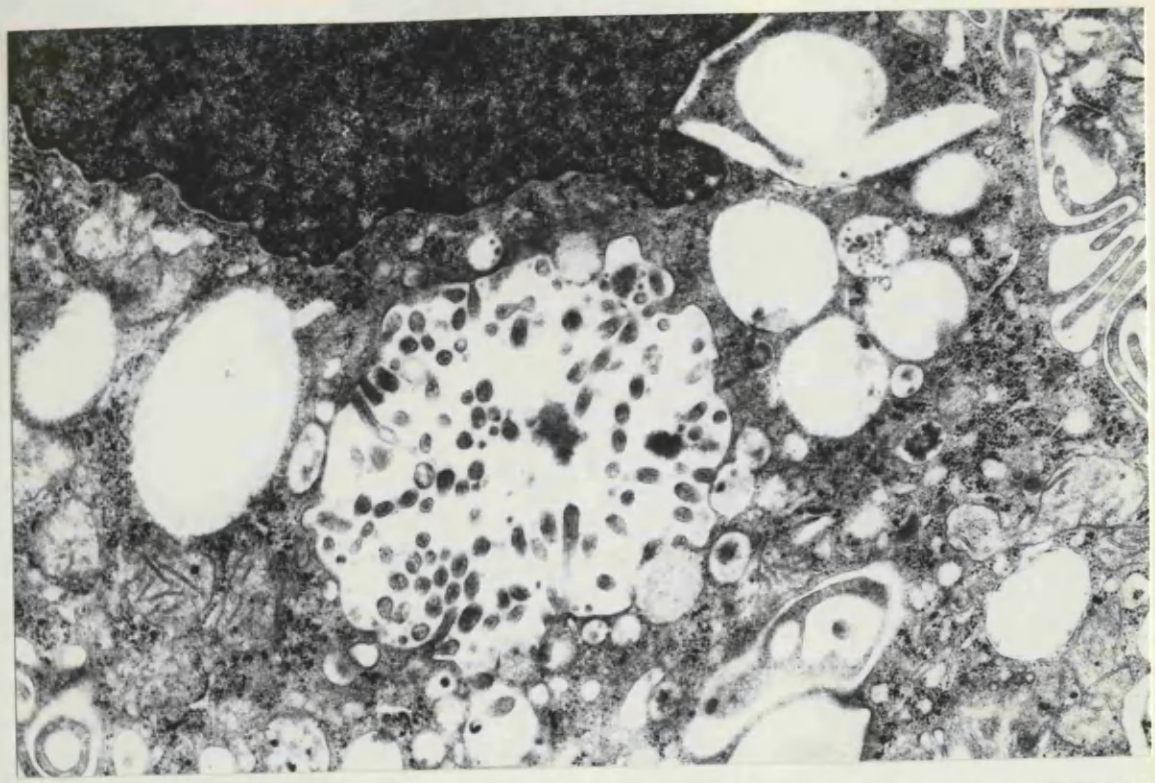

165

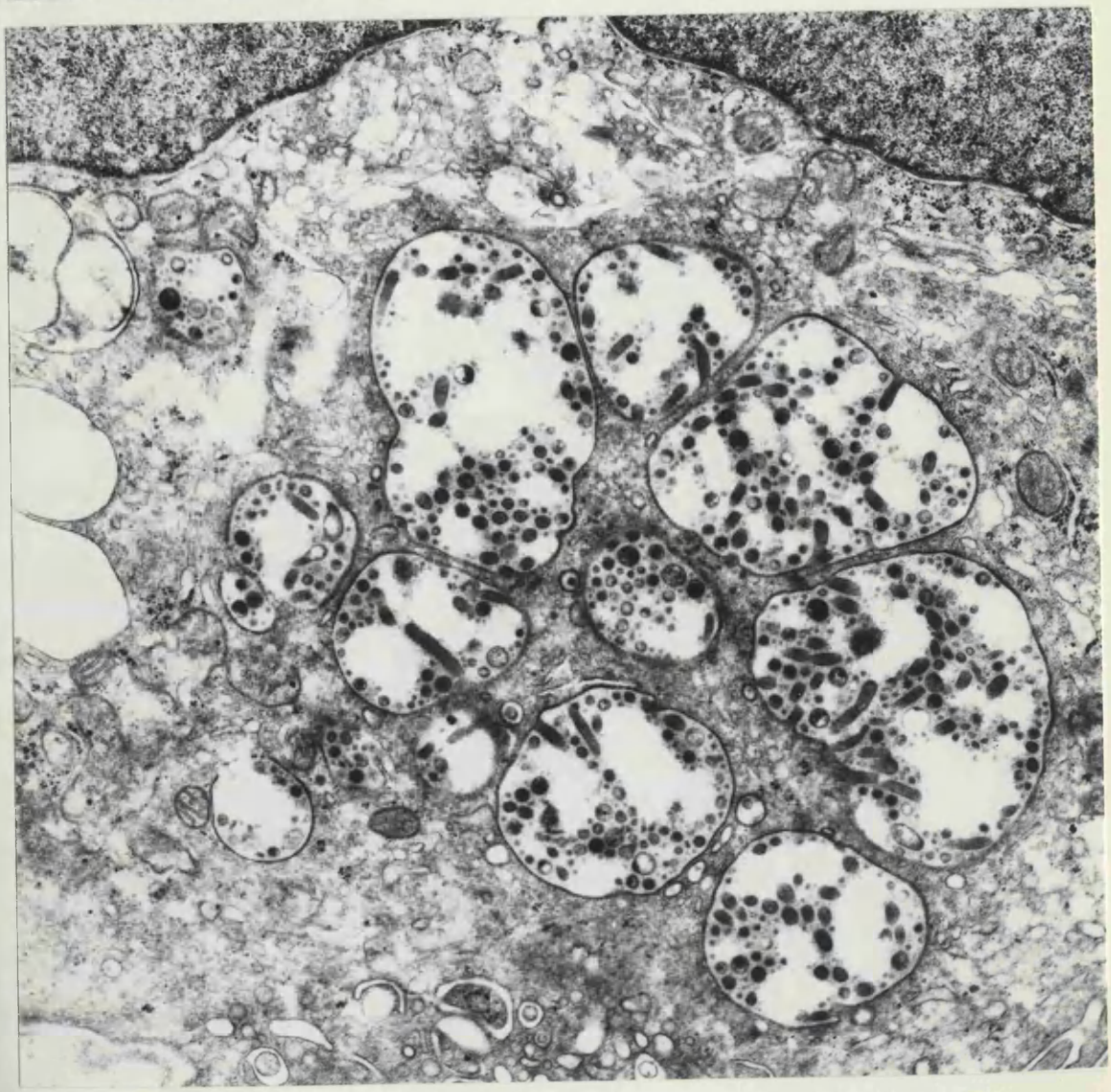

166

GASTRIC TUMOURS

Figure 167. Metastatic signet ring cell gastric carcinoma. The microvilli projecting into the intracytoplasmic saccular inclusion are seen to have a microfilamentous core extending to the cytoplasm.

Magnification 88250

Figure 168. Metastatic signet ring cell gastric carcinoma. The tubulovesicular inclusions of the signet ring cell are similar to those of gastric parietal cells(Fig.48). A cytoplasmic invagination into the vesicle is seen at two points (arrows).

Magnification 116500

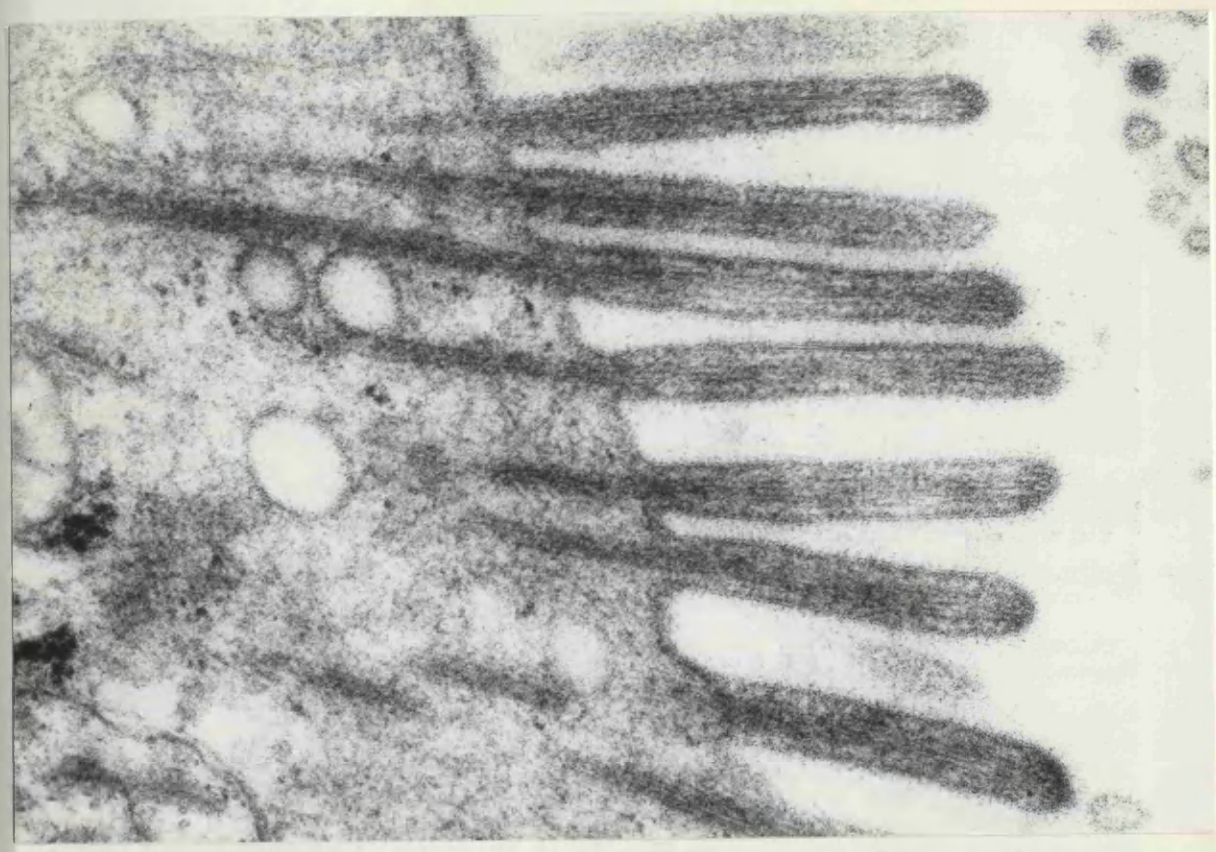

167

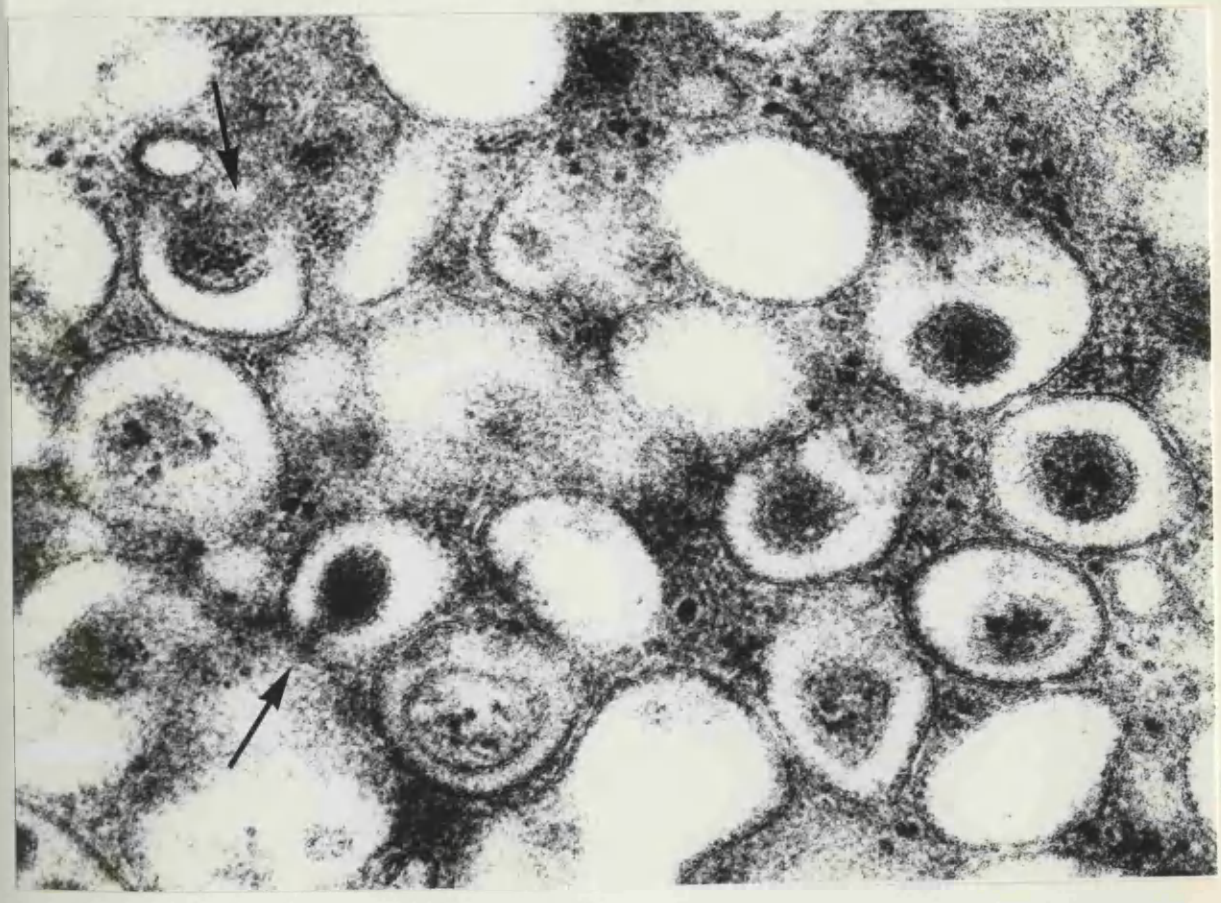

168

GASTRIC TUMOURS

Figure 169. Metastatic signet ring cell gastric carcinoma.

Intranuclear tubules are seen.

Magnification 69900

Figure 170. Metastatic signet ring cell gastric carcinoma.

Numerous intranuclear dense inclusions are seen. These inclusions are separated by a clear halo from the surrounding chromatin.

Magnification 155000

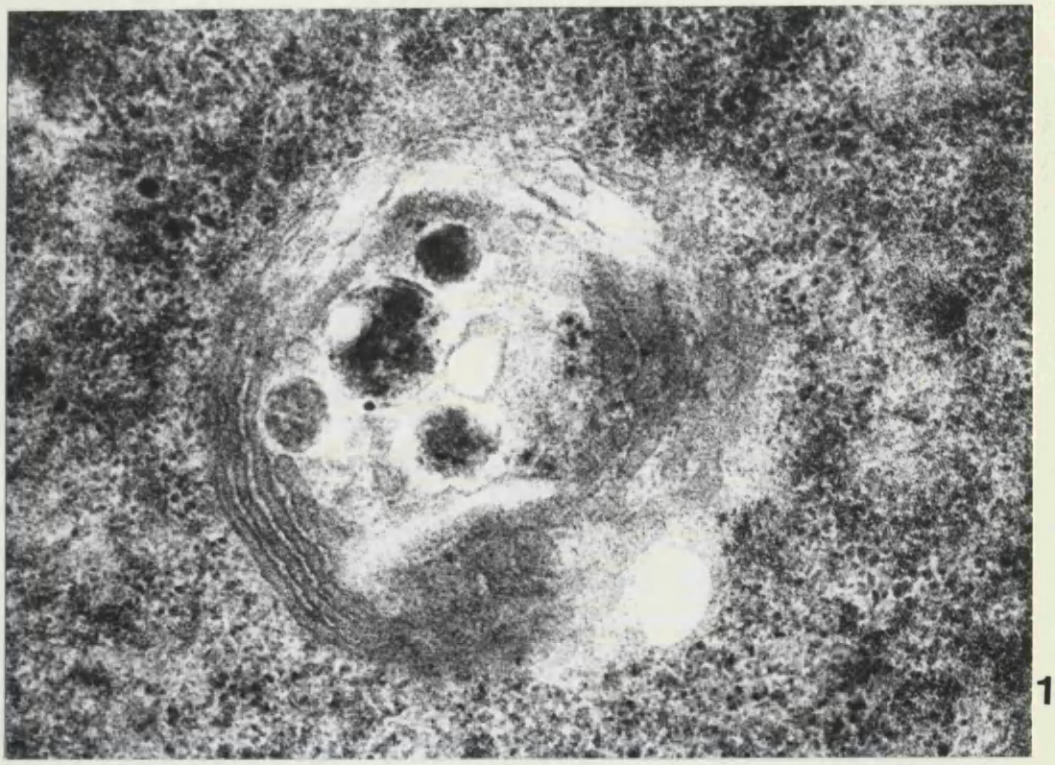

169

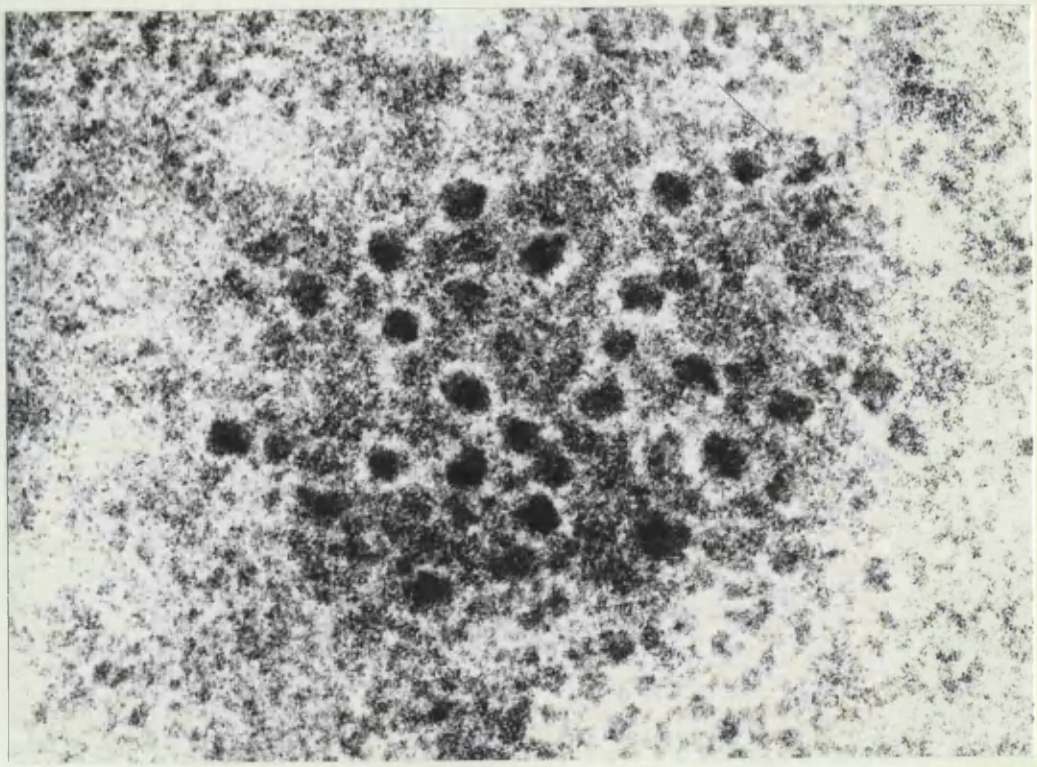

170

COLONIC TUMOURS

Figures 171, 172. The histology of a typical case of villous papilloma is shown.

Magnification 225

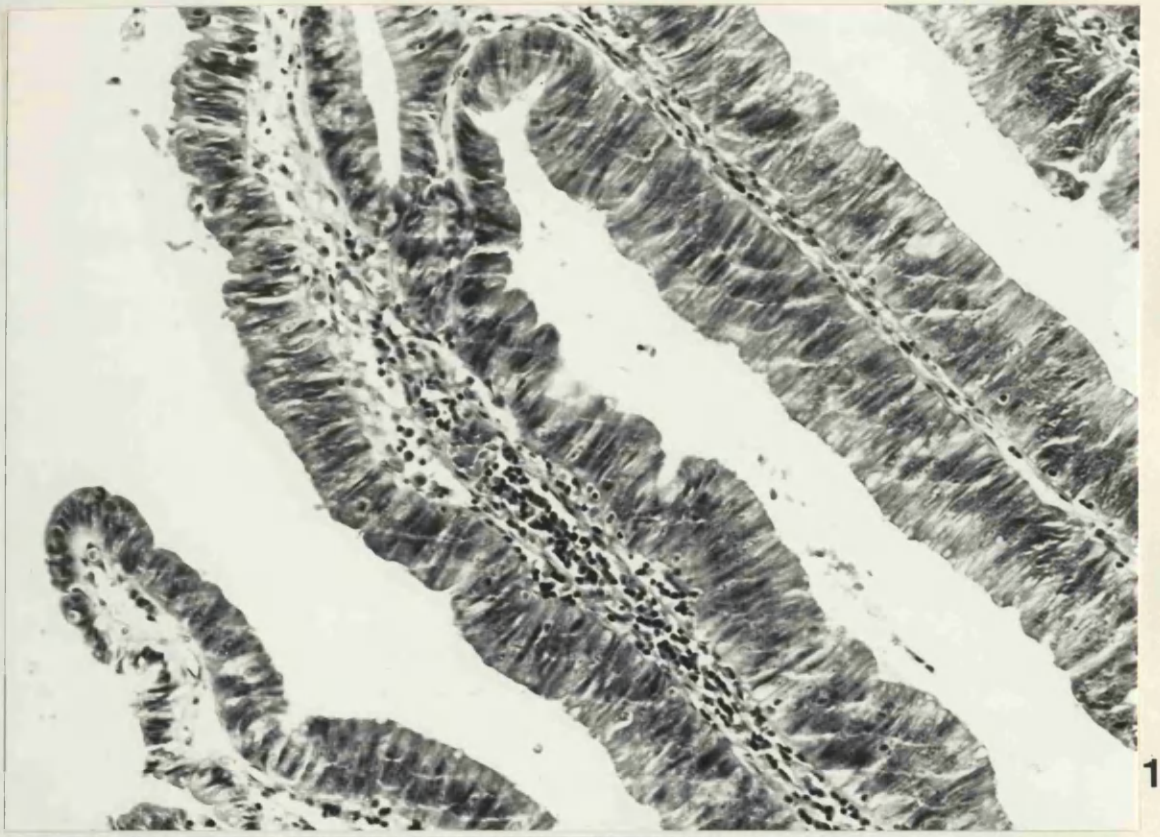

171

172

COLONIC TUMOURS

Figure 173. Villous papilloma. The apical parts of the neoplastic cells of villous papilloma are shown.

Magnification 10750

Figure 174. Villous papilloma. The basal parts of several cells are seen.

Magnification 8600

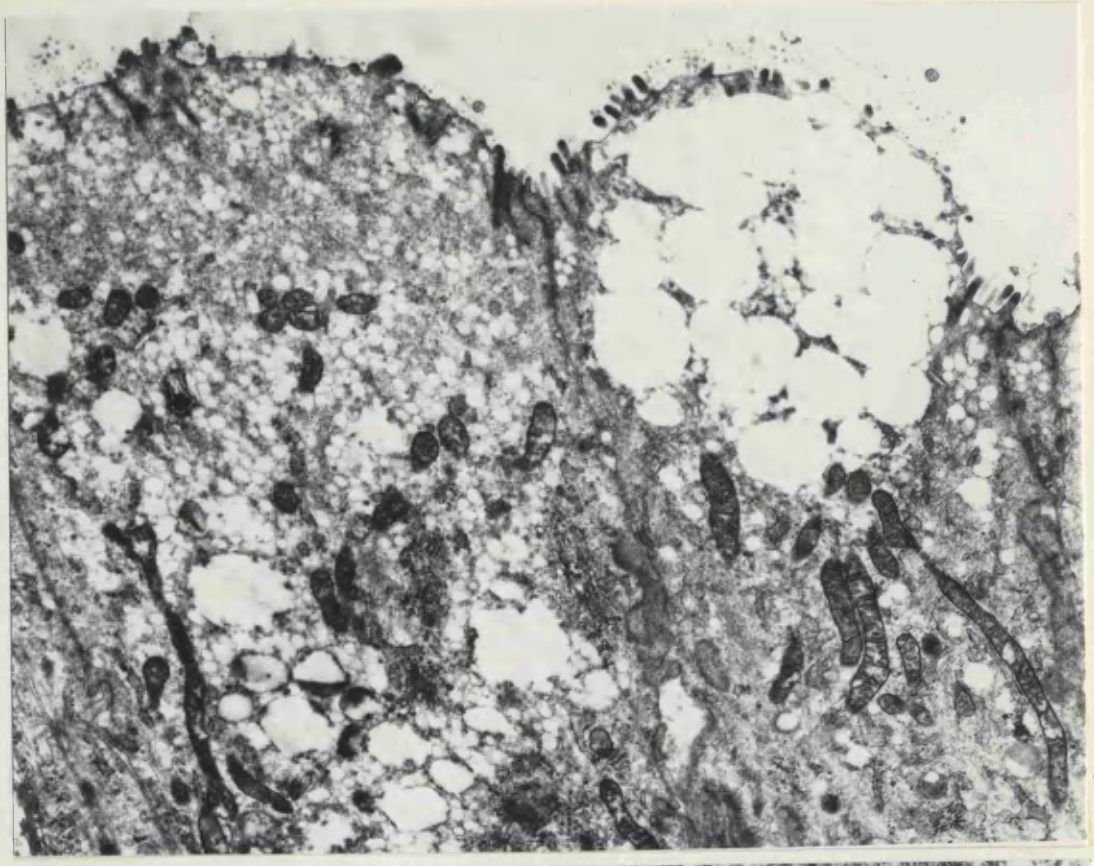

173

174

COLONIC TUMOURS

Figure 175. Villous papilloma. Villous papilloma cells have quite prominent mitochondria, aggregatesof secretion granules in the apical cytoplasm and numerous membrane-limited vesicles. Note the large nucleus and the short irregular microvilli.

Magnification 9890

Figure 176. Villous papilloma. A group of mitochondria lies in basal cytoplasm of the neoplastic cell.

Magnification 51250

175

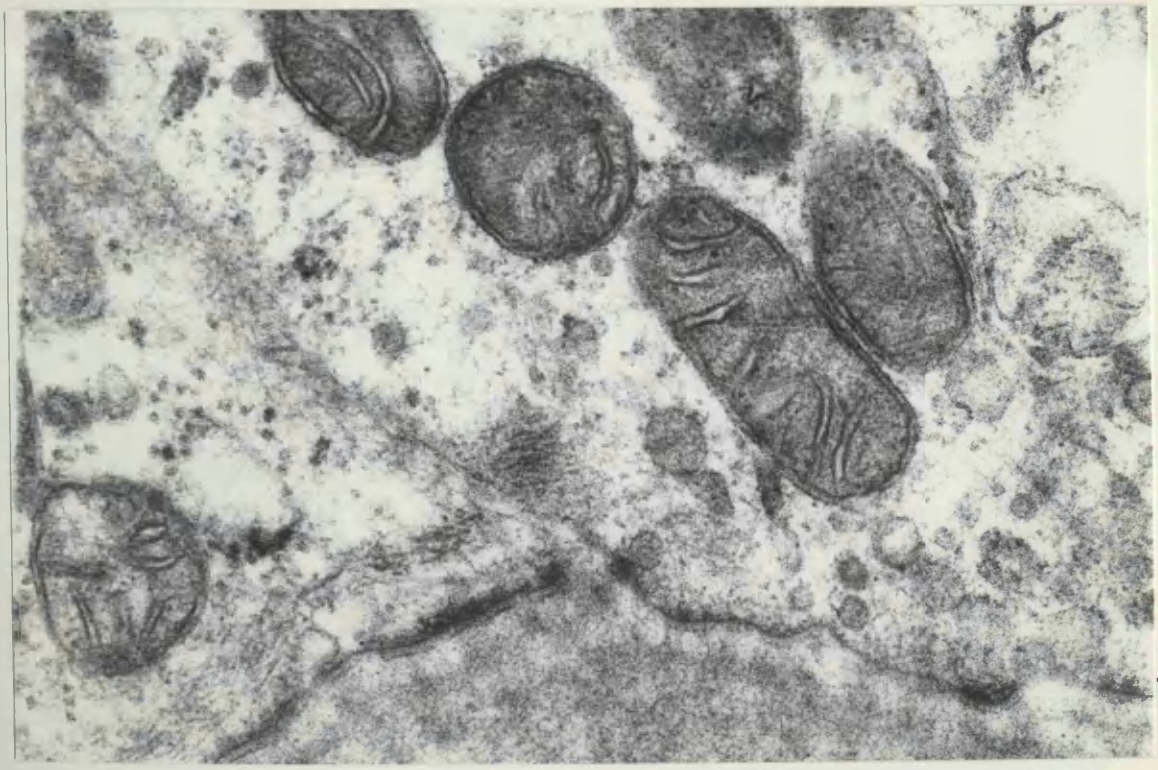

176

COLONIC TUMOURS

Figure 177. Villous papilloma. Dense deposits of carbohydrate staining are seen on the apical cell membrane and just inside the membrane of the vesicles . Note the lumen(L).

Magnification 51250

Figure 178. Villous papilloma. Positive carbohydrate staining is seen again just inside the membrane of the vesicles.Note the lumen(L).

Magnification 88250

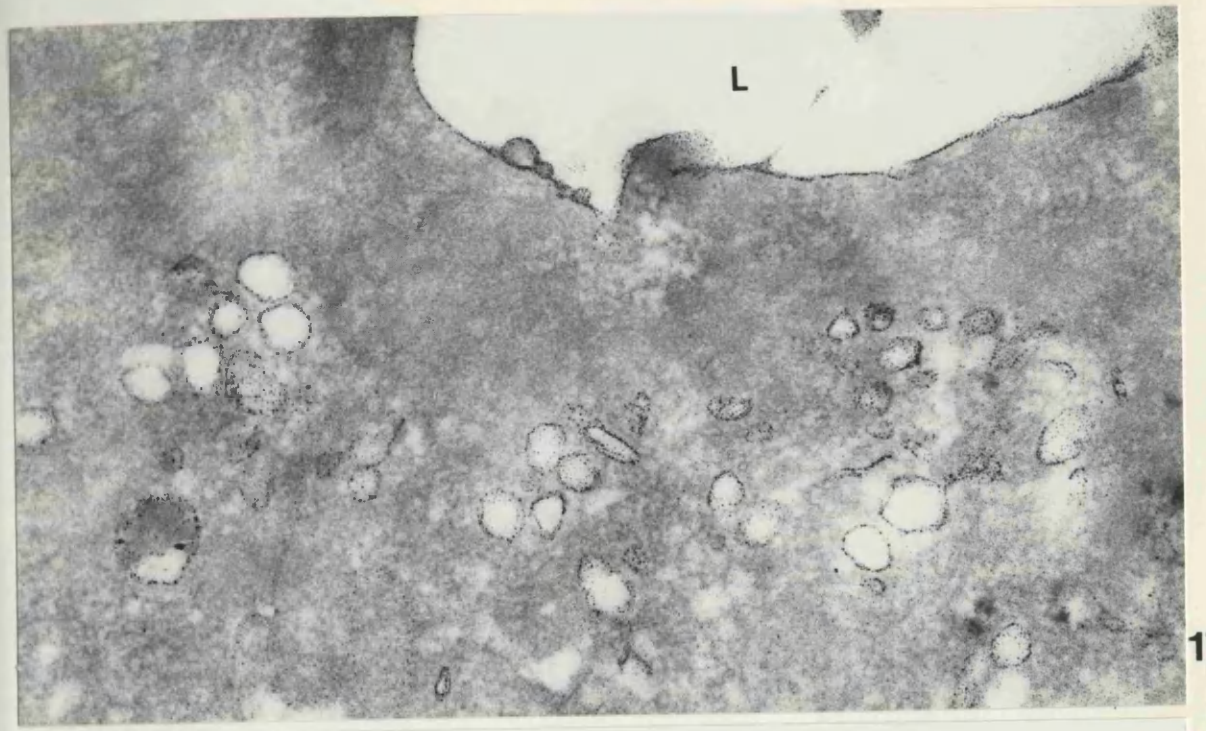

177

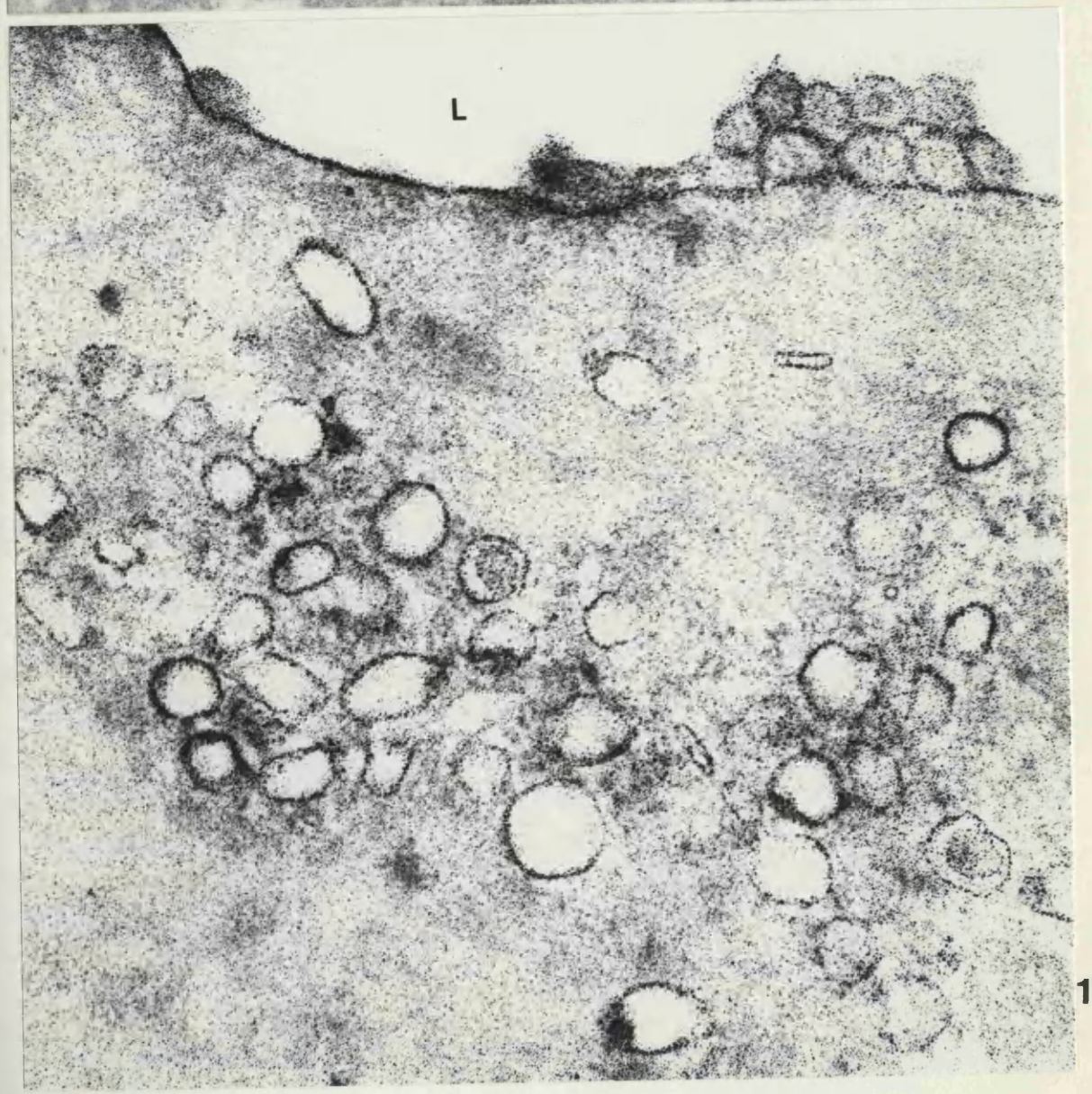

178

COLONIC TUMOURS

Figure 179. Villous papilloma. The prominent nucleolus of a villous papilloma cell is shown.

Magnification 70000

Figure 180. Intracytoplasmic membrane-bound inclusions (M) of villous papilloma are seen. Note the nucleus(N) of adjacent cell. These inclusions bear a strong resemblance to nuclear material.

Magnification 17500

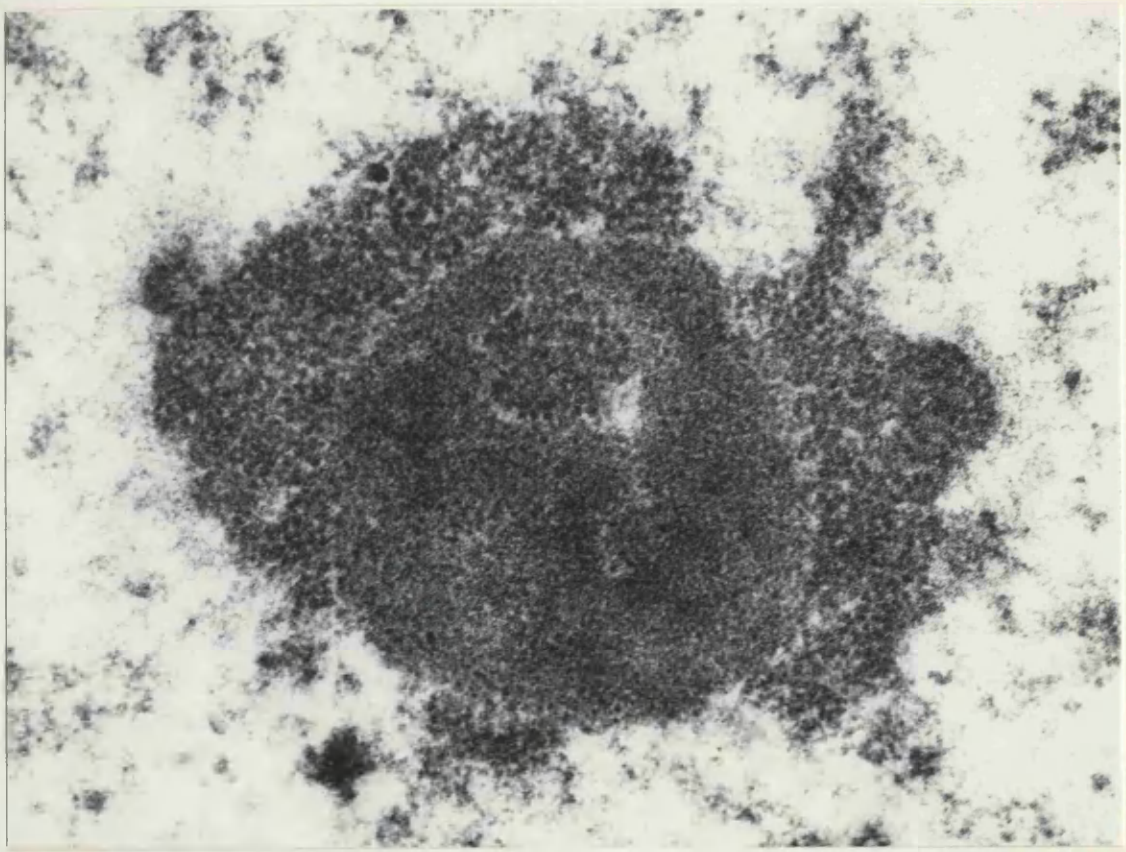

179

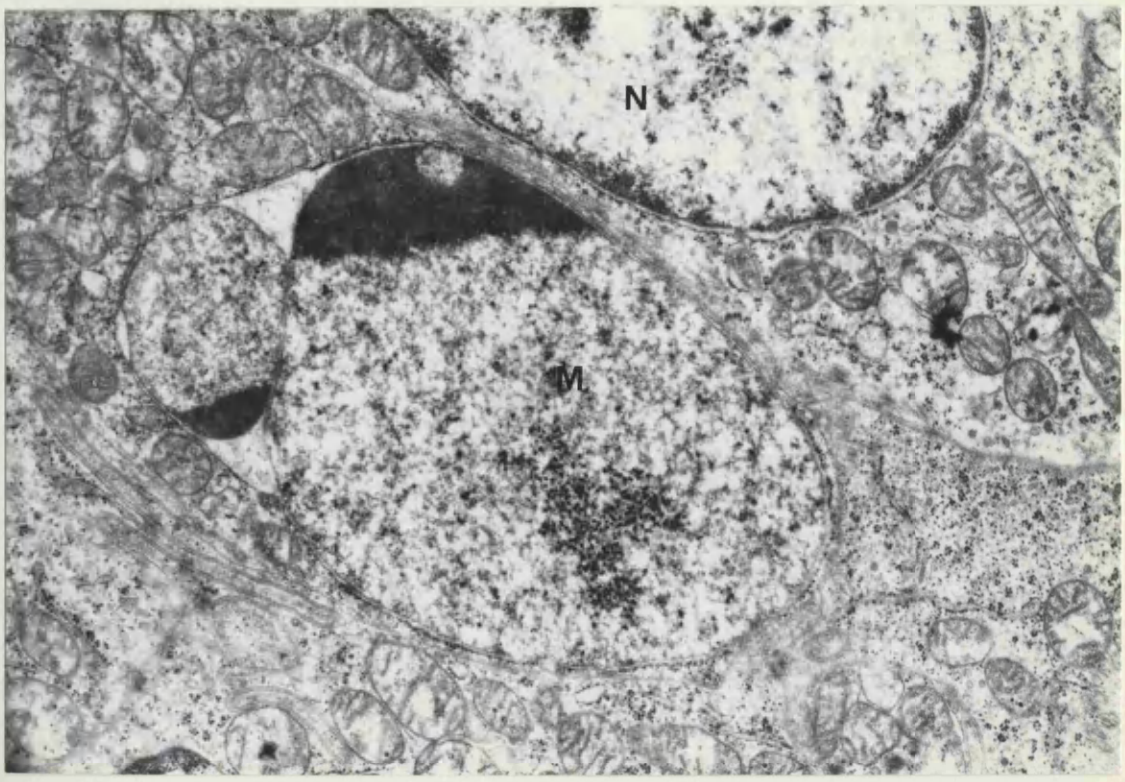

180

COLONIC TUMOURS

Figure 181. Villous papilloma. Aggregates of dark cells are shown to have numerous mitochondria, lateral interdigitations and intracellular vacuoles.

Magnification 8600

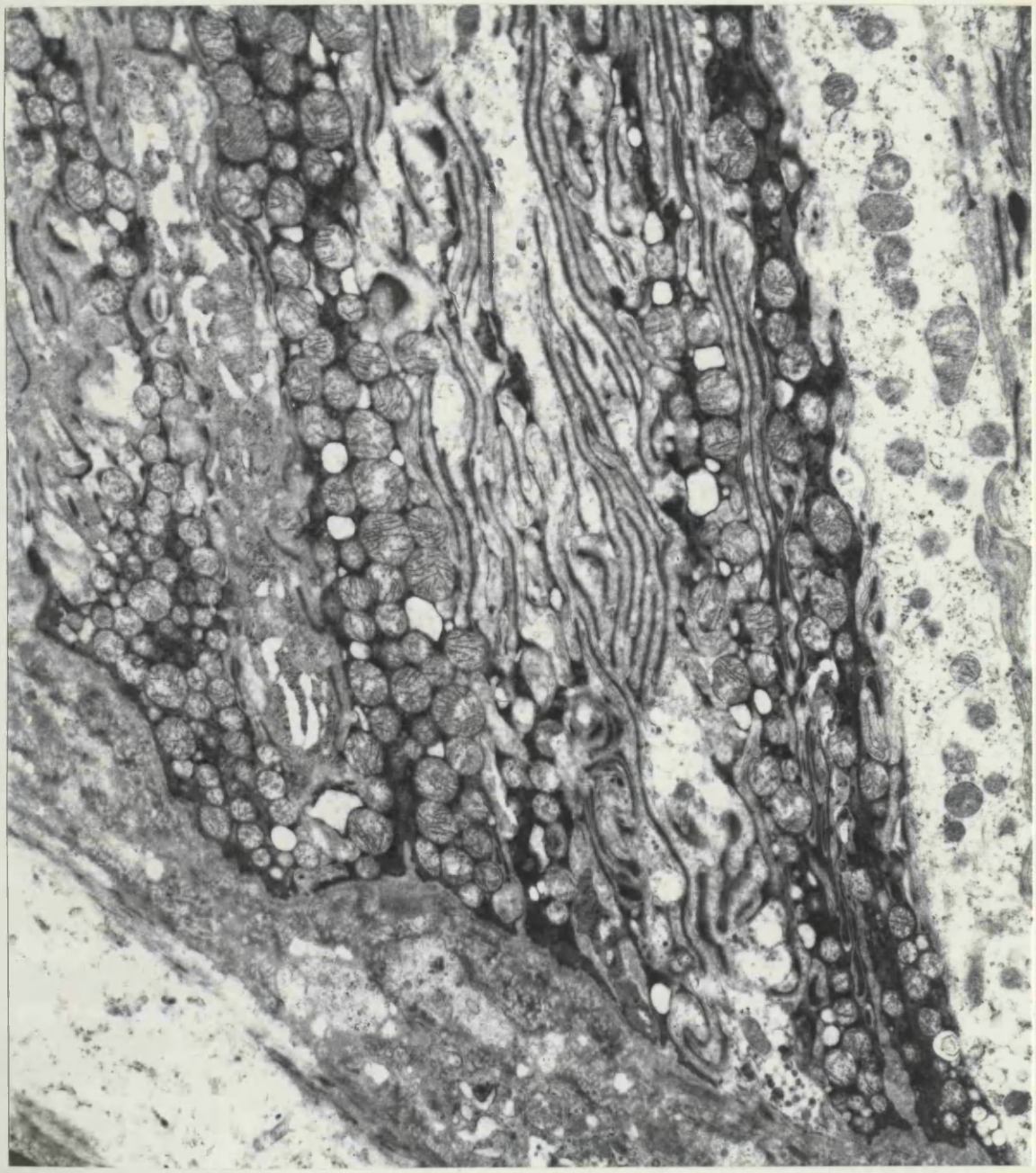

181

COLONIC TUMOURS

Figure 182. Villous papilloma. The cytoplasm of the dark cell has numerous mitochondria. A dark nucleus is also seen.

Magnification 17500

Figure 183. Villous papilloma. Basal region of dark cell showing the closely packed mitochondria and intracellular vacuoles.

Magnification 17500

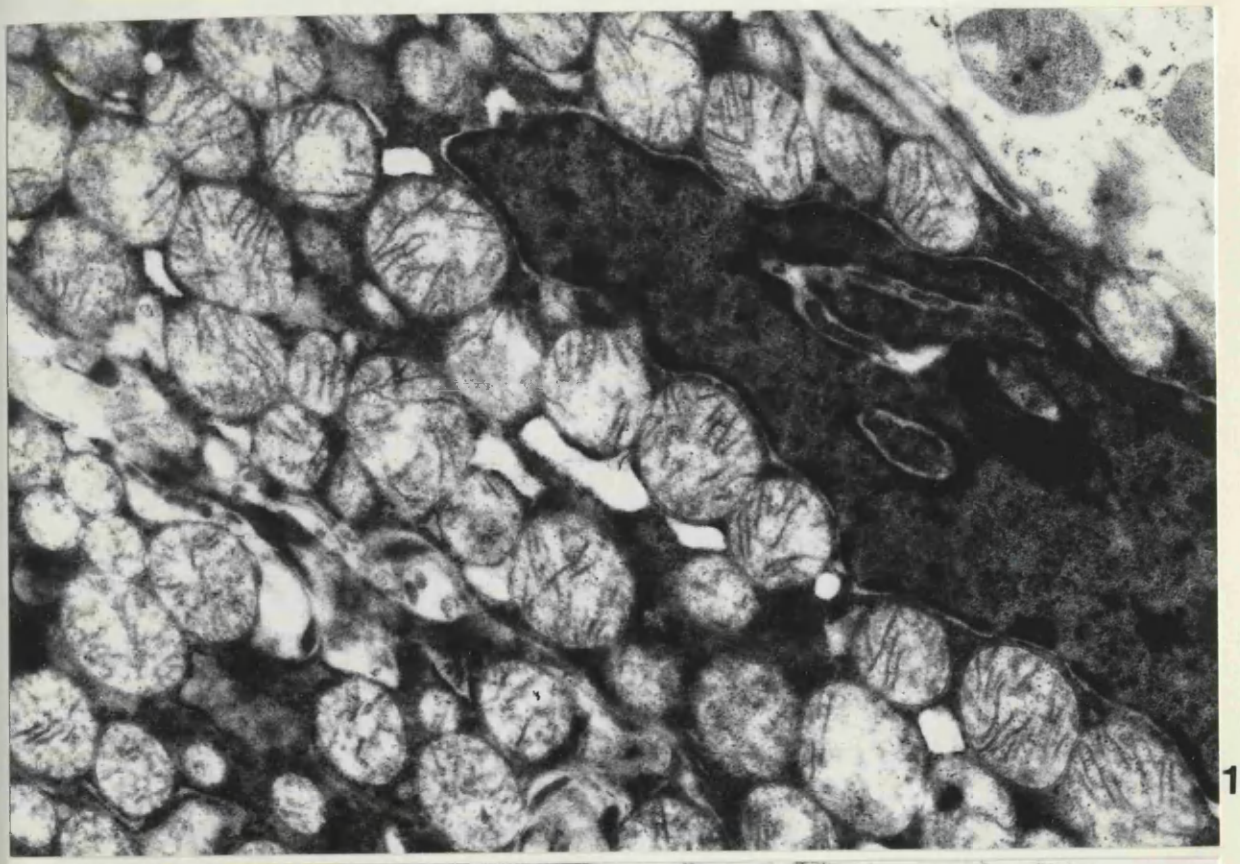

182

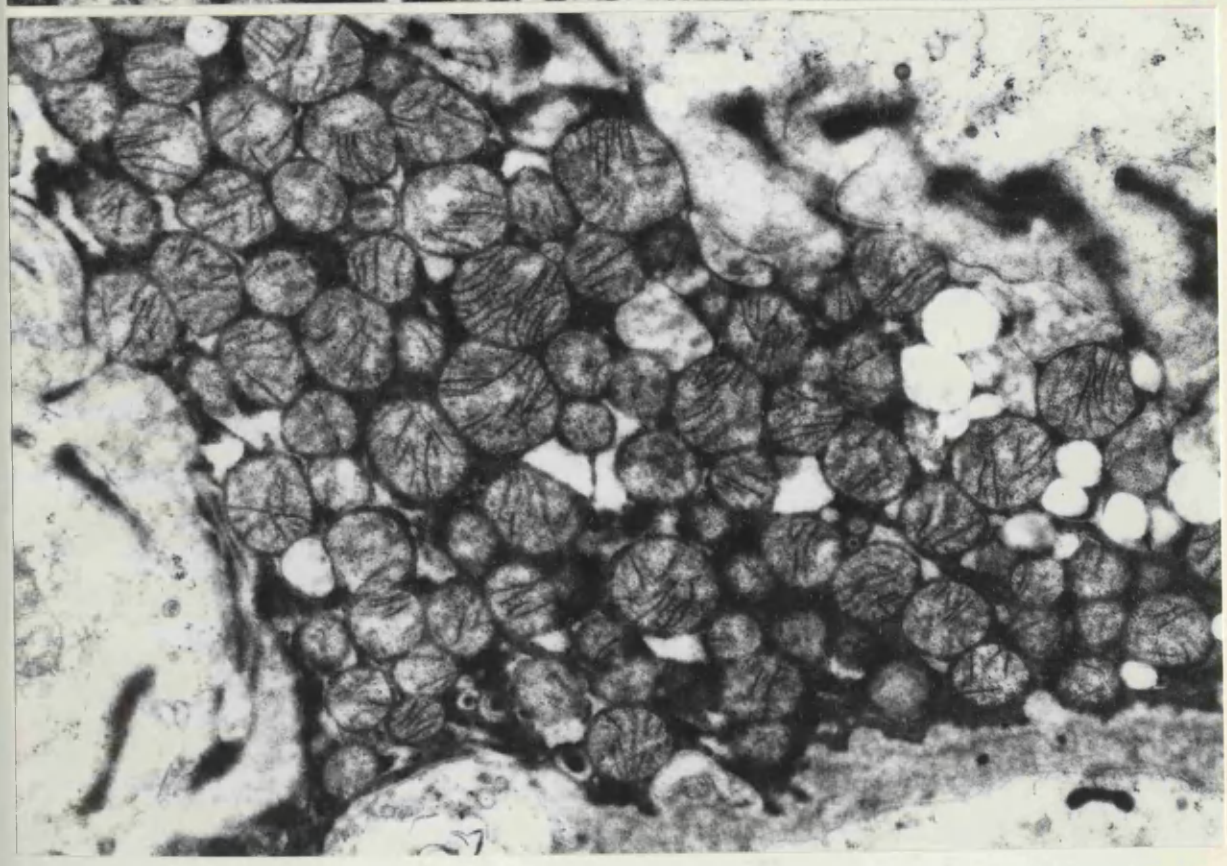

183

COLONIC TUMOURS

Figure 184. The histology of a typical case of well differentiated primary colonic carcinoma is shown.

Magnification 225

Figure 185. The histology of a typical case of well differentiated metastatic colonic carcinoma is seen.

Magnification 225

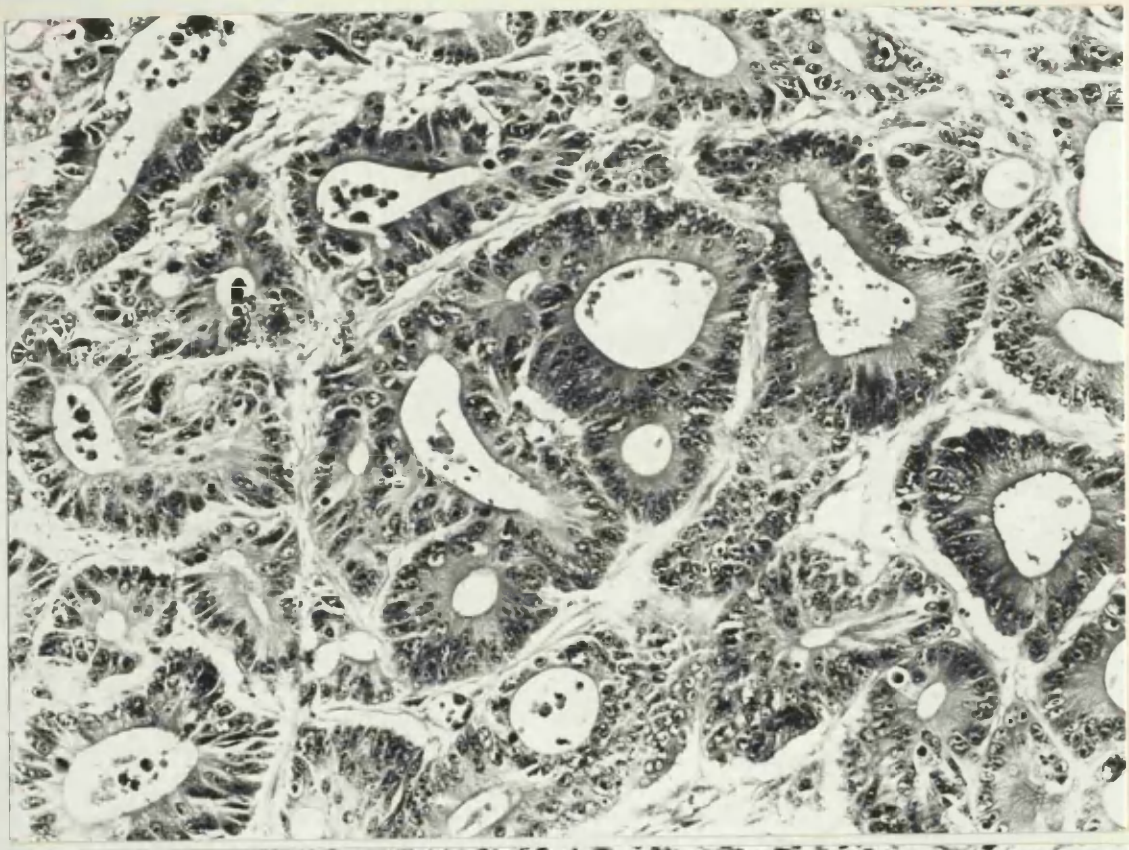

184

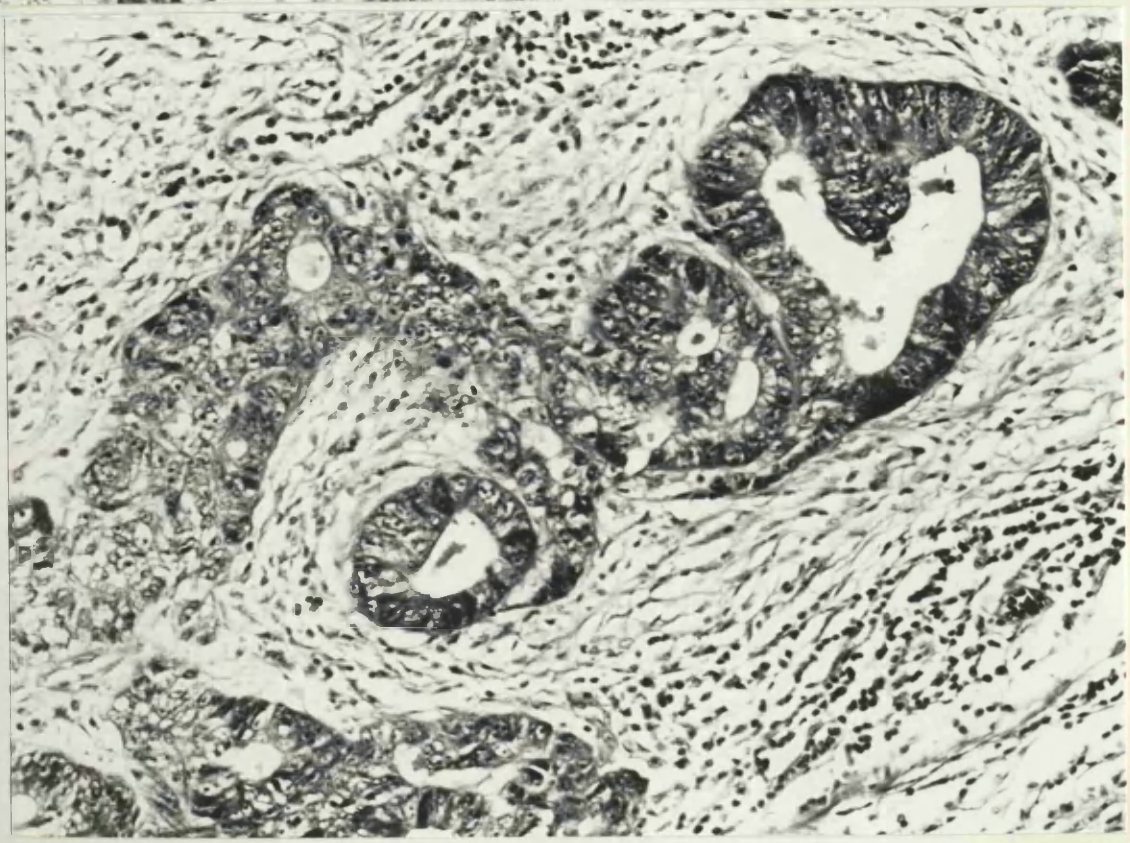

185

COLONIC TUMOURS

Figure 186. Well differentiated primary colonic carcinoma.

A group of neoplastic cells is arranged around a wide lumen. Their apical surfaces bear irregular microvilli. The lumen is seen to contain moderately dense material.

Magnification 6000

Figure 187. High magnification of the apex of a cell of well differentiated primary colonic carcinoma. This shows the typical microvilli and the intermicrovillous vesicles.

Magnification 39000

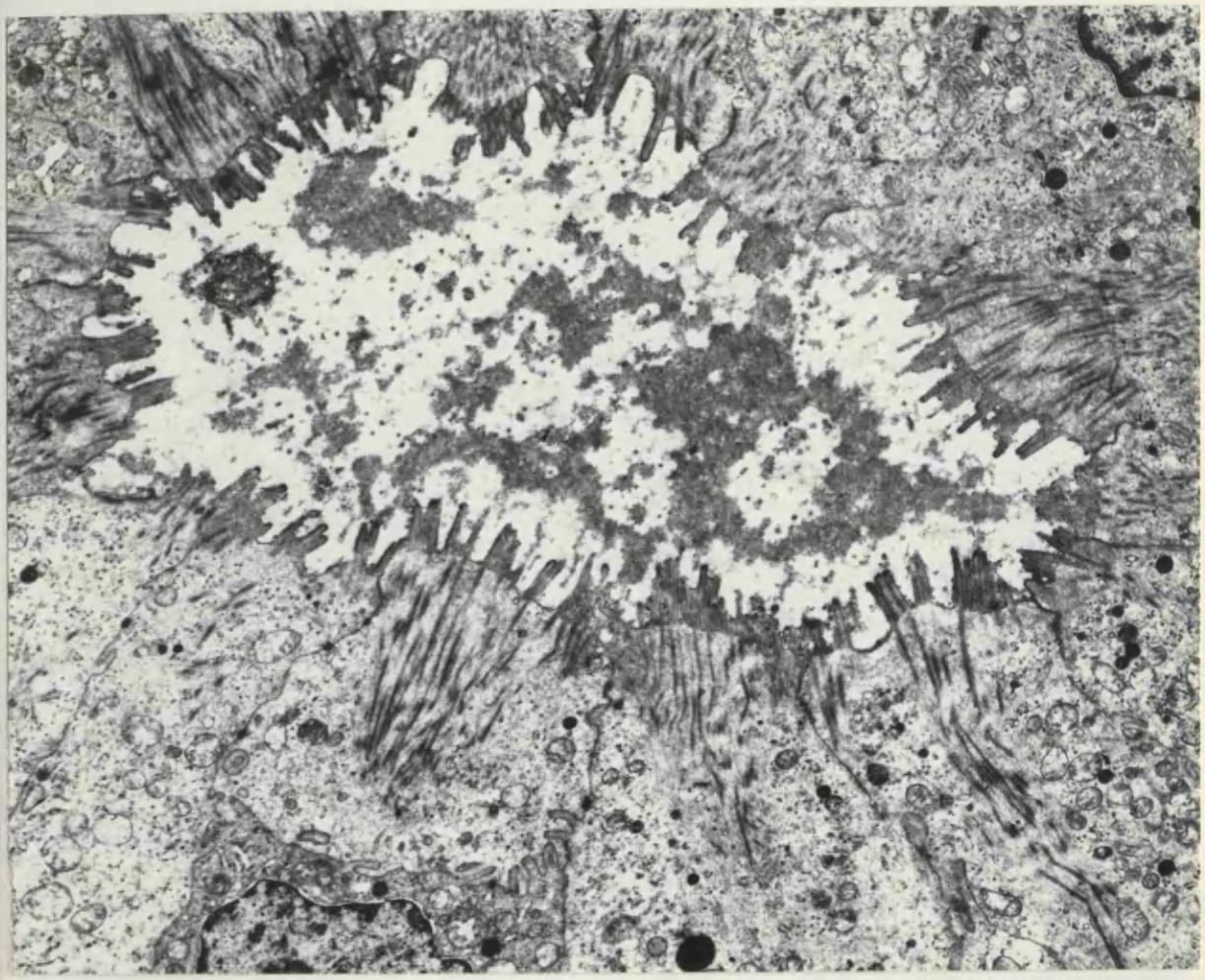

186

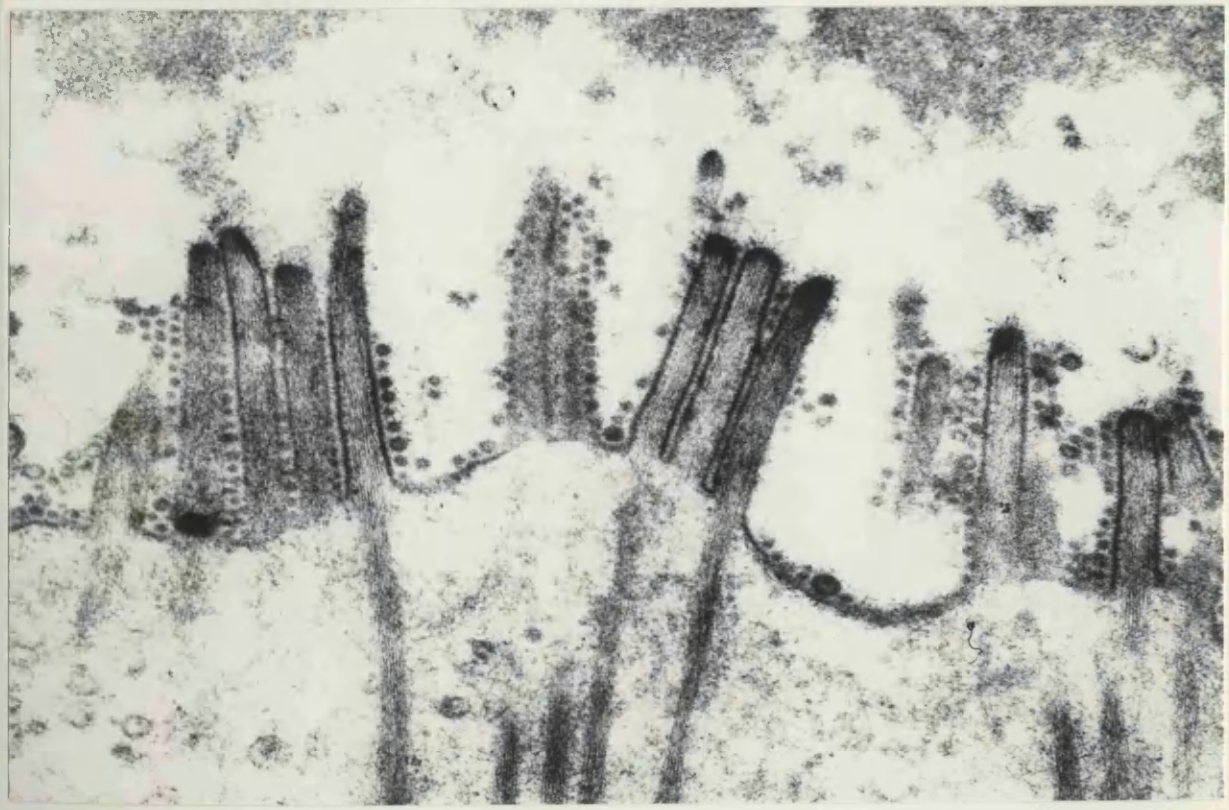

187

COLONIC TUMOURS

Figure 188. Well differentiated primary colonic carcinoma.

Apical regions of cancer cells show lateral interdigitations, numerous cytoplasmic dense bodies and a small Golgi apparatus(G).

Magnification 12900

Figure 189. Well differentiated primary colonic carcinoma.

The neoplastic cells rest on a continous basal lamina, heaped on each other with pseudostratification.

Magnification 8600

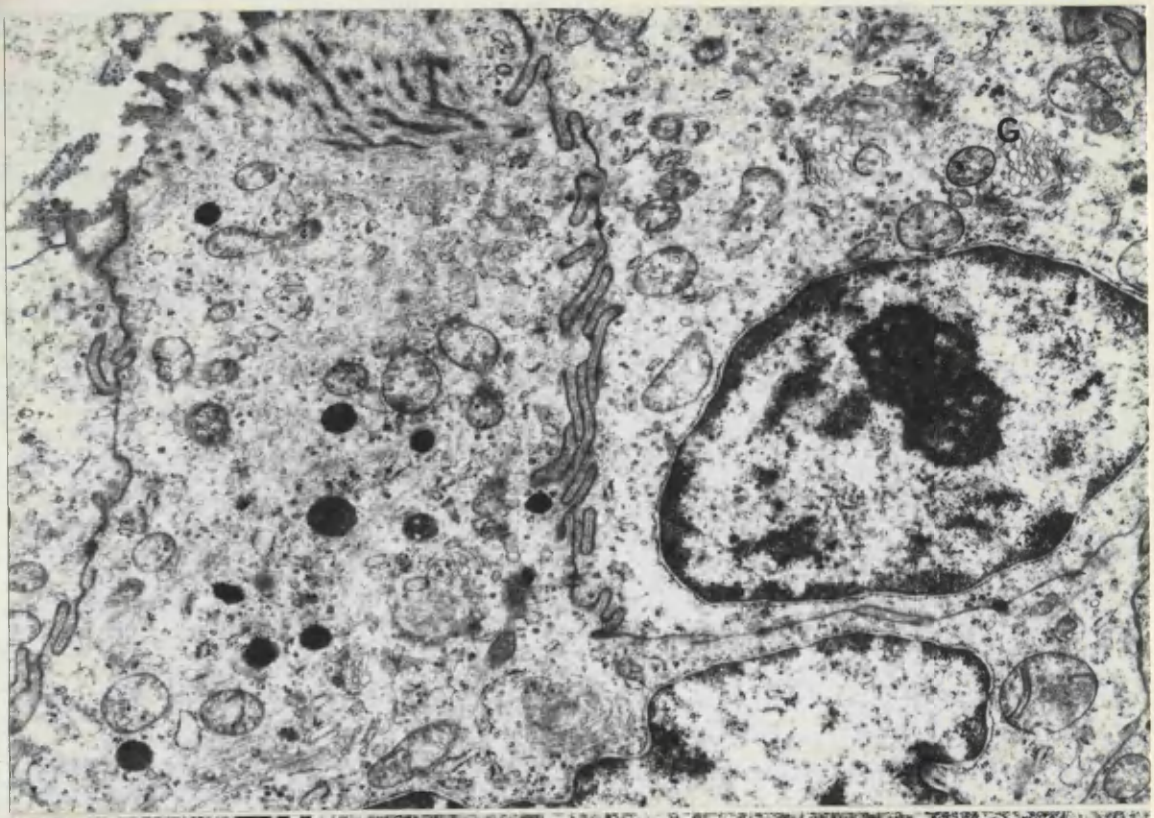

188

189

COLONIC TUMOURS

Figure 190. Well differentiated primary colonic carcinoma.

A large cancer cell with segmented nucleus is shown.

Magnification 3360

Figure 191. Well differentiated primary colonic carcinoma.

Pseudopodial cytoplasmic protrusions(P) from cancer cells are seen to project through the basal lamina into the stroma(S).

Magnification 13800

190

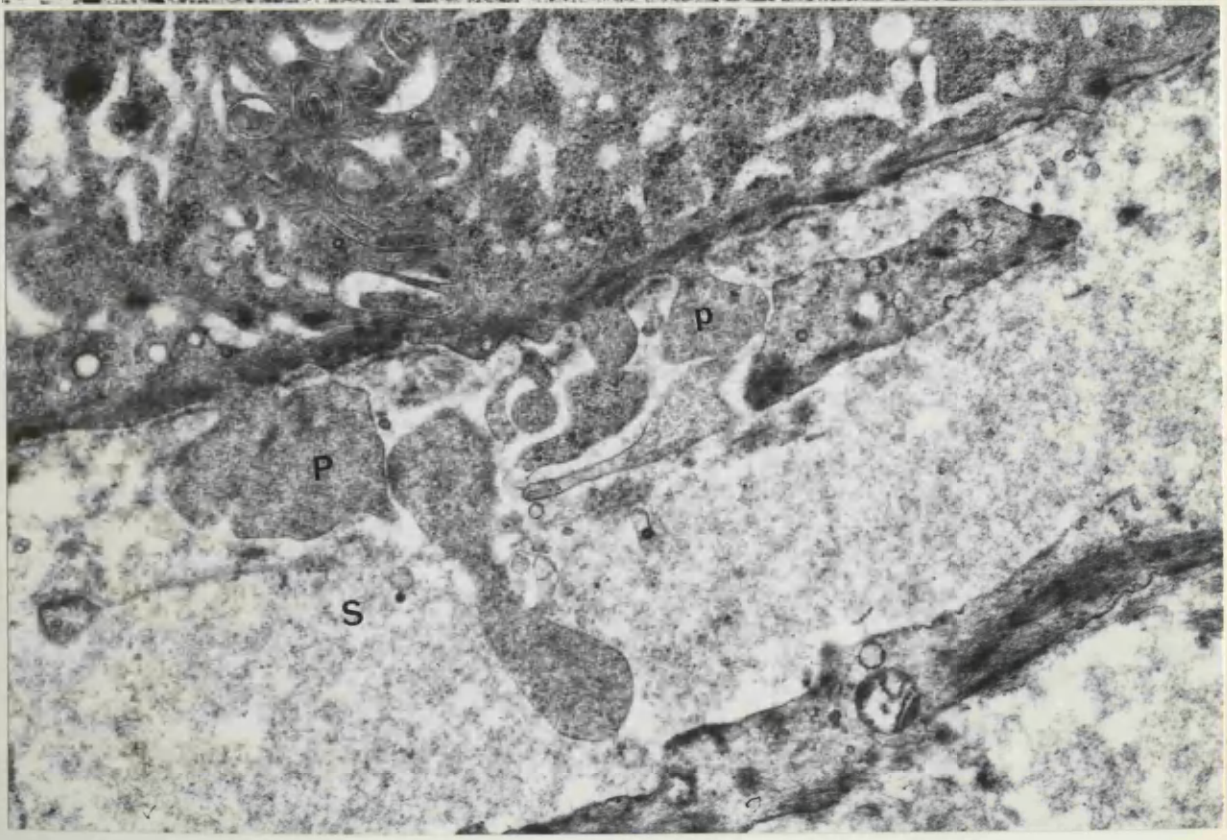

191

COLONIC TUMOURS

Figure 192. Well differentiated primary colonic carcinoma.

A bizarre-shaped nucleolus with several holes is shown.

Magnification 30500

Figure 193. Well differentiated primary colonic carcinoma.

Apical regions of cancer cells showing numerous doughnut-like inclusions.

Magnification 32500

Figure 194. Well differentiated primary colonic carcinoma.

Doughnut-like inclusions and membrane-limited vesicles are seen.

Magnification 88250

192

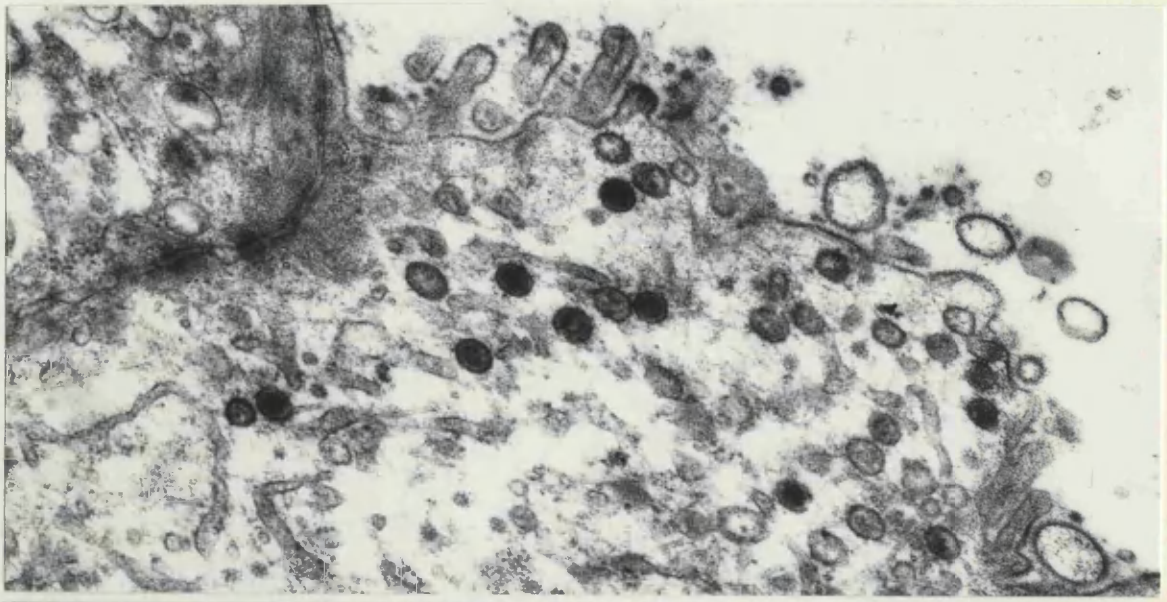

193

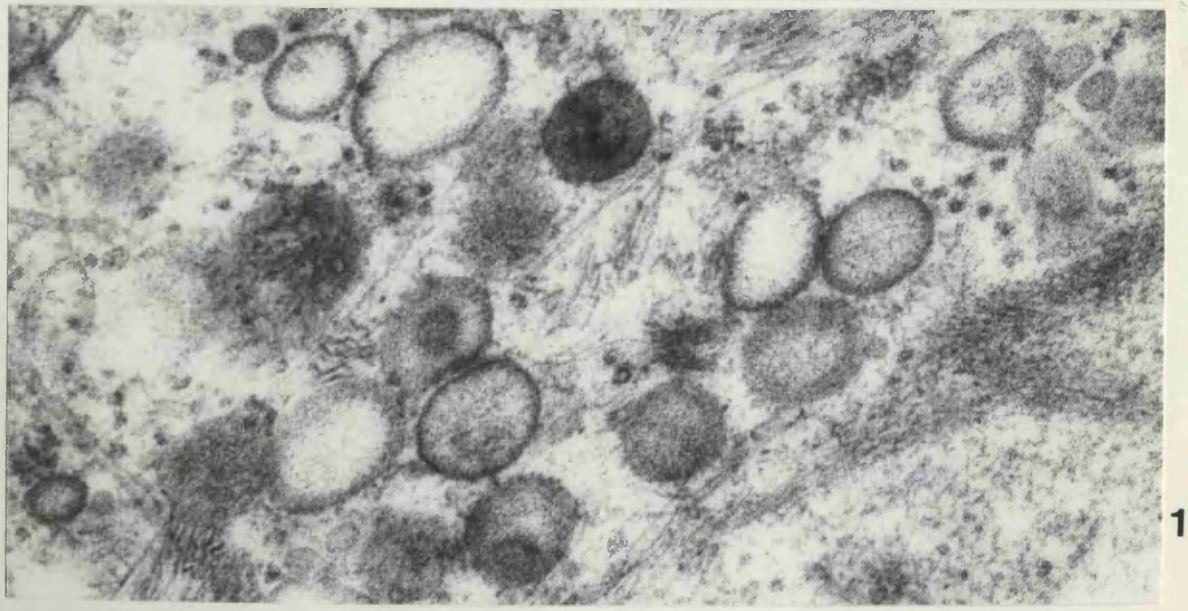

194

COLONIC TUMOURS

Figure 195. Well differentiated primary colonic carcinoma.

A network of tubular structures is seen to be continous with the granular endoplasmic reticulum.

Magnification 95200

Figure 196. Well differentiated primary colonic carcinoma.

Another network of tubular structures is shown.

Magnification 41000

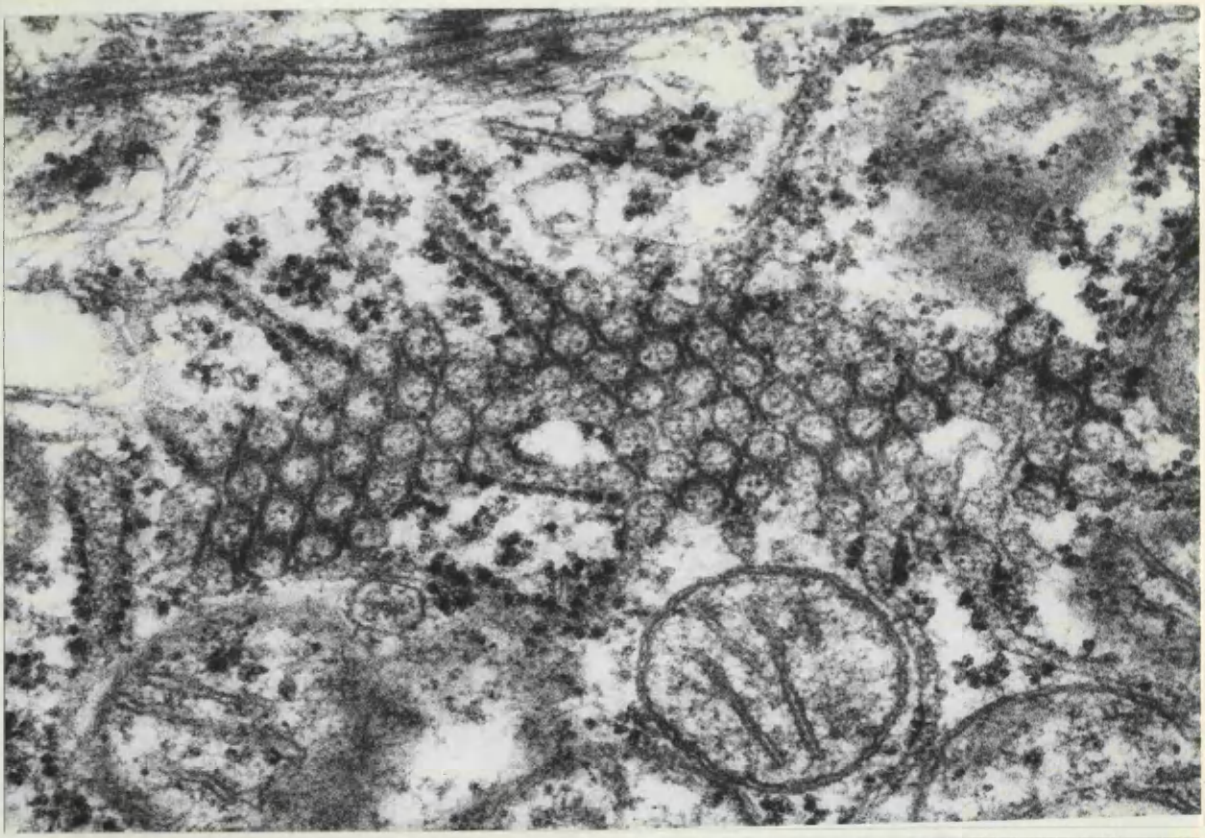

195

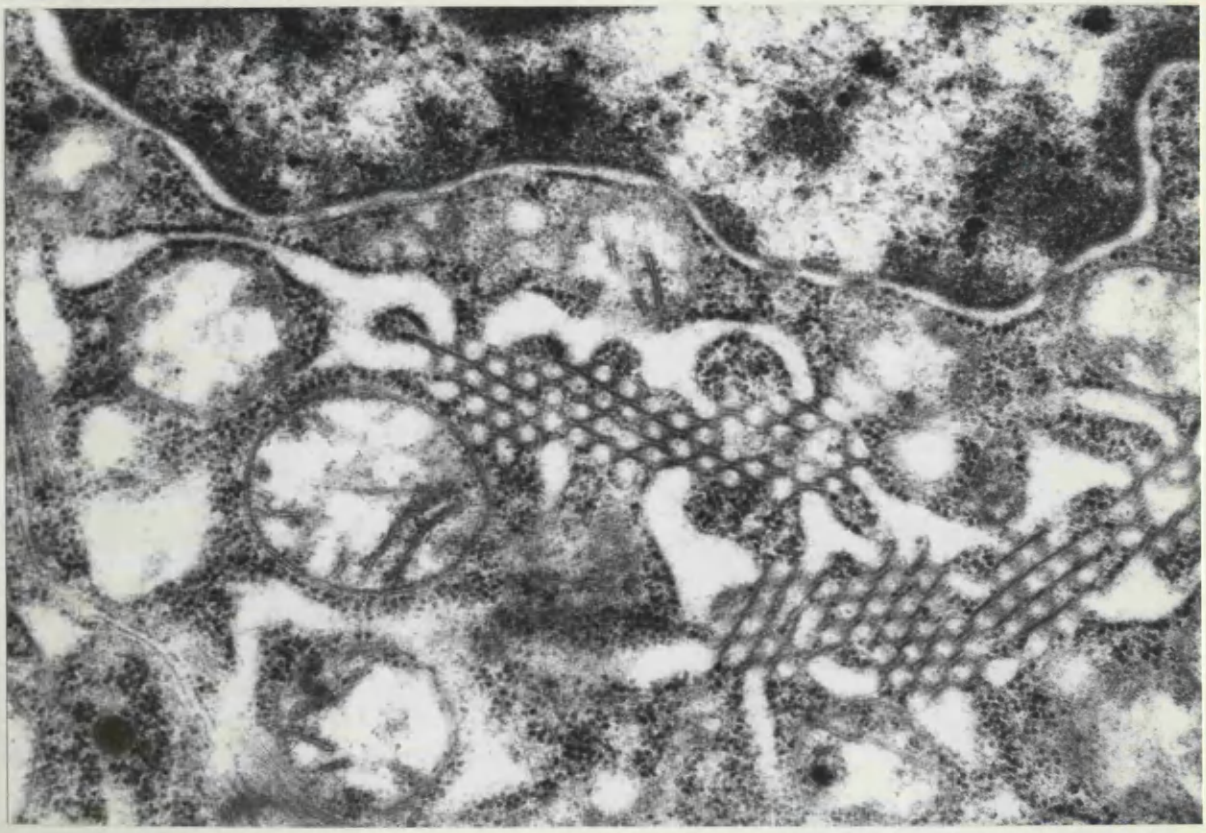

196

COLONIC TUMOURS

Figure 197 . Well differentiated primary colonic carcinoma.

Nuclear invagination has produced a channel of cytoplasm leading to three prominent nucleoli.

Magnification 10750

Figure 198. Well differentiated primary colonic carcinoma.

An island of cytoplasm is stranded within the nucleus. Two prominent nucleoli are seen to lie in contact with the cytoplasmic island.

Magnification 22750

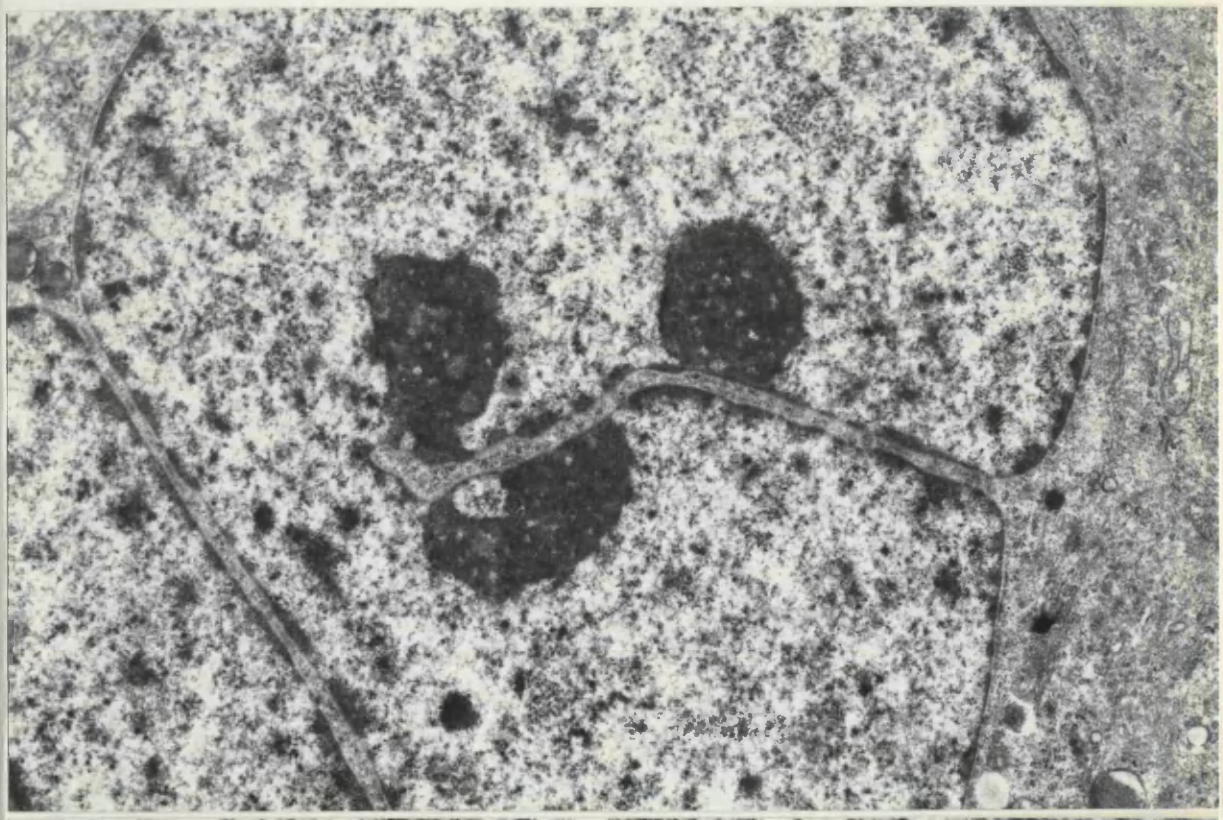

197

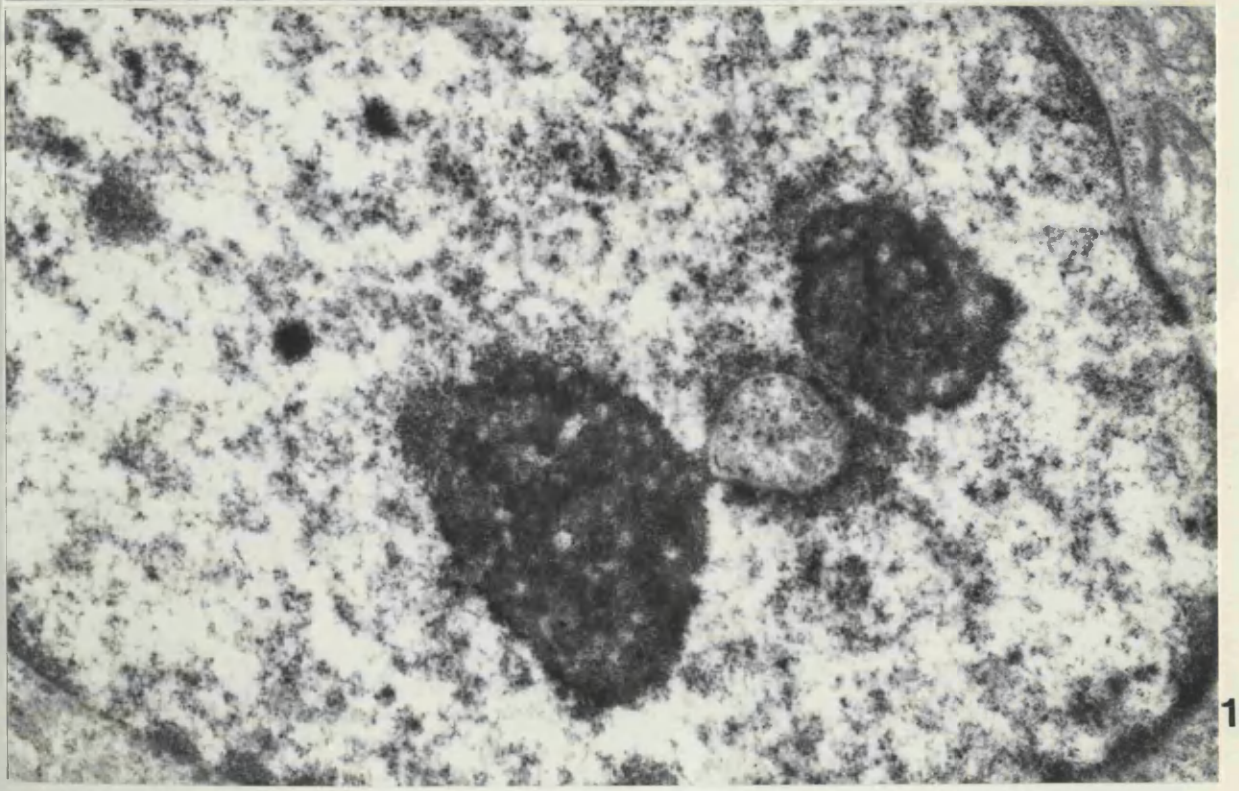

198

COLONIC TUMOURS

Figure 199. Well differentiated primary colonic carcinoma.

The cytoplasm contains numerous ribosomes and membrane-limited heterogeneous dense inclusions.

Magnification 22750

Figure 200. Poorly differentiated primary colonic carcinoma.

Light and dark cells are seen. The light cells are predominant. The few dark cells seen in the left upper corner of the micrograph have dark nuclei.

Magnification 6720

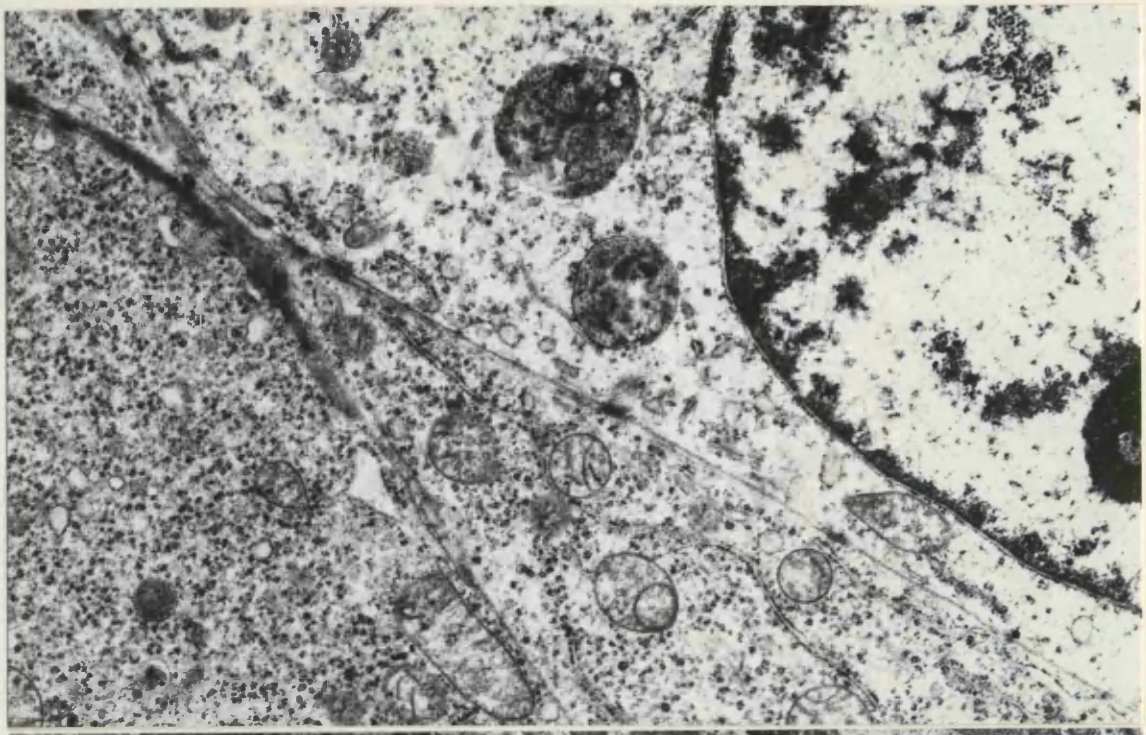

199

200

COLONIC TUMOURS

Figure 201A. The histology of a typical case of poorly differentiated primary colonic carcinoma is shown.

Magnification 225

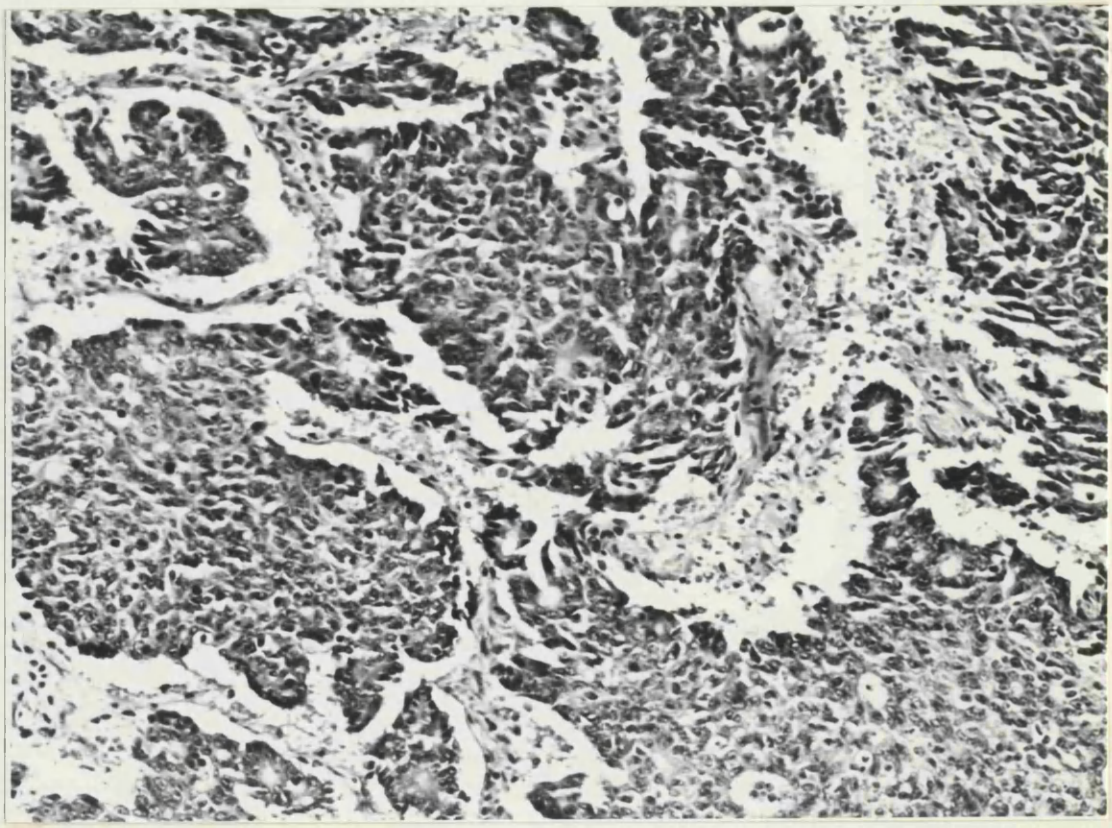

201A

COLONIC TUMOURS

Figure 201. Poorly differentiated primary colonic carcinoma. The apical regions of cancer cells are shown. The neoplastic cells are connected by typical desmosomes (D). Note the lumen(L) of the gland.

Magnification 8600

Figure 202. Poorly differentiated primary colonic carcinoma. The basal regions of the neoplastic cells are shown. The cells rest on a basal lamina.

Magnification 10750

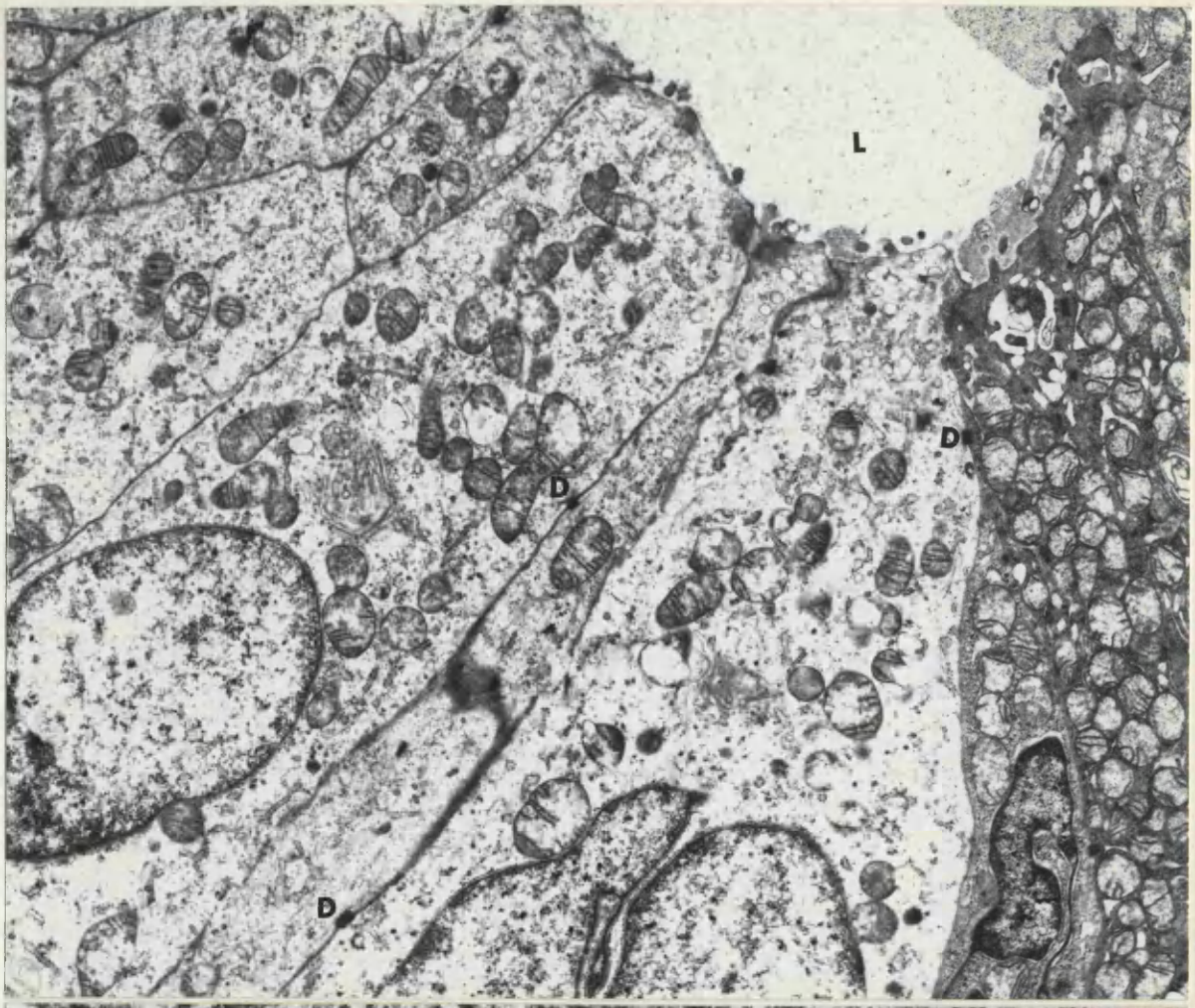

201

202

COLONIC TUMOURS

Figure 203. Well differentiated metastatic colonic carcinoma. The cells are columnar in shape and have basally situated nuclei. Their apices bear short irregular microvilli.

Magnification 8600

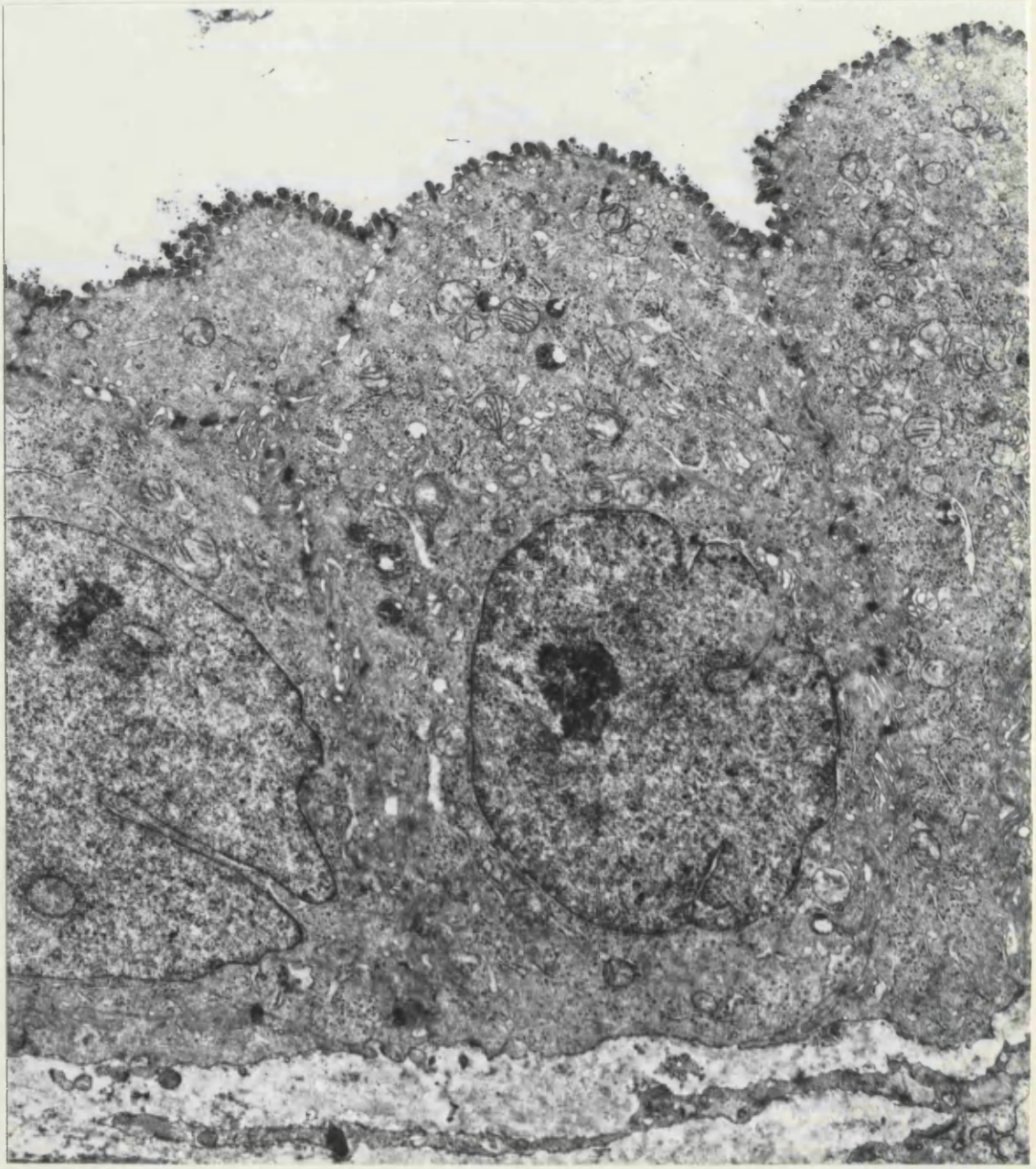

203

COLONIC TUMOURS

Figure 204. Well differentiated metastatic colonic carcinoma.

There are numerous small vesicles between the microvilli and in the lumen. Notice the mitochondria and membrane-limited vesicles in the apical cytoplasm.

Magnification 22750

Figure 205. Well differentiated metastatic colonic carcinoma.

The basal regions of the cells show aggregates of mitochondria.

Magnification 17500

Figure 206. Well differentiated metastatic colonic carcinoma .

Two channels of cytoplasm lead to a prominent nucleolus.

Magnification 17500

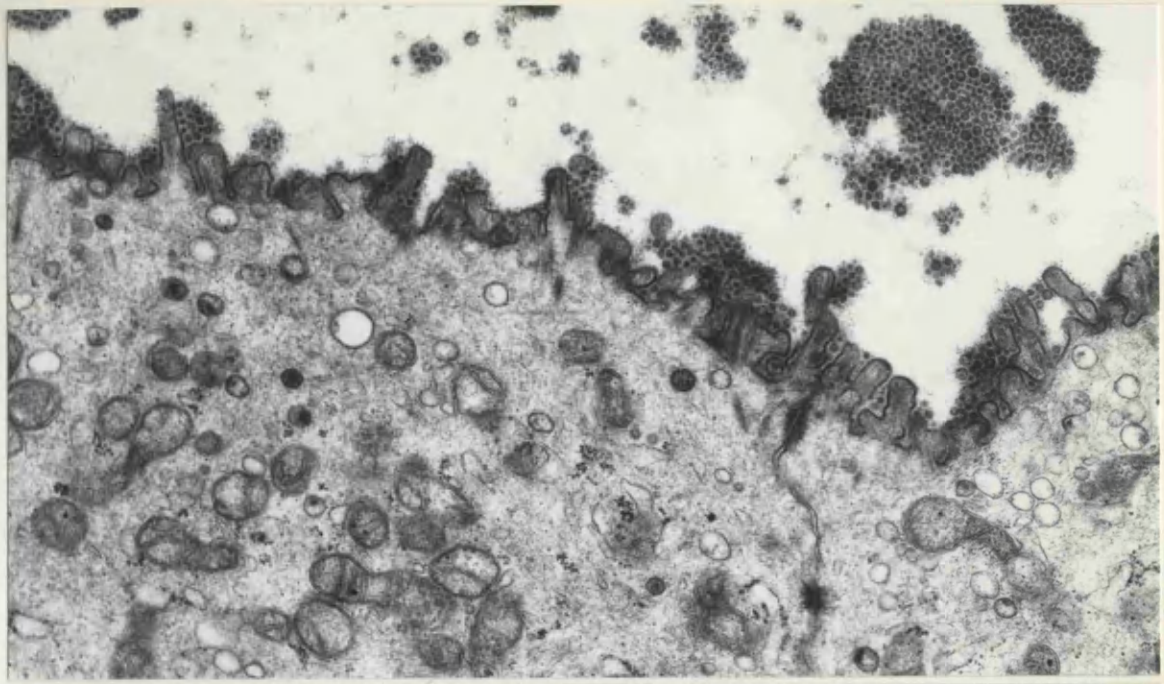

204

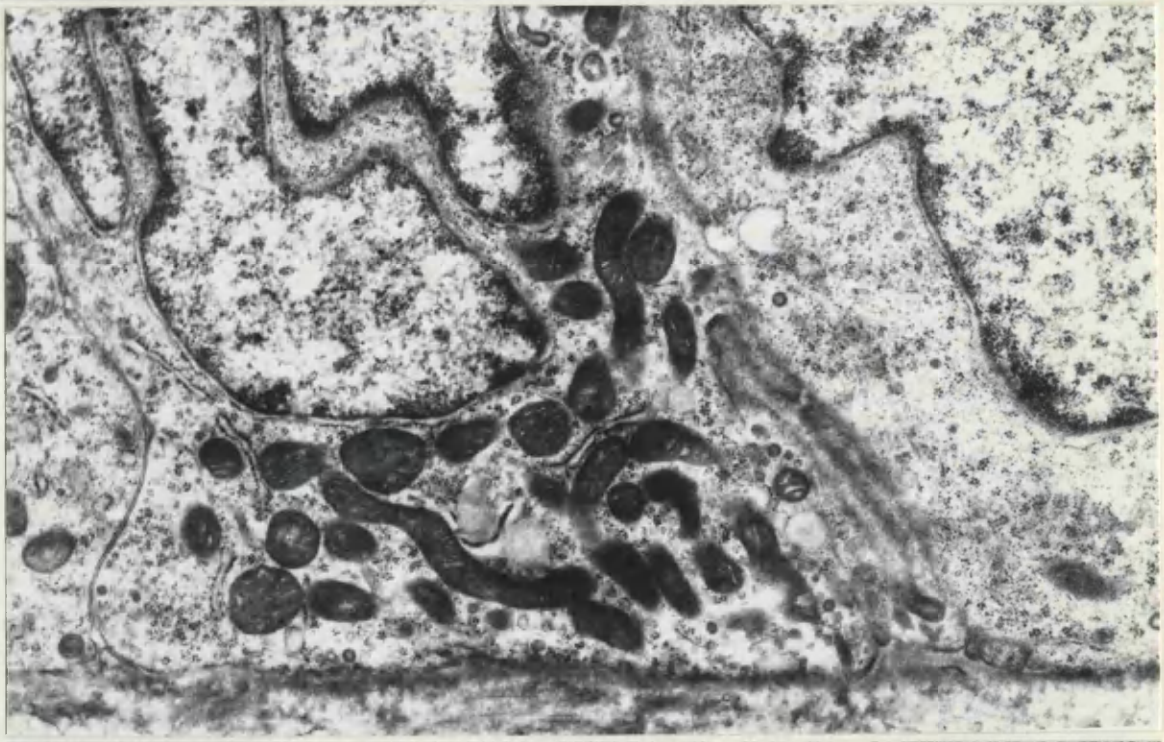

205

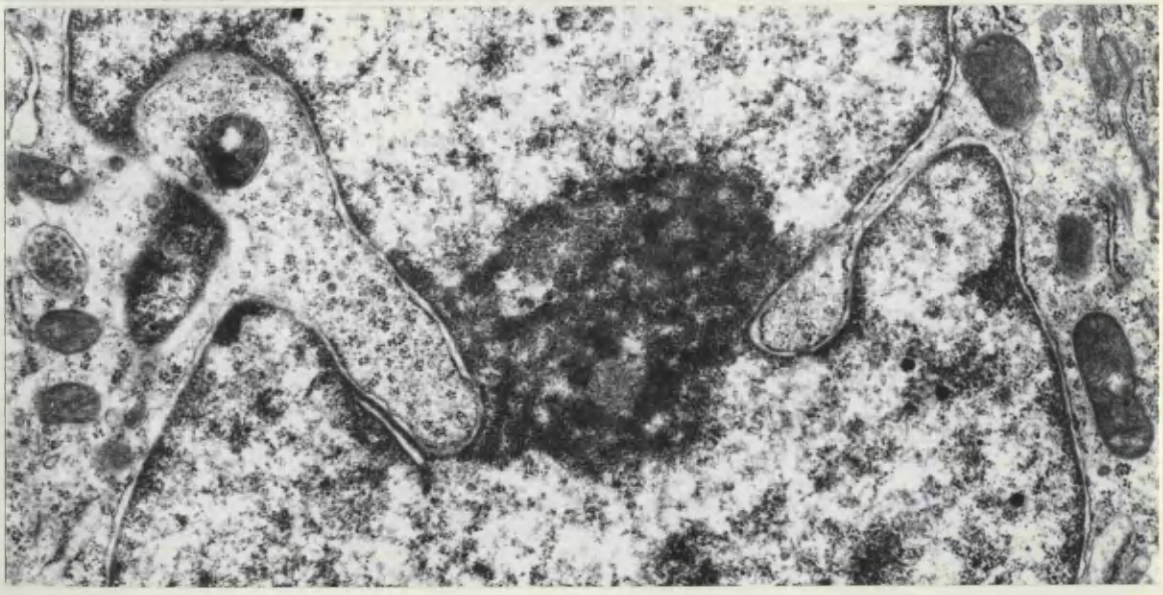

206

COLONIC TUMOURS

Figure 207. Well differentiated metastatic colonic carcinoma.

The lumen of the gland contains moderately dense material and assorted cellular debris.

Magnification 17500

Figure 208. Well differentiated metastatic colonic carcinoma.

Dense deposits of carbohydrate staining are seen in the cytoplasmic vesicles, fuzzy coat and the moderately dense luminal material shown in figure 207.

Magnification 31200

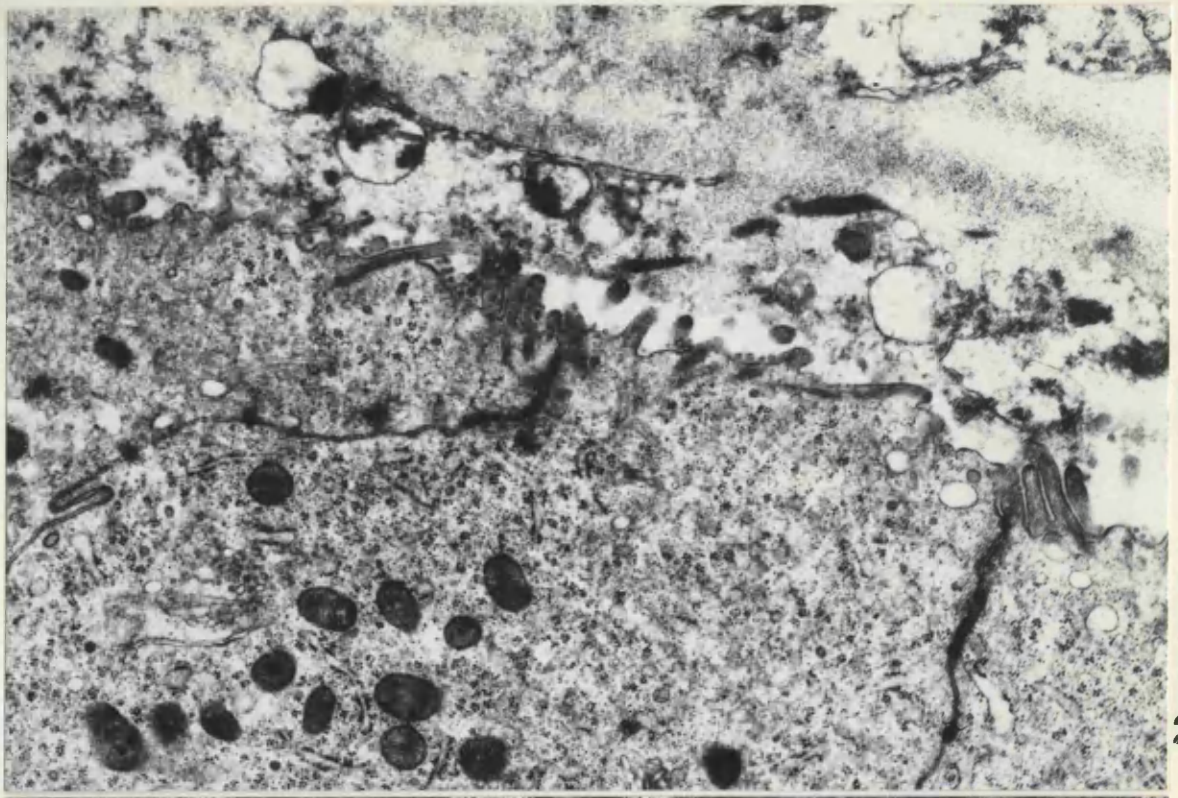

207

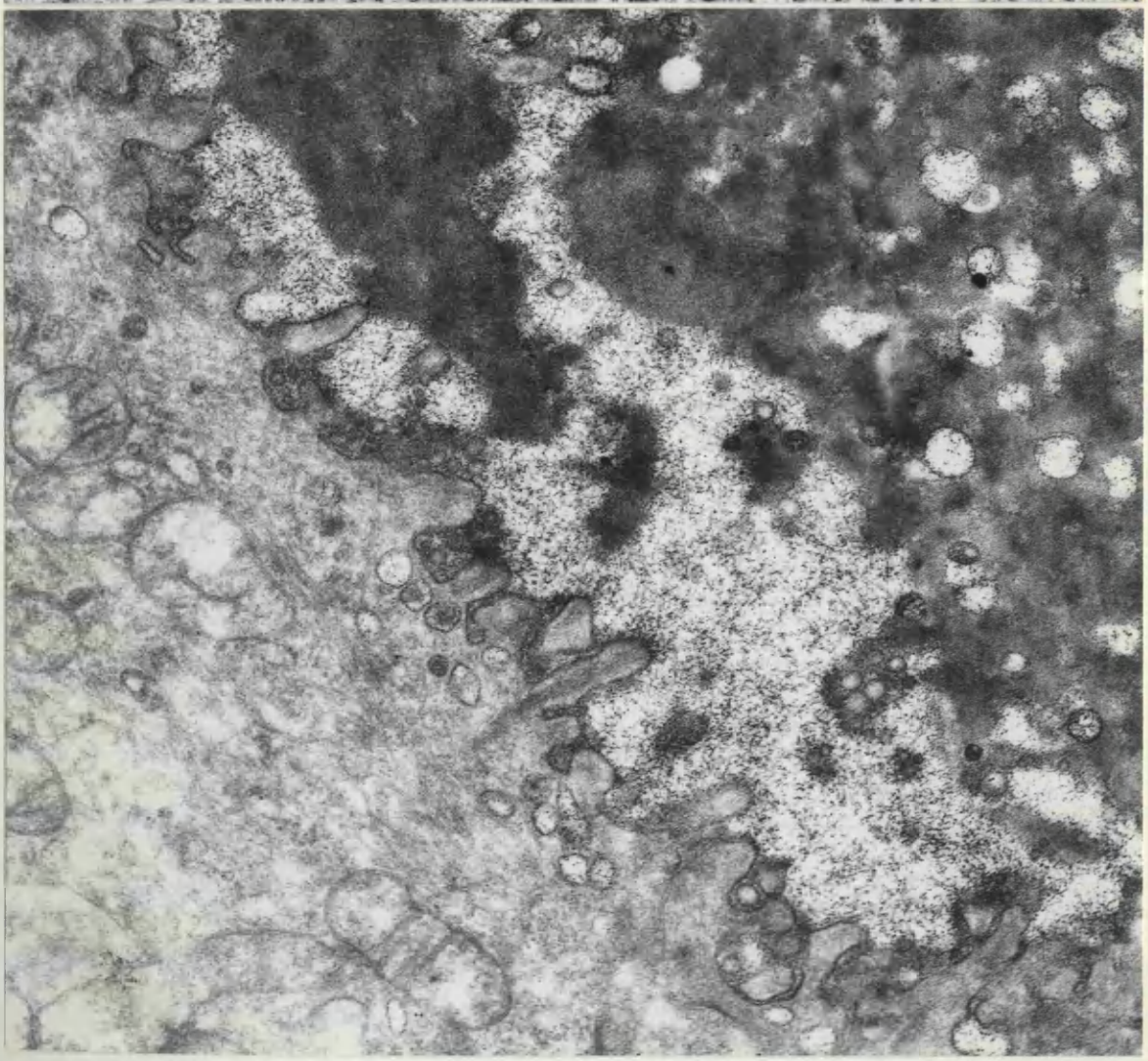

208

COLONIC TUMOURS

Figure 209. Carbohydrate-staining of normal colonic mucosa shows fine granular dense deposits in the fuzzy coat and cytoplasmic vesicles.

Magnification 51250

Figure 210. Positive carbohydrate staining is shown in the fuzzy coat of primary colonic carcinoma.

Magnification 88250

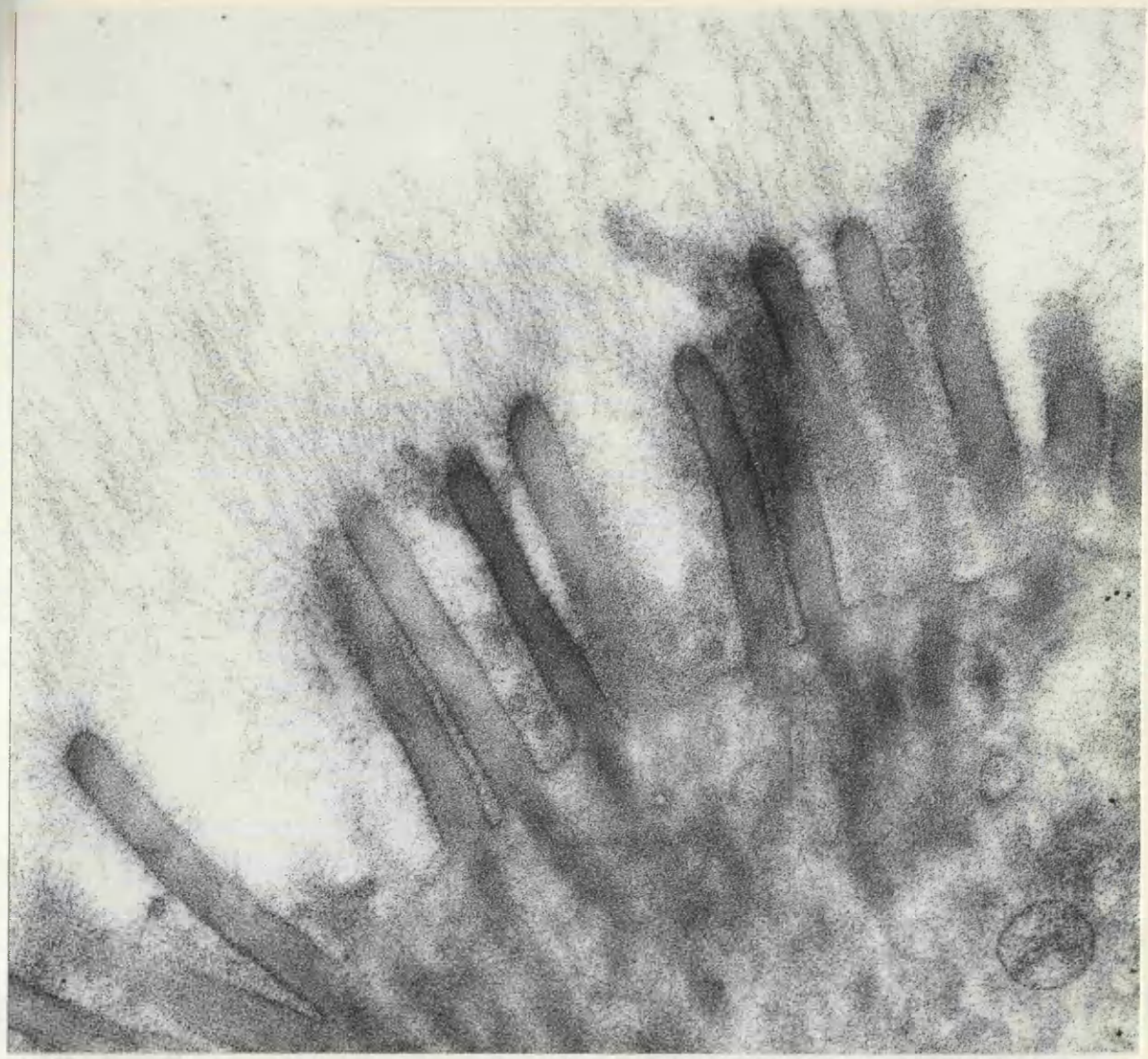

209

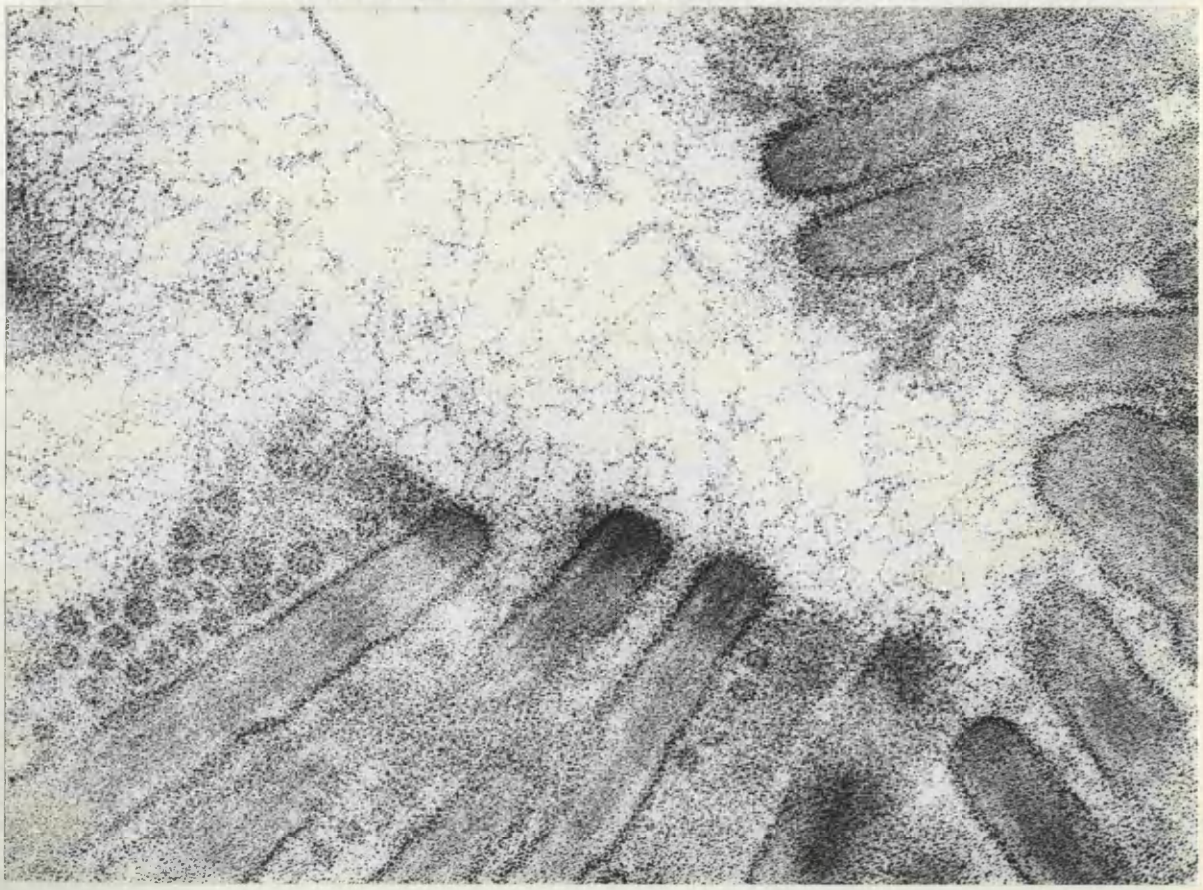

210

COLONIC TUMOURS

Figure 211. Positive carbohydrate-staining in the membrane-limited vesicles of colonic carcinoma.

Magnification 61500

Figure 212. Positive carbohydrate-staining is also seen in the doughnut-like inclusions of colonic carcinoma.

Magnification 39000

Figure 213. Positive carbohydrate-staining is again shown in the doughnut-like inclusions of primary colonic carcinoma.

Magnification 51250

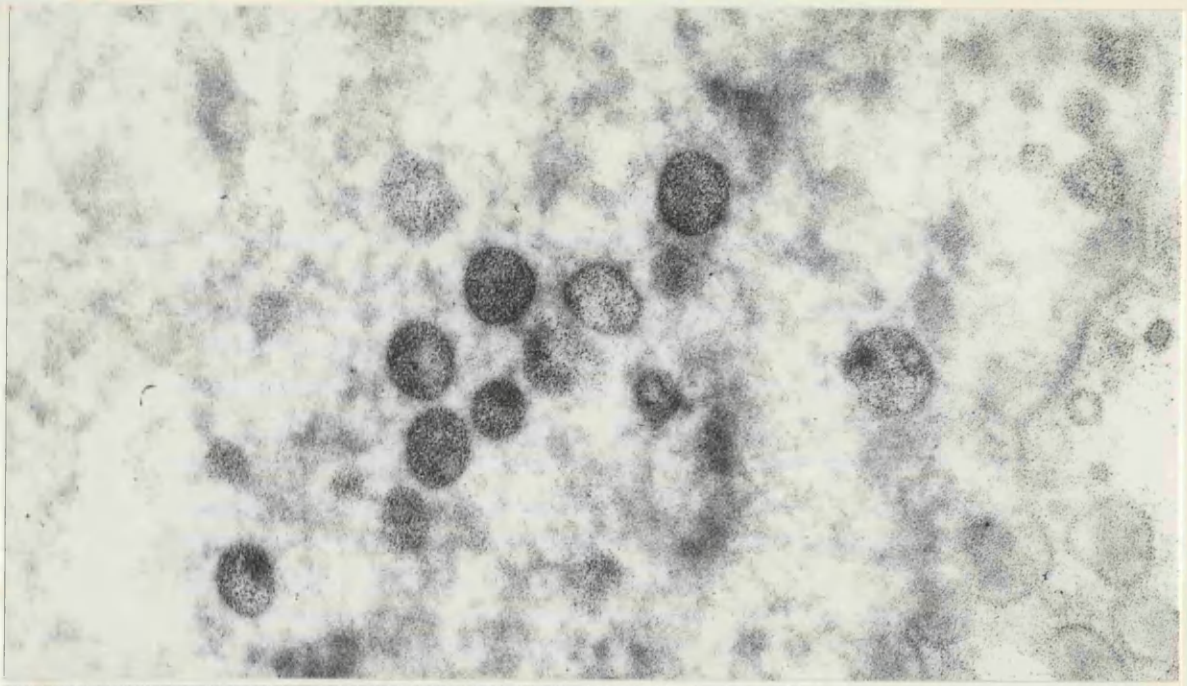

211

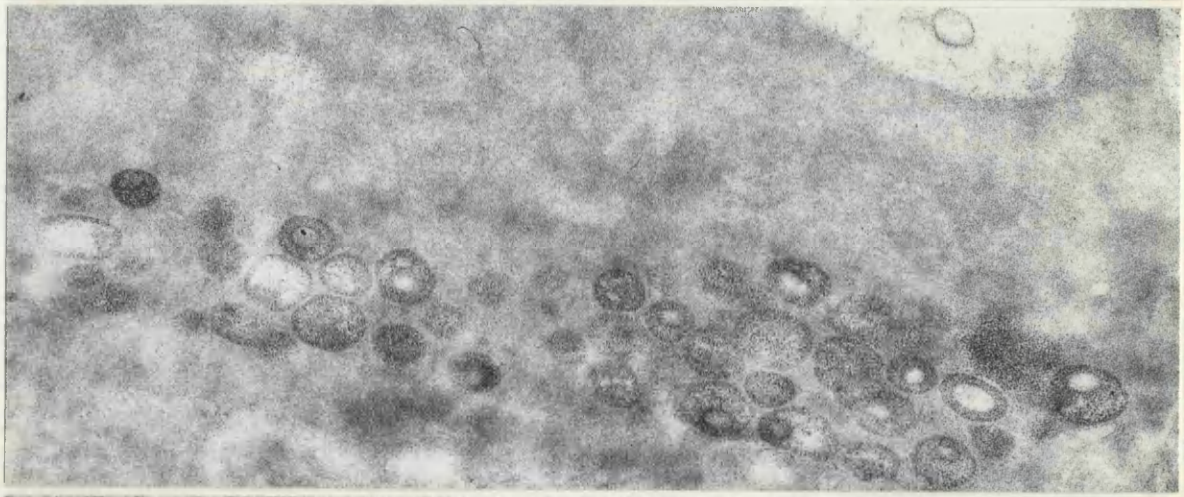

212

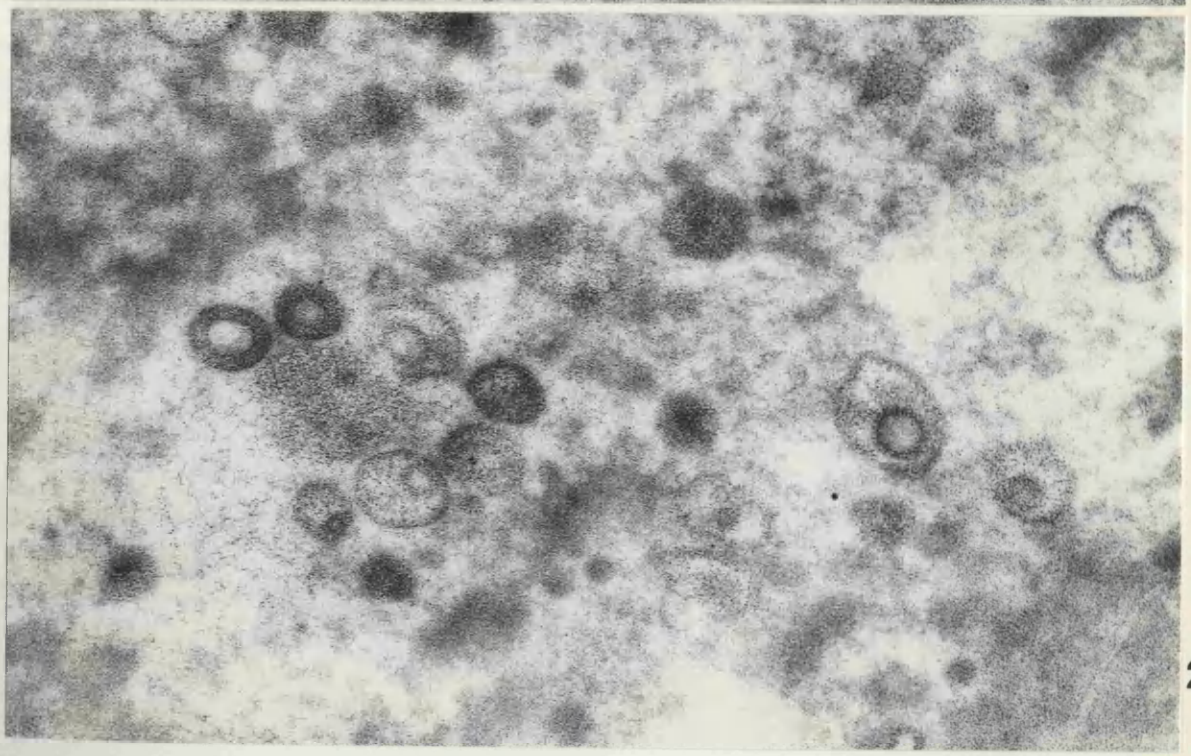

213

COLONIC TUMOURS

Figure 214. Positive acid phosphatase activity is shown in the small dense bodies of colonic carcinoma.

Magnification 22750

Figure 215. Acid phosphatase activity in the dense inclusions of colonic carcinoma.

Magnification 22750

Figure 216. Two heterogeneous bodies showing acid phosphatase activity are seen in colonic carcinoma.

Magnification 27300

Figure 217. Colonic carcinoma. Positive acid phosphatase activity is seen in a large heterogeneous inclusion.

Magnification 27300

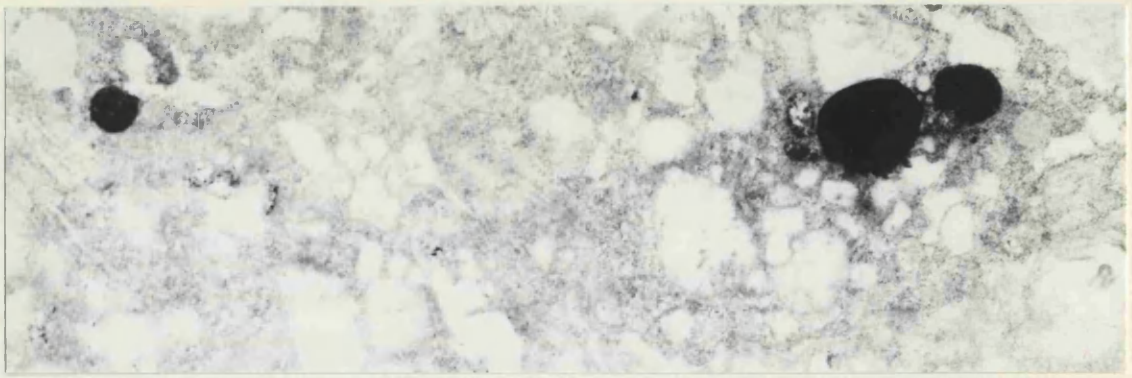

214

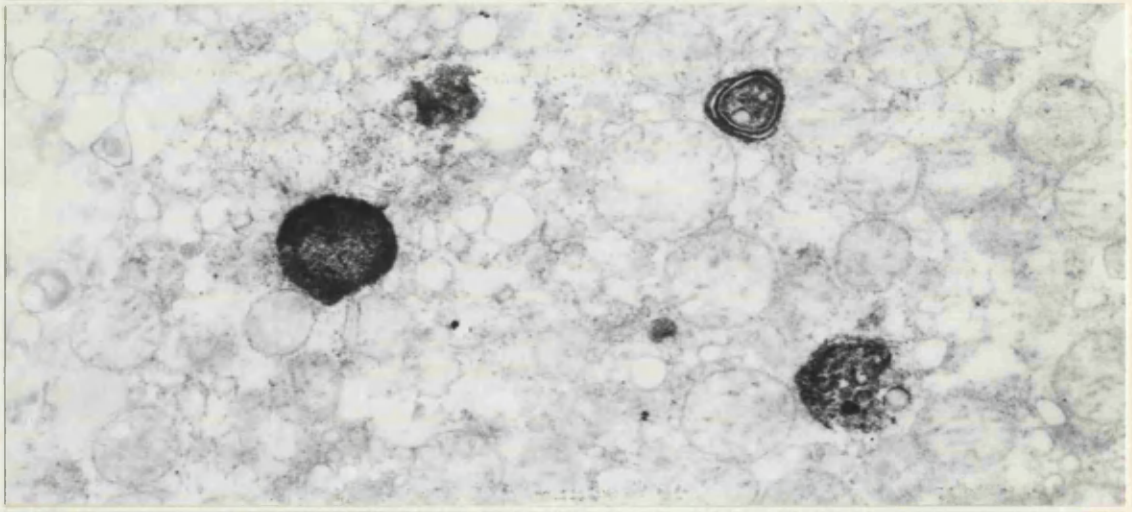

215

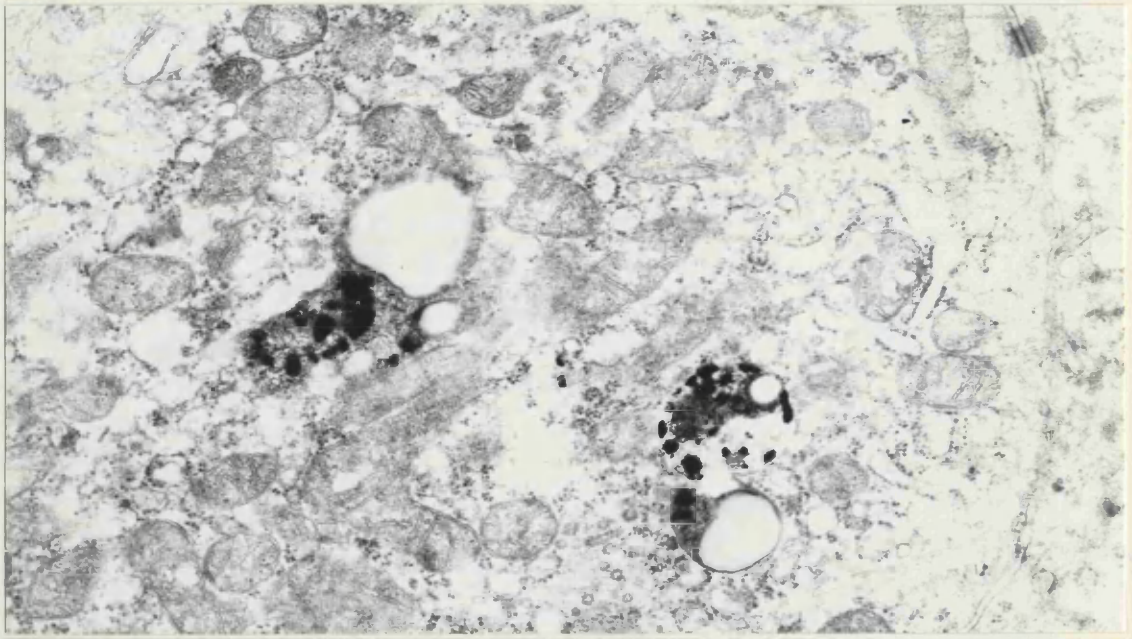

216

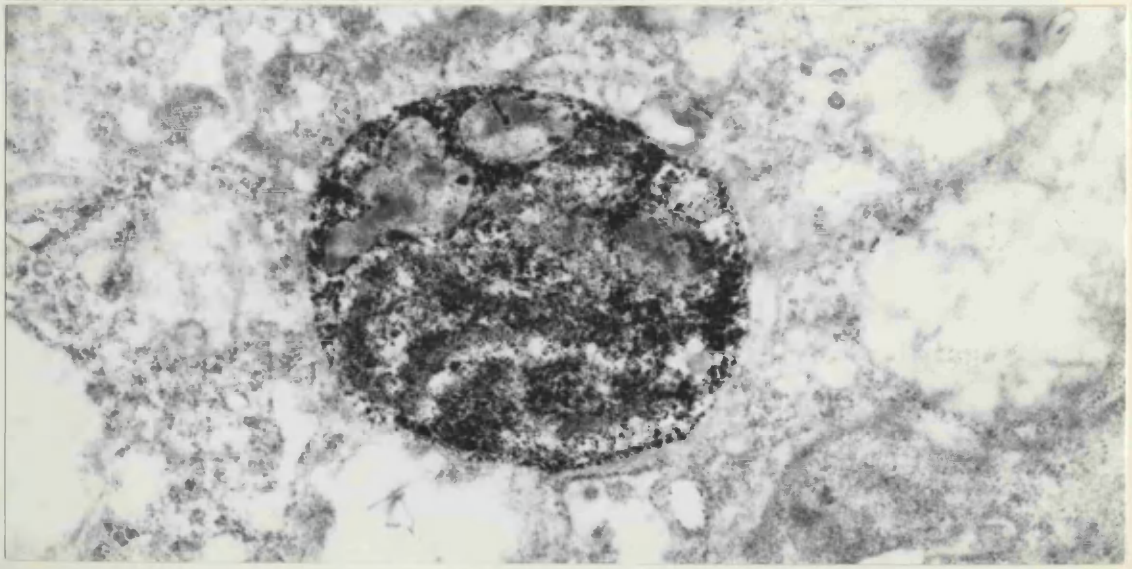

217

Figure 218. Nuclear body from normal epithelial cell of small intestine. It consists of microfibrillar material.

Magnification 88250

Figure 219. Microfibrillar nuclear body from squamous epithelium of oesophagus. Notice the clear halo which separates the nuclear body from the surrounding chromatin.

Magnification 88250

Figure 220. A microfibrillar nuclear body from colonic mucosa is shown.

Magnification 88250

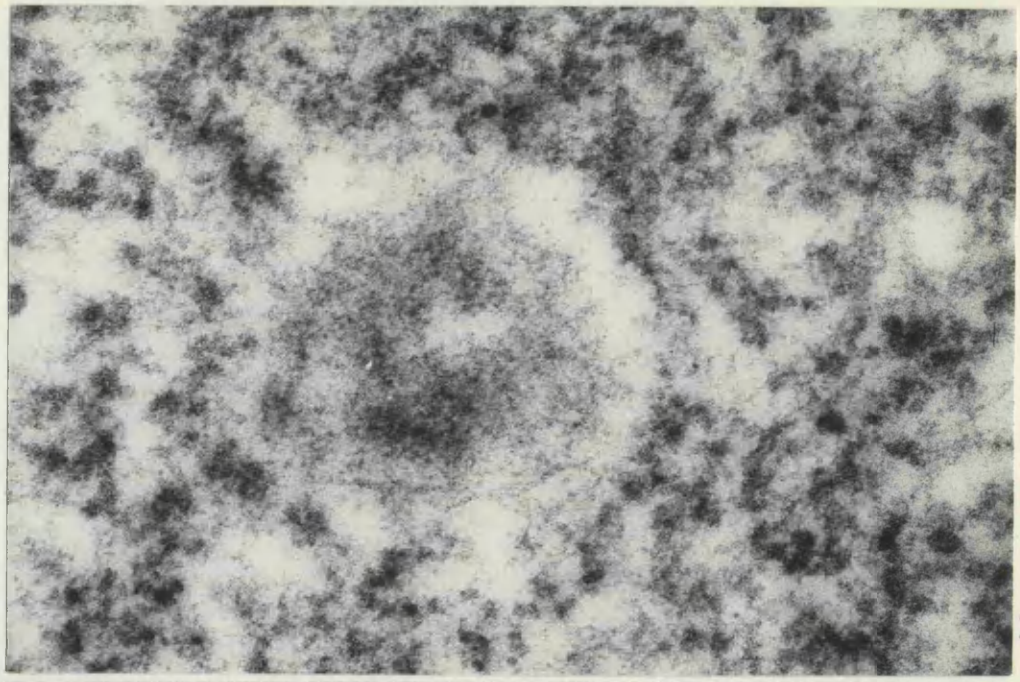

218

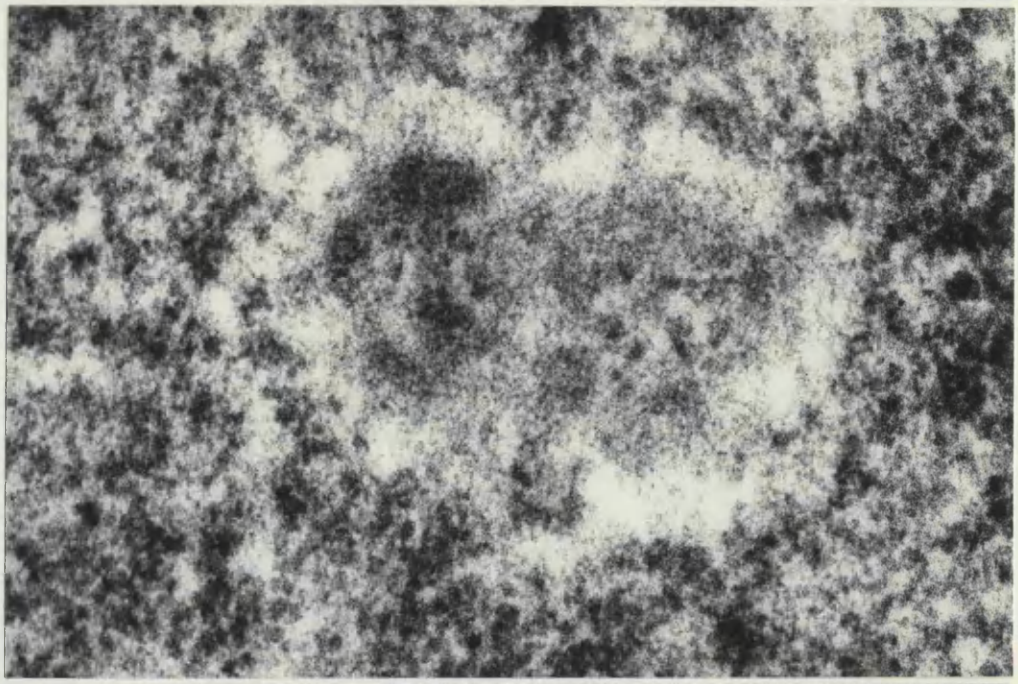

219

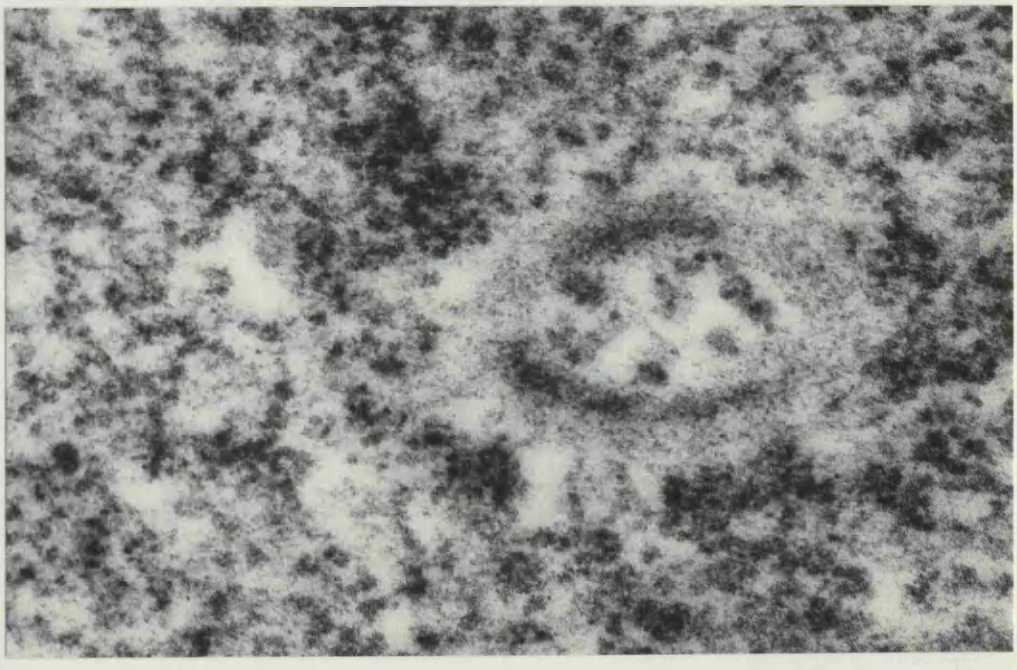

220

NUCLEAR AND CYTOPLASMIC INCLUSIONS

Figure 221. Well differentiated primary gastric carcinoma. Two microfibrillar nuclear bodies are seen in proximity to the nucleolus.

Magnification 93200

Figure 222. Squamous cell carcinoma of oesophagus. A single nuclear body is seen close to the nucleolus.

Magnification 39000

Figure 223. Primary colonic carcinoma. Two nuclear bodies are seen in close contact with each other.

Magnification 93200

Figure 224. Adenocarcinoma of the ampulla of Vater. Two nuclear bodies are seen close to each other.

Magnification 39000

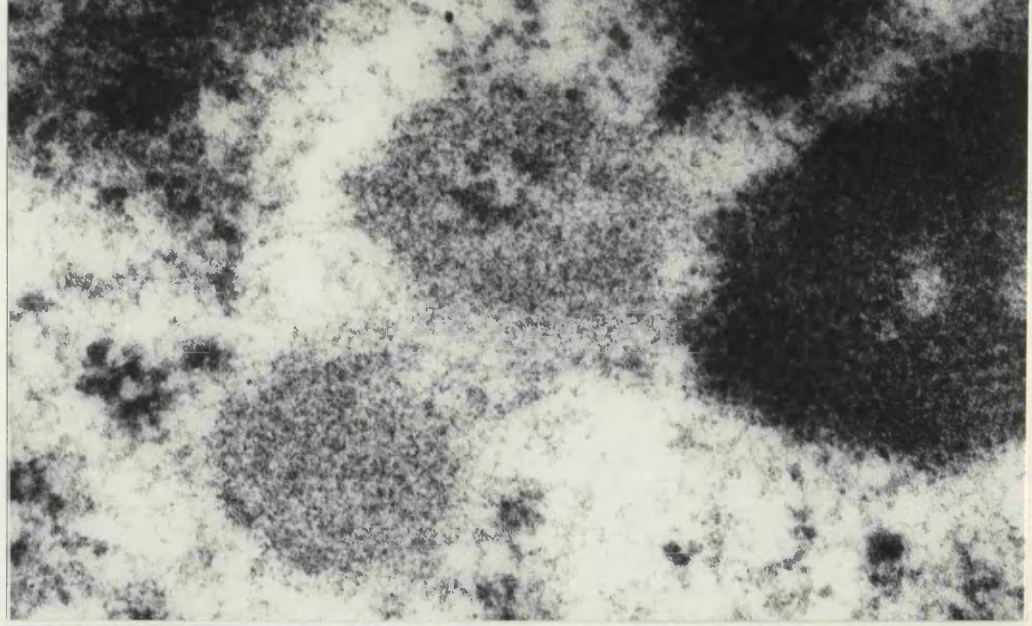

221

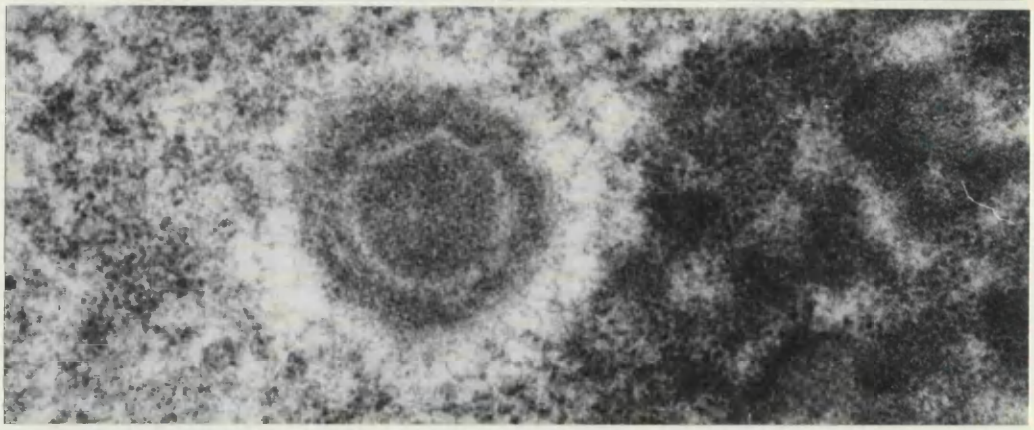

222

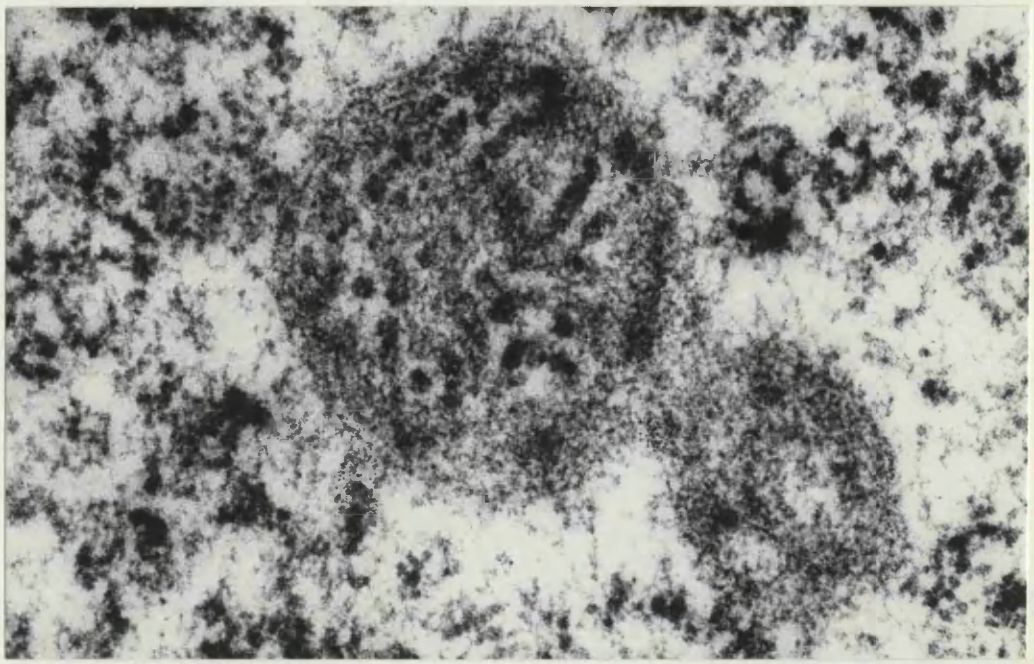

223

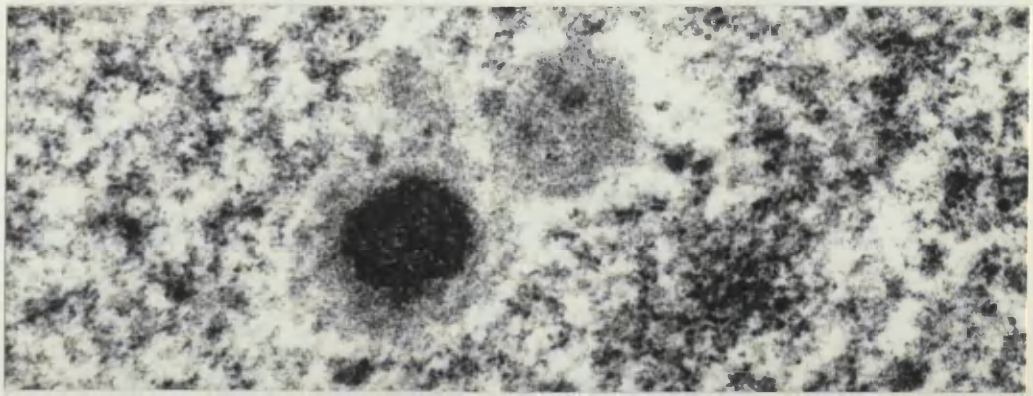

224

NUCLEAR AND CYTOPLASMIC INCLUSIONS

Figure 225. Primary colonic carcinoma. The nuclear body displays a dense homogeneous core and a microfibrillar cortex.

Magnification 93200

Figure 226. Metastatic gastric carcinoma, showing a nuclear body consisting of a dense granular core surrounded by microfibrillar material.

Magnification 88250

Figure 227. Primary colonic carcinoma, showing a nuclear body consisting of microfibrillar material.

Magnification 88250

Figure 228. A microfibrillar nuclear body from a case of gastric carcinoma.

Magnification 93200

Figure 229. Squamous cell carcinoma of oesophagus. A nuclear body is seen with a vacuolated central core and a microfibrillar cortex.

Magnification 84000

Figure 230. Colonic carcinoma. The nuclear body displays a vacuolated central core and microfibrillar cortex.

Magnification 105900

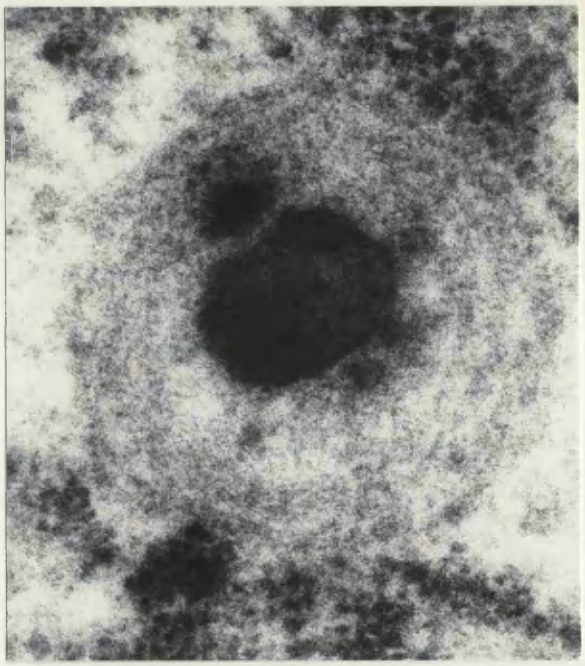

2 25

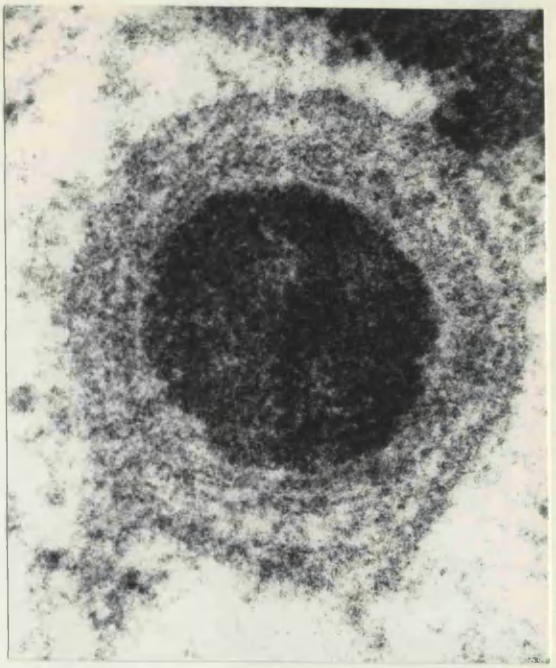

2 26

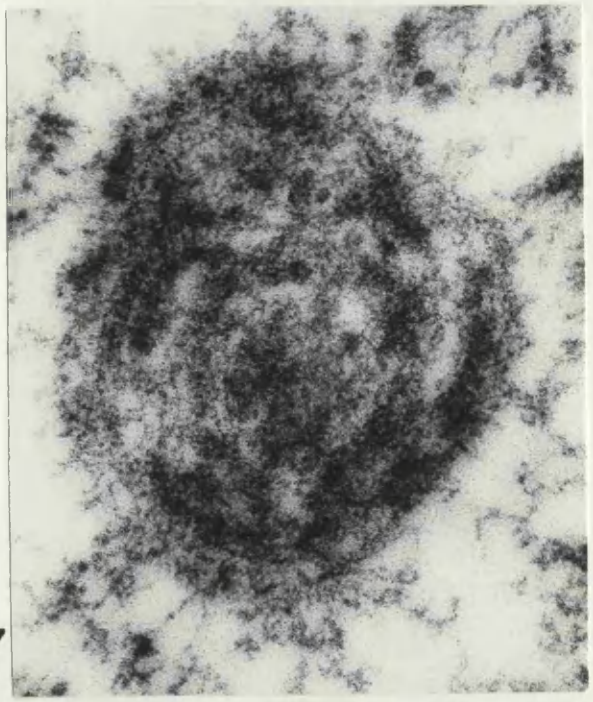

227

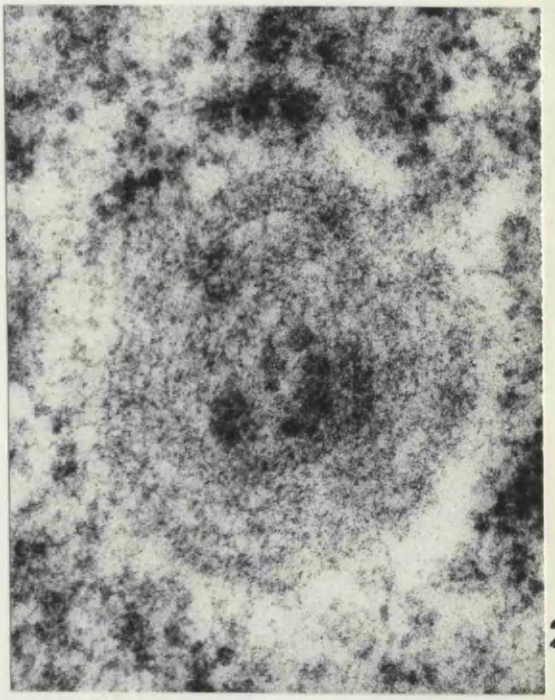

2 28

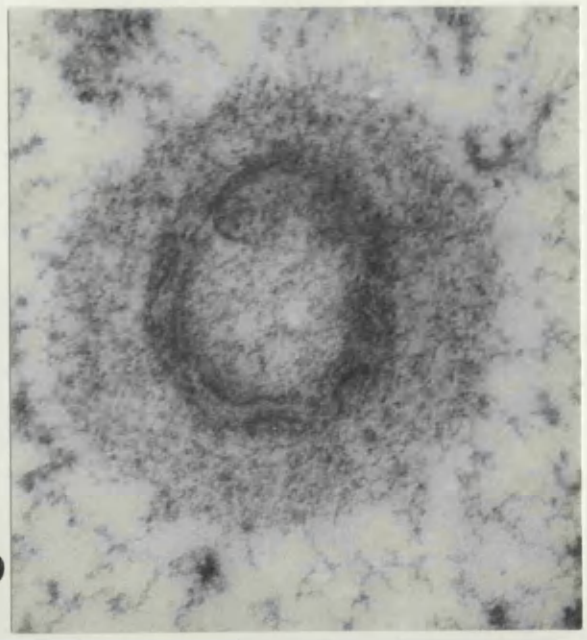

229

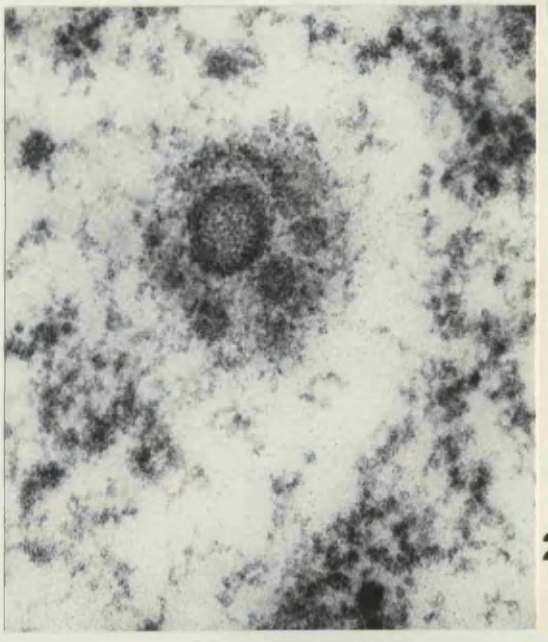

2 30

NUCLEAR AND CYTOPLASMIC INCLUSIONS

Figure 231. Squamous cell carcinoma of oesophagus.

A microfibrillar nuclear body is shown.

Magnification 37500

Figure 232. Deep level of the nuclear body shown in figure 231. Notice the appearance of the dense central core at this level.

Magnification 37500

Figure 233. Deeper level from the nuclear body shown in figure 231. Note the prominence of the dense central core which is not seen in figure 231.

Magnification 37500

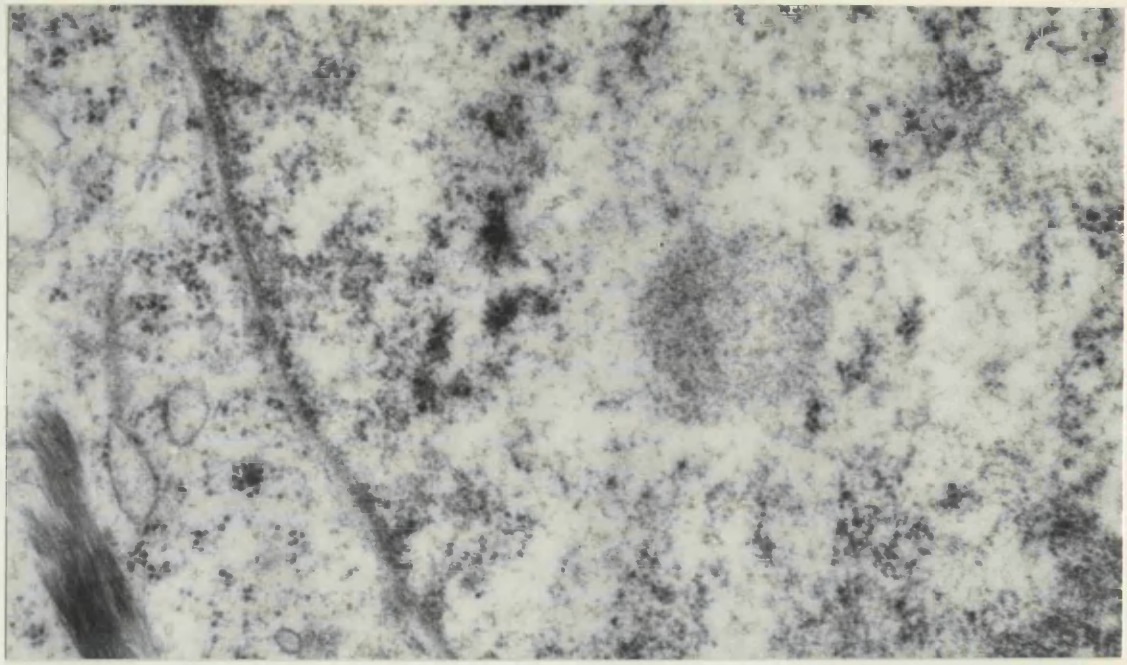

231

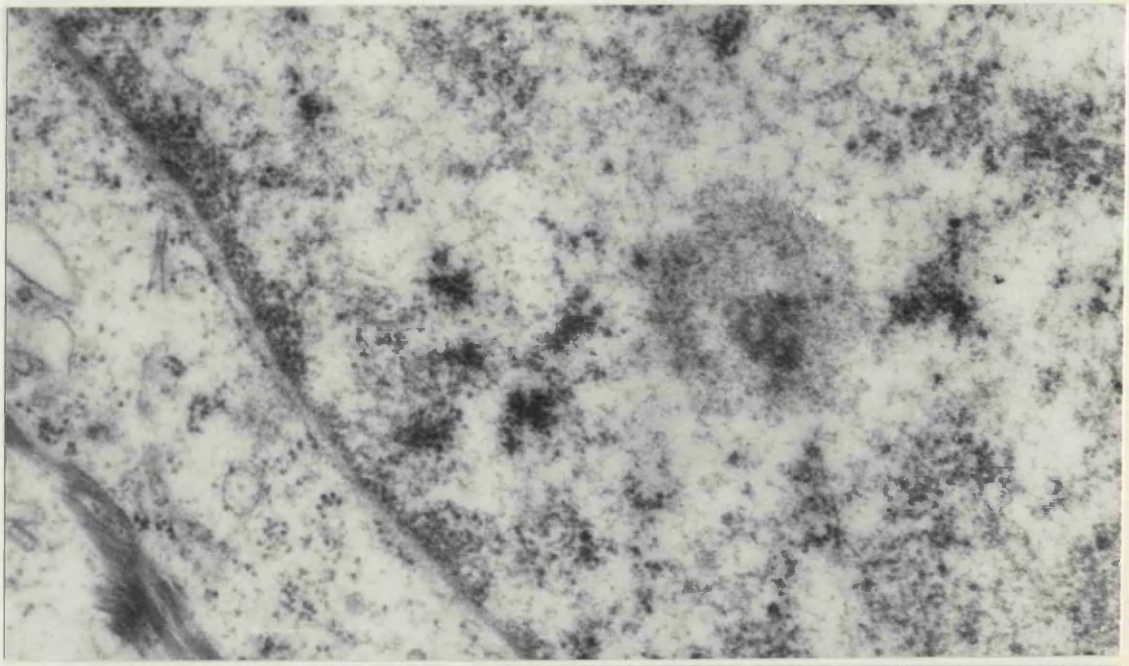

232

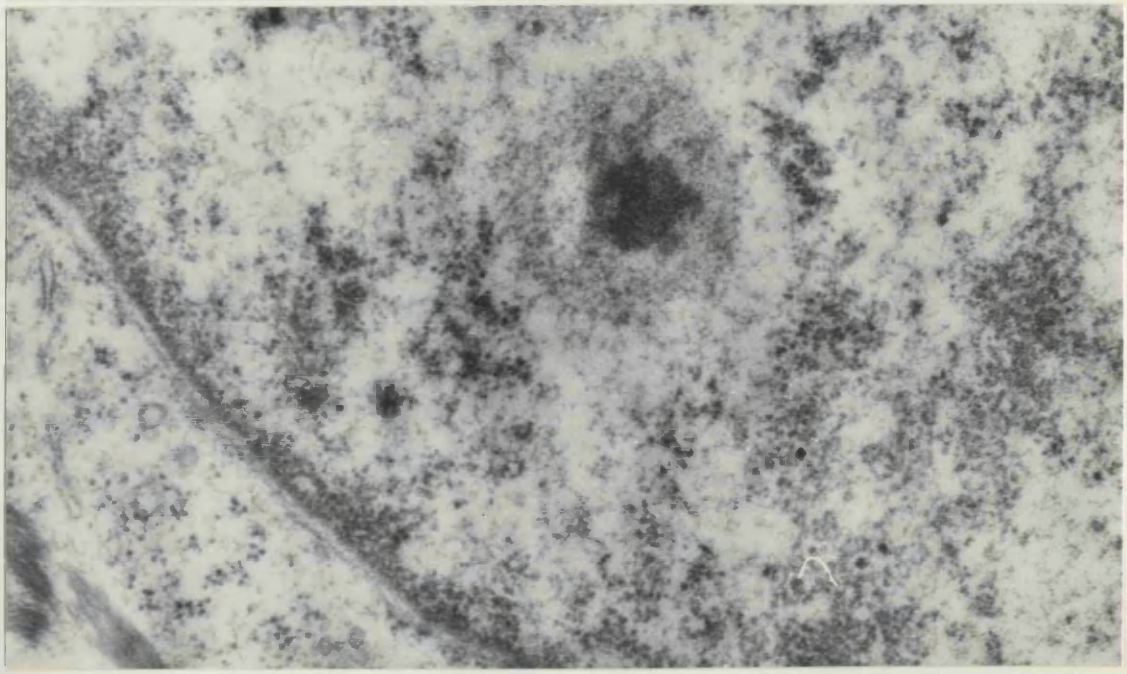

233

NUCLEAR AND CYTOPLASMIC INCLUSIONS

Figures 234, 235, 236. Three levels from a single nuclear body from squamous cell carcinoma of oesophagus. Notice how the appearance of the dense central core of this nuclear body changes at different levels of section.

Magnification 80700

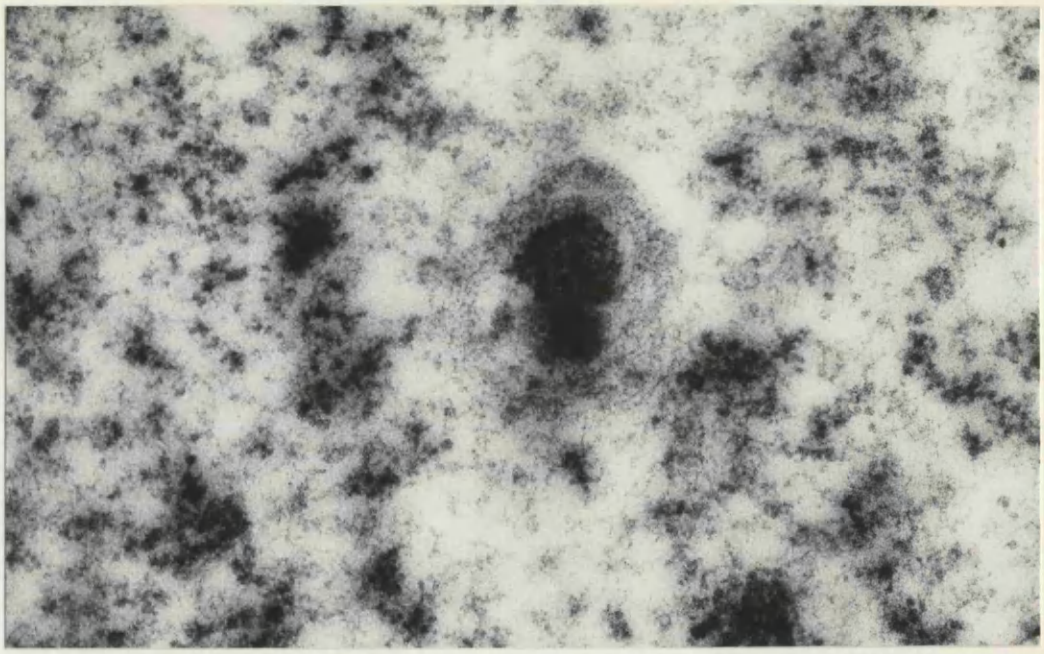

234

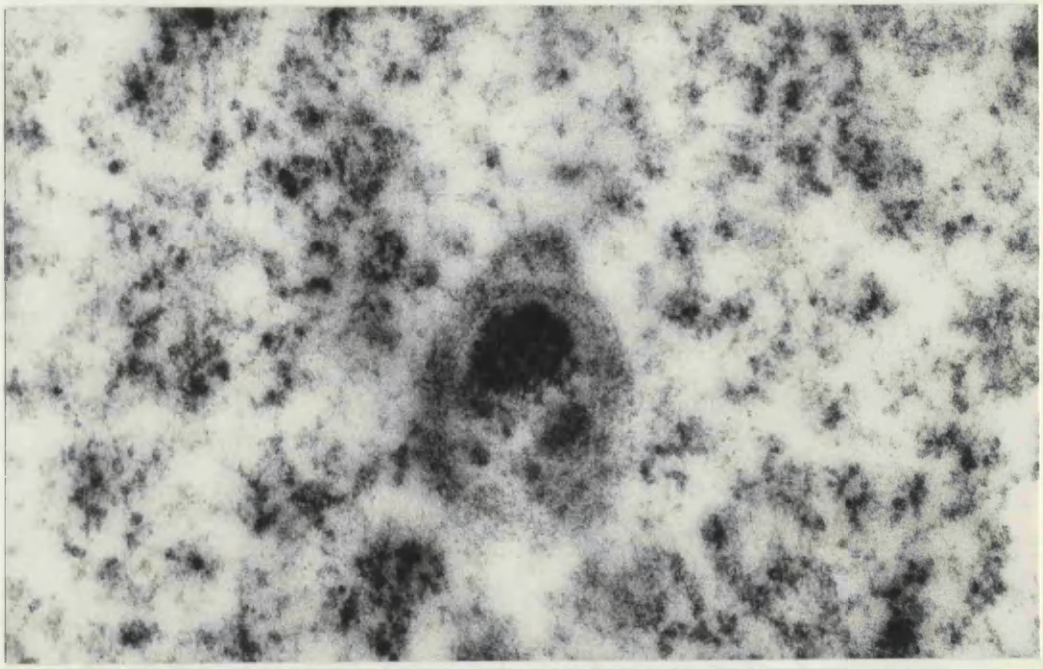

235

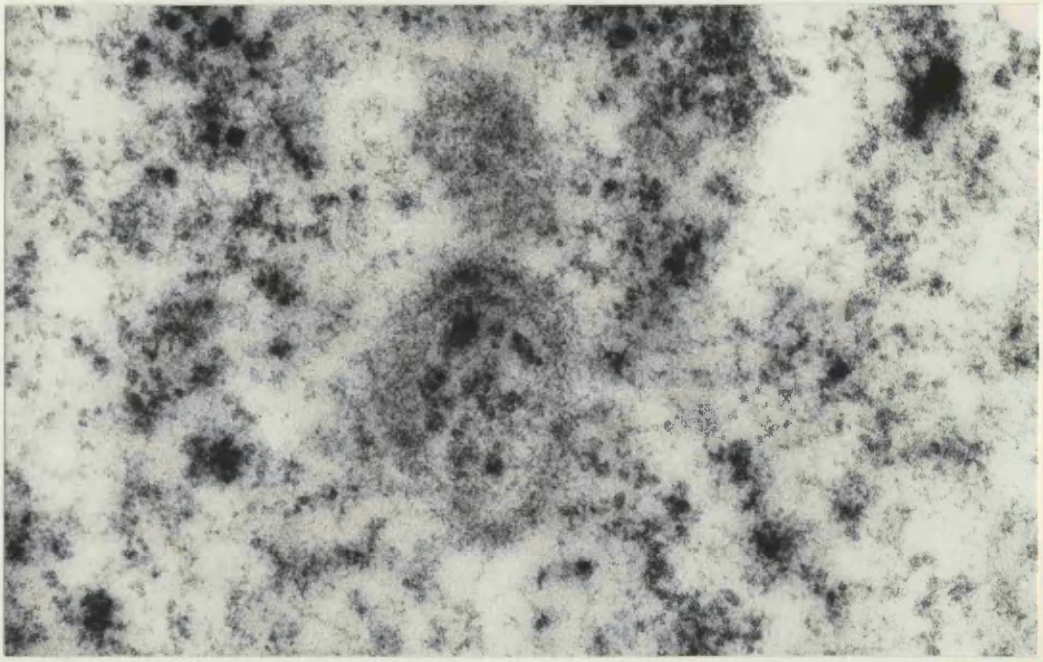

236

NUCLEAR AND CYTOPLASMIC INCLUSIONS

Figure 237. Paired profiles within the nucleus in a case of rectal carcinoma.

Magnification 177000

Figure 238. Intranuclear paired profiles of rectal carcinoma. The appearance of the paired profiles in this micrograph is suggestive of sectioned microtubules.

Magnification 116500

Figure 239. Intracytoplasmic paired profiles of rectal carcinoma, showing alternating linear and punctate structures.

Magnification 107500

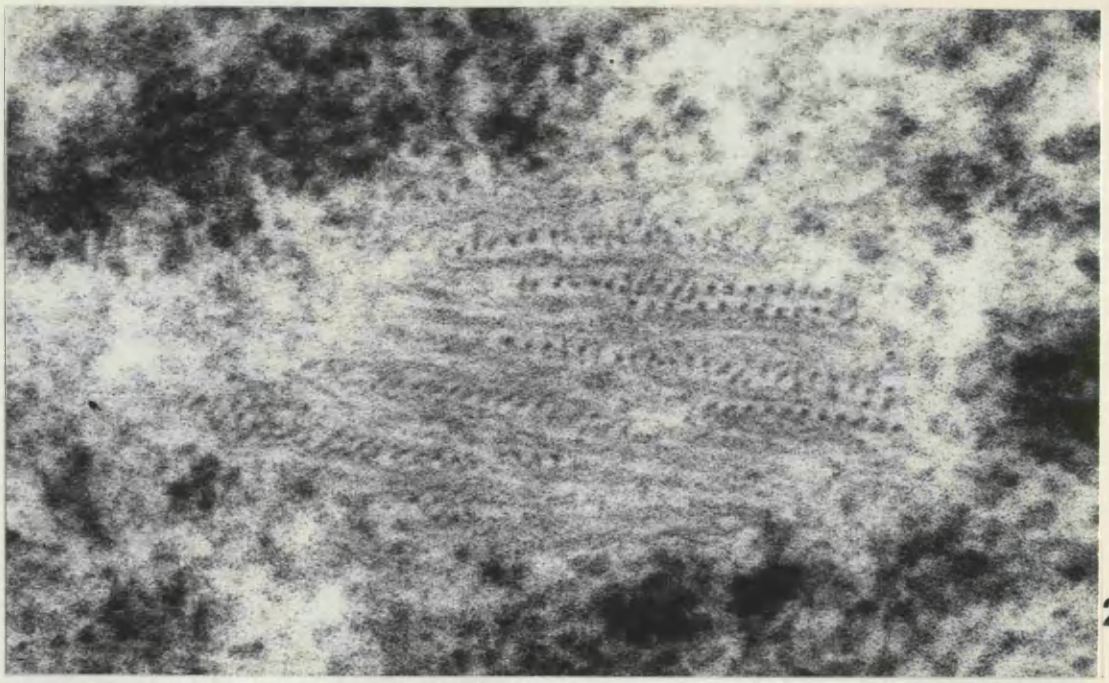

237

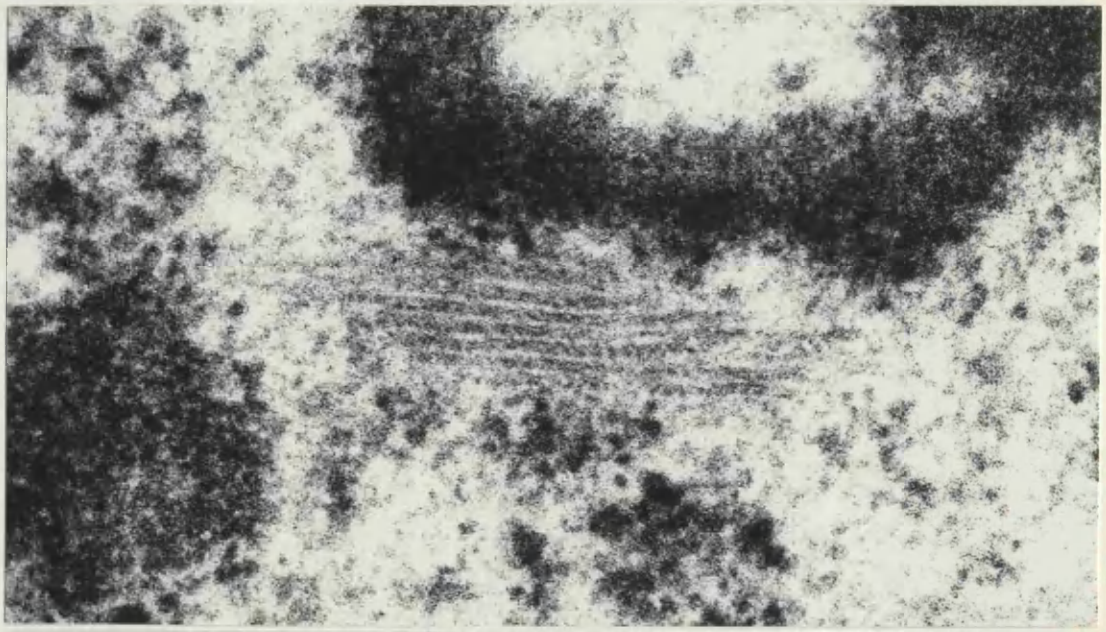

238

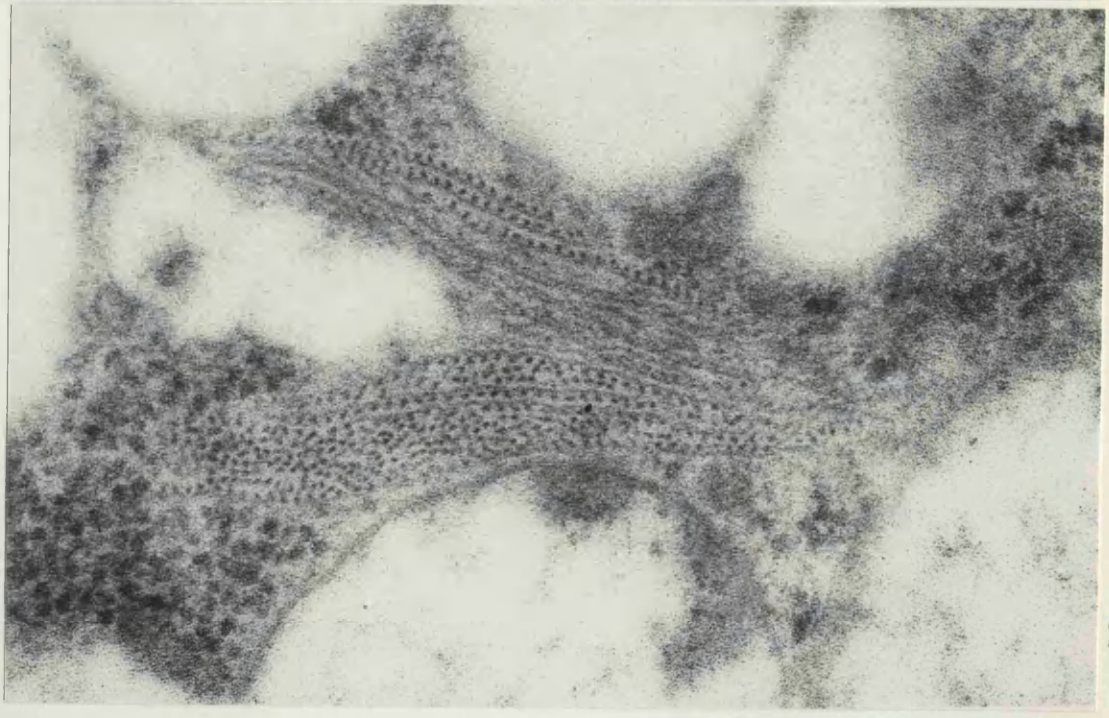

239

NUCLEAR AND CYTOPLASMIC INCLUSIONS

Figure 240. Intranuclear fibrillar inclusion of metastatic rectal carcinoma, occupying an area apparently free from chromatin granules.

Magnification 67250

Figure 241. An intranuclear fibrillar inclusion of primary rectal carcinoma.

Magnification 32500

Figure 242. An intracytoplasmic fibrillar inclusion of rectal carcinoma consisting of undulating microfibrils.

Magnification 39000

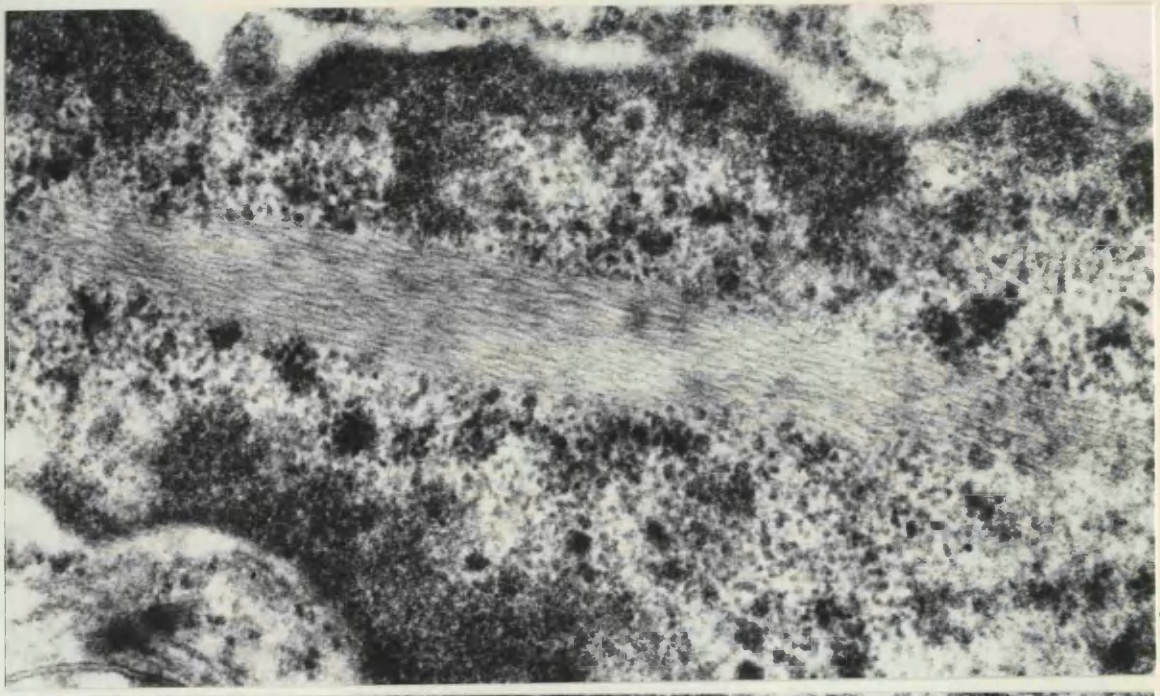

240

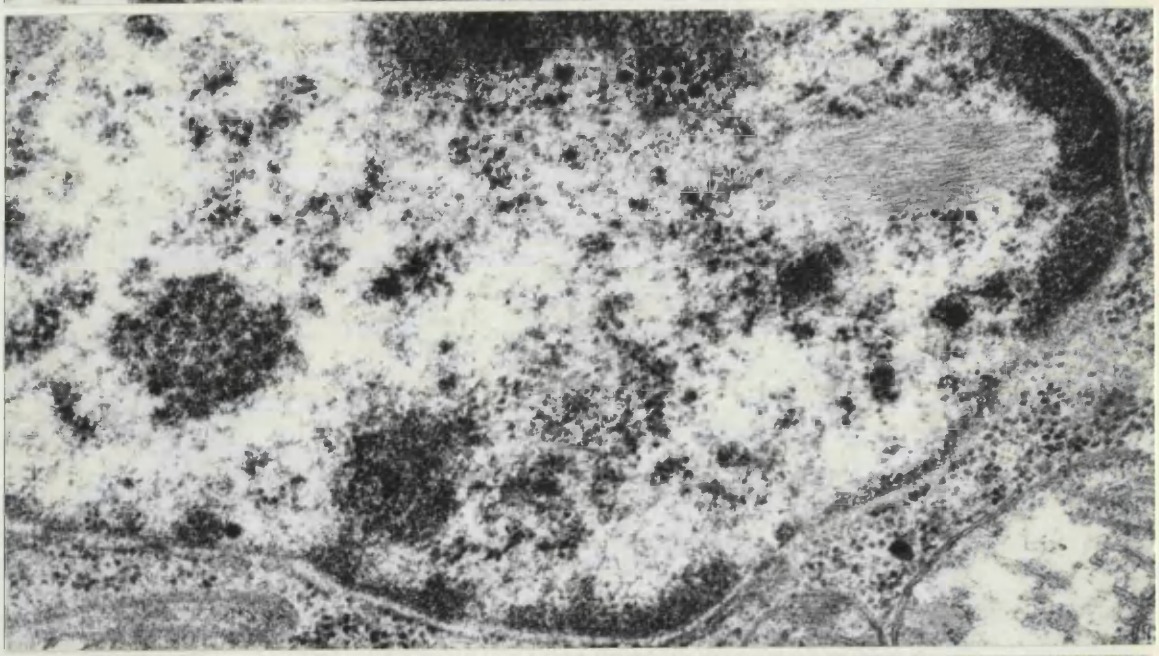

241

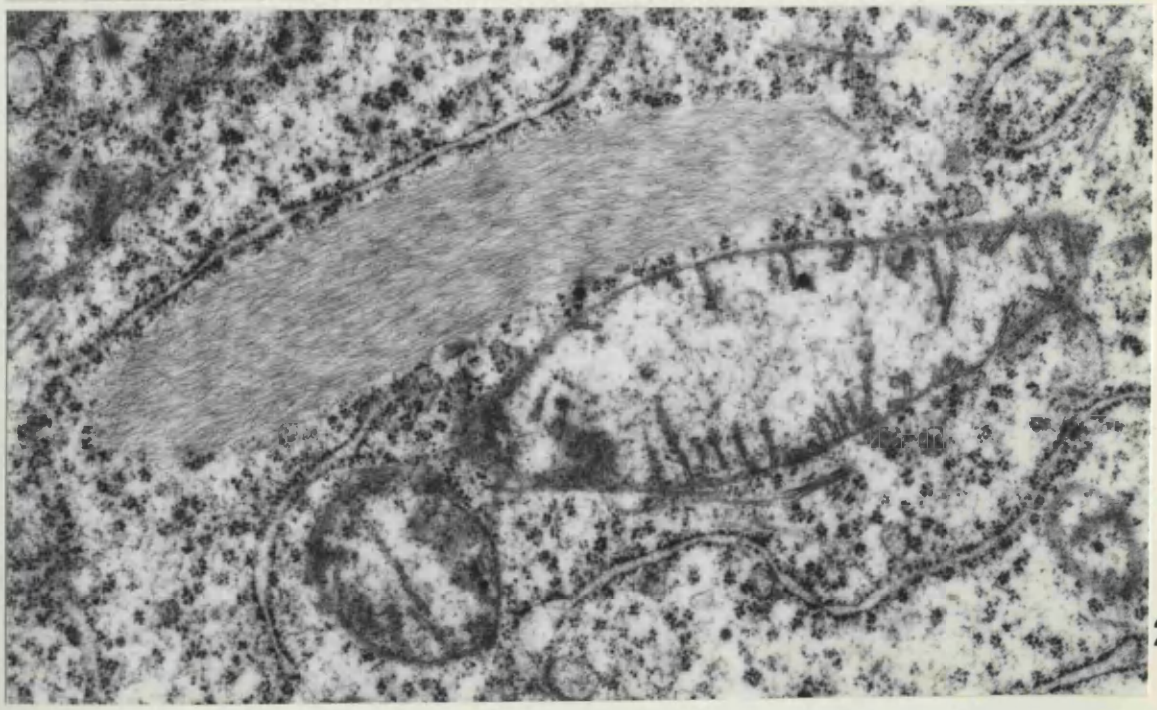

242

NUCLEAR AND CYTOPLASMIC INCLUSIONS

Figure 243. Fibrillar inclusion(F) within the cytoplasm of a mitotic figure from rectal carcinoma . The cell membrane of the mitotic figure is identified by arrows. Notice the intercellular space(S) which separates the mitotic figure from the adjacent cell.

Magnification 22750

Figure 244. Lattice inclusion within a nucleus from rectal carcinoma.

Magnification 93200

Figure 245. Obliquely sectioned intranuclear lattice structure(L) near a microfibrillar nuclear body(B).

Magnification 93200

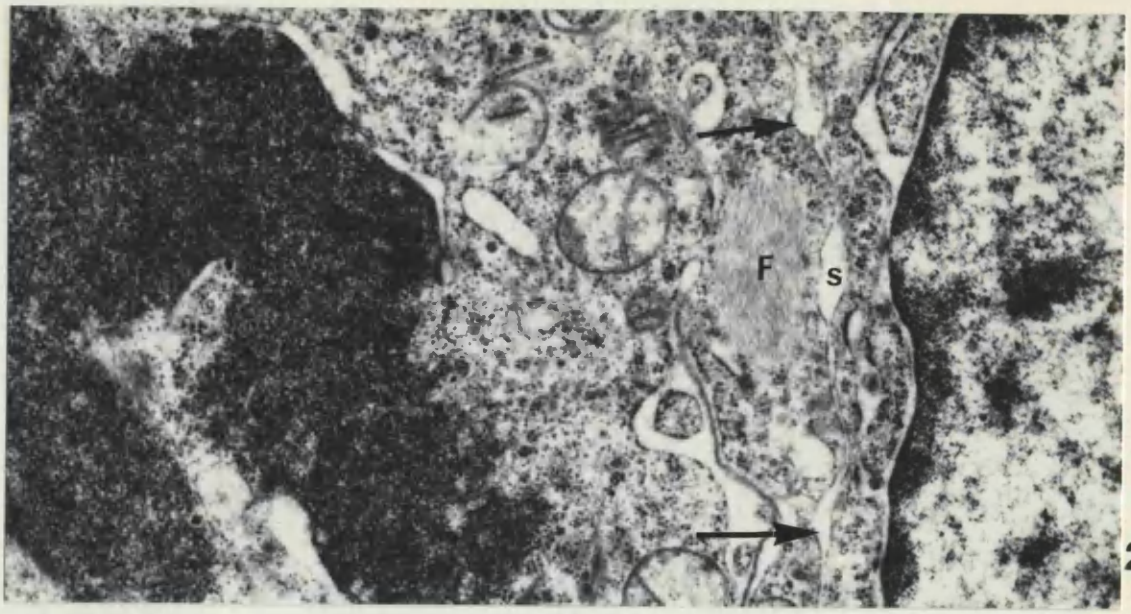

243

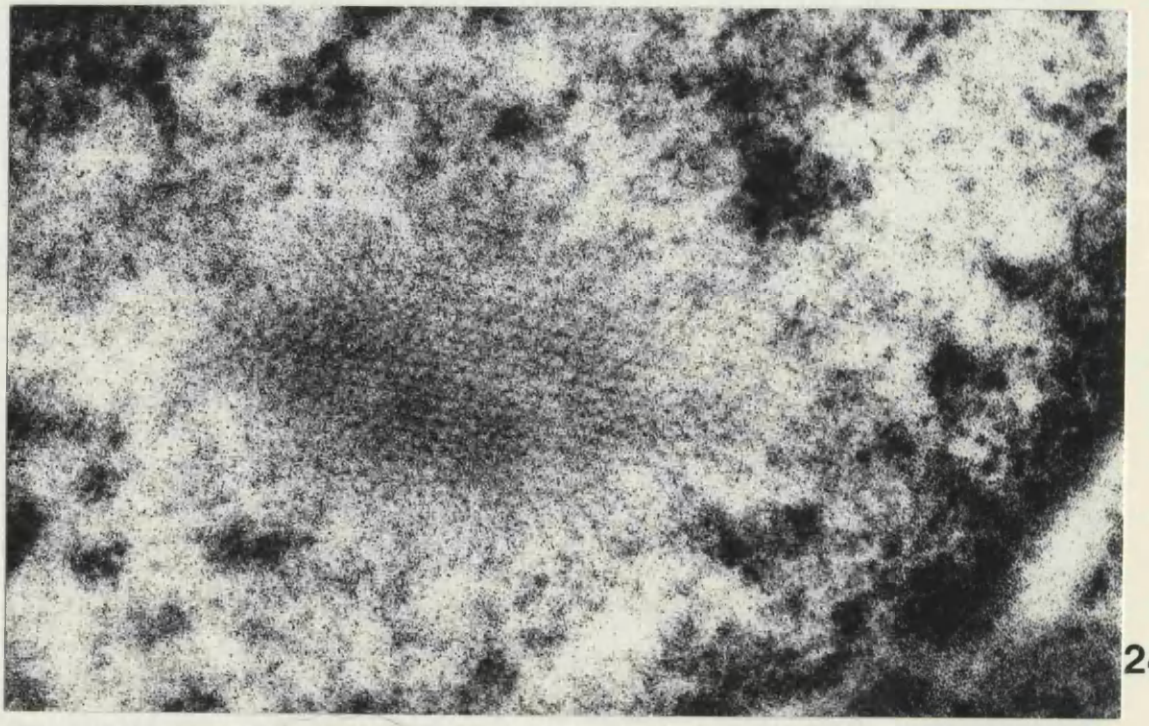

244

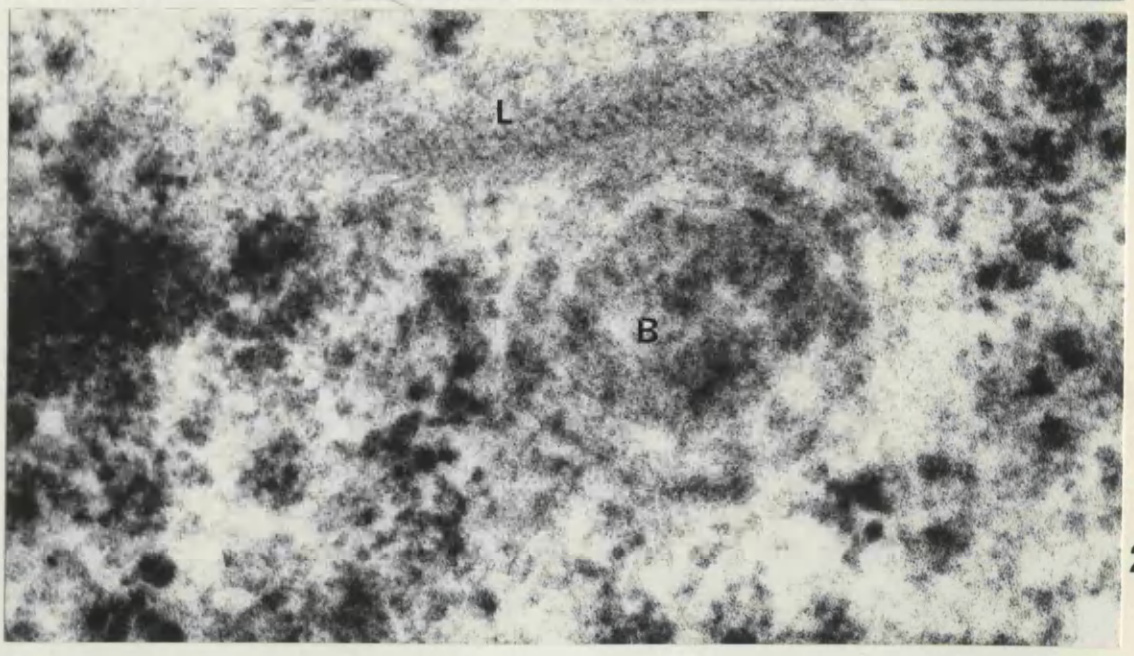

245

NUCLEAR AND CYTOPLASMIC INCLUSIONS

Figure 246. Intranuclear coiled structure of gastric carcinoma.

Magnification 129000

Figure 247. Higher magnification of the intranuclear coiled structure of gastric carcinoma.

Magnification 198000

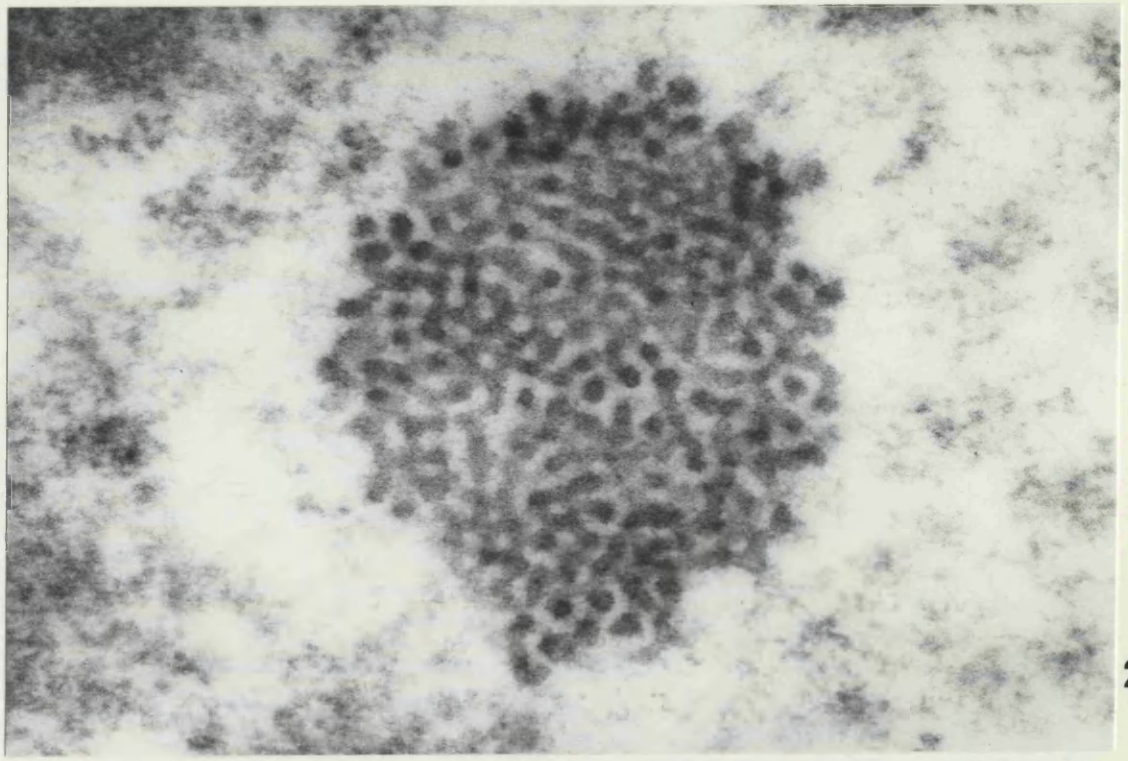

246

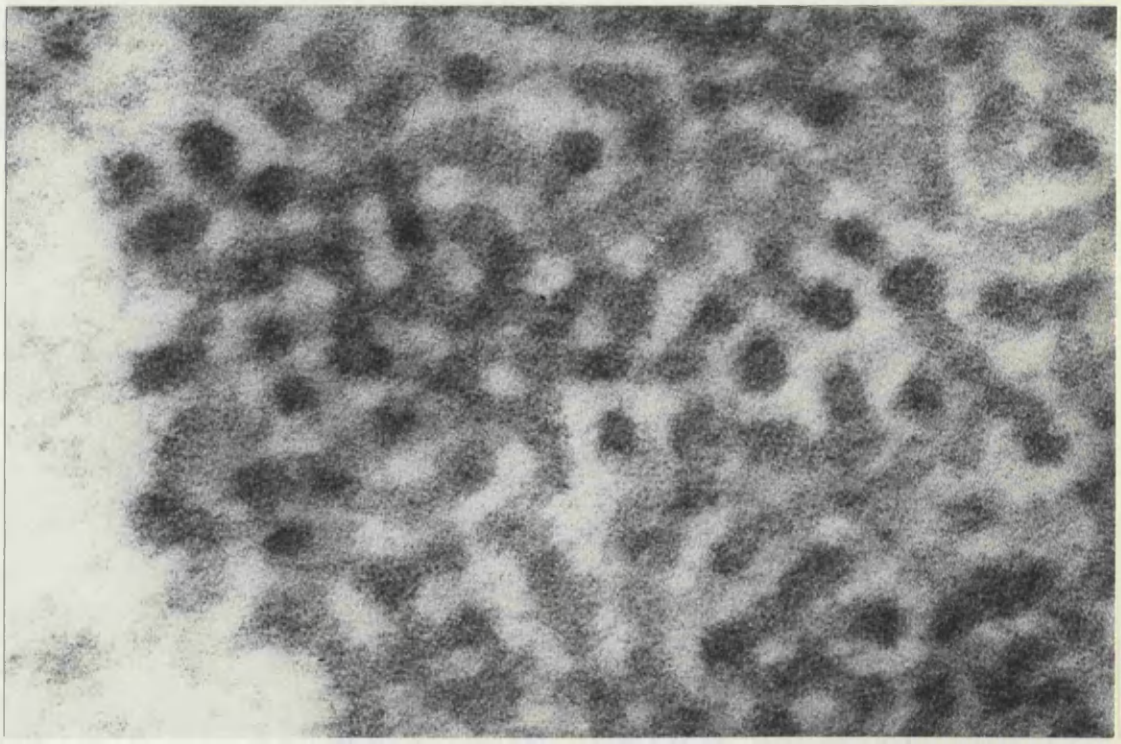

247

X-RAY MICROANALYSIS

Figure 248. This spectrum was obtained from a deposit of the reaction product of the periodic acid thiocarbohydrazide silver proteinate procedure in squamous epithelium of oesophagus. It shows a small sulphur Kα peak at 2.307KeV and a large silver Lα peak at 2.984KeV.

b0
b1
b2
b3
b4
VS: 500 10EV/CH

X-RAY MICROANALYSIS

Figure 249. A spectrum from the cytoplasm of the same cell analysed in figure 248. No significant spectral line is seen.

b4
b3
b2
b1
b0
VS: 500 MS: 10EV/CM

X-RAY MICROANALYSIS

Figure 250. This spectrum shows the result of analysis of the dense reaction product of acid phosphatase in the intercellular spaces of squamous cell carcinoma of oesophagus (See figure 90). A very large M line of lead is seen at 2.365KeV. There is only a small osmium component.

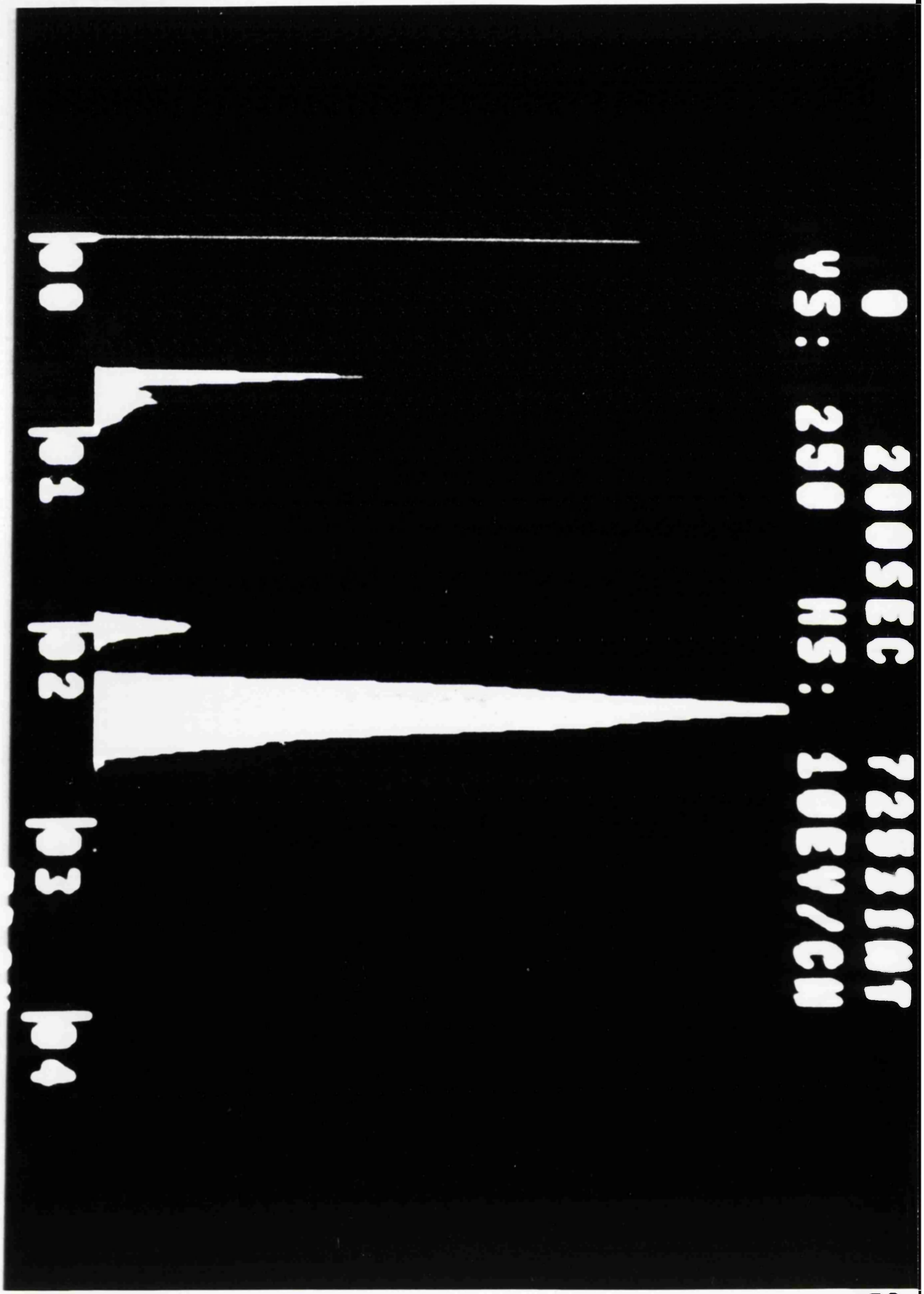
0 200SEC 72831MT
VS: 250 HS: 10EV/CM
0
1
2
3
4

X-RAY MICROANALYSIS

Figure 251. The spectrum shows the analysis of clear cytoplasm from same cell analysed in figure 250. No significant lead deposit is present.

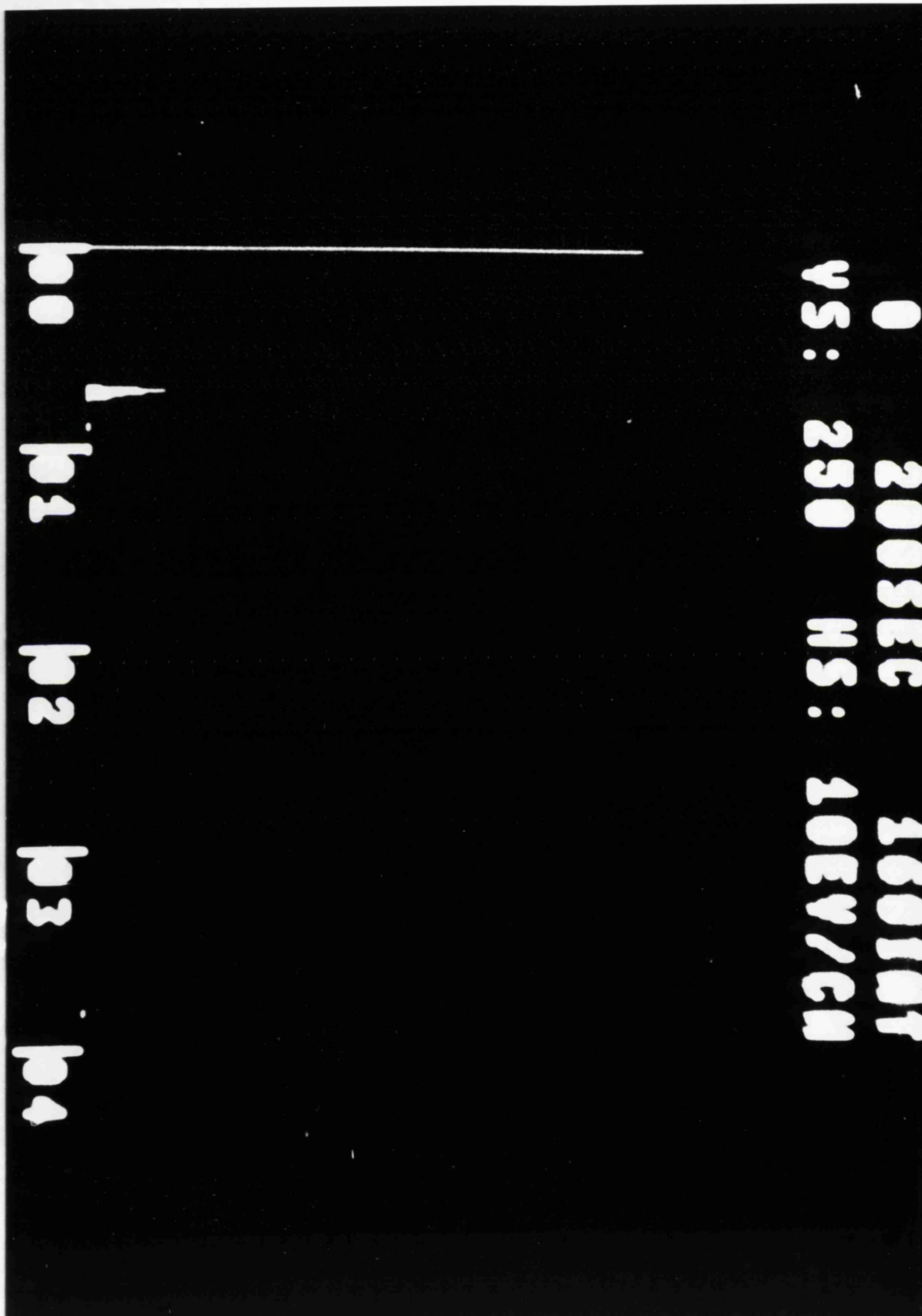
0 200SEC 160INT
VS: 250 HS: 10EV/CM

X-RAY MICROANALYSIS

Figure 252. This specrum was obtained from the analysis of a lysosome in the case of adenocarcinoma of colon demonstrated in figure 214. The principal spectral lines present are the osmium M line at 1.914KeV, and the lead M line at 2.365KeV, confirming the presence of lead in the deposit .

MS/CM 10EV/CM
VS:1000 MS: 10EV/CM
0
d4 d3 d2 d1 d0

X-RAY MICROANALYSIS

Figure 253. The analysis of a clear area of cytoplasm 50 nm distant from the lysosome analysed in figure252. No significant lines are demonstrable.

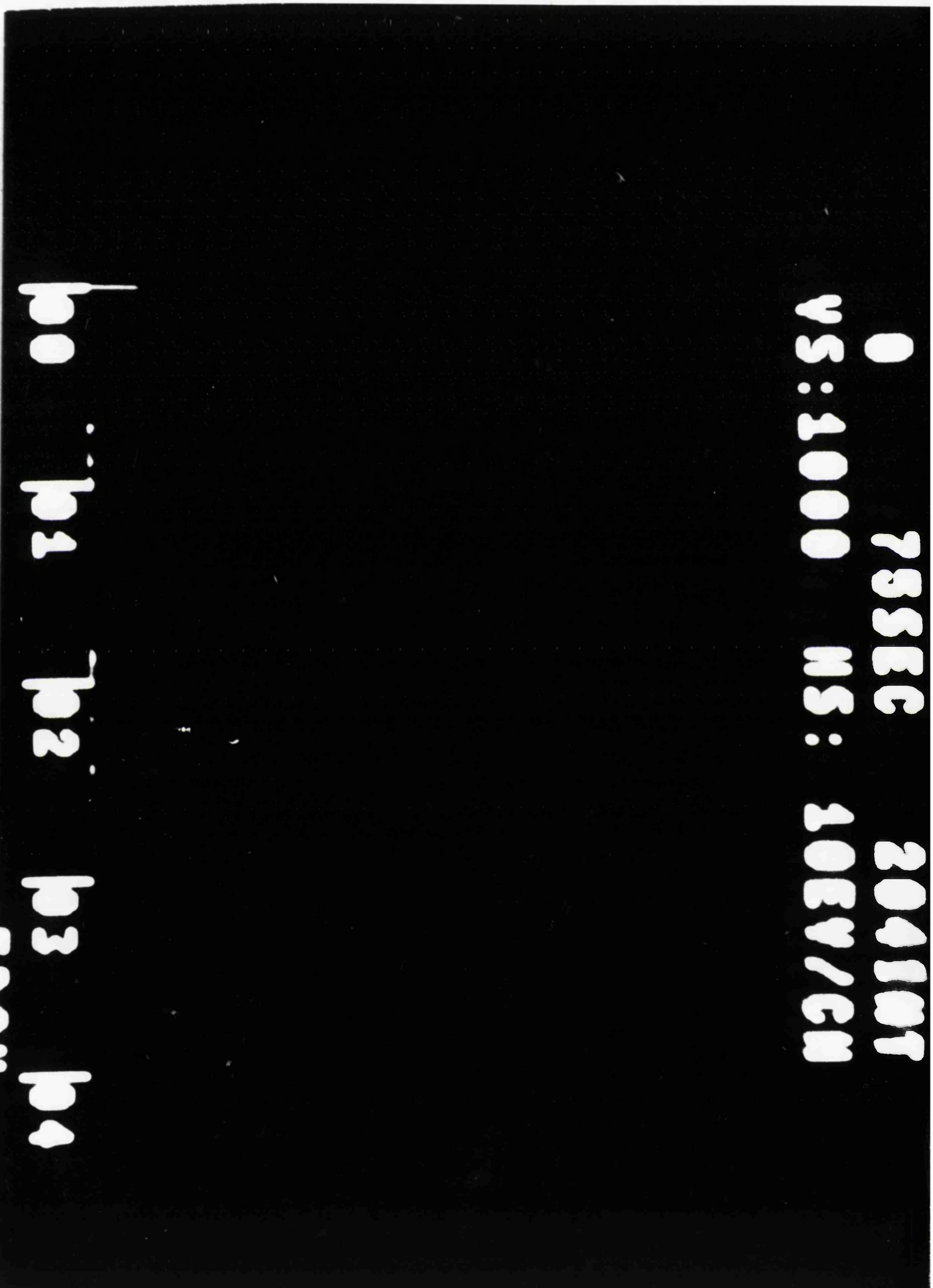
VS:1000 HS: 10EV/CM